UNIVERSITE DE LILLE 1 – UFR SCIENCES DE LA TERRE

ECOLE DOCTORALE DE LA MATIERE, DU RAYONNEMENT ET DE

L'ENVIRONNEMENT

THESE

Présentée par

Pitaksit DITBANJONG

STRATIGRAPHY AND TECTONICS
OF CENOZOIC DEPOSITS
AT THE SOUTHWESTERN BORDER OF THE
MESOHELLENIC BASIN, CONTINENTAL GREECE

En vue de l'obtention du grade de:

DOCTEUR EN SCIENCES DE LA TERRE DE L'UNIVERSITE DE LILLE 1

Soutenue le 17 octobre 2013 devant la commission d'examen :

Michel LOPEZ	Rapporteur	Université Montpellier 2
Siegfried LALLEMANT	Rapporteur	Université de Cergy-Pontoise
Julien BAILLEUL	Examinateur	Institut Polytechnique Lasalle-Beauvais
Jacky FERRIERE	Examinateur	Université de Lille 1
Frank CHANIER	Co-directeur de thèse	Université de Lille 1
Jean-Yves REYNAUD	Directeur de thèse	Université de Lille 1

Acknowledgements

I would like to express my gratitude to Jean-Yves Reynaud, my supervisor, for his confidence and help and for giving the opportunity to attend to this thesis topic under his direction. Without his support, suggestions and geniality, this work would never have been done. I am also indebted to Frank Chanier and Jacky Ferrière who are my professors, my colleagues, my friends and my 'papas'. This manuscript could never have been completed without them. I have earned uncountable experience and learned million of things, geology, field method, friendship, adaptation and life in each generation.

Jacky, Frank, grâce à vous j'ai passé un moment formidable. Merci du fond du cœur!

I am grateful to all jury members; Michel Lopez, Université Montpellier; Siegfried Lallemant, Université de Cergy-Pontoise; Julien Bailleul, for their time, their critics and suggestions that will help greatly to improve this manuscript and my future work.

I would like to pay special tribute to all the people who have taken part in the sedimentological and paleontological analyses, in particular, Silvia Gardin and Daniel Vachard.

I would like to acknowledge all colleagues and personnels in the laboratory who have consistently supported in any administrative procedures and kindly helped in the reprography of this manuscript.

My thanks must go to all my Thai and French friends inside and outside the laboratory SN5 who are always available to share the opinions and always ready to help since my first day in the Université Lille 1.

I also thank all of my family for furnishing constantly the support and encouragements all along my life and my coming future.

Finally, my thesis would never have been completed without support from the Development and Promotion of Science and Technology Talents Project (DPST) conducted jointly by the Royal Thai Government Agencies and the Institute for the Promotion of Teaching Science and Technology (IPST). They gave me a great opportunity and a scholarship covering the entire duration since my High School until my PhD (1998-2012).

RESUME

Le bassin méso-hellénique est un bassin oligo-miocène intra-chaîne situé dans le nord de la Grèce continentale, à la limite entre les zones externes et les zones internes de la chaîne des Hellénides. Ce mémoire présente une analyse détaillée des séries sédimentaires affleurant sur la bordure occidentale du bassin dans sa partie la plus méridionale. Trois blocs, séparés par des failles majeures, sont étudiés successivement, du point de vue des faciès, de leur stratigraphie et des structures tectoniques. Une carte géologique détaillée est produite, fondée sur les formations lithologiques élevées au rang d'unités stratigraphiques. La structure est un monoclinal faillé à vergence vers le bassin. Les failles sont essentiellement des failles normales, mais des mouvements compressifs existent. Des failles listriques synsédimentaires précoces sont enregistrées à la base du comblement. Les failles majeures interblocs sont inversées tardivement. Les faciès indiquent pour l'essentiel des épandages sous-marins d'origine gravitaire. Les sources sédimentaires sont d'abord locales (couverture mésozoïque) puis, pour l'essentiel du comblement, lointaines (socle pélagonien des zones internes). Les directions de paléocourants indiquent un approvisionnement depuis le NE, dans le secteur des Météores. La succession stratigraphique est marquée par des ruptures de faciès abruptes et érosives ainsi que des discordances enregistrant essentiellement un signal tectonique. Les analyses micropaléontologiques permettent de préciser l'âge des séries sur l'intervalle Oligocène supérieur-Miocène inférieur. Cet âge est plus jeune que le démarrage du bassin méso-hellénique plus au nord, mais sub-contemporain de la mise en place des conglomérats des Météores, dont le contrôle tectonique a également été mis en évidence.

ABSTRACT

The Mesohellenic Basin is an Oligo-Miocene intermontane basin preserved in Northern continental Greece, at the boundary between the external and internal zones of the Hellenides. This memoir presents a detailed analysis of the deposits outcroping in the southernmost part of the basin, on its western border. Three fault-bounded blocks are presented successively, including facies, stratigraphic and tectonic data. A detailed geological map is provided, featuring lithological formations of chronological significance. The main structure is a faulted monocline dipping toward the basin. Faults are mostly normal faults, although compressional features are observed. Synsedimentary listric faults are recorded in the lower part of the basin fill. The major block-bounding faults were lately inverted. The facies indicate mainly submarine gravity flows and associated turbidites. The sediments were supplied first locally (erosion of the mesozoic cover) and then, for most of basin fill, from denudation of the pelagonian basement (internal zones). Paleocurrent directions, related to this main part of the infill, indicate a source to the Northeast, in the area of the Meteora. The stratigraphic succession is marked by facies gaps and erosional unconformities which point to a dominant tectonic control. The micropaleontologic analyses provide an overall Upper Oligocene-Lower Miocene age of the series. This age is younger than that of the early stages of the basin more to the north, but rather contemporaneous with the Meteora conglomerates, the tectonic origin of which was previously demonstrated.

4

CHAPTER I – Introduction

I. Geological outline

A. The Hellenides

This work concerns a major sedimentary basin of Northern continental Greece, the Mesohellenic Basin (Mesohellenic Trough: Brunn, 1956; Aubouin, 1958 or Albano-Thessalian Basin: Bourcart, 1925). This basin is part of the Hellenides, which are part of the alpine orogen of the Western Tethys (Fig. I. 1).

The Hellenic chain is composed of two main realms (Brunn, 1956): the internal zones (to the east) on which the Tethys oceanic crust was obducted in the Late Jurassic, and the external zones (to the west) which were tectonized in the Cenozoic due to collision between Adria and European tectonic blocks. The external zones are understhrusted beneath the internal zones starting in the mid- to late-Eocene (Fig. I. 1).

The internal zones are basically composed of two domains: the Vardar domain to the east and the Pelagonian domain to the west. The Vardar was thrusted above the Pelagonian in the Paleogene.

The Pelagonian domain is the basement of most of the Mesohellenic Basin. It underwent several major tectonic episodes:

1) In the Upper Jurassic, obduction of ophiolites, the origin of which remains debated (cf. discussion in Ferrière et al., 2012). Maliac nappes related to the pelagonian oceanic margin are preserved between the Triassic-Jurassic pelagonian shelf series and the ophiolites.

2) In the late Mesozoic-early Cenozoic, a generalized compressional tectonic phase.

    a. Until the early Eocene, the internal zones are strongly tectonized and metamorphozed, namely to the northeast of Hellenides (phases CT1 and CT2 of Vergely, 1984).

    b. Starting in the late Eocene, southwestward verging thrusts propagate from the internal to the external zones (CT3 of Vergely, 1984).

The Mesohellenic Basin developed at this time as a piggyback basin, due to the eastward subduction of first the Pindos flysch basin and second the thick Gavrovo-Tripolitza platform beneath the Pelagonian zone.

3) In the Plio-Quaternary, the Pelagonian is marked by extensional tectonics, which also affects most of the Aegean plate.

From the major compressional Eocene phase to the recent extensional regime, the Pelagonian zone records several additional tectonic episodes which are marked by vertical motions, some being related to compressive features in the Upper Miocene-Lower Pliocene and Lower Pleistocene (Mercier et al., 1979; Vamvaka et al., 2006).

B. The Mesohellenic Basin (MHB)

The MHB is a 4.5 km deep, 300 km long and 30-40 km wide basin, striking NW-SE from Albania to Northern Greece. It has some conspicuous caracteristics (Brunn, 1956; Doutsos et al., 1994; Kontopoulos et al., 1999; Zelilidis et al., 2002; Ferrière et al., 1998, 2004, 2011; Vamvaka et al., 2006) (Fig. I. 2):

- It is located inside the Hellenic chain, at the boundary beween the external and internal zones;

- It is Cenozoic in age (late Eocene to middle Miocene) and therefore contemporaneous to collision between Adria (to the West) and Europe (to the East, corresponding to the Pelagonian block in Greece);

- It is mainly 'molassic' because, starting from the early Oligocene, its deposits unconformably rest on the rocks of the previously deformed internal and external zones;

6

- It is also 'piggyback', in spite of its large scale, because it is contemporaneous of the propagation, below it, of underthrusting of part of the external zones, as evidenced in the Olympos-Ossa tectonic windows to the east (Fig. I. 1B)(Godfriaux, 1968).

- Its infilling mostly consists in siliciclastic deposits sourced by the rising external zones until the latest Oligocene and then by the internal zones (starting with the Pentalofon Formation);

- It hosts 7 major stratigraphic units: 2 Eocene formations coresponding to two small basins (Krania Fm to the west and Rizoma to the east); 2 Oligo-Miocene formations corresponding to the main basin fill (Eptachorion Fm and Pentalofon Fm); 1 Lower-to-Middle Miocene formation restricted to the eastern part of the main basin (Tsotyli Fm); 2 Middle Miocene formations outcroping forming the last deposits in separate areas of the basin (Ondria and Orlias Fms);

- It records three main palaeogeographic changes: (i) a dissected topography with deeps and shelves (Krania and Rizoma Fms); (ii) a shallowing-up, large foreland trough (Eptachorion and Pentalofon Fms); (iii) an eastward jump of the foreland trough during the last and shallowest stages of infilling (Tsotyli to Orlias Fms);

The last of those points shows that the MHB basically records the topographic evolution of the orogen, although eustatic variations may have a subdued effect on its architecture (Ferrière et al., 2004, 2011). In its early stages (late Eocene), subsidence is localized in restricted areas of the pelagonian margin above the deep, Pindos basin subduction. During the main, later stages (Oligo-Miocene), the generalized subsidence reflects the collision and later underthrusting toward the east of the thick Gavrovo-Tripolitza ridge (Ferrière et al., 2004).

The MHB has been mapped at 1/50000: Brunn, 1969; Savoyat *et al.*, 1969a, 1969b, 1971a, 1971b, 1972a, 1972b; Mavridis *et al.*, 1979, 1993; Koumantakis *et al.*, 1980; Vidakis *et al.*, 1998). On these maps, except for the youngest Formations in the northern MHB, only the main lithologic Formations as recognized by Brunn (1956) have been distinguished.

More detailed works or additional data in large studies have been proposed. They concern:

i) Paleontological data especially for datings using Foraminifera and nannofossils: Bizon et al., 1968; Soliman H.A. & Zygojiannis N. 1980; Zygojiannis N. & Müller C., 1982; Barbieri R. ,1992; Kontopoulos *et al.*, 1999; Zelilidis *et al.*, 1997, 2002; Ferriere *et al.*, 2004;

ii) Sedimentological analysis: Desprairies, 1979; Ori and Roveri, 1987; Papanikolaou *et al.*, 1988; Wilson, 1993; Zelilidis A. & Kontopoulos N., 1996; Zelilidis *et al.,* 2002; Ferriere *et al.*, 2004;

iii) Tectonic structures: Doutsos et al., 1994; Ferriere et al., 2004, 2011; Vamvaka et al., 2006.

The MHB narrowend to the south, due to the presence of an indentor of the Pelagonian margin which intrudes the growing accretionnary prism (Ferrière et al., 2004, 2011). This study aims to understand how the basin continues to the south of this indentor. While Eocene to Miocene deposits largely crop out in the main, northern part of the MHB, they are, where they exist, mostly covered by Plio-Quaternary deposits to the south of Kalambaka in the Trikala – Thessalian plain (Fig. I. 1 and Fig. I. 2). The Cenozoic counterparts of the MHB deposits are only exposed in a restricted, western part of this plain, at the border of the Koziakas Mountains, and this is where this study was undertaken.

C. The study area versus MHB

The study area in a new part of the MHB developed during the Early Miocene, while the main part of the MHB developed since the Early Oligocene (locally late Eocene).

This area represents the SW border of the MHB with thick terrigenous deposits (especially sandstones and conglomerates) but the pebble, mainly pelagonian nmarbles and gneisses, come frome the NE border of the basin.

In the study area, normal faults and compressive structures are observed. Some of these normal faults are synsedimentary faults of Early Miocene age, at the base of the series.
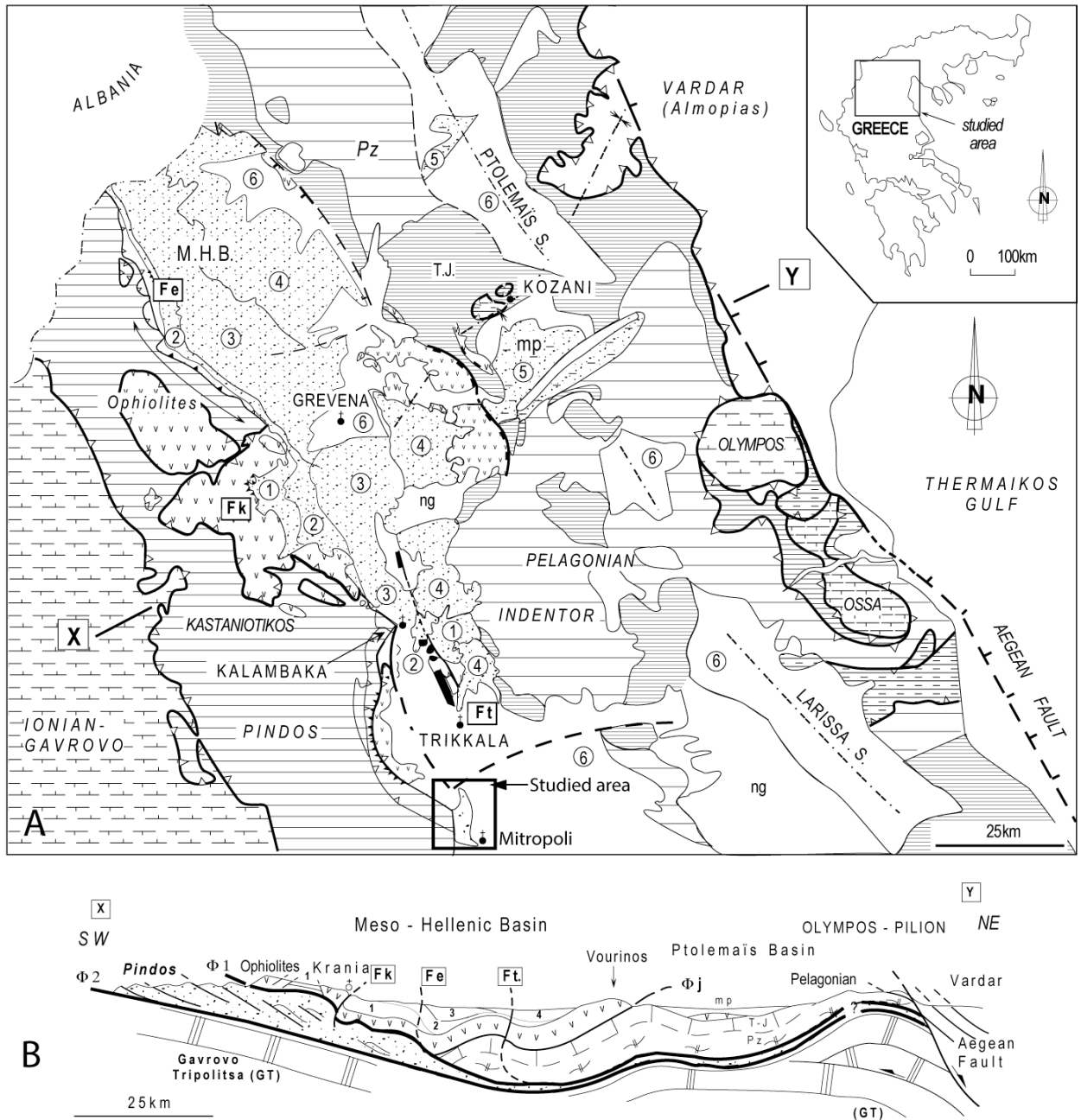
Fig. I. 1: A) Geological of the Mesohellenic basin (MHB). The inset frame in the main map corresponds to the study area. Number in circles, 1: Krania and Rizoma Fm, 2: Eptachorion Fm, 3: Pentalofon Fm and 4: Tsotyli Fm. B) Cross-section of the MHB (Ferrière et al., 1998).
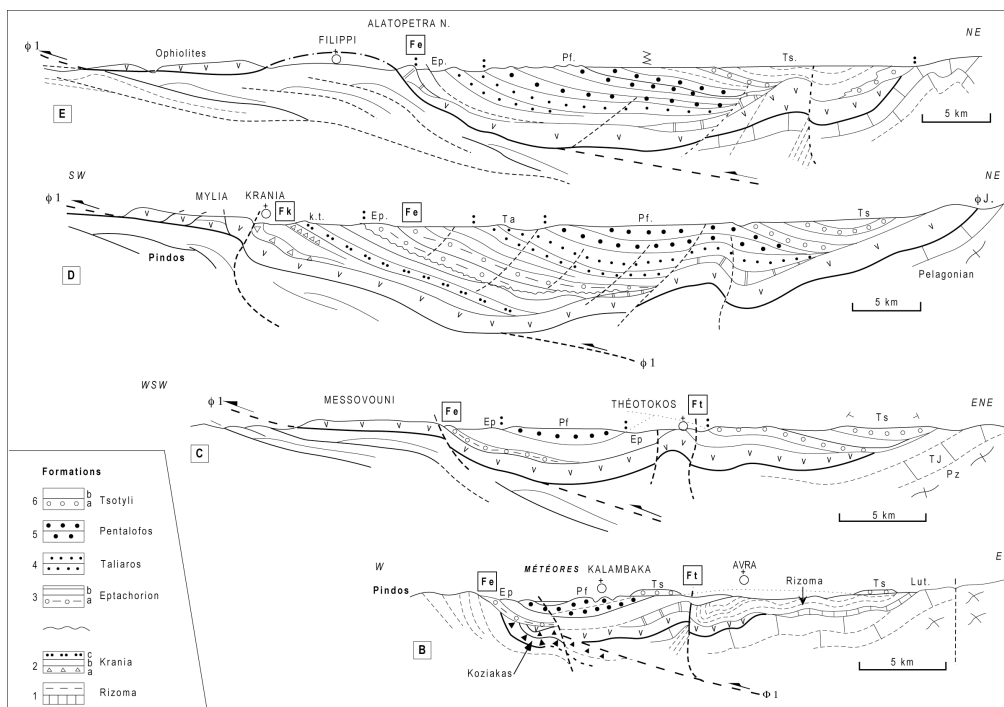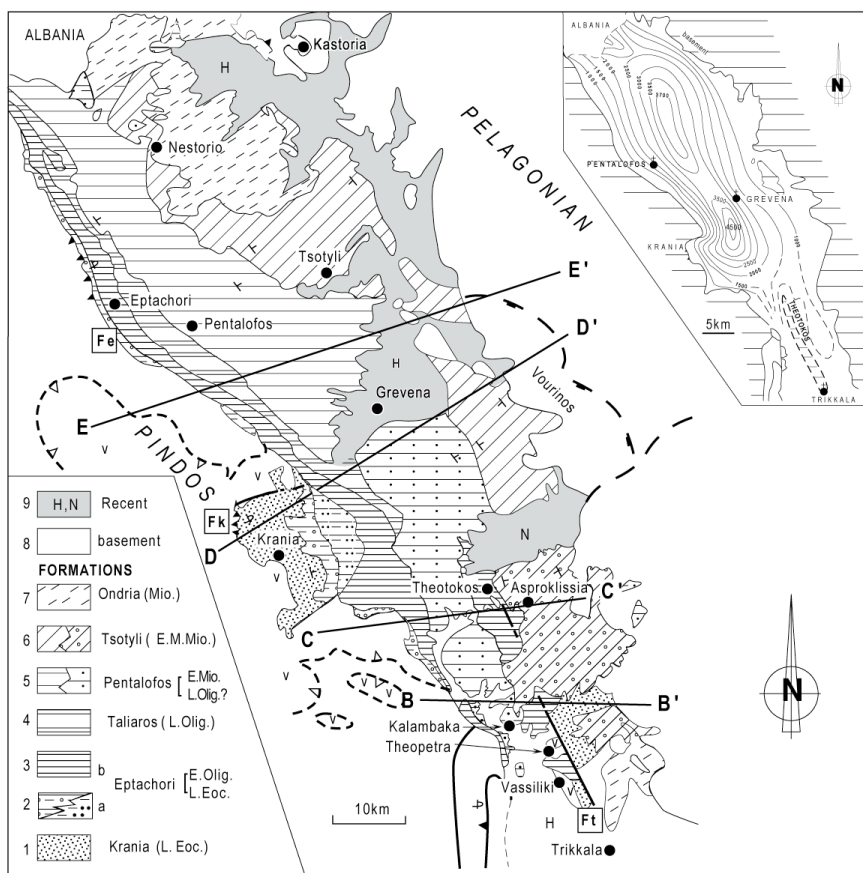
Fig. I. 2: (Top) Detailed map and (bottom) cross-sections of the MHB (Ferrière et al., 2004).

II. Previous work on the study area

The outcrops at the border of the Koziakas Mountains have never been studied beyond the need of geological mapping. Our fieldwork was devoted to the southern most ones, which have recently been expanded on new road cuts.

The study area, a hilly landscape with elevations ranging from 200 m to the east and 700 m to the west, is about 60 km^2. It is located at the western border of the Thessalian plain, about 10 km west of Karditsa and 20 km south of Trikala (Fig. I. 1 and Fig. I. 3). It encompasses an area bounded by Mitropoli and Morfovouni to the south, Fanari to the north, and centered on Kanalia, Livadhia and Aghios Akakios villages (Fig. I. 2 and Fig. I. 3). The cumulated thickness of outcroping deposits is about 1 km. To the west, these deposits rest above the folded, calcareous strata of the Koziakas (belonging to the external zones), or locally above lavas or radiolarites of the Koziakas or the Maliac zone (belonging to the internal zones).

Among the former descriptions of this area, Aubouin (1958) first identifies these outcrops and provides some lithologic information. Later, geological maps were published with some more details (Savoyat, 1969b; Jaeger, 1979; Lekkas, 1988; Karfakis, 1993) (Fig. I.4 and Fig. I.6). On the 1:50,000 map, Savoyat (1964) makes a difference between two lithologies: Oligocene limestones and siliciclastic facies (Fig. I. 4). Jaeger (1979) only provides a few more informations. Lekkas (1988) improves the mapping, adding one new lithologic formation (Fig. I. 5). The cross sections of Lekkas (1988) are unfortunately limited to very restricted areas (Fig. I. 6). This author adds some details on the facies of the Oligocene limestone. A slight angular unconformity is visible on the B cross-section to the south of Aghios Akakios but we could not evidence it again on the field.

The scarcity of good exposures may explain that only a few pieces of field works were undertaken until the 2000's. Then, a new EW tarmac road joining Mitropoli and Morfovouni was cut, revealing extended and meaningful outcrops of the southernmost deposits. Two more NS roads are still in construction, cross cutting most of the key outcrops. One joins the Mitropoli-Morfovouni road, and the other connects the Aghios Akakios village to this one.

III. Objectives and methods

A. Objectives

On the basis of these new outcrops, the objectives of this work are as following:

- Assess the facies stratigraphy and tectonics of the study area to build a depositional model of this part of the MHB;

- Discuss the processes controlling the basin evolution and associated base level changes;

- Extrapolate the stratigraphic model to the subsurface to propose a stratigraphic correlation with the northern part of the MHB.

B. Methods

To achieve these objectives, several field campaigns have been performed over 5 years (about 50 working days). They have been devoted to detailed geological mapping, sedimentologic descriptions and logging, and the assessment of the tectonic structures.

Due to the poor time resolution of available datations, we mapped lithologic units. We reasonably think that these units have a time-stratigraphic value (see Chapter II).

Detailed sedimentologic logs were drawn, aiming to gather the maximum information about the depositional settings. They consist in type-sections, which are correlated in distance to supplementary sections for assessing the 2D or 3D stratigraphic geometries.

The detailed clast lithology of coarse-grained siliciclastic deposits, as weel as paleocurrents as indicated by sedimentary structures, have been carefully documented to reconstruct the sources and routing paths of depositional systems.

The tectonic analysis was mainly based on the documentation of small-scale faults and their stratigraphic calendar. The main, block bounding faults (Fig. I. 3), did not provide much information.

The petrography of rock samples was determined at the laboratory based on thin section analysis. XRD anaylses were carried out on the clay mineral fraction of the finest-grained deposits but the results are not incuded here for they did not allow to raising stratigraphically discriminating categories. By contrast, some of those finest-grained deposits (silty marls) delivered nannofossils which were used for age determinations.

IV. Outline of the memoir

A. Contents

After this introduction (Chapter I), several parts will be presented, as following:

i) One main part (Chapter II) devoted to the sedimentology and stratigraphy of each of the three fault-bounded blocks (Fig. I. 3). More than 48 outcrops have been studied in detail (Fig. I. 7).

The Mitropoli block (UM, to the SW) is considered as the most comprehensive stratigraphic succession of the area. The Kanalia block (UK, to the center), and the Fanari block (UF, to the NE) comprise shorter successions. These blocks are bounded by the Livadhia (between UM and UK) and Kanalia faults (between UK and UF).

The three blocks comprise stratigraphic units that are first considered as specific to them, and identified from one dominant lithology: UM1 to UM7 in Mitropoli block, UK1 to UK3 in Kanalia block, and UF1 to UF4 in Fanari block.

The facies and stratigraphic successions within each block are interpreted in terms of depositional setting and sequence stratigraphy.

Finally, the stratigraphic correlation between the blocks is discussed, giving way to a more general assessment of basin evolution.

ii) A specific part devoted to the assessment of the most documented tectonic structures at various scales (Chapter III). These are mainly synsedimentary faults preserved within UM3, but some were originated after basin inversion. The observations were made in numerous localities (Fig. I. 8).

iii) A general overview and conclusion (Chapter IV) pointing to the conspicuous pattern of this basin fill. This allows to compare with the stratigraphic pattern of the main MHB to the north and to propose a basin scale correlation and evolution sketch. Last but not least, the main result of this work is to propose a new detail geologic map of the area (Fig. I. 9).

iv) Some addings are provided at the end of the memoir, after the reference list **(Annexe-I and -II)***.*

B. Figures

The figures are numbered by chapter (e.g. Fig. II.47 means the 47th figure of Chapter II). The studied outcrops are localized by numbers on maps (e.g. Fig. II.1). Detailed maps of specific sites are also provided in Chapter II for the three blocks. The sedimentologic logs are numbered as the related outcrops or sites. They comprise standardized information, such as:

- Grain-size: S: Silt, G: Gravel, P: Pebble, C: Cobble, B: Boulder. The S-G range corresponds to the sand grain-sizes: vf: very fine-, f: fine-, m: medium-, c: coarse-, vc: very coarse-grained;

- Thickness in meters;

- Capital letters pointing to the labels of photographs (which are displayed in another figure);

- Additional data pointing to specific samples (for nannofossil determinations).
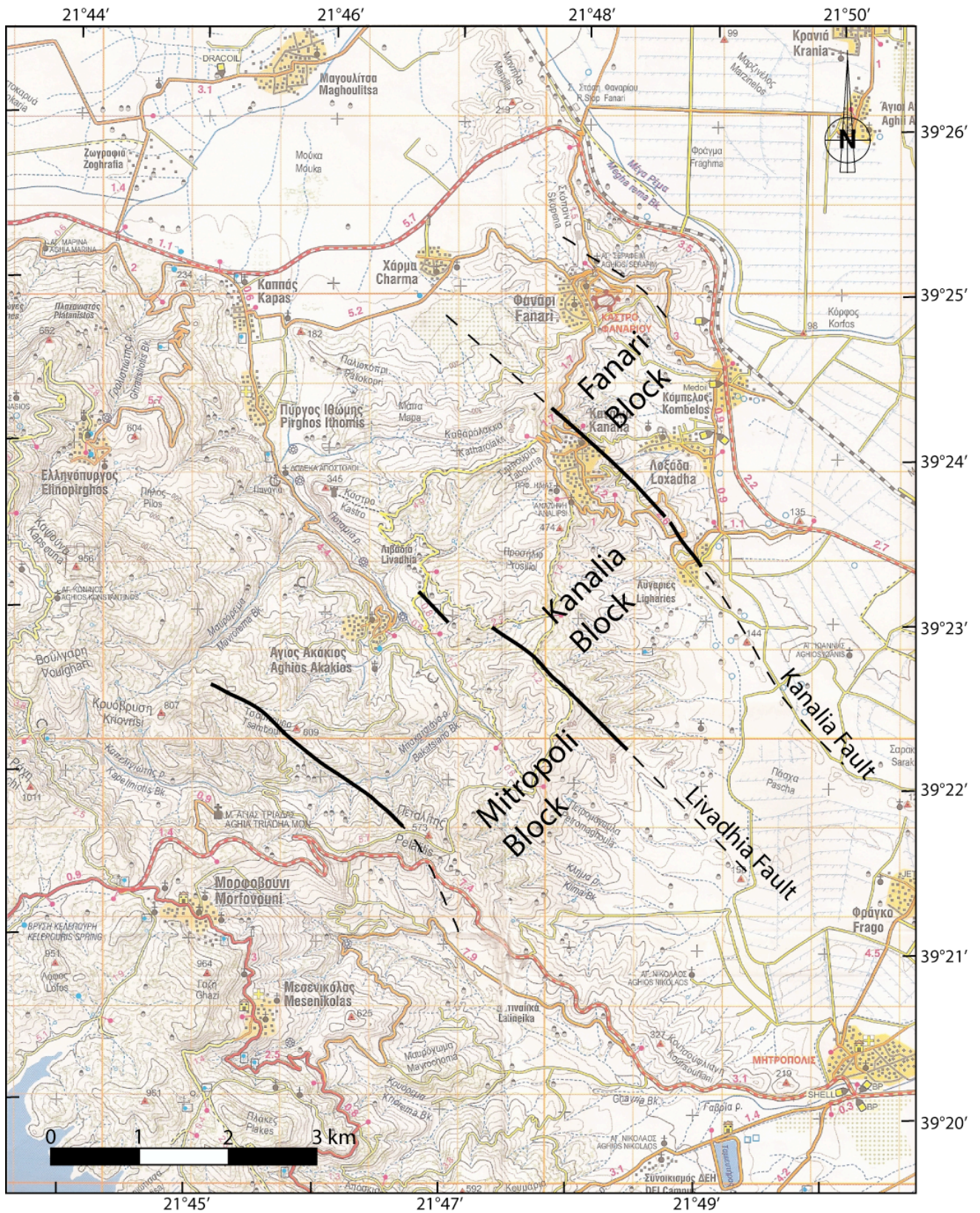
Fig. I. 3: Morphologic map with the roads of the Morfovouni-Mitropoli-Fanari area. Three blocks bounded by faults are outlined, each of whose has been studied separately for stratigraphy and tectonics (see Chapters II and III).

Fig. I. 4: Geological map and cross section (line A-A') of the study area (Savoyat, 1969b). Note that one of the main faults of Fig. I. 3, crossing Kanalia village to the north, was already reported by Savoyat. The added numbers point to the Pindos flysch (1 and 2), the Koziakas limestones (3), and the MHB deposits (5). Added white arrow indicates Oligocene limestone resting on the Koziakas Limestones.

Fig. I. 5: Geological map by Lekkas (1988). Added numbers indicate the three lithologic formations distinguished by this author: flysch (1), conglomerate (2), sandstone. However, in our work, we could not come to the same general architecture.
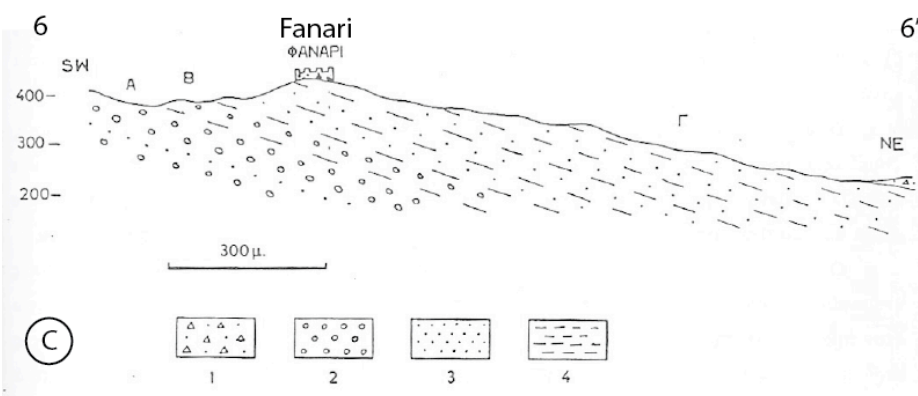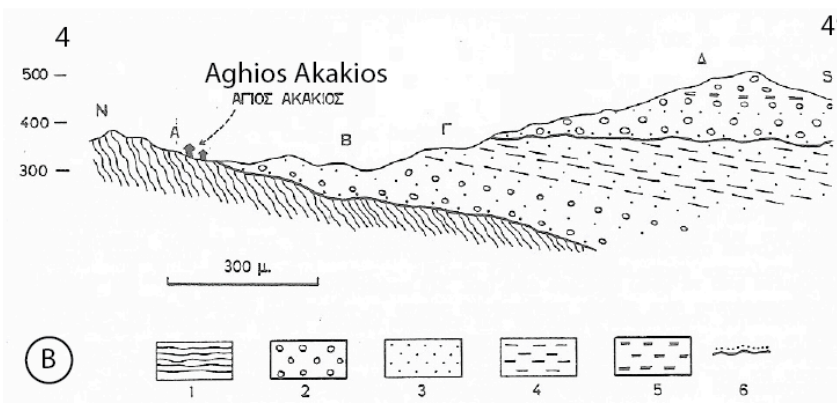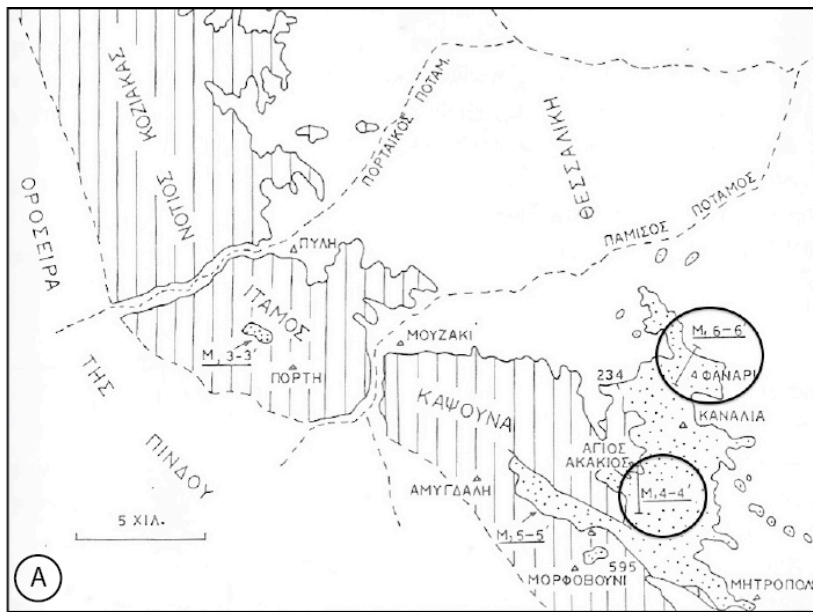
Fig. I. 6: Cross-sections (B) and (C) located on the map (A). From Lekkas (1988). For (B) 1- Koziakas basement, 2-Conglomerate, 3-Sandstone, 4-Sandstone and siltstone, 5-Siltstone and 6-Plio-Quaternary sediment. For (C) 1-Brecia conglomerate, 2- Conglomerate, 3-Sandstone, 4-Siltstone.

18
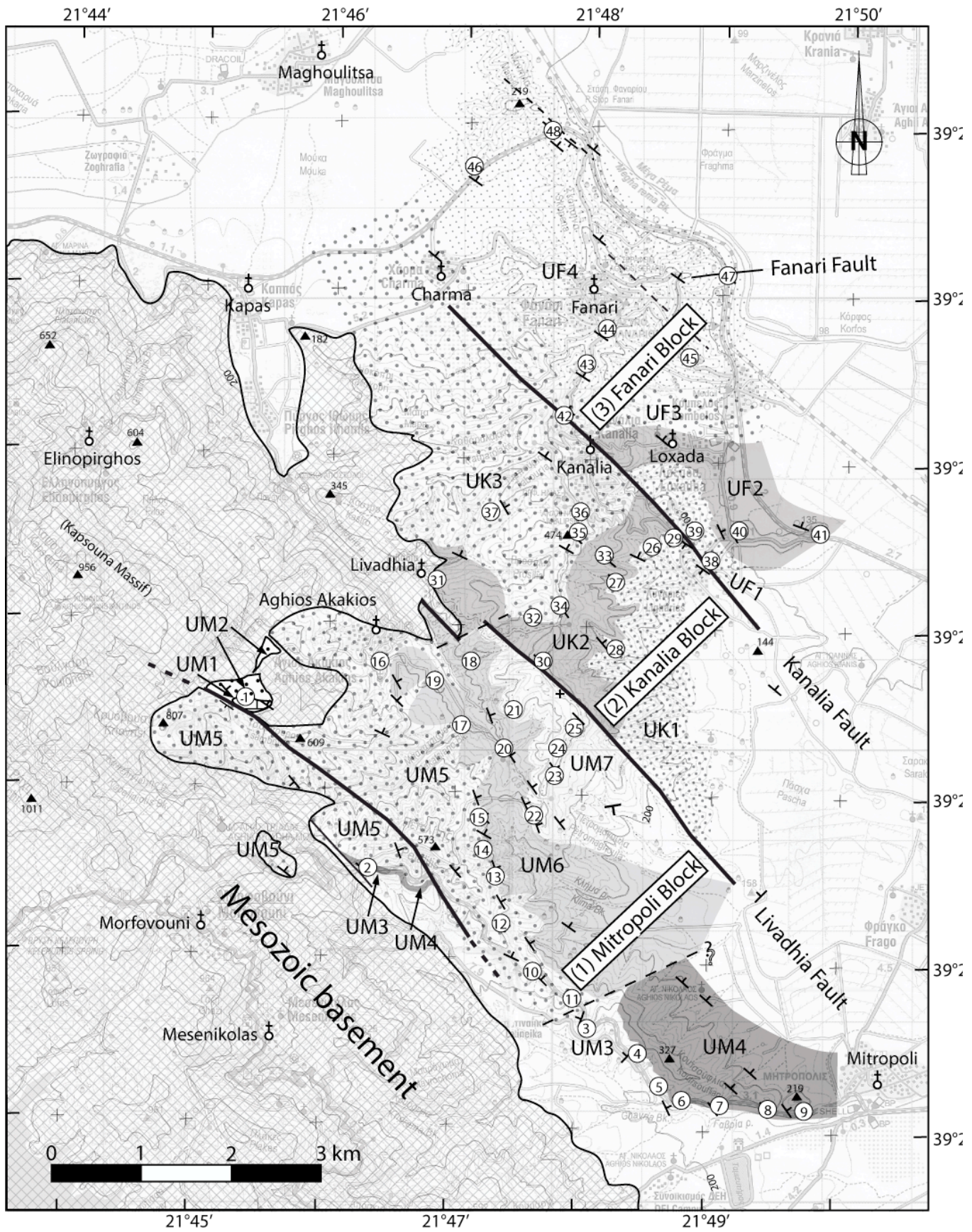
Fig. I. 7: Locality map of sedimentary site (1-48; Chapter II).
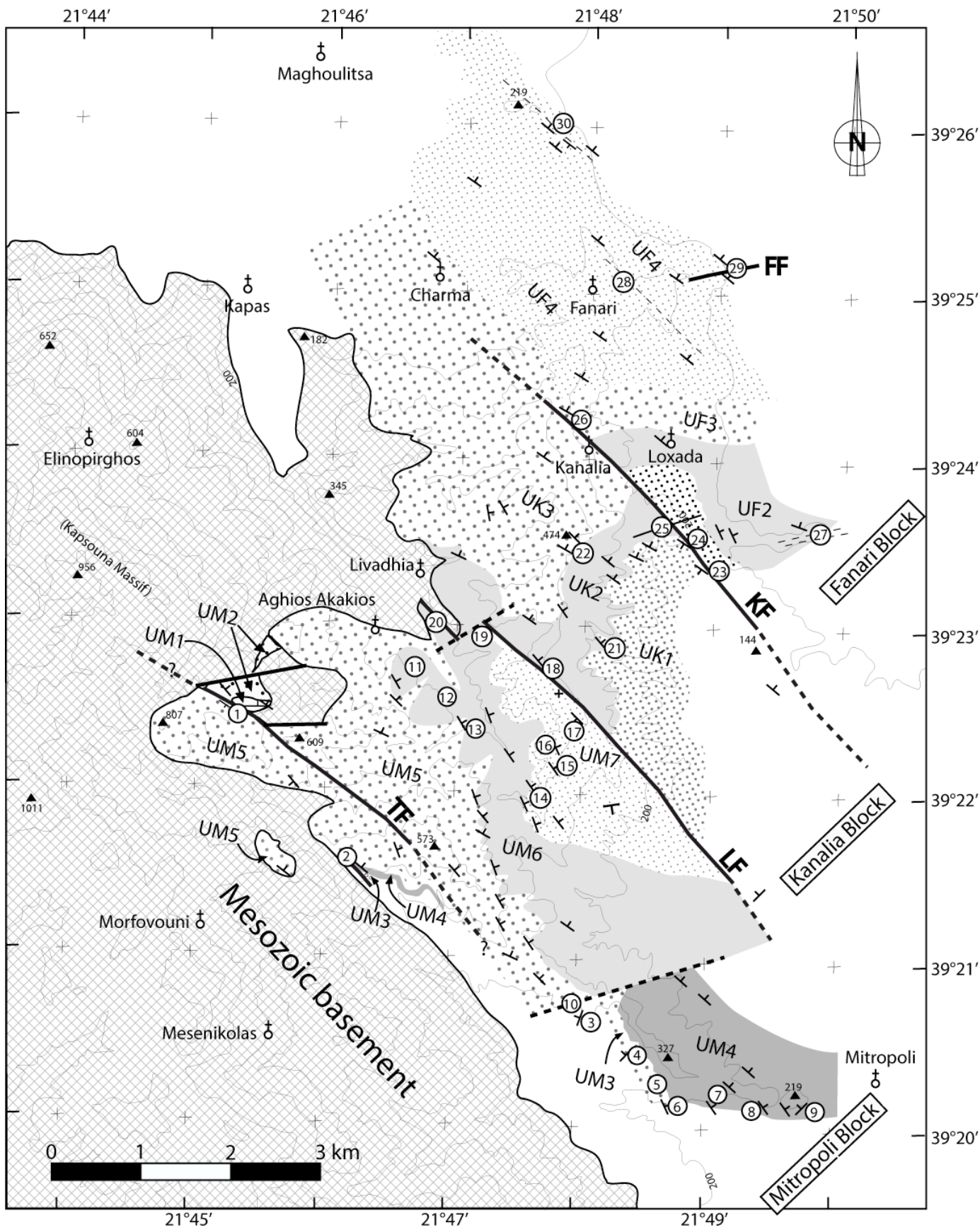
Fig. I. 8: Locality map of tectonic site (localities 1-30; Chapter III).
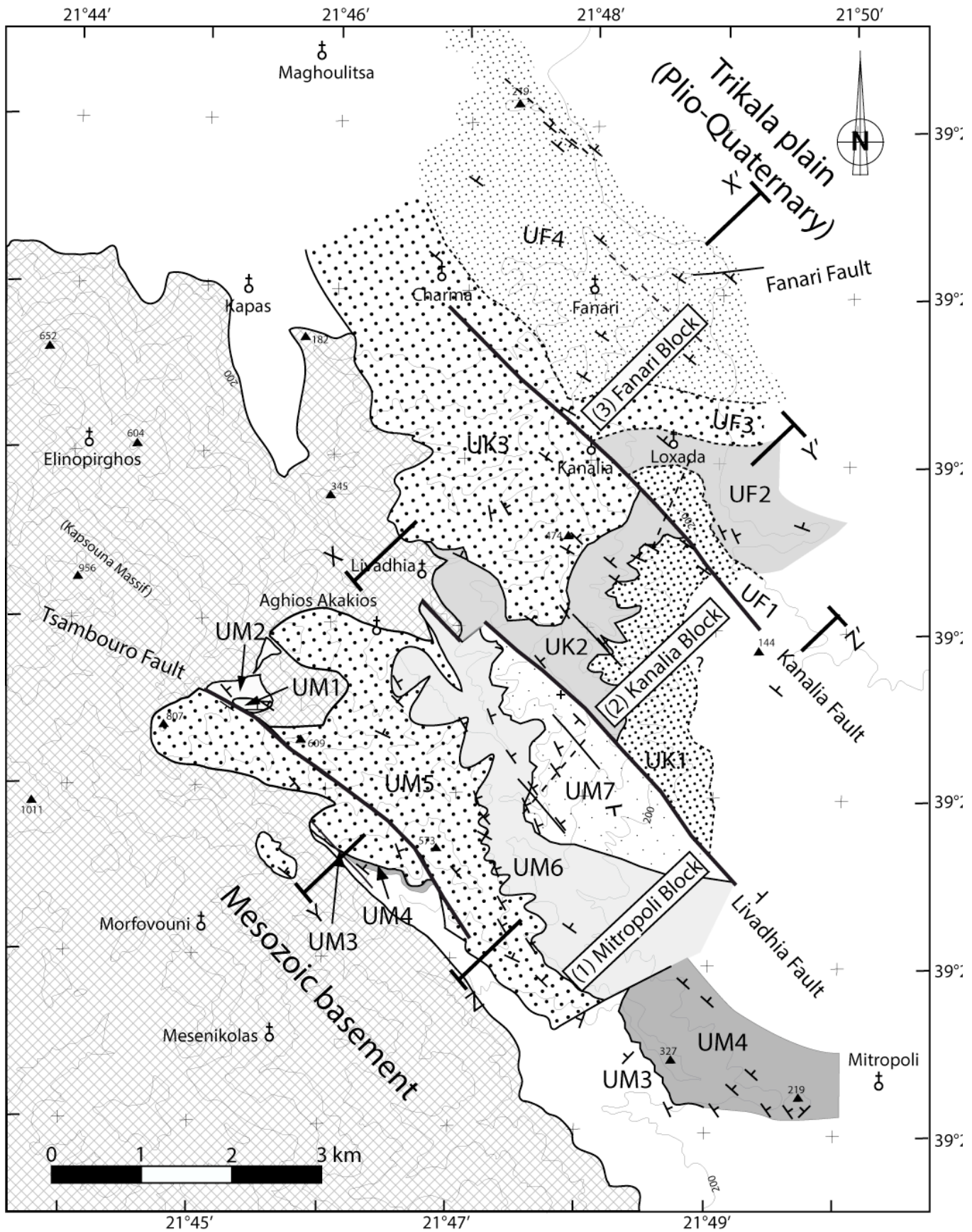
Fig. I. 9: A - Geological map of studied area (details see text Chapters II and III). B - (next page): Cross-sections of the study area with NE-SW direction (X-X', Y-Y' and Z-Z').
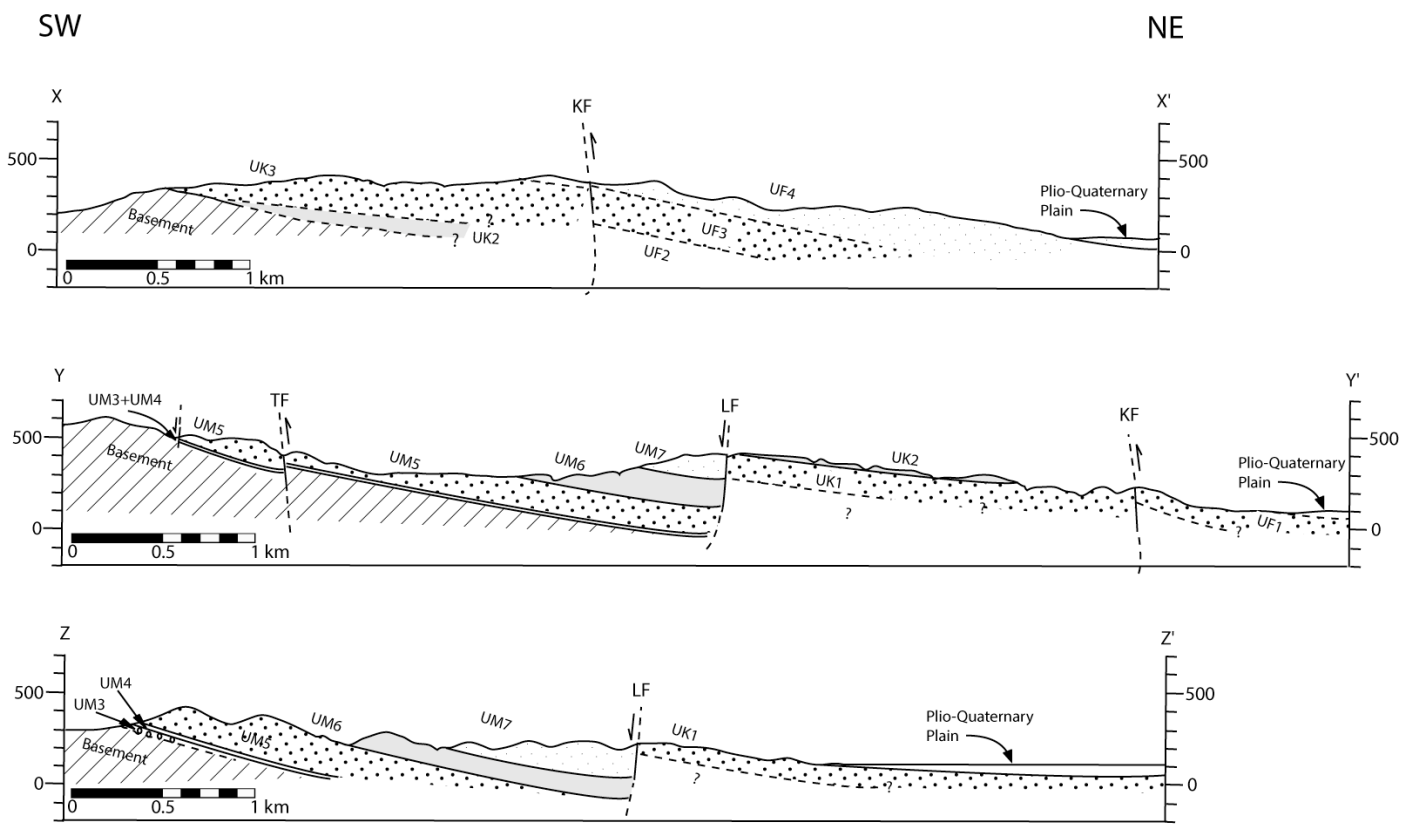
Fig. I. 9: B) - Cross-sections of the study area (X-X', Y-Y' and Z-Z', see Fig. I. 9A for locations)

CHAPTER II - Sedimentology and stratigraphy

This chapter presents the results of the sedimentology and stratigraphy of the studied outcrops. The results are presented block by block and unit by unit. The interpretations are presented at the end of each unit and consist of the primary facies and depositional setting assessment of the units.

The references in sedimentology and sequence stratigraphy supporting our conclusion are basics of fluvial sedimentology as regarding to the processes and deposits of alluvial fans and braided conglomerate-rich rivers (Collinson, 1996) and the classical rationale of sequence stratigraphy (Posamentier et al., 1988) as regarding to the definition of systems tracts. A more detailed attention was paid to submarine deposits because they represent most of those observed in the basin. The synthesis of Shanmugam (2000) on gravity deposits was used as to understand the facies tracts related to the transformation of coarse grained submarine gravity flows (Mutti, 1979). The Mutti model was not used because we did not find enough detail to document all the facies but we retained the idea of a seaward transition between matrix-supported conglomerates (proximal debris flows) toward coarse grained turbidites with erosion scour and gravel, « traction-carpet » bases (Lowe, 1982 sequences), and then finally the « classical » sandy turbidites of Bouma (1962) or interbedded sheet-like turbidites and hemipelagites (Stow & Shanmugam, 1980). The related grain-support processes were taken from Mulder and Alexander (2001), namely the reference to flow density. We also used the Stow et al. (1996) synthesis to conceive our facies model as within a « slope fan » large-scale geometry and especially the reference to the early Normark (1970) model to relate the sandy channel-and-lobe facies to a distal turbiditic system.

V. Mitropoli-block

Mitropoli-block is located in the southwesternmost part of the studied area, around Mitropoli and Aghios Akakios villages (Fig. II. 1). The deposits rest unconformably by way of an onlap surface on the Mesozoic basement to the south and to the west. The Mitropoli-block is bounded to the north by the Livadhia fault. The total thickness of the type section in this block is about 600 m.

It has been divided into 7 stratigraphic units. Each unit is described from the lower (UM1) to the uppermost unit (UM7; Fig. II. 2).
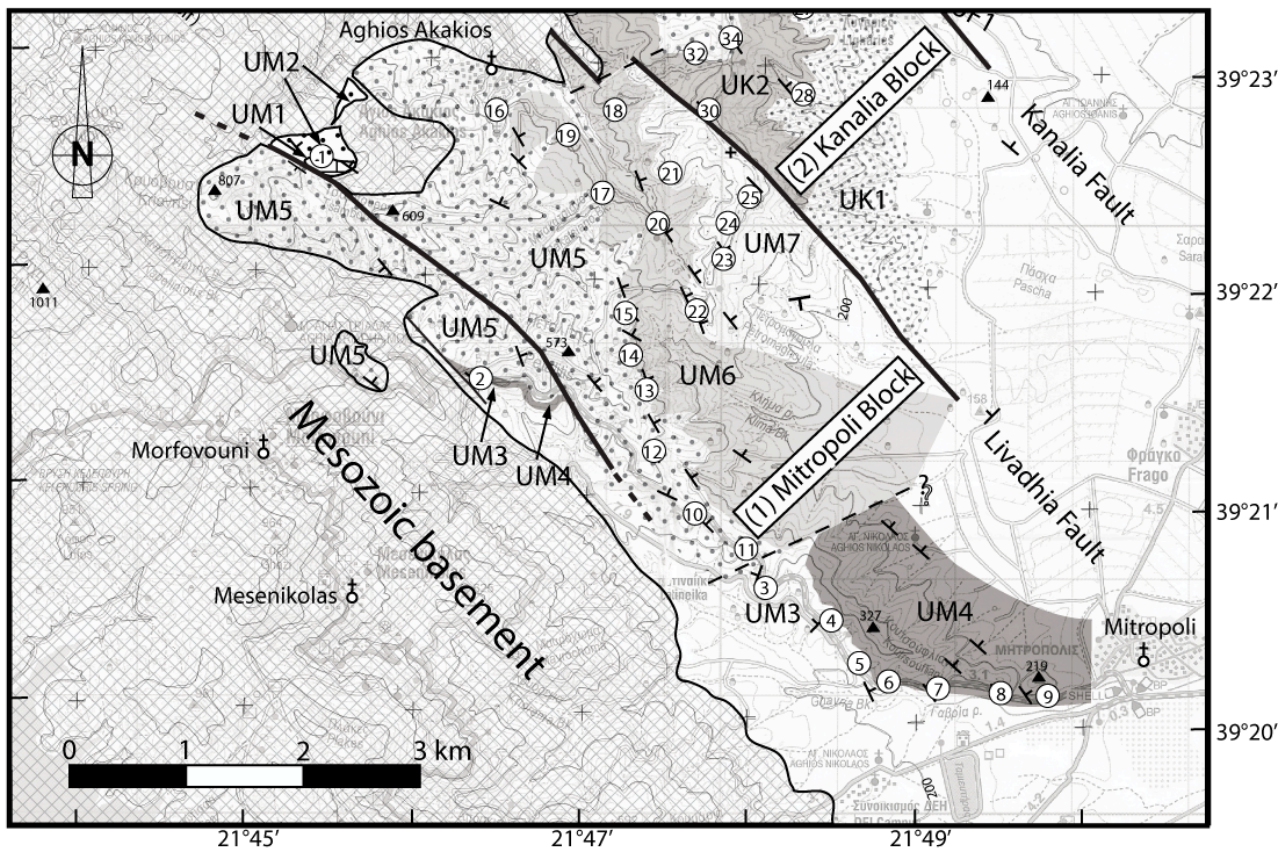
Fig. II. 1: Location of the UM1 to UM7 outcrops (localities 1 to 25).
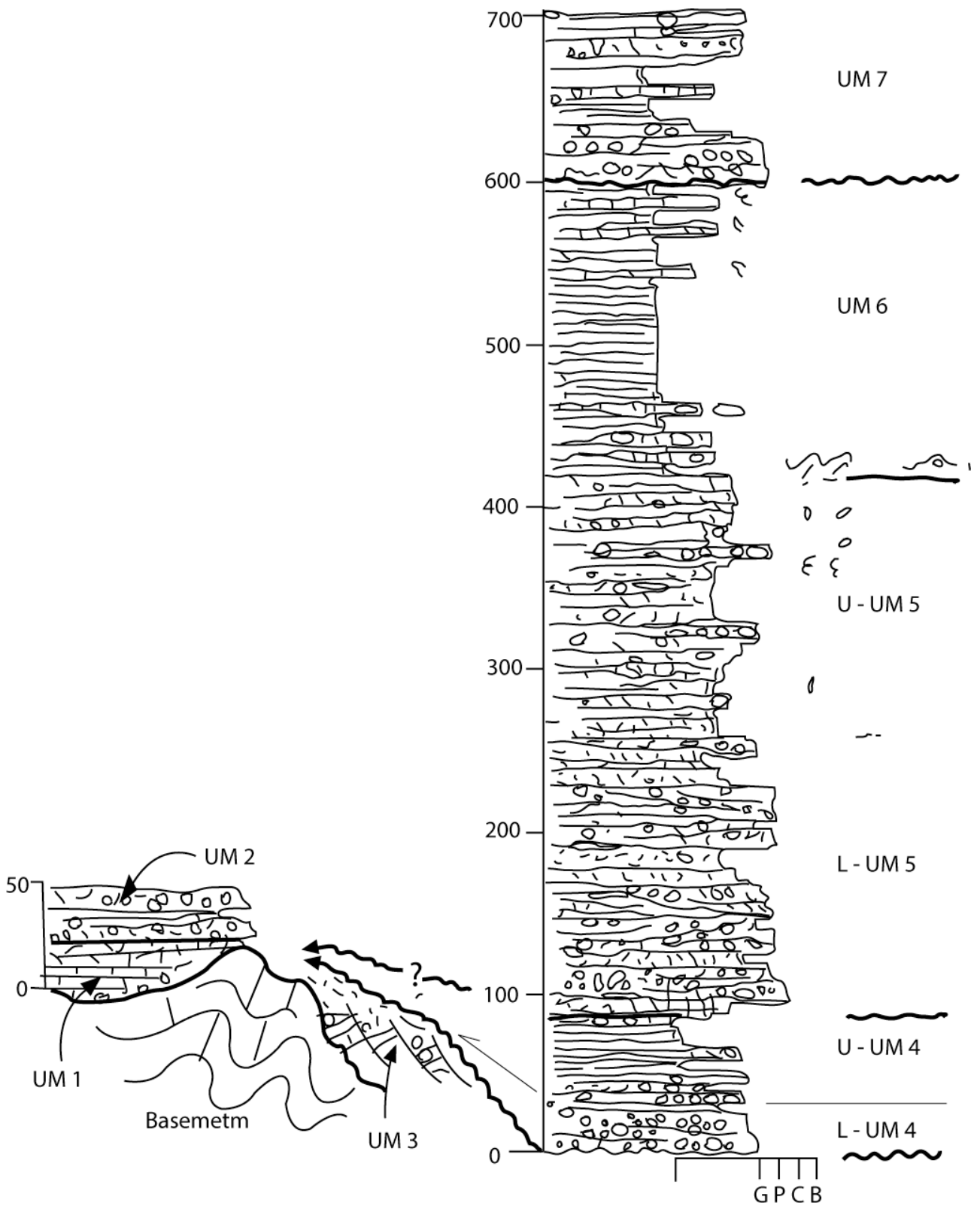
Fig. II. 2: Sedimentary log of Mitropoli block (UM1 to UM7).

A. Unit M1 (UM1): Oligocene limestone

A basal limestone unit in the studied area was first evidenced by Savoyat (1969b) who described it as an organogenic limestone 10-20 m thick. It was attributed to Aquitanian-Burdigalian owing to the presence of *Spiroclypeus sp.* associated with red algae, Bryozoaires, Echinoderms and miliolidae. Later, Jaeger (1979) attributed this limestone to the Late Oligocene from the occurrence of *Heterostegina sp.*, *Operculina sp.*, *Asterigerina sp.*, *Nephrolepidina sp.* and *Amphystegina sp.* Lekkas (1988) confirmed this Late Oligocene age based on the occurrence of *Eulepidina dilatata* MICHELOTTI, *Nephrolepidina sp.*, *Lepidocyclina sp.* and *Nummulites sp.*

UM1 is exposed in locality-1 (Fig. II. 1 and Fig. II. 3) only at the westernmost part of Mitropoli-block, about 1.5 km southwestward from Aghios Akakios and 3 km northward from Morfovouni village. It crops out in sections 1a to 1c, where section-1a is the type section. Sections-1c and -1d also shows the overlying conglomerates of UM2. UM1 is the only limestone deposit in the studied region. It likely corresponds to the initiation of sedimentation in the southern termination of the MHB.
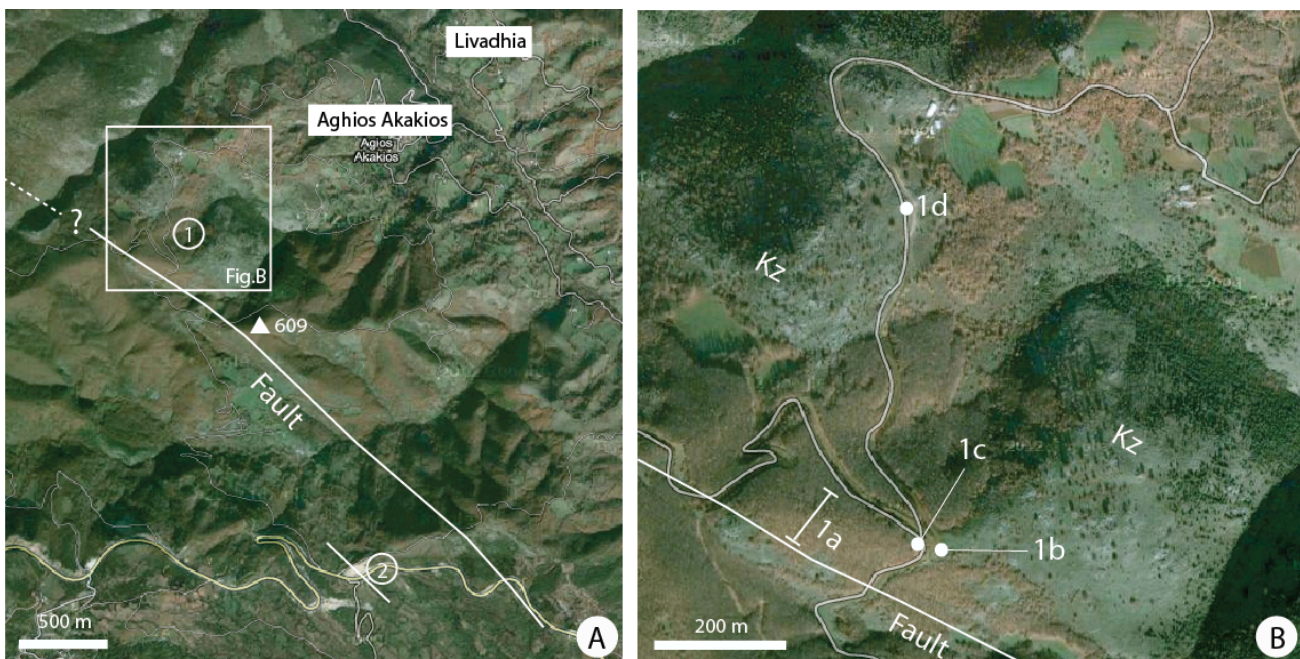
Fig. II. 3: Map of locality-1, satellite Google image. A) Locality-1, in a square, is located at the northern side of hill-609 and southwestward from Aghios Akakios village. B) Zoom showing the precise locations of sections-1a to -1d. (Kz = Koziakas Mesozoic basement).

1. Lower UM1: the thick-bedded limestones

a) Type section: section-1a

Section-1a (Fig. II. 4, log-1a) is dominated by a massive, pale grey limestone, approximately 20 m thick. It forms a small hill culminating at elevation 620 m asl (Fig. II. 3 for location). The lower boundary is not exposed in section-1a (for this, see log-1b, Fig. II. 4).
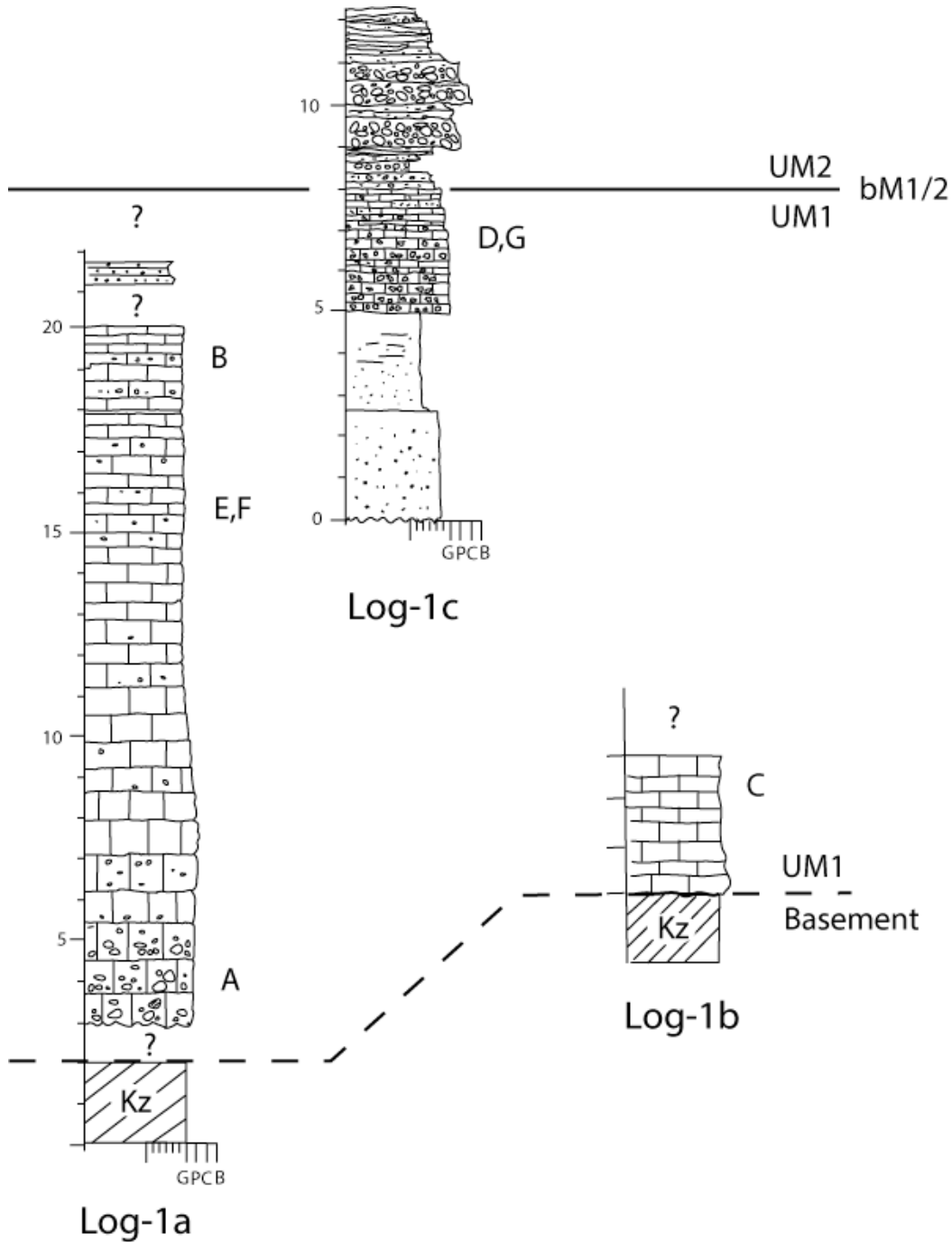
Fig. II. 4: (UM1) Sedimentary log-1a (A), log-1b (B) and log-1c (C). A to G: see Fig. II. 5.

The basal part of section-1a consists of a 1-3 m thick clast-supported limestone conglomerate (Fig. II. 4, log-1a). Conglomerate ranges from gravel to cobble size (maximum clast size is up to 10x20 cm) and are sub-angular to sub-rounded and poorly sorted.

Clasts are composed of limestone 90%, igneous 5% and radiolarites 5% clasts. Fossils consist of *Nephrolepidina sp., Lepidocyclina sp., Heterostegina sp., Asterigerina sp., Amphistegines sp., Rotalidae* (D. Vachard and C. Baumgartner determining) (Fig. II. 5).
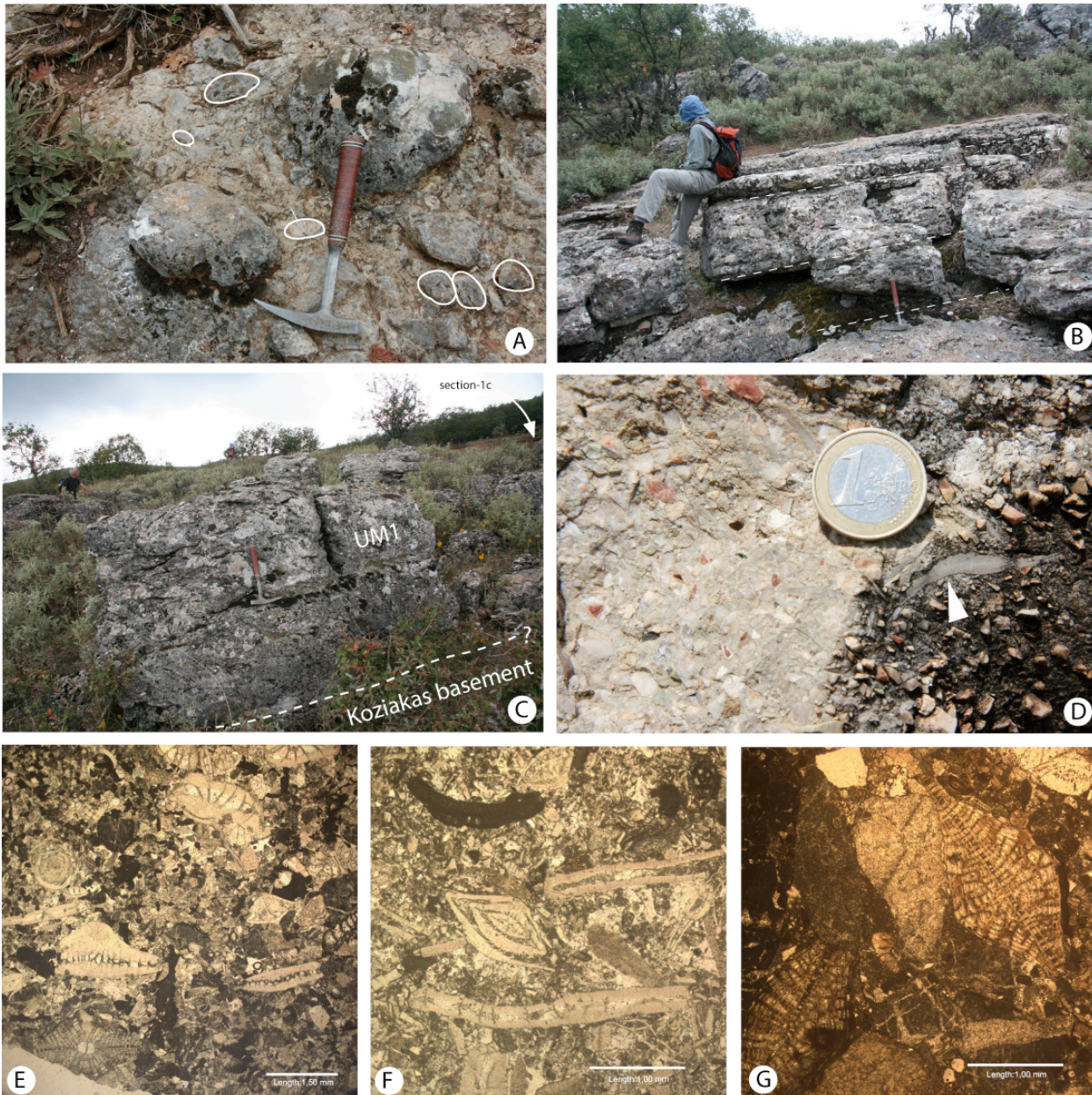
Fig. II. 5: Facies of the limestones (UM1). A) Gravel to cobble conglomerate at the base of section-1a. B) At the top of section-1a, limestone is moderately bedded. C) Section-1b: bioclastic limestone resting directly on the Koziakas Mesozoic basement. D) Section-1c: brechic limestone above the sandstones with Foraminifera. E) to G) Thin sections of facies showing benthic foraminifera (*Nephrolepidina sp., Lepidocyclina sp., Amphistegina sp., Rotalidae*).

28

The lowermost layers are predominantly composed by limestone clats, likely sourced from the underlying calcareous Koziakas basement. Conglomerate clasts are decreasing in abundance and fining upward the succession. However, some gravel clasts are present up to the top where beds are thinner and well bedded (Fig. II. 5B). Thin sections of 5 rock samples have been analyzed to document the texture of the limestone forming the matrix of the conglomerate. The facies is a micrite (Folk, 1959) or a grainstone-to-packstone (Dunham, 1962).

b) <u>Basal contact of UM1: Section-1b</u>

Section-1b is located at about 200 m eastward from section-1a, close to the main track and to the section-1c (Fig. II. 3 for location). It exhibits an about 3-5 m thick limestone, which rests directly on the Koziakas Mesozoic basement (Fig. II. 4, log-1b). In the field, it is difficult to distinguish UM1 limestone from the basement because they are of the same kind of lithology. However, UM1 can be evidenced by the presence of large foraminifera fossils such as *Nephrolepidina sp., Lepidocyclina sp., Amphistegina sp., Rotalidae.*

2. The upper part of UM1: the first terrigenous beds

a) <u>Type section: section-1a</u>

A few meters of fining-upward sandstone lay on the massive, Foraminifera-rich limestones, with the same dip of strata, in a top of section-1a (Fig. II. 4). The upper bed of limestone is a homogeneous conglomerate dominated by carbonates both in the matrix and elements. The contact with the overlying sandstone is not clearly exposed but no strata dip change can be seen across it.

The section-1c is a better outcrop (Fig. II. 4), with the same kind of sedimentary beds than in the section-1a, but the basal contact is not well exposed.

b) <u>Additional section: section-1c</u>

This outcrop is located on the western flank of the main track, situated at about 30m westward from section-1b (Fig. II. 3, 1c for location). As it looks like the upper part of log-1a, this succession is attributed to the upper part of the main bioclastic limestone.

The basal part is made of weathered pale brown, coarse-grained sandstones and siltstones (5 m thick) (Fig. II. 4, log-1c). They are covered by a 3 m thick conglomeratic

limestone with abundant bivalves, lepidocyclines and unidentified fossils. The contact between this limestone bed and the underlying sandstone siltstone is sharp. Clasts range from very angular to sub angular, gravel sized. Clast components consist of chert, green rocks, quartz and limestone. The source seems to be the close basement (Koziakas and/or Maliac series). This calcareous bed is covered by huge conglomeratic gneiss-rich conglomerates owing to UM2, the pebbles of which come from an area far to the east (Pelagonian basement series).

3. UM1: Interpretation

The UM1 limestones of the studied area are the first transgressive sediments on the local basement (Koziakas and maybe Maliac series). The lowermost, conglomeratic beds (sections-1a, -1b and -1c), are interpreted as intraformational conglomerates formed by wave ravinement at the early stages of development of the carbonate shelf. The overlying packstones (section-1a) correspond to the later development of the shelf, in slightly deeper waters. They are dominated by benthic heterozoan species (large Foraminifera), keeping well pace with some terrigenous supply. From time to time, the nearby coastal topography still supplies conglomeratic lenses to the basin (a top of section-1a, at the contact with the terrigenous beds). An abrupt change shuts down the carbonate production, which is replaced by a siliciclastic, high energy setting (the next UM2 conglomerate). The first terrigenous deposits, which are also the finest-grained, announce either a tectonic event in the hinterland or a significant base-level fall. The first hypothesis is supported by the fact that the source of the conglomerates is no longer the nearby Koziakas but the Pelagonian basement, to the east of the basin (beginning of UM2 unit).

B. Unit M2 (UM2): gravel to pebble gneissic-rich conglomerate

UM2 is exposed at the western part of Mitropoli-block where it overlies conformably UM1 (Fig. II. 1 and Fig. II. 3, locality-1). It crops out along the main track and in the surrounding area (Fig. II. 3, sections-1c and -1d). UM2, at least about 20 m thick, is dominated by matrix-supported, pebble conglomerate and interbedded sandstone. It either rests directly on the basement or overlies conformably the bioclastic limestone of UM1. Two successions (sections-1c and -1d) are described below. The upper boundary of UM2 is not exposed.

1. Section-1c: the stratigraphic contact between UM2 and UM1

The contact between UM1 and UM2 is defined as the base of the conglomerate bed at 9 m in section-1c (Fig. II. 4, log-1c; and Fig. II. 6). Above this surface, the deposit is dominated by gneiss-rich conglomerates.
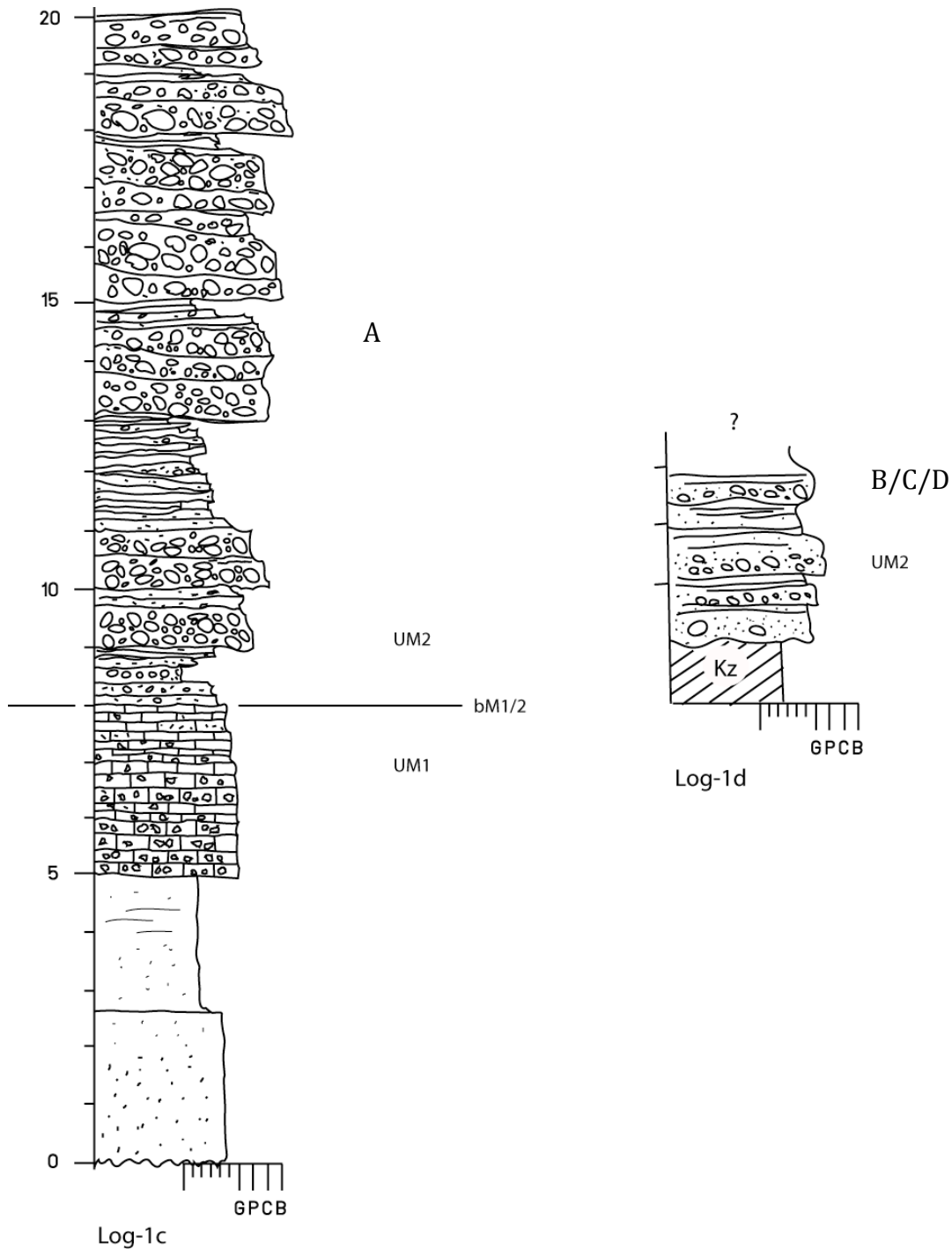
Fig. II. 6: UM2, Log-1c and log-1d (location Fig. II. 3). A to D see Fig. II. 7.

UM2 at section-1c consists in a roughly bedded, dominantly clast supported conglomerate, interbedded with meter thick intervals of planar bedded to low angle oblique beds of medium-grained sandstones. The beds in the conglomerate and the sandstone form an overall conformable succession of strata dipping 10-20° to the NE.

The conglomerate beds, dominantly clast-supported, have a lens shape over ten of meters in lateral extent and sharp, locally erosional bases. They are about 0.2-1 m thick. They are grouped into slightly thinning- and fining-up successions, 2-3m thick each, passing upwards to the sandstone. The clasts in the conglomerates are composed of white marbles and easily recognized gneiss sized up to 20 cm. In some beds, they are tightly imbricated, with their great axis vertical, indicating a shear towards the SW.

2. Section-1d: UM2 unit on the Koziakas basement

About 500 m from section-1b, going northward along the track, section-1d is exposed at the western side of the track (locality-1d in Fig. II. 3). The base of measured section is an erosional, angular unconformity above the basement. This unconformity dips to the east at a higher angle than the overlying strata, which form therefore an apparent onlap to the west (Fig. II. 7B).

The succession is at least 5 m thick and it consists of conglomerates and sandstones, which rest directly on the Koziakas Mesozoic basement (Fig. II. 6, log-1d and Fig. II. 7B, C and D). As in the type section-1c, the succession shows conglomerates and sandstones. Minor sandstone beds are medium to coarse grained with planar cross bedding.

Conglomerates dominate. They are massive, moderately to poorly sorted, matrix- or clast- supported. Clasts consist of limestone, ophiolitic rocks, red chert and gneiss. They commonly range from gravel to pebble size. The maximum size of the clasts about 20x40 cm are made of sub angular to sub rounded, limestone corresponding to the close Koziakas basement (Fig. II. 7C and D). Clast imbrications, in general, indicate a SW-direction, however it varies from S to W. This section confirms that this UM2 conglomerate deposit onlaps from the east to the west on the Koziakas Mesozoic basement.
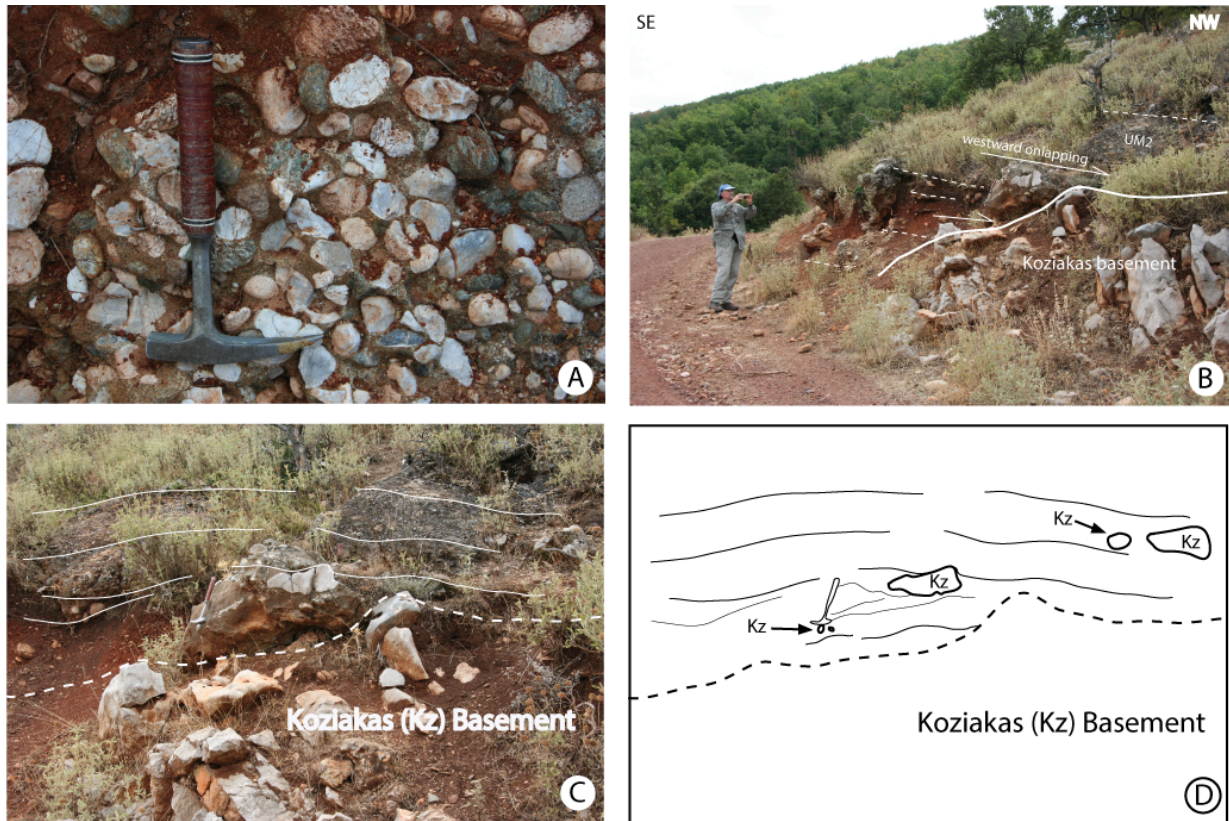
Fig. II. 7: Facies of the UM2 conglomerates. A) View of conglomerates (log-1c, Fig. II. 6). B) to D) outcrop of log-1d, Fig. II. 6). Transgressive contact is well exposed.

3. UM2: Interpretation and conclusion

Even in the lack of paleontological data, it is obvious that the UM2 conglomerates are younger than the underlying UM1 limestones above, which they rest sub-conformably at the scale of our observations. Their polygenetic composition suggests that they were supplied by a large catchment area, including the Pelagonian continent to the east. Their clast-supported nature shows the dominant control of tractive processes. The abrupt sandy interbeds suggest either a pulsed regime of deposition and/or the occurrence of a concentrated suspension load as well. The lens-shaped beds with erosional bases also point to thin, amalgamated channel forms which are constistent with thin flows. As a consequence, the UM2 conglomerates are interpreted as energetic river deposits, possibly at the transition between alluvial fans and braided plain. The imbrications indicate a paleocurrent to the SW, which is consisting with the main Pelagonian source to the NE. As hypothesized in the interpretation of UM1, the UM1-UM2 transition would thus correspond to a significant base-level fall of several tens of meters in this area (from a carbonate shelf to a proximal alluvial setting).

C. Unit M3 (UM3): Conglomerates with syn-sedimentary normal faults

UM3 is well characterized by reddish, poorly sorted, clast- and matrix- supported, pebble- to cobble-conglomerates interbedded with sandstones and pale brown, grey or reddish siltstones. The conspicuous feature of UM3 is the occurrence of well-exposed, syn-sedimentary normal faults.

Outcrops of UM3 are exposed along the Mitropoli-Morfovouni road, at the southern part of Mitropoli-block (Fig. I. 7, localities 2 to 6). There, UM3 deposits locally rest on the Koziakas-Maliac basement and their thickness is at least 25 m (Fig. II. 1, locality-4 and -5). The upper boundary of UM3 is marked by a sharp erosional surface and capped by conglomerate or siltstone package of UM4. We describe exposures of UM3 from the western to the eastern localities. The proposed type-section of UM3 is at locality-2.

1. Western outcrops: Type-section of UM3 deposits (section-2)

An excellent road-outcrop, section-2, is located at about 2 km from Morfovouni village, on the Morfovouni-Mitropoli road (Fig. II. 3A, locality-2). It laterally extends up to 500 m along the road, subparallel to the strike direction but the lower boundary of UM3 is not exposed in locality-2 (Fig. II. 8).

The characteristic conglomerates of UM3 are well observed at section 2b (Fig. II. 8 and Fig. II. 9).

Fig. II. 8: UM3, panorama relative to section-2, with location of log-2b and-2c.
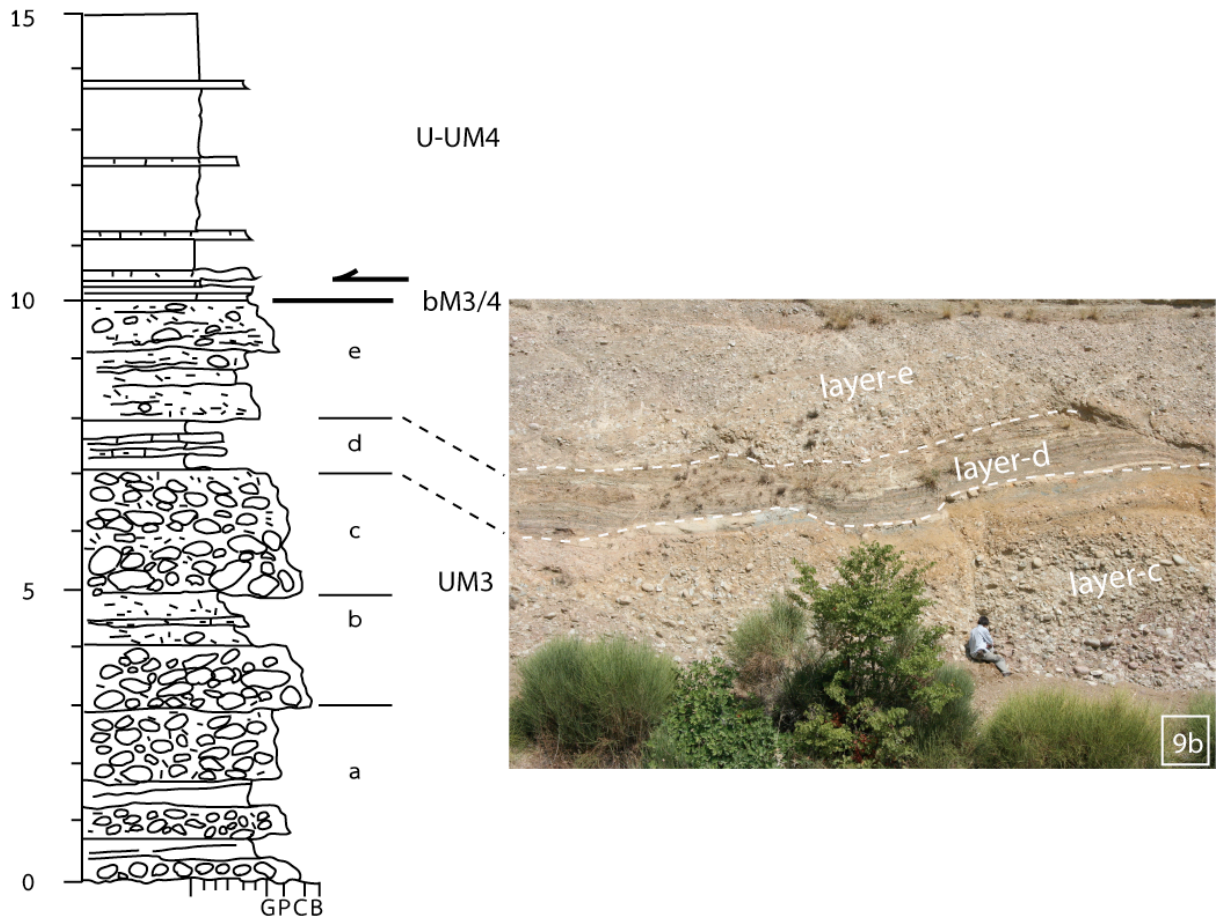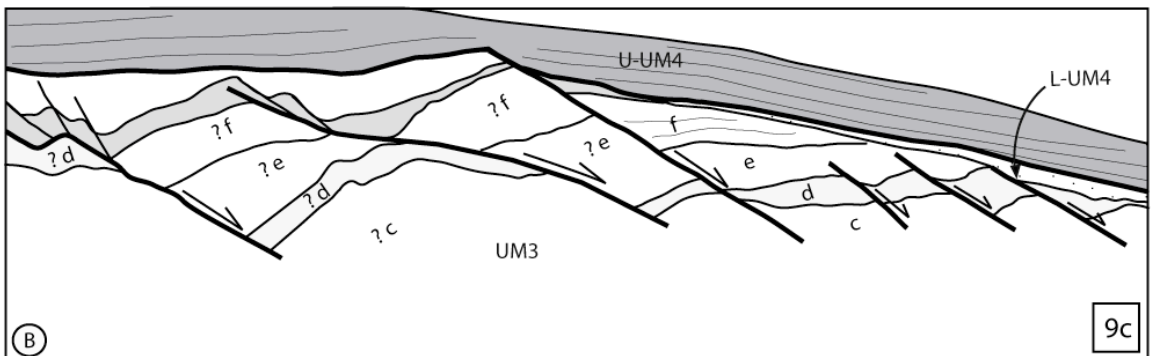
Fig. II. 9: a- Log of section-2b (UM3); b- Detail of sediments between two faults; c- Outcrops of UM3 with syn-sedimentary normal faults (A, panorama view and B, line drawing of A).

Layer-a is an about 3 m thick massive, poorly sorted, matrix-supported, gravel- to pebble-conglomerate forming the base of log-2b. The conglomerate is interbedded with reddish, gravel-bearing sandstone intervals. The sandstone beds are thin- to medium-bedded with tiny trough cross beds.

Layer-b rests with an erosional surface above the underlying layer-a. It commences by 1 m thick of massive, structureless, poorly-sorted, clast-supported conglomerates. Clasts range from sub-angular to sub-rounded, moderate- to low-sphericity, and pebble- to boulder-size. Clast components consist of gneiss, limestone, ophiolite, quartz and red chert. This conglomerate bed grades upward into 1 m thick reddish, gravelly coarse-grained sandstone punctuated by gravel layers.

Layer-c rests above layer-b by way of an apparently conformable but sharp surface. It is characterized by a westward thickening, from 1 to 4 m thick (cf. Fig. II. 9). It is composed of a massive, structureless, moderately- to poorly-sorted, clast- and matrix-supported, and pebble- to cobble-conglomerate.

Layer-d is a fine-grained layer. It sharply overlies conformably layer-c. It is a good marker bed about 1 m thick, with pale brown to pale grey siltstones interbedded with very thin- to thin-bedded, medium-grained sandstone (Fig. II. 9). The upper contact is an erosional surface at the base of layer-e or UM4.

Layer-e is a medium-grained conglomerate, which is preserved in the lows of the erosion surface truncating the layer-d. Its upper boundary is a sharp erosion surface at the bottom of UM4. As a consequence, the UM4 deposits rest unconformably on layers-e or -d.

Well-exposed syn-sedimentary normal faults occur through UM3 in section-2 (Fig. II. 8 and Fig. II. 9C). Tilting of sedimentary strata of UM3 to the west and thickness variations into triangular wedges can be found within the UM3 unit as a result of these normal faults.

2. UM3: Eastern outcrops (section-3 to -6)

Along the eastern part of the Mitropoli-Morfovouni road, close to Mitropoli village, outcrops of reddish conglomerates interbedded with sandstones and siltstones show normal faults, as in the western area. At least 4 outcrops (section-3 to -6, Fig. II. 1 and Fig. II. 10) have been observed.

a) <u>Type-section: Section-3</u>

At about 3 km, west from Mitropoli village, section-3 is well exposed at the northern side of the road (Fig. II. 1, locality-3). The outcrop can be followed up to more than 50 m. Sedimentary strata are dipping to the SW as a result of the normal faults. Syn-sedimentary faults are also well observed here. The succession is composed of reddish conglomerates interbedded with few sandstones and siltstones (Fig. II. 10, log-3).
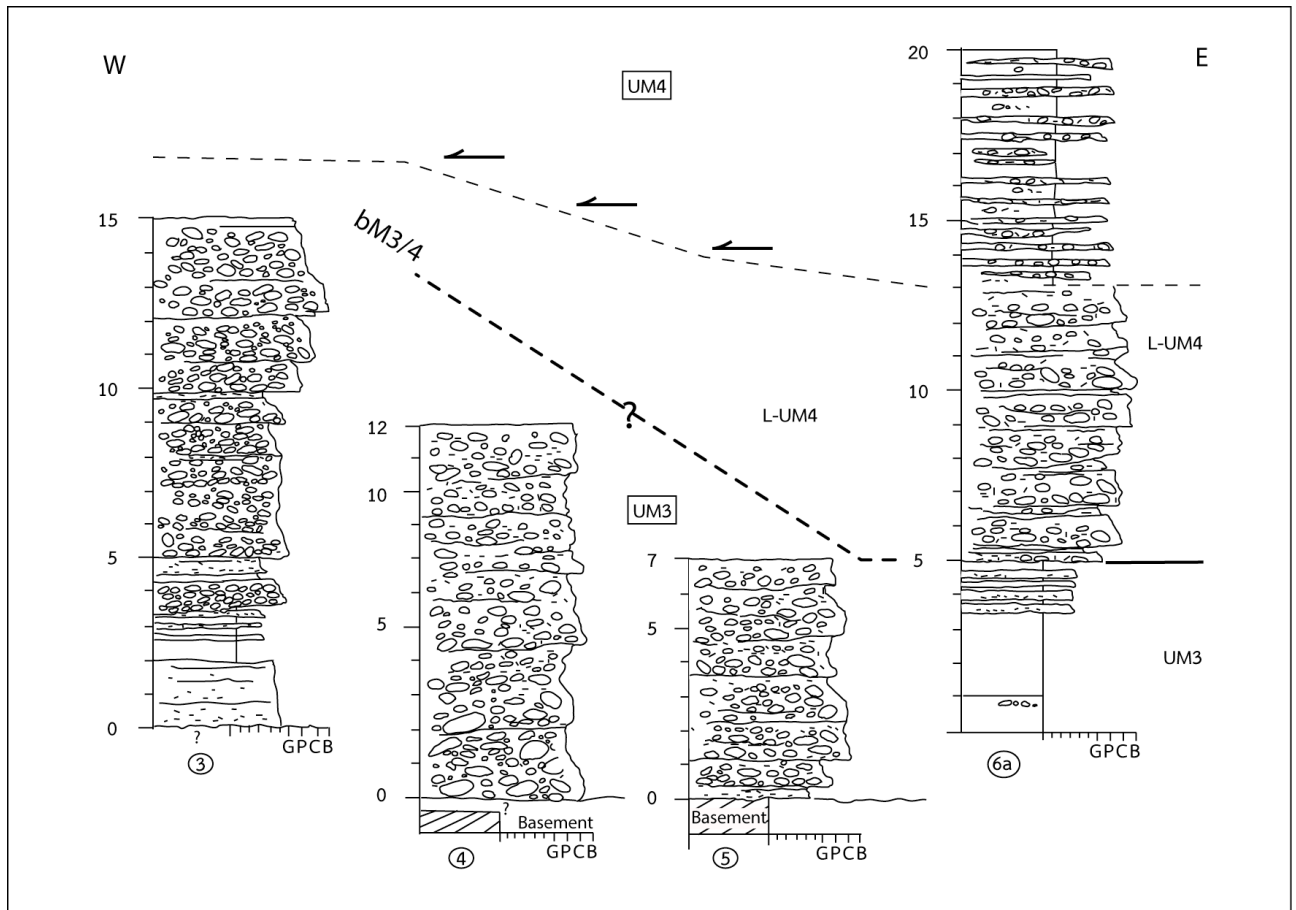
Fig. II. 10: UM3, Sedimentary logs-3 to -6 from the eastern part of Mitropoli block (close to Mitropoli village). See Fig. II. 1 for location.

The section-3 begins with 2 m thick brownish to violet weathered, medium- to coarse-grained sandstone, the lower boundary of which is not exposed. The sandstone is sharply overlain by 1 m thick, pale brown to pale green, sandy siltstone interbedded with very thin-bedded, lenticular, medium-grained sandstone veneers. Above this, the section exhibits a 10 m thick reddish conglomerate, commonly massive, poorly-sorted and matrix-supported. They are rich in gneiss, marbles but also, radiolarites, ophiolitic rocks and cretaceous limestones.

b) Complementary sections of UM3: Sections-4 and -5

(1) Section-4 (Fig. II. 10, log-4): massive conglomerates

About 300 m eastward of section-3, section-4 is exposed at the northern side of the road (Fig. II. 1, locality-4). This section is dominated by a massive conglomerate, up to 12 m thick. The strata are gently dipping westward. They rest at the base against deformed basement, but the contact is not clear, probably controlled by a fault. The conglomerates are reddish, massive, poorly- to very poorly-sorted, matrix-supported and disorganized. Clast ranges from pebble to boulder size, very angular- to sub-rounded. Maximum clast size is up to 30 x 50 cm. The clasts are composed of gneiss, limestone, green volcanic rock and red chert. The matrix is a brown-reddish, coarse- to very coarse-grained sandstone. Conjugate normal faults occur and some conglomerate clasts are clearly deformed near the fault planes.

(2) Section-5: UM3 deposits on the basement

At about 300 m eastward from section-4, section-5 exhibits about 7 m thick massive conglomerate resting directly on the deformed Koziakas-Maliac basement (Fig. II. 10, log-5). A thin 30 cm thick sole of coarse-grained sandstone separates the main conglomeratic beds from the basement. The sandstone exhibits flute-casts indicating a southward flow.

(3) Section-6a

This outcrop is not dominated by conglomerates but by sandstones and siltstones (5 m thick, Fig. II. 10; log-6a). The conglomerates resting on these fine-grained beds belong to the lower UM4 and not to UM3 as they are bounded at their base by main erosional surface.

3. UM3: Correlation between western and eastern outcrops

Conglomerates of UM3 from western and eastern part share similar facies and sedimentary characteristics, *i.e.* reddish clast- to matrix-supported, pebble- to cobble-conglomerates dominated.

Moreover, well-exposed syn-sedimentary normal faults cross cut these conglomerates both in the western and eastern outcrops. This is particularly clear in site-4, where the basement is exposed to the SW on the hanging wall and conglomerates are infilling to the NE the footwall. In the western part, the basement is not exposed but normal faults are also well developed.

38

Even if 4 km exist between eastern and western outcrops and if paleontological data are not enough accurate, because of these similar characteristics (facies and faults), we consider that all these outcrop belong to the same UM3.

4. UM3: interpretation and conclusion

a) Syn-sedimentary faults control the nature of the basal unit contact

The UM3 stratigraphic unit is one of the most interesting in the studied area because of the well-exposed syn-sedimentary normal faults. These faults are the first evidences of subsidence in this area of the basin. They deepen the basin on their eastern side. Also, in the eastern outcrops (sections-4 and -5) the first UM3 sediments are directly overlying the Koziakas-Maliac basement. This suggests that the previously deposited UM1 and maybe UM2 units could have been removed by erosion before deposition of UM3. This could be the affect of such faults. In more detail, the observed faults control the stratal thickness variations that are observed in large and continuous outcrops, and the associated triangular wedges. They also explain the vertical facies variations across the related fills. Section-2 is thought to reflect the best the control of these faults on deposition.

b) A debris-flow dominated triangle fill

The lowermost deposit is a poorly bedded, matrix-supported conglomerate. The heterogeneity of clast shape and lithology suggests that they were emplaced as debris flows in the lows of the topography created by faulting. The interbedded sandstone and siltstone, locally several meters thick, suggest relatively long stages of settling of the suspended load (siltstones) in a quiet environment, alternating with more energetic bedload transportation stages (crossbedded sandstones). Combining these interpretations, these lower UM3 conglomerates could have taken place on a subaqueous slope supplied by debris flows and swept by turbidity currents.

These debris flows alternate with more homogenous and well-rounded, clast-supported conglomerates which have an erosional, channelized base (layer-b, layer-e). Section-2 suggests that these conglomerates are emplaced during peak activity of the faults, because of the local angular unconformity at their base. After this active stage of relief evolution in the vicinity of the faults, the depositional profile would be regarded toward a renewed, more conformable debris-flow dominated deposition (layer-c). The overall upward

increase of sandstone and siltstone intervals matches the progressive flattening of the relief associated with the fault and the correlative decrease of energy of the deposit.

D. Unit M4 (UM4): Post-faulting terrigenous conglomerates and siltstones

UM4 is exposed on the southern part of Mitropoli-block. Good outcrops exist along Mitropoli-Morfovouni road (Fig. I. 7, sites-2 and -6 to -9). It unconformably overlies syn-stectonic UM3 conglomerates and is capped by the thick UM5 conglomerates. It is up to 50 m thick with a thickness increasing eastward.

The lower part of UM4 (L-UM4) is composed of conglomerates, at least 10 m thick to the east, that pinch out in a westward direction (Fig. II. 11 and Fig. II. 1, site-2). They locally, angular unconformity, overlie on the UM3 conglomerates. Several features allow to distinguish between the UM3 and L-UM4 conglomerates (see previous section): (i) reddish, yellowish to grayish siltstones and sandstones occur within UM3 and not in L-UM4; (ii) triangular wedges of syn-sedimentary strata with thickness increasing to southwestward are well express in UM3 and not in L-UM4; (iii) syn-sedimentary normal faults are only found within UM3 and not in L-UM4; (iv) as an effect of syn-sedimentary normal faults, tilting strata of UM3 dip to the SW while strata of L-UM4 are subhorizontal to slightly NE-dipping.

The upper part of UM4 (U-UM4) is composed of siltstones, mostly massive pale-grey to grey. Very thin- to medium-bedded sandstones beds are interbedded in these siltstones. The proposed UM4 type-section is section-2 (Fig. II. 1). Supplementary data relative to section-6 to -9 are also exposed (Fig. II. 15).

1. UM4: Western outcrops

a) General view: the UM4 Type-section (Section-2)

This section is an excellent continuous outcrop where four sub-sections were logged: section-2a to -2d from west to east (Fig. II. 1, locality-2, the same locality for type-section that UM3 described above as Fig. II. 8 and Fig. II. 9). Thick massive siltstones are well exposed at all sub-sections. The largest exposures (Fig. II. 11) show the conglomerates of L-UM4 (Lower-UM4) and the siltstones of U-UM4 (Upper-UM4) overlying unconformably the reddish, syn-

40

tectonic conglomerates of UM3 and capped by conglomerates of UM5. The lower- and upper-boundary of UM4 are defined here.

The lower boundary of UM4 is well observed at section-2b and -2c (bM3/4 on Fig. II. 12 and Fig. II. 13). It is irregularly to sharply erosional. It cuts into the underlying UM3 and is slightly dipping (approximately 3-5°) eastward. At the western side of section-2b, bM3/4 forms an angular unconformity above UM3 (Fig. II. 12 and Fig. II. 13B). Commonly, both conglomerates of L-UM4 and massive siltstones of U-UM4 onlap to the west on this surface.

The upper boundary of UM4 (bM4/5) is well exposed at section-2a and -2d (Fig. II. 11 and Fig. II. 13A, E and D). It is a sharply erosional surface. UM4 is approximately 25 m thick in section-2.
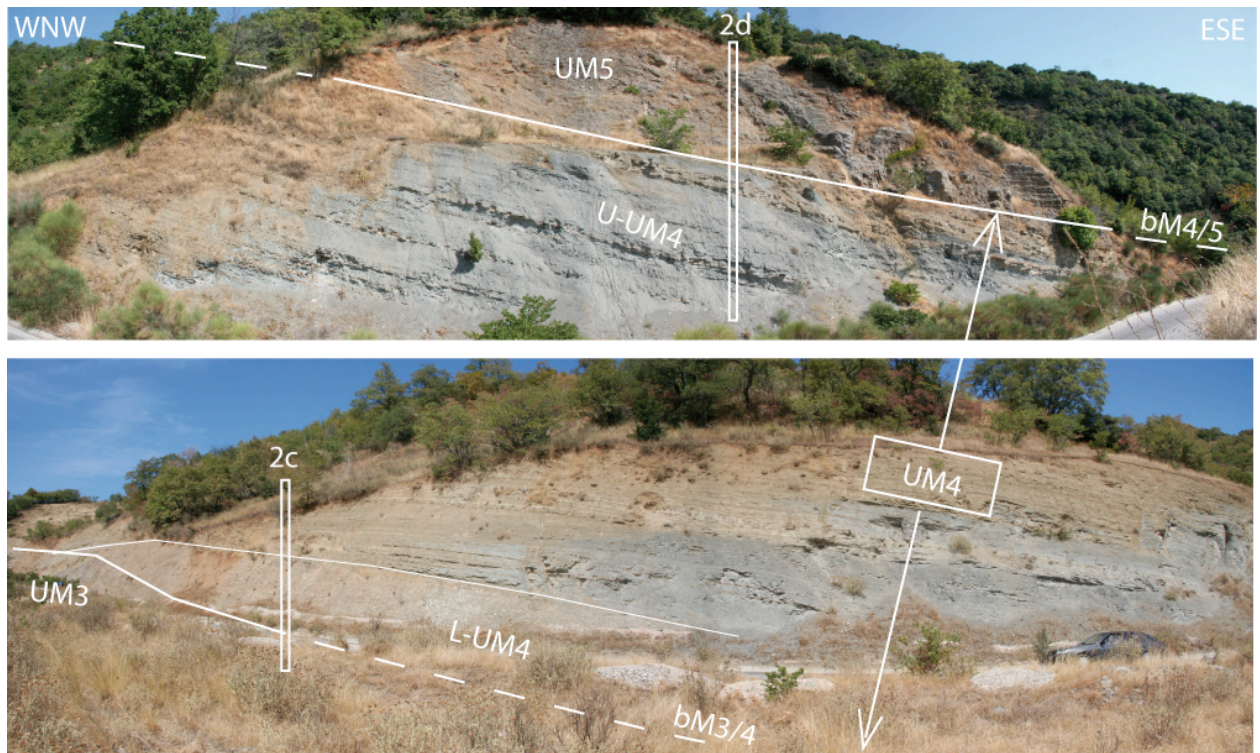
Fig. II. 11: (UM4) - Views of section-2 (with location of log-2d) looking to north, showing UM4 as a fine-grained unit between UM3 and UM5 coarse-grained units. Approximate thickness of UM4 is 25 m. Bottom: view showing the lower erosional contact of Lower-UM4 (bM3/4) conglomerates above UM3 and location of log-2c. Top: view located at about 250 m from section-2c, showing massive siltstones of UM4 overlain by conglomerates of UM5. The upper contact of UM4 is sharply erosional (bM4/5).
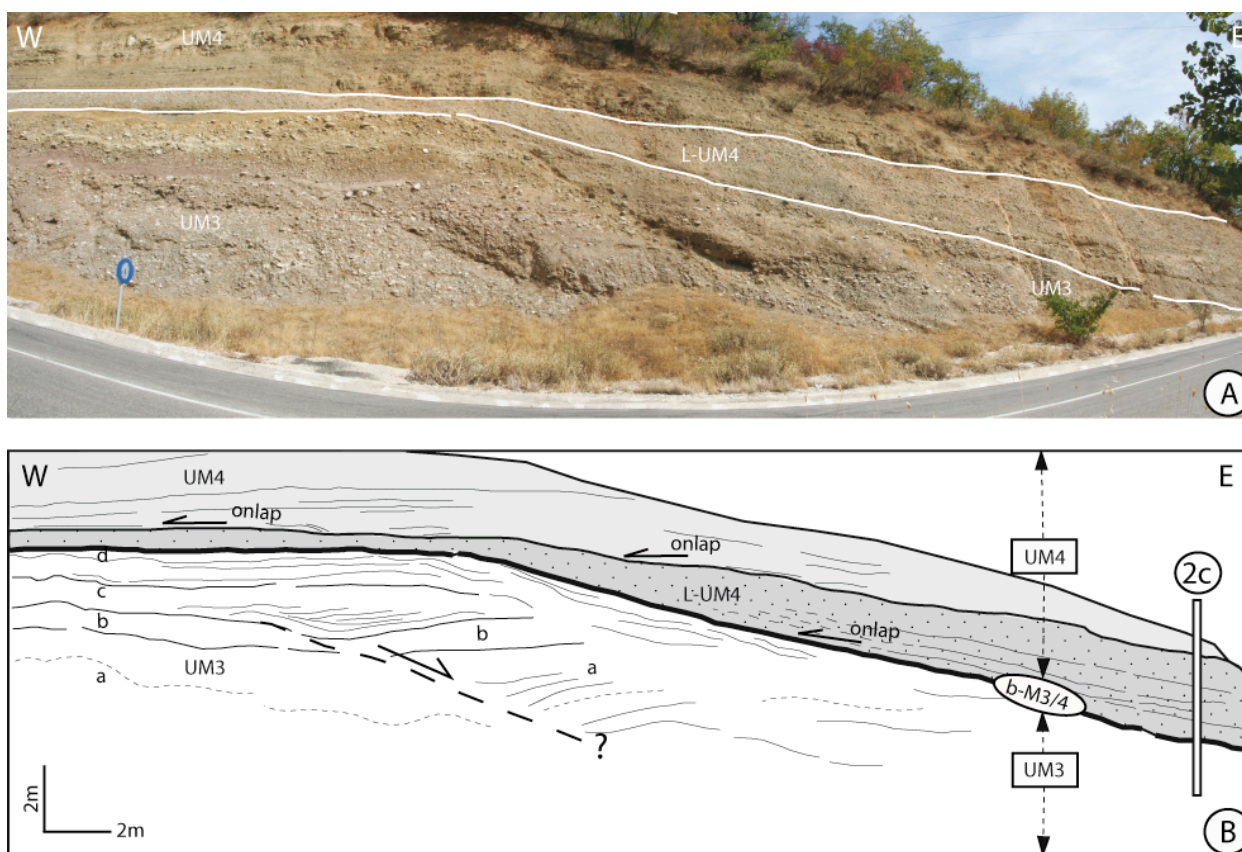
Fig. II. 12: (A) UM4: view of section-2c. (B) Line drawing showing the erosional lower boundary of UM4 (labelled as b-M3/4). Conglomerates of L-UM4 onlap this surface (bM3/4) and is sharply capped by the massive siltstones of U-UM4.

b) UM4 basal conglomerates (L-UM4)

The base of UM4 is well exposed at section-2c (Fig. II. 12 and Fig. II. 14). L-UM4 starts with an about 20 cm thick planar-bedded sandstones. It passes upward into a 2 m thick, massive, matrix- to clast-supported, moderately cemented, gravel- to large pebble-conglomerate. The conglomerate is overall fining-upward. Large-scale tiny trough cross beds are observed. Clasts mainly consist of quartz, limestone, gneiss, marble, red chert and igneous rock. They are sub-angular to sub-rounded. Clast imbrication indicates a westward shear (with a vertical long axis of clasts). Lenticulary, coarse-grained sandstones beds with planar cross-laminae are interbedded in this conglomerate.

The conglomerate thickens eastward, from 0 m to more than 5 m over 30 m in distance (Fig. II. 12). The upper surface bounding L-UM4 is sharp and overlain by massive siltstones with westward onlapping (Fig. II. 13A and C).

42

c) UM4: Massive siltstones (U-UM4)

In site-2, U-UM4 is dominated by pale grey massive siltstones (Fig. II. 13A, E and D). This deposit has weak organic matter content. Three samples have been collected from section-2a, -2b and -2d (Fig. II. 14) for nannofossil analysis, but the results do not permit to determinate ages from these localities.
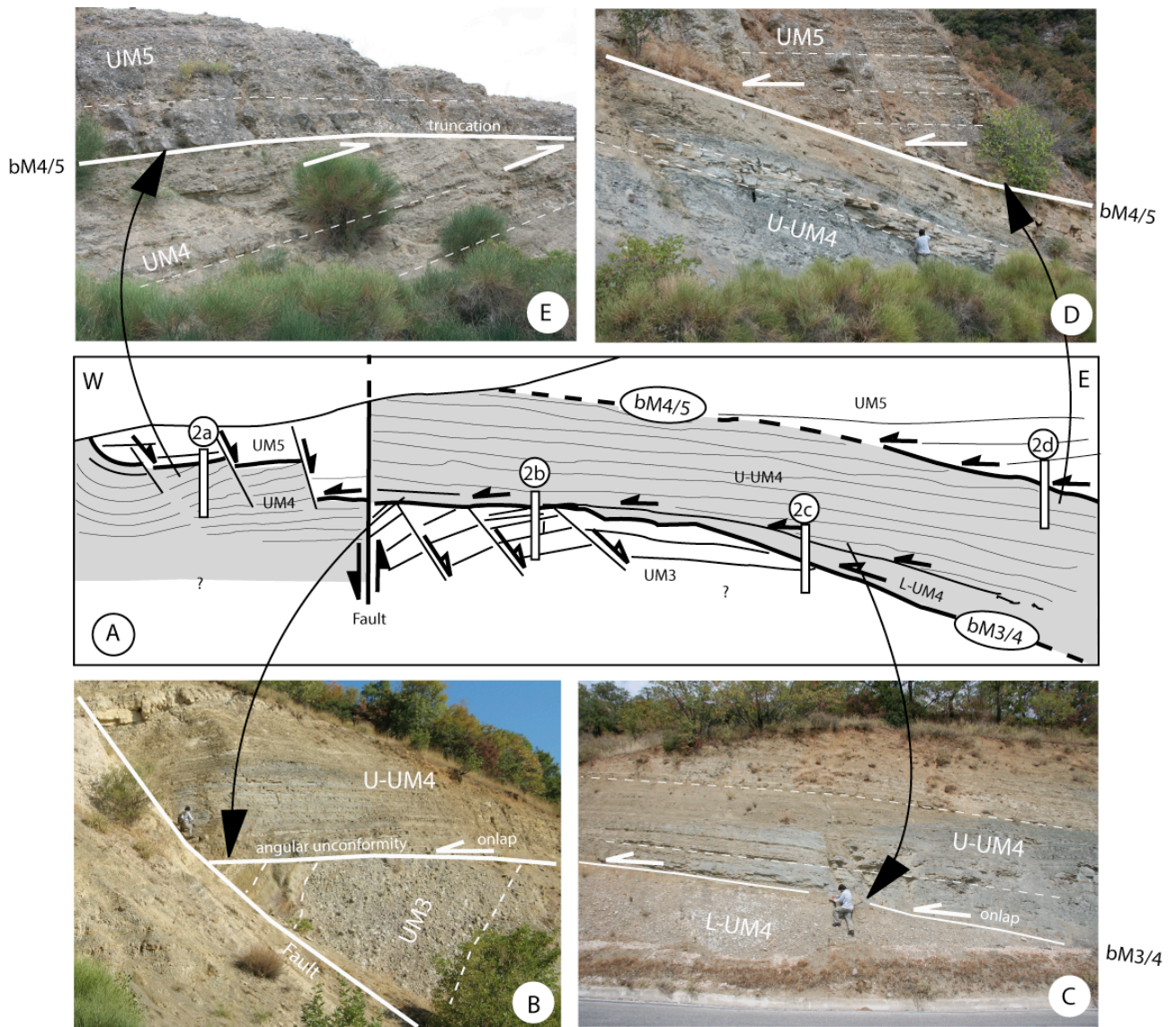
Fig. II. 13: UM4. A) Synthetic sketch of outcrops at locality 2, showing the geometric relationships between UM3, UM4 and UM5. Note the general onlap of deposits onto the lower unit boundary of UM4, as well as the onlap onto the internal boundary of UM4 between the conglomerates (L-UM4) and the siltstones (U-UM4). B) UM4 rests by way of an angular unconformity on the UM3 at the western part of section-2 (log 2b). C) UM4 shows clearly eastward thickening and westward onlapping at the lower boundary. D) From log 2-d, the upper part of UM4 is onlapped by conglomerates of UM5. E) From log2-a, the upper part of UM4 is truncated by UM5.
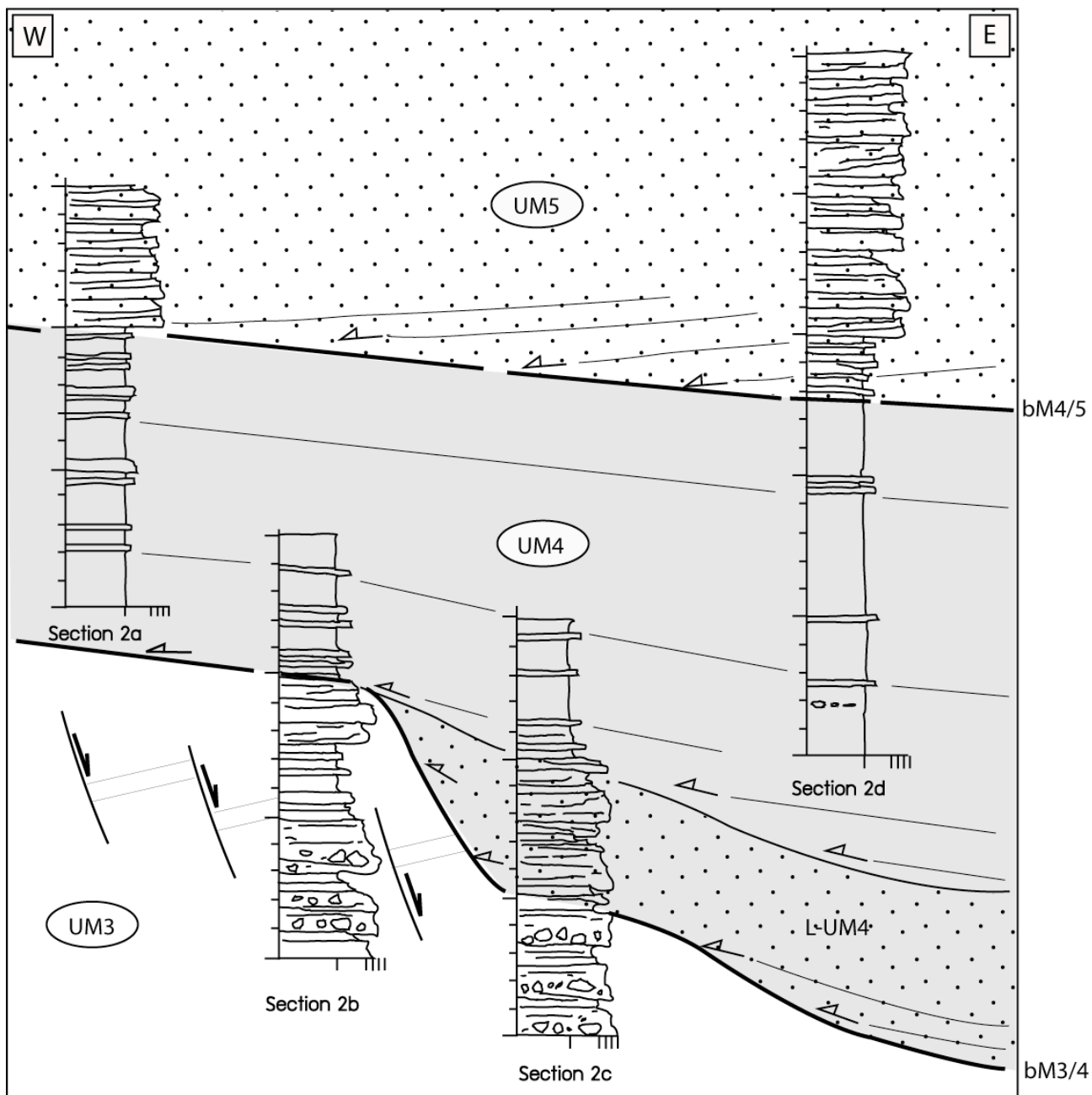
Fig. II. 14: UM4. Correlation of sedimentary logs from section-2. It shows the lower UM4 boundary (base of L-UM4 on the east, base of U-UM4 on the west) incised into UM3 and with westward onlap and pinch out of underlying deposits.

Sandstones beds are scattered within the siltstones. The overall proportion of sandstones/siltstones is approximately 1:4. Sandstones range from very thin- to medium-bedded, fine- to coarse-grained and they are very well cemented. Commonly, sandstones beds have flat, sharp and slightly erosional base and locally slightly normal gradings to the overlying siltstones. Planar bedding is rare as well as bioturbation. Locally, at section-2d, lateral accretion within a thicker package sandstone beds is observed. This package laterally thins and grades to the siltstones.

44

2. UM4: eastern outcrops

At about 3 km to the east of locality-2, close to Mitropoli village, massive siltstones of UM4 form an elongated hill trending NW-SE (Fig. I. 7and Fig. II. 1, hill-327 m and hill-219 m). Siltstones are well cropping out along the Mitropoli-Morfovouni road at locality-6 to -9 (Fig. II. 15). The basal conglomerate of L-UM4 is also exposed at locality-6a (Fig. II. 10). The upper boundary of UM4 at these eastern localities is not exposed.
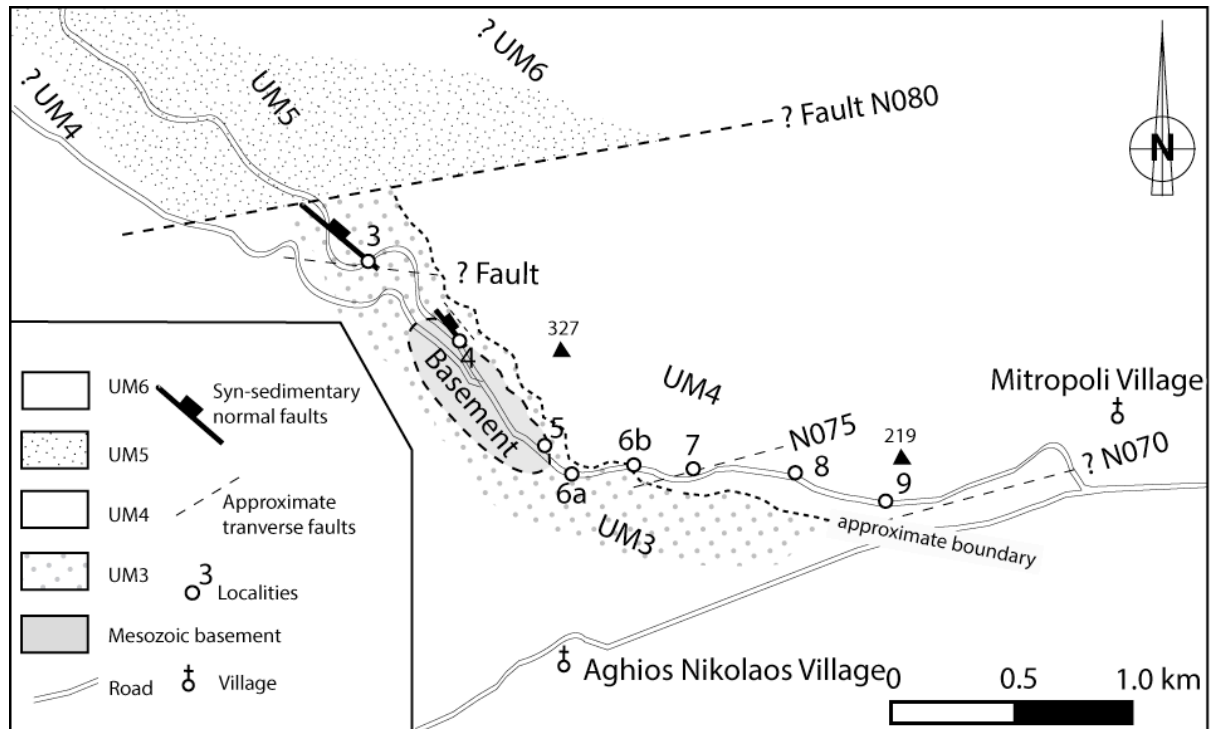
Fig. II. 15: Map of the eastern part of Mitropoli-Morfovouni road, close to Mitropoli village. Well-exposed siltstones (U-UM4) are going younger from locality-6 to -9.

a) The basal conglomerates (L-UM4): Section-6

The lower boundary of L-UM4 is exposed in the upper part of section-6a (Fig. II. 10). It shows an erosional contact of L-UM4 above UM3. At locality-6b (Fig. II. 15) the L-UM4 conglomerate shows a gradational upward fining (Fig. II. 17A and B). It passes gradationally upwards into a thick siltstone unit interbedded with very thin- to thin-bedded sandstone beds.

b) The siltstones (U-UM4): sections –7, -8, -9

The upper UM4 (U-UM4) siltstones with interbedded sandstones are very thick near Mitropoli (Fig. II. 16).

45
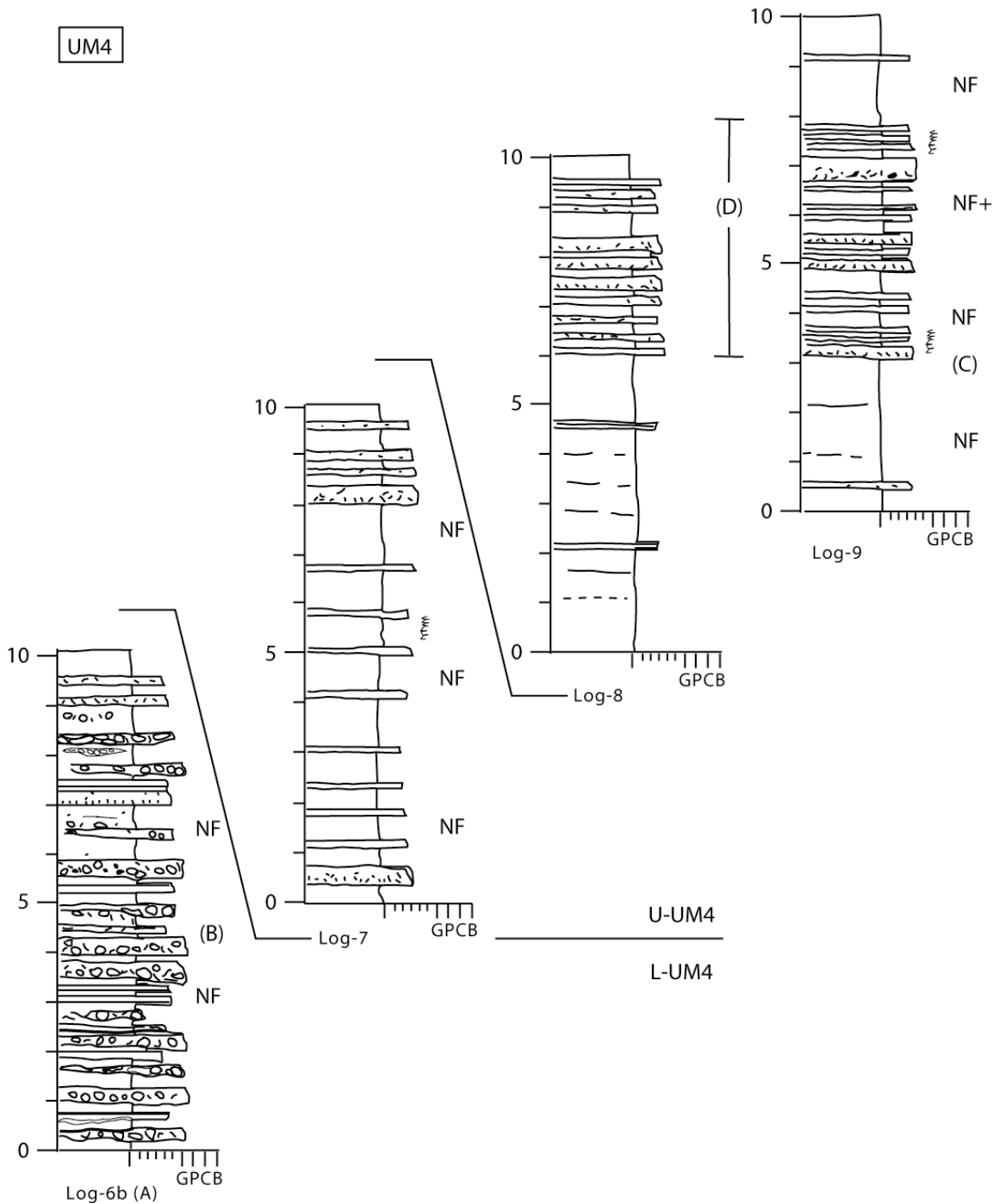
Fig. II. 16: UM4, Sedimentary log-6b to –9 with location of samples for nannofossils (NF, NF+ with fossils) and location of view of facies (A, B, C and D: see Fig. II. 17).

(1) Section-7

This section-7 is located at about 300 m eastward from section-6b (Fig. II. 15, locality-7) and it is the continuation of the succession in section-6. Total thickness of section-7 is 10 m. It is composed mostly by pale-grey to grey (fresh) and pale-brown (weathered) siltstones. Floating gravel and pebble clasts are observed. Rhythmic sandstones with sharp-base, very

thin- to thin-bedded occur within the siltstone (Fig. II. 16). Sandstone form fine- to coarse-grained, non-graded to slightly normal-graded beds.

Three samples of siltstones have been collected and nanofossils have been observed but the results of nannoanalysis do not provide a constraining age.

(2) Section-8

Taking into account the dippings, section-8 is the continuing succession above section-7, about 500 m eastward from section-7 (Fig. II. 15, locality-8). The base of this section is composed by a 5 m thick layer of massive, grey siltstone typical of UM4 (Fig. II. 16, Log-8). It is overlain by a series of interbedded sandstone and siltstone beds, about 4 m thick. The sandstone beds show a thickening upward trend. They have sharp, erosive bases and they range from thin- to medium-bedded, medium- to coarse-grained. Slightly normal grading and planar bedding are present in the sandstone, as well as mud clasts 1-2 cm in diameter. Bioturbations are rare.

(3) Section-9 (Fig. II. 16)

This section is exposed at the foothill located at about 300 m eastward from section-8 (Fig. II. 15, locality-9) and stratigraphically rests above it. The succession shares similar facies with section-8 namely the interbedded sandstones and siltstones but the proportion of sandstones/siltstones is slightly increasing to 1:2. Siltstones are pale-grey, massive and occasionally have a higher load of dark organic matter.

Sandstones range from very thin- to medium-bedded, organized in tabular and sheet-like beds. Sedimentary structures are observed including scour bases, normal-grading, planar lamination better expressed than in the lower sections (Fig. II. 17C). Mud clasts with 1-3 cm in diameter are locally abundant in the sandstones. Vertical and subhorizontal bioturbations occur both in sandstones and siltstones.

This sandstone package is probably equivalent to the sandstones package (Fig. II. 17D) at the top of section-8, if not, it would be above (Fig. II. 16). Several samples of siltstones have been collected with good results. The nannoanalysis indicates an Early-Miocene age (Fig. II. 16, NF+ log-9).

Fig. II. 17: UM4, log-6b to -9. A) Outcrop view of L-UM4 (log-6b), dominated by conglomerates lenses interbedded with siltstones and sandstones. B) Detail of A. C) U-UM4, dominated by grey siltstones interbedded with sandstones. D) Outcrop view of U-UM4 (log-9), flysch-like deposits.

3. Correlation between western and eastern UM4 outcrops

UM4 is characterized by the succession of U-UM4 siltstones and interbedded sandstones, overlying a conglomerate (L-UM4) which might be preserved in the lows of the erosional, unit-base surface (Fig. II. 18).

It is worth noting the following points:

i) all sub-unit bounding surfaces could not be observed in each section;

ii) UM4 shows an eastward thickening: massive siltstones thicken from 25 m in the west to more than 50 m at about 4 km to the east;

48

iii) sandstones are less developped in the western outcrops;

iv) nanofossils might indicate an Early Miocene age for U-UM4 to the east but no correlation could be established with the western outcrops.

Despite all these observations, we have estabished the correlation between the UM4 western and eastern outcrops (section-2 to section-9) taking into account their overall dip, their facies attributes and (locally) their location between UM3 and UM5.
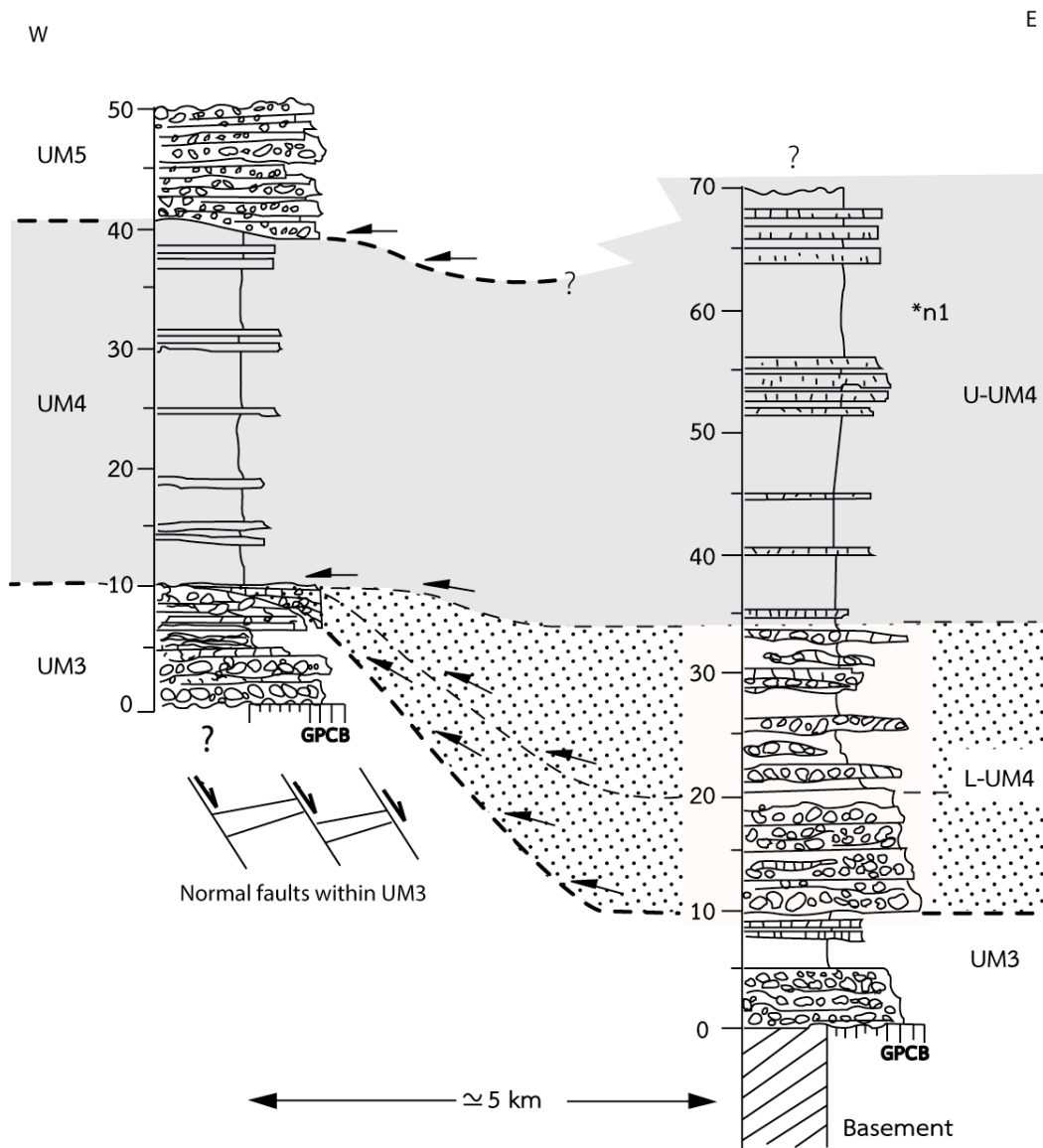
Fig. II. 18: Correlation between eastern (locality-2) and western logs (combined from localities 6 to 9) of UM4 included conglomerates (L-UM4) and siltstones (U-UM4).

4. UM4: Interpretation

The sedimentologic characteristics (silt dominantly) and fossils (marine nanofossils) show that the U-UM4 silststone was deposited in a marine setting, below wave base. While the siltstone corresponds to the hemipelagic, bulk sedimentation, the thin sandstone intercalations would record turbiditic events. This is supported by the Bouma-like Ta style of most of the sandstone beds in the lower to middle part of the sub-unit (sharp, slightly erosional base, not laminated, normal grading). The absence of ripples on top of the graded sand suggests that the density of the turbiditic flow was not high during its waning stage. This suggests that the submarine path of these turbidites was not long and its catchment relatively small. As a consequence, we suggest that the basic facies of U-UM4 represents the submarine slope of a small basin: the first true MHB at this place.

The depositional setting of the L-UM4 conglomerates remains debatable. The matrix-supported fabric and absence of prominent erosion between the parallel, isopachous beds suggest these conglomerates would have been emplaced as debris-flows. The conglomerate clasts are of the same nature as those in UM3 and, except that they are generally smaller, of the same shape. Thus, the L-UM4 conglomerates could correspond to a more distal slope margin deposit. This would explain the basinward lateral interfingering of the conglomerate with siltstone beds in section-6b.

E. Unit M5 (UM5): a thick conglomerate and sandstone unit

UM5 up to 250-300 m thick is volumetrically the most important in Mitropoli-block. It is well cropping out at Petalitis hill (hill-573), along Kanalia-Morfovouni road (Fig. I. 7, localities-12 to -15), Mitropoli-Morfovouni road (Fig. II. 1, localities-2, -10 and -11) and also along the Aghios Akakios road (Fig. II. 1, localities-16 and -17).

In general, UM5 rests above the massive siltstone of UM4 with locally westward, apparently, downlapping geometry. The basal contact is a sharply erosive surface and it is only exposed at the western part of the studied area (Fig. II. 1, locality-2). UM5 also rests unconformably on the Koziakas basement to the west.

UM5 is composed of conglomerates, sandstones and few siltstones. It is subdivided into two parts: conglomerates dominate in the lower part while the upper part is dominated by sandstones.

1. The conglomerate-dominated lower part of UM5 (L-UM5)

Lower UM5 is well exposed along Mitropoli-Morfovouni road (Fig. II. 1, locality-2 for the west and locality-10 and -11 for the east) and also along Kanalia-Mitropoli road (Fig. II. 1, locality-12).

The lower UM5 is dominated by massive, medium- to thick-bedded, gravel- to pebble-conglomerates. Conglomerates have sharp to irregular erosional base. They are matrix- to clast-supported, locally bedded and reverse-, normal- or non-graded. There is an overall gradational fining upward of the conglomerates within, ending up with the upper UM5 sandstones.

a) <u>Lower boundary of UM5 to the west: Section-2</u>

A fresh road-cut provides the only section where we found the lower boundary of UM5 exposed at the western part of the Mitropoli block (Fig. II. 1, locality-2). At this site, UM5 is only exposed at section-2a and -2d, respectively (Fig. II. 13). The lower boundary of UM5, defined as bM4/5, is a sharp and erosional surface (Fig. II. 19). The subsection-2a (Fig. II. 14), shows the surface bM4/5 truncating underlying siltstones of UM4 (Fig. II. 19A and B). In a nearby ancient quarry, we also found this surface truncating UM4 and the conglomerates of UM5 resting above, with an apparent westward onlap on this surface (Fig. II. 19C). In subsection-2d (Fig. II. 13A and D), bM4/5 is slightly erosional above siltstones of UM4 and the conglomerates of UM5 overlie this surface with clearly westward down-lapping.

Conglomerates at the base of UM5 are commonly massive, matrix-supported and moderately sorted. In places they are crudely stratified. Clasts range from sub-rounded to well-rounded, gravel- to pebble-size and clasts up to 5x10 cm are observed. Clast components include gneiss, marble, quartz, igneous rock and red chert clasts (Fig. II. 19D). Upward on the sequence, following a small pathway to the top of hill-573, individual conglomeratic beds with clast-supported, normal grading, gravel- to cobble-conglomerates occur (Fig. II. 19E).

Fig. II. 19: (L-UM5). A) Panorama views from the west of section-2d showing the erosional lower boundary of UM5 (labeled as b-M4/5). Siltstones of UM4 are truncated by b-M4/5 and conglomerates of UM5 rest with apparent westward onlaps on this surface. B) Zoom of (A), showing clearly sharply erosive and truncated surface of b-M4/5. C) Upward from section-2a, at an ancient quarry, b-M4/5 is sharp and slightly incised into underlying UM4 with the overlying conglomerates of UM5 downlapping westward. D) Clast-supported, poorly sorted, gravel to pebble conglomerate. Clast components include ophiolite (o), radiolarite (r), marble (m), quartz, limestone and gneiss (g). E) Massive, thick bedded, matrix to clast-supported, normal grading, pebble to boulder conglomerates capped by very coarse-grained sandstones.

52

b) The lower conglomeratic part of UM5 to the east: Section-10

This section is located along Mitropoli-Morfovouni road, at about 4 km westward from Mitropoli village (Fig. II. 1, locality-10). The measured section is exposed at the northern-side of the road cutting.

The succession exhibits massive heterogeneous conglomerates, poorly- to moderately stratified, with tabular to lenticular beds 20-80 cm thick (Fig. II. 20 and Fig. II. 21). The beds locally show a crudely erosional base. Clasts range from gravel- to cobble-size and are subangular to subrounded. Maximum clast size is up to 10x20 cm. Clast components include gneiss, marble, limestone, ophiolite and red chert. Some imbrications (great axis vertical) indicate a south-southwestward direction of shear.
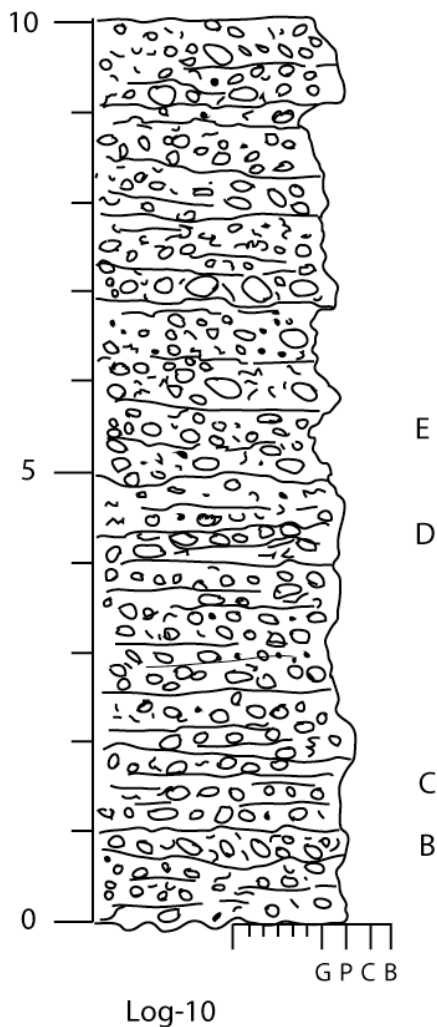
Fig. II. 20: (UM5), Sedimentary log-10. B to E see Fig. II. 21.
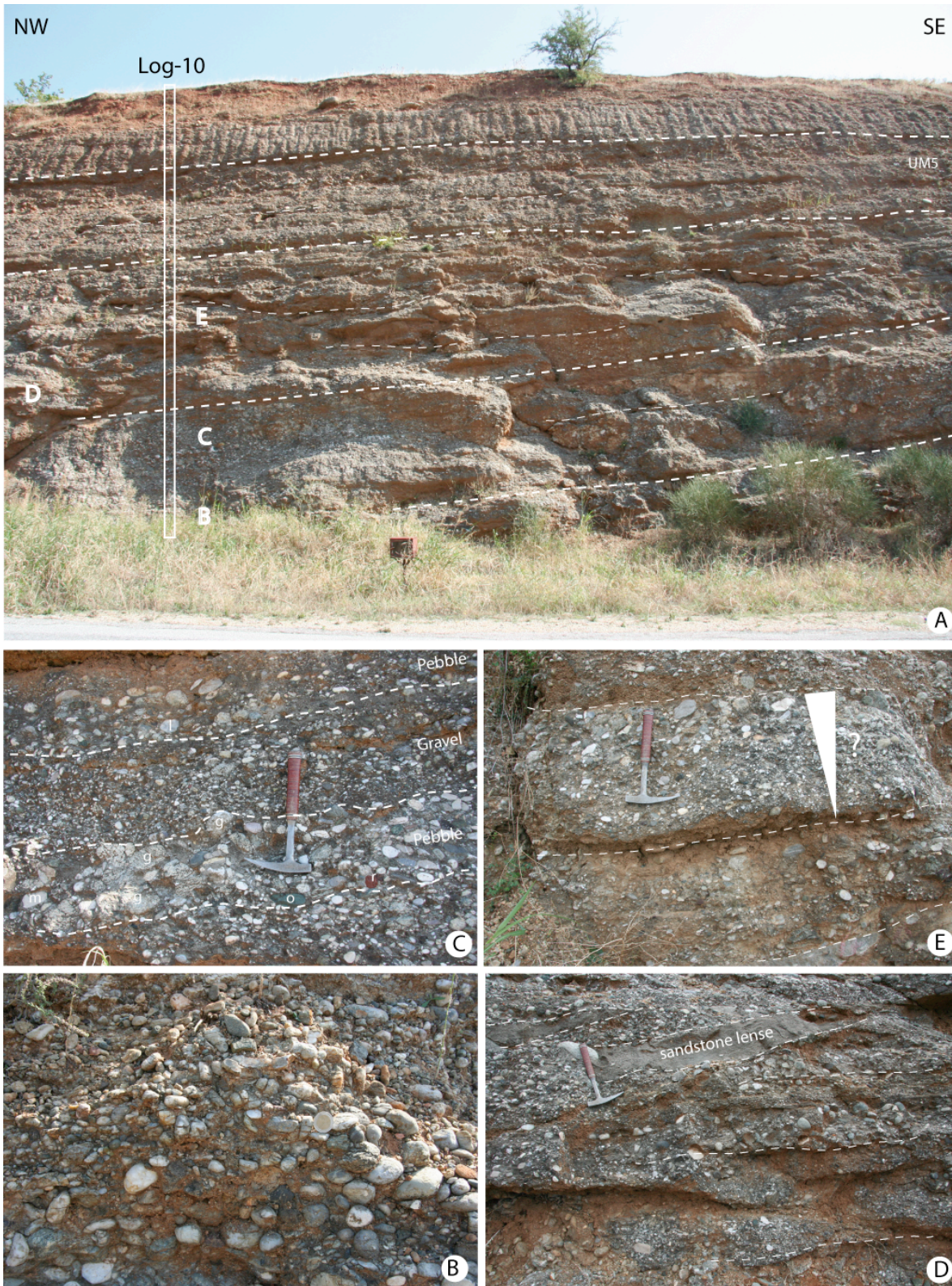
Fig. II. 21: UM5, log-10. A) Outcrop of conglomeratic beds of section-10. B) Poorly cemented, pebble conglomerates. C) Non-grading, poorly sorted, gravel to pebble conglomerate. Organized in lenticular beds. D) About 20 cm thick of sandstone lens occur. E) Crudely stratified, matrix-supported, moderately to poorly sorted, gravel to pebble conglomerate. Large pebble capped a top of bedding. Reverse grading, medium-bedded.

2. Upper part of UM5: sandstones with conglomerates

The upper UM5 is marked by an increasing percentage of sandstones versus conglomerates. The upper UM5 is thus dominated by moderately to well-bedded sandstones interbedded with lenticular conglomerates and siltstones. The transition between the lower and upper parts of UM5 is generally gradational so that no sub-units are considered.

The sandstones in upper UM5 range from thin- to thick-bedded, fine- to very coarse-grained and mica grains occur. Organic matter is common in medium- to thin-beds. Sedimentary structures such as scour bases, normal-grading and planar-bedding are common in the sandstones. Bioturbations including *Skolithos* and *Ophiomorpha* are abundant.

The interbedded conglomerates are lenticular, thin- to thick-bedded. They are of gravel- to cobble-grain size, moderately- to poorly-sorted, matrix- to clast-supported and with normal- to non-grading of the individual beds.

Upper UM5 is well exposed along the Kanalia-Mitropoli road (Fig. II. 1, locality-13 to -15).

a) <u>Section-13: example of the sandstone-rich upper UM5</u>

This section is situated on Kanalia-Mitropoli road, exposed on the western side of the road (Fig. II. 1, locality-13). It is about 15 m thick, dominated by sandstones with conglomerates (Fig. II. 22). The sandstone beds are well-bedded and 20-50 cm thick. They are medium to very coarse-grained and well cemented. Their bases are sharp and erosional.

Sedimentary structures include normal grading or non-grading and planar bedding. Beds show an apparent, low angle, downlap toward the south. Scattered organic matters occur. An exceptional, well preserved dark organic matter, with 5 cm thick and 50 cm long, is observed (Fig. II. 23B and C). The sandstones are interstratified with about 1-2 m thick pebble to cobble conglomerate beds (Fig. II. 22). The conglomerates are matrix-supported, poorly-sorted, non-graded. Clasts in the conglomerates are rounded- to very well-rounded with maximum clast size is up to 15x25 cm. The long-axis of pebbles or cobbles is commonly dipping to the NE. Clast components are marble, limestone, gneiss and ophiolite (Fig. II. 23D) while the matrix varies from coarse-grained sandstone to granule conglomerate. The conglomerates are slightly erosional above the sandstones but overall form a conformable succession of strata.
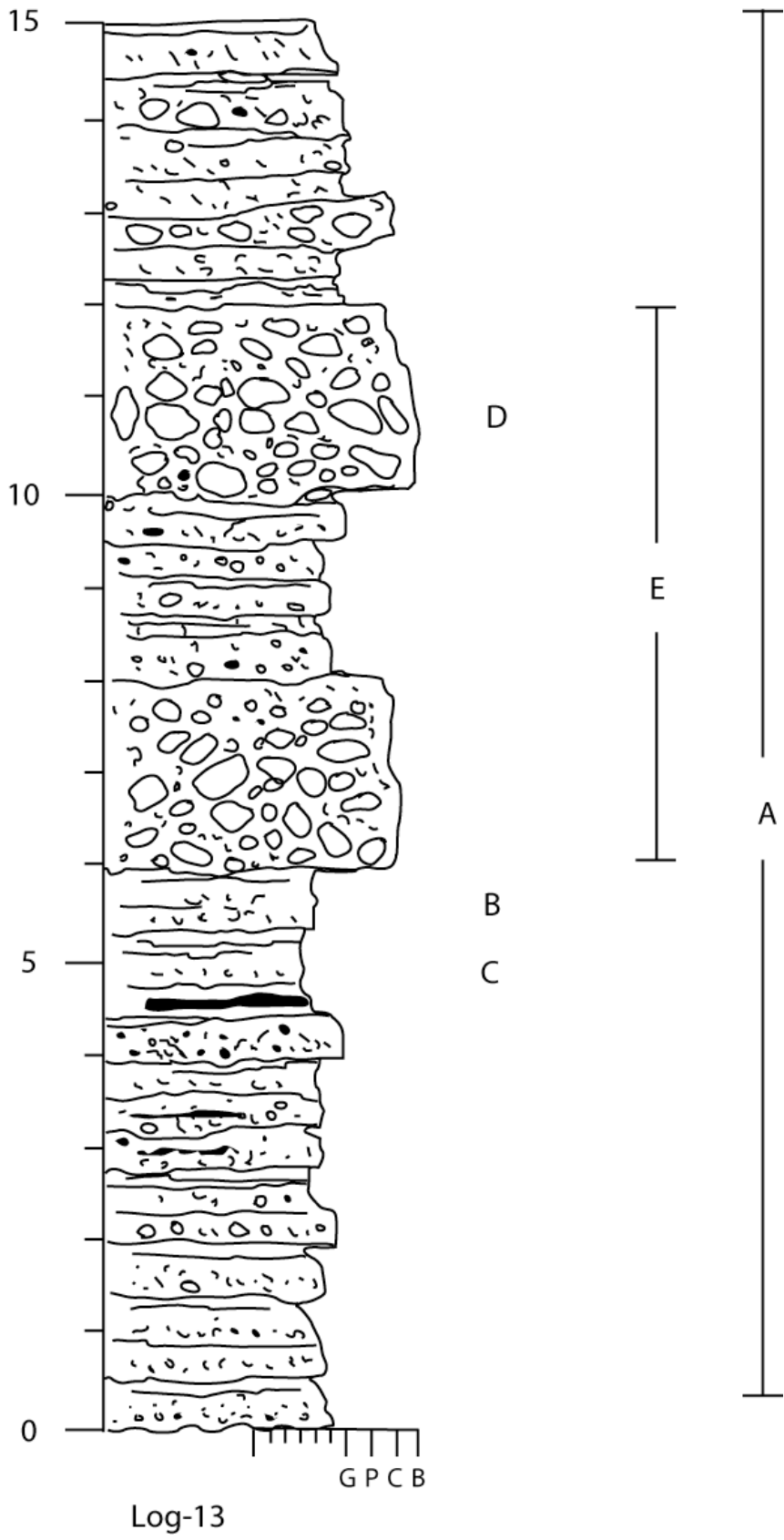
Fig. II. 22: UM5, Sedimentary log of section-13. A to E: see Fig. II. 23.
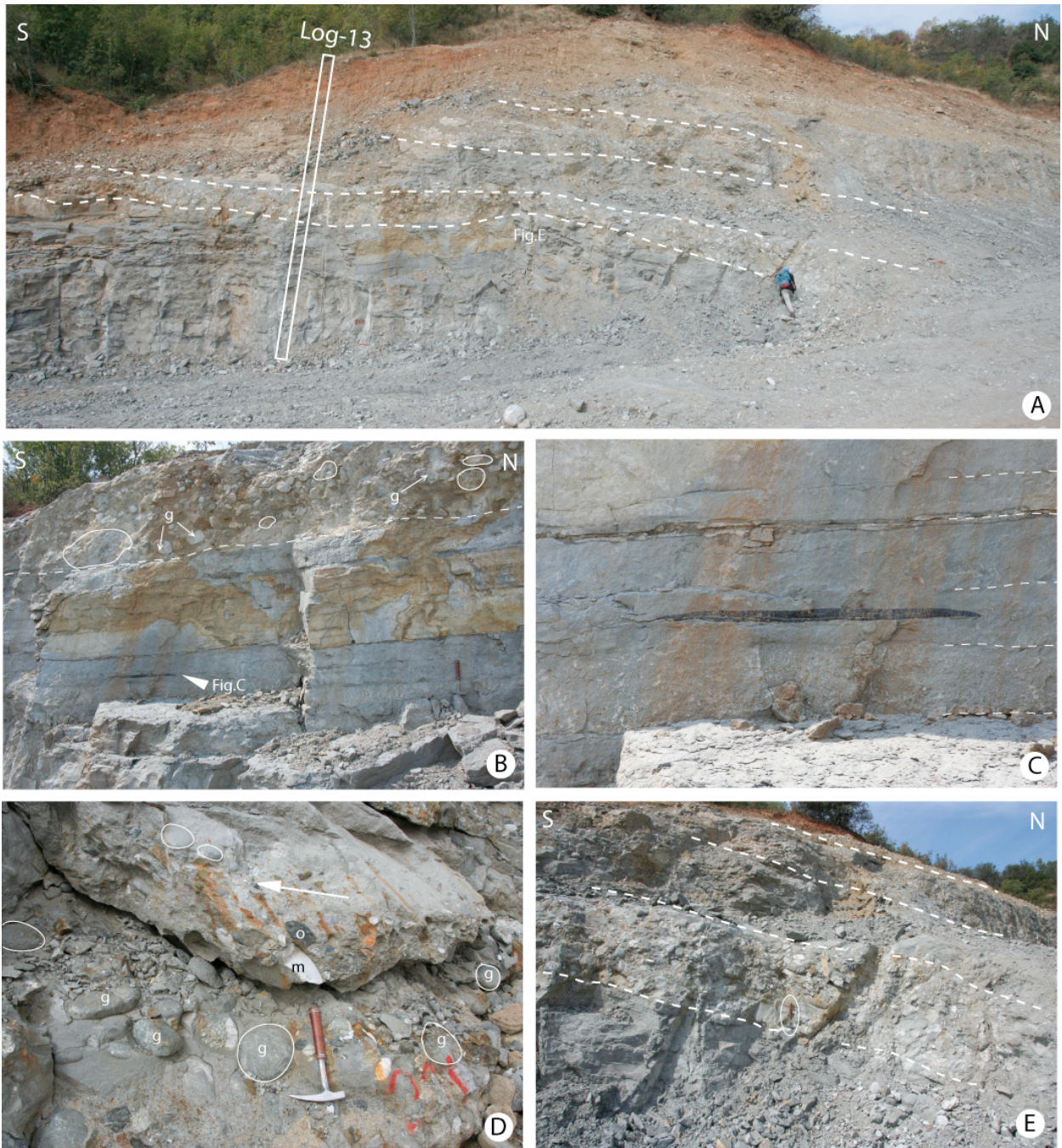
Fig. II. 23: UM5. A) Panorama view from section-13 logged in Fig. II. 22. Note the pebble conglomerate bed at the middle part of the succession, as labeled in dash line. A person for scale. B) Planar bedding in coarse-grained sandstones overlain by a 2 m thick cobble conglomerate (g: gneiss pebble). C) A dark organic matter lens 5 cm thick and 50 cm long well preserved in the coarse-grained sandstone beds. The lowermost bed is a medium bedded, gravel conglomerate showing normal grading. D) Matrix supported, moderately to poorly sorted, pebble to cobble conglomerate bed. Clasts are well rounded with 15x25 cm size (g: gneiss pebble, o: ophiolite rocks). E) Conglomerate beds within dominating sandstone deposits (see location on A).

b) UM5: Additional data on upper UM5 (Section-14 and -15)

Section-14 is located about 100 m northward from section-13, on Kanalia-Mitropoli road (Fig. II. 1, locality-14). It exhibits a 20 m thick succession comparing with that of section-13 comprising sandstones interbedded with minor medium- to thick-conglomerate beds (Fig. II. 24).

The lower part is composed of subtly bedded sandstone interbedded with pebble conglomerate. Upward in the succession, the bedding in the sandstones becomes more prominent. The beds base is sharp and erosive. Grain size ranges from medium to very coarse sands. Bioturbations are very abundant especially *Ophiomorpha* and *Skolitos.*

Fig. II. 24: Upper-UM5 form log-14. A) Rounded trace: *Ophiomorpha* and elongated trace: *Skolitos*. B) Mud clasts with a large one in the middle (20x30 cm). C) Organic matter-rich in sandstone. D) View of the lower part of log-14.

Section-15 is located immediately above section-14 and shows alternations of sandy-matrix supported conglomerates alternating with organic-rich, fine sandstone beds. Maximum clast size is locally up to 50 cm (Fig. II. 25 and Fig. II. 26).

58
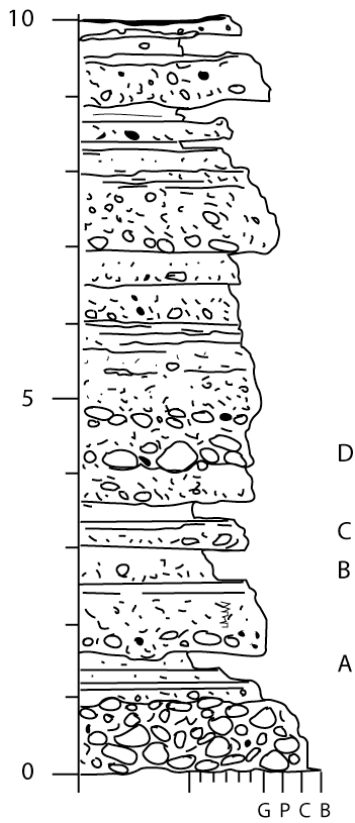
Fig. II. 25: Upper-UM5. Sedimentary log of section-15.
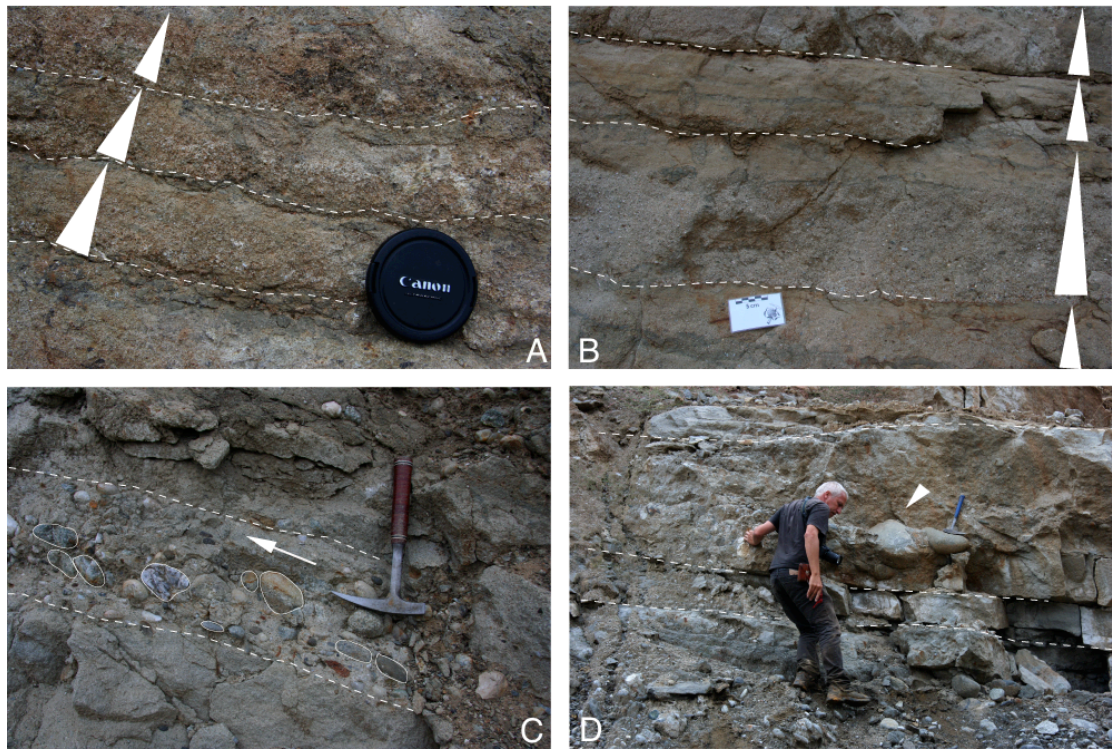
Fig. II. 26: Upper-UM5. Detail of sedimentary facies of log-15. A) Thin bedded, normal gradded sandstone. B) Coarse grained sandstones with bioturbation *"Skolitos".* C) Clast imbrication indicating flow from NE to SW. D) Floating boulder (white arrow) within conglomerate bed.

3. UM5: Complementary sections from the north-western area (Aghios Akakios village)

a) <u>Section-16: Alternation of conglomerates and sandstones</u>

This section is located to the west of Mitropoli block, at about 300 m in elevation, southeastward from Aghios Akakios (Fig. II. 1, site-16). It is up to 45 m thick and comprises sandstones interbedded with 4 main levels of conglomerates (Fig. II. 27). Sedimentary strata are striking N140-160° and dipping 15-25° to NE. Most of the deposit is pale bown to reddish at the outcrop, locally greenish, both in weathered and exposures and fresh sections (Fig. II. 28A).

The conglomerates bedsets, up to 5 m thick, are poorly sorted and matrix-supported (Fig. II. 28B). Clasts are dominated by quartz, limestone, gneiss and mable. Red chert and ophiolites clasts are also present but less important. Clasts range from sub-angular to sub-rounded and from gravel to pebble size. Pebble- to cobble-clasts are occasionally observed. The conglomerate bedsets have a sharp, erosional base, locally exhibiting channel-like incisions of several meters in amplitude. Most of them crop out as a massive, loose deposit, but they also locally form a crudely bedded facies where they are mixed with sandstone veneers (less than 20% in average volume). This latter facies mostly occurs as the infill of the channel-like forms, onlapping the erosion surface or showing oblique accretion sets parallel to it, the whole facies exhibiting a complex cut-and-fill architecture (Fig. II. 28F).

The sandstones, medium- to coarse-grained, are also moderately cemented. They form up to 8 m agradational successions above the conglomerates. Their lower bounding surface, although overall conformable, is locally scoured (Fig. II. 28C). Individual, <1 m thick, lens-shaped, clast-supported conglomerate beds with large-scale internal oblique bedding are observed within the sandstone, less than 20% in average volume (Fig. II. 28D). The sandstones are dominantly massive (Fig. II. 28E), except in the upper part of the section where they exhibit planar bedding conformable to the top surface of the underlying conglomerate. There, the sandstone beds exhibit slightly normal gradings and floating gravels. They are locally interbedded with thin, grey siltstones.
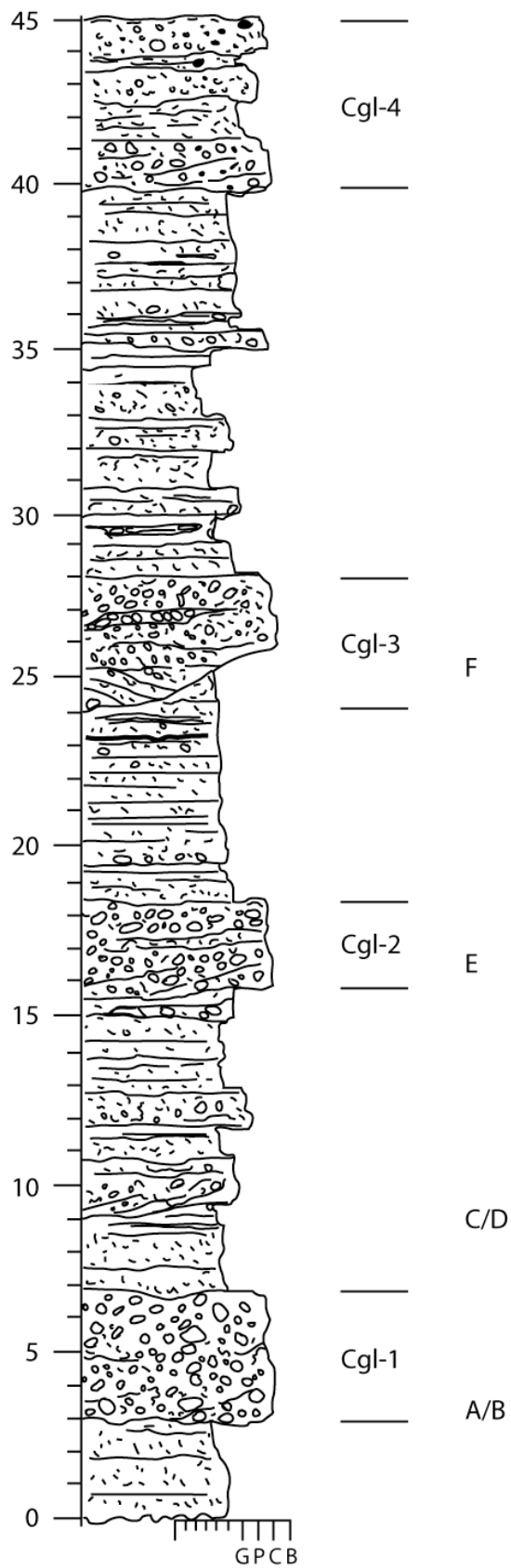
Fig. II. 27: UM5. Sedimentary log from section-16. A to F and Cgl-1 to Cgl-4: see text and Fig. II. 28.

61

Fig. II. 28: UM5. Views of section-16. A to F: for details see text.

b) **Upper limit of UM5 at SE of Aghios Akakios: Section-17**

Section-17 is exposed at 1.5 km southeastward from previous section-16, on the Aghios Akakios to Kanalia- Mitropoli road, at about 280 m high altitude (Fig. II. 1, locality-17, close to a stream name Bakatsiano). This section provides another view of the large-scale interbedding of sharp-based, erosional conglomerates and overlying agradational sandstones to siltstones (Fig. II. 29). The rocks are less reddish and more greenish to grey here.
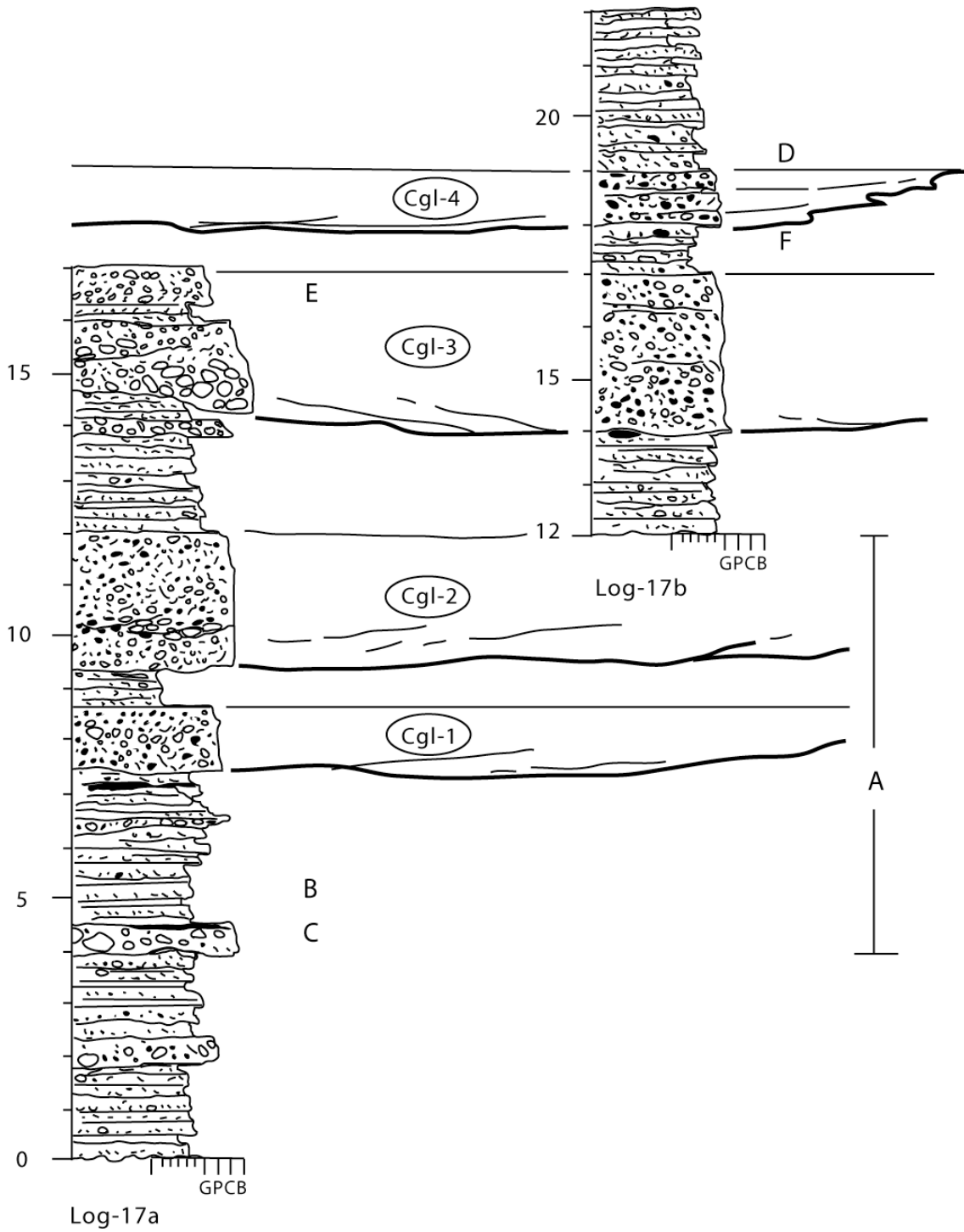
Fig. II. 29: UM5. Sedimentary log from section-17. A to F and Cgl-1 to Cgl-4: see text and Fig. II. 30.

The conglomerates, as in section-16, occur as <1m-thick lenses interbedded within the sandstones or as up to 12 meters-thick bedsets formed by the amalgamation of lens- or wedge-like, locally erosional beds, internally massive or exhibiting crude oblique bedding. In the latter case, even clearer than in section-16, they fill in channel-like erosion forms, up to 3

63

in amplitude, incised in the underlying sandstones (Fig. II. 30A, Cgl-2). The conglomerate beds are dominantly matrix-supported, moderately sorted and overall fining upward. Clasts are composed by gneiss, marble, quartz, limestone, ophiolite and rarely red chert. Maximum clast size is about 20x30 cm (Fig. II. 30C, D).
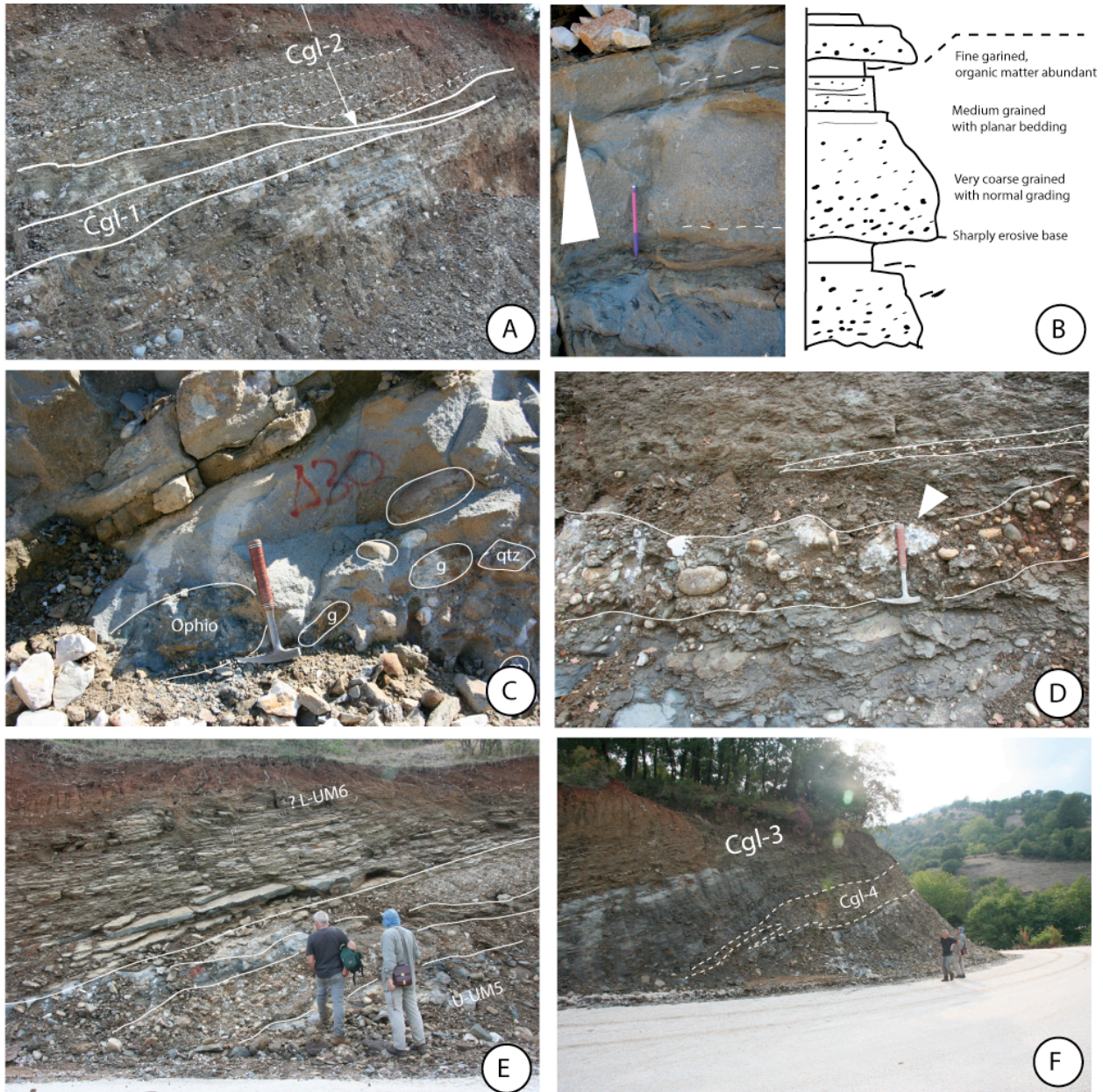
Fig. II. 30: UM5. Views of section-17. A to F: location Fig. II. 29, for details see text.

In section-17, there might be a somewhat increased number of silstones interbedded within the sandstone bodies, as compared to section-16. The sandstones range from fine- to very coarse-grained, and they pervasively form 10- 20 cm thick, planar beds, with sharp to erosional flat bases and normal gradings (Fig. II. 30A). Ripple lamination can be observed in

64

the upper part of the sandstone beds (Fig. II. 30B). The siltstones are present at the top of the sandstone beds (Fig. II. 30E). They contain thin ripple trains and dark organic matters clasts. One notes an upward increase of the siltstone amount at the top of section-17. This is how the boundary with the overlying UM6 is defined.

4. UM5: Interpretation

As for other conglomerate-rich units, the depositional setting interpretation of UM5 is not straightforward. The conglomerates have a scoured base, and generally infilling channel-like forms and the clasts are dominantly well rounded. The cut-and-fill architecture of the conglomerate beds infilling the channels suggests the predominance of bedload deposition. Besides, the dominantly matrix supported fabric of the conglomerates (except for those interbedded within the sandstones) suggests a highly concentrated flow and/or a rapid flow waning at the place of deposition. As a consequence, we suggest that the conglomerates are deposited at the outlet of channels carrying heterometric sediments mixed together under high-energy conditions. The large extent and isopachous character of beds points to a submarine, likely slope-margin setting.

The conglomerate grades upward to a sandstone dominated succession in which small conglomeratic channels remain present. The occurrence of numerous plant remains in these sandstones, suggest a direct connection to a fluvial feeder. The scoured bases and flat-bedded, normal grading of the sandstone beds indicates a pulsed, high-energy supply of sediments. This is consistent with a proximal turbiditic system. The occurrence of *Ophiomorpha* in these sandstones suggests a nearshore setting, but some species of this burrow type are also observed in the *Nereites* ichnofacies, in deepsea sediments (Uchman, 2009).

F. Unit M6 (UM6): Massive siltstones interbedded with thin bedded sandstones

UM6 is rarely exposed, the most complete and continuous succession is cropping out in a dry river to the east of Aghios Akakios at section-18, which has been therefore proposed as a type-section of UM6 (Fig. II. 1). Other successions (section-19 and -20) are presented as complementary sections.

About 100 m thick, UM6 is dominated by massive, grey siltstones interbedded with sharp based, thin- to medium-bedded sandstones. It is a fine-grained unit, between the coarse-grained UM5 and UM7. It conformably overlies the conglomerates and sandstones of UM5 and probably also unconformably the Koziakas Mesozoic basement. However, the latter contact is not clearly exposed in the field. UM6 is capped, probably conformably, by conglomerates and sandstones of UM7.

1. Type-section of the siltstone-rich UM6: Section-18

Section-18 is taken from a dry bank and is located to the SE of Livadhia village (Fig. II. 1, locality-18). It is about 80-100 m thick limited a the top by the Livadhia fault (Fig. II. 31).
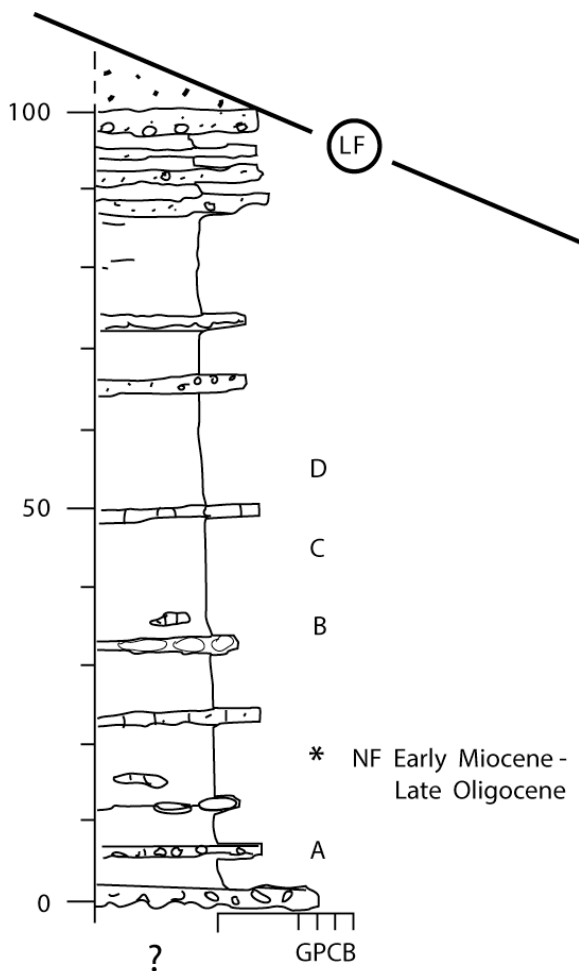
Fig. II. 31: UM6. Sedimentary log of section-18. A to D: see Fig. II. 32. LF: Livadhia fault. NF: nannofossils.

The section has its base on the top of a thin matrix-supported, gravel to pebble conglomerates (Fig. II. 32A). Above this basal conglomerate, corresponding to UM5, siltstones

66

dominate upward the section. In the lower part, thin- to medium-bedded calcareous sandstones occur within the siltstones. Calcareous nodules and lenses are also present (Fig. II. 32B) as well as locally numerous small burrows (Fig. II. 32D). Small scale slumps and slides affect the deposit. At the top of the succession, medium bedded sandstones are present forming a slumping-like structure, about 10 m thick.
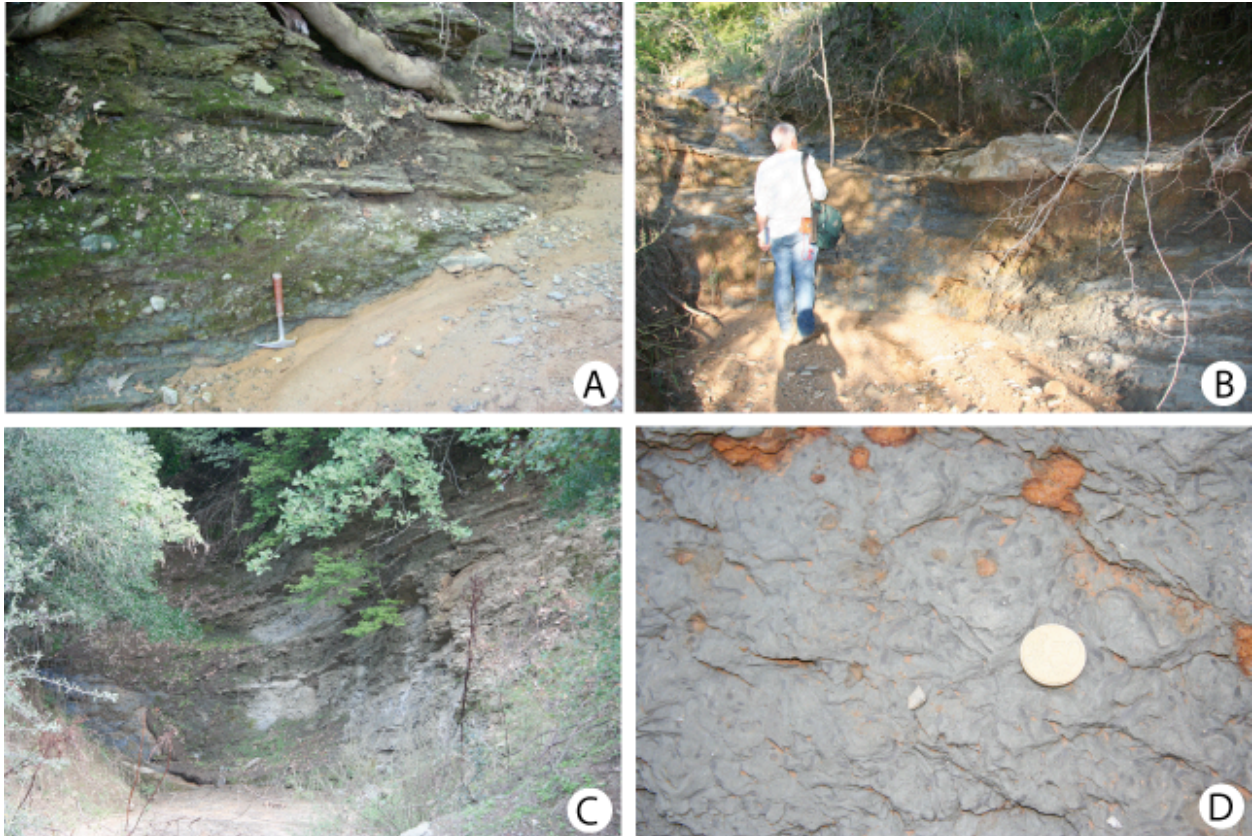
Fig. II. 32: UM6. Details of section-18. A) Matrix-supported, poorly sorted, gravel to pebble conglomerates from the base of section-18 (near boundary between UM5 and UM6). B) Lenticular limestone diagenetic (?) body (lower part of the section). C) Massive, pale grey, siltstones with interbedded thin-bedded sandstones (upper part of the section). D) Unknow bioturbations on sandy siltstones.

Two samples of siltstone have been collected from the lower part of this section. One gives a Late Oligocene to Early Miocene age (Fig. II. 31).

2. UM6: Complementary data (Sections-20 and -19)

a) Section-20

At a junction of Aghios Akakios-Mitropoli road and a small pathway, on the northern bank of a dry creek, UM6 forms a foot-hill where section-20 is exposed. It consists of about 10 m thick of siltstone interbedded with minor sandstone beds (Fig. II. 33, log-20 on the left). The

pale grey siltstones are massive (Fig. II. 33, A on the right). The sandstones are fine to medium bedded with planar cross bedding and sharp locally erosional flat base (Fig. II. 33, B on the right). The beds are non-graded to slightly normal grading. They are organized in tabular and lenticular "sheet-like"bodies. Bioturbation is rare.
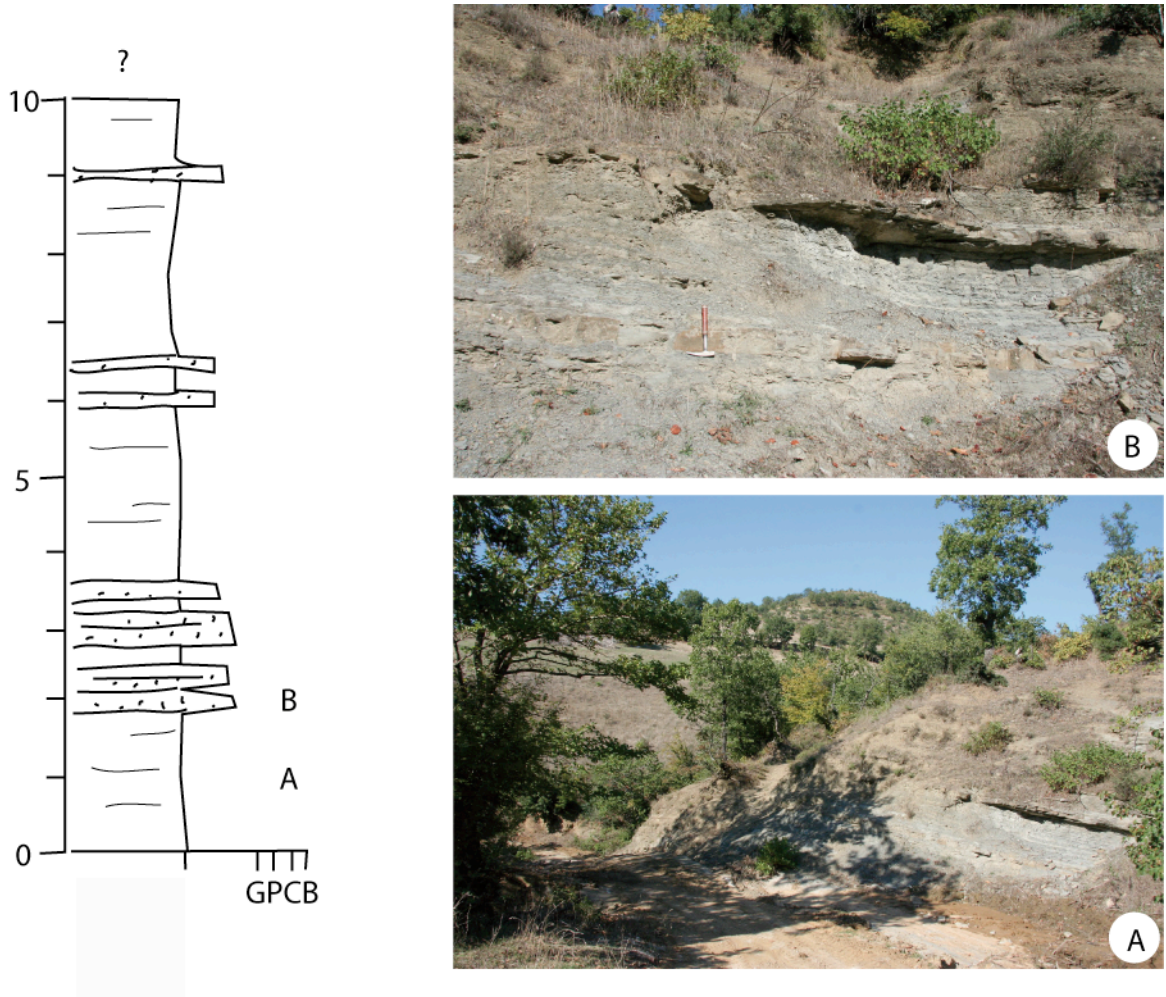
Fig. II. 33: UM6. Left) Sedimentary log from section-20. A and B: location of views at the base of log-20. Right) Views of section 20. A) Massive siltstones at a foothill. B) Medium bedded, sandstone with sharply erosive base encased in massive siltstones.

b) Complements on the lower part of UM6: Section-19

Section-19 is a combination from several exposed outcrops along road-cuttings between section-16 and -17. It is located along the road between Aghios Akakios and the Kanalia-Mitropoli road (Fig. II. 1, locality-19). The top is completed by the section-21.

Planar laminated sandy siltstone (UM6) overlies both well bedded, medium- to thin, coarse grained sandstones and thick, massive conglomerate beds of UM5. In this section, the contact between the underlying UM5 and the overlying UM6 is gradational but rapid. The

68

UM6 sandy-siltstones show planar- to ripple lamination, hummocky cross stratification-like (?
HCS), sliding-slumping sedimentary structure and calcareous nodules.

3. UM6: Outcrops of the main Kanalia-Mitropoli road

Further east, along the saddle of the Kanalia-Mitropoli road (between section-15 and -
22 see Fig. II. 1 for location), UM6 is exposed at the northern side of the road.

They are massive sandy siltstones with interbedded sandstones. The siltstones are
pale-grey to grey in fresh and pale brown when weathered. The sandstones are fine- to
coarse-grained, very thin- to thin bedded (sheet-like) and sharp-based. Compared to the other
outcrops, the amount of sandstone beds increases in this area.

4. UM6: Interpretation

The occurrence in one place of a planktic nannoflora which can reasonably associated
to the bulk siltstone facies suggests that the whole deposit is marine. The siltstone was even
emplaced below the wave base, and most of it can be considered as hemipelagic deposit.
Furthermore, the slumps recorded in this deposit suggest that it was emplaced on the
submarine basin slope. A significant supply of carbonate, likely produced by the planktic
ecosystem, may be responsible of the formation of carbonate nodules at early stages of
diagenesis.

The thin interbedded sandstones are interpreted as turbidites (sharp bases, normal
gradings, ripples). The few HCS found at the top must be considered with caution. They
normally are associated with shoreface settings but may also occur in turbidites, which is the
preferred interpretation here in the absence of any other hint of shallow water dynamics.

G. Unit M7 (UM7): sandstone-rich unit with few conglomerates and siltstones sub-units

UM7 is the youngest unit of the Mitropoli-block. It is well exposed along the Kanalia-
Mitropoli road located on the crest of the area (Fig. II. 1, localities 22 to 25) and in dry river
channels near this road (Fig. II. 1, locality-21). The lower unit boundary is not well exposed in
outcrops, however, panoramic views show the coarser-grained UM7 unit overlying the

siltstones of UM6 (Fig. II. 34). The UM7 upper boundary is not found as the Mitropoli block is limited by the main NW-SE Livadhia fault (Fig. I. 7).

The stratigraphic succession of UM7 is complicated by faults and graben structures especially in vicinity of Livadhia Fault. As the offsets of faults seem to be of limited importance, and taking into account the dippings of the beds (about 10° to 20° to NE) we estimate though that UM7 is more than 50 m thick.

The succession of UM7 deposits is complex. It consists of conglomerates, sandstones, and siltstones. Siltstones and particularly sandstones dominate over conglomerates. We subdivided UM7 into several parts: i) the lower part is composed of massive, pebble- to cobble-conglomerates; ii) the middle part is dominated by alternation of metric to decametric siltstones and sandstones; iii) the upper part is dominated by alternation of decimetric sandstone beds and thin siltstone levels*.

Fig. II. 34: Panorama view from hill-609, located SW of Aghios Akakios village, looking to NE direction. It shows reddish weathering conglomerates of the L-UM7 overlying siltstones of UM6. Limit between UM6 and UM7 is defined as bM6/7. 21 to 24 are the described sections for UM7.

1. Lower part of UM7 (L-UM7): a 30 m thick conglomeratic unit

The lower boundary of UM7 is placed at the contact of the conglomerates above the massive siltstones of UM6. Section-21 is proposed to be the type-section of L-UM7 and, further southeastward, section-22 is a complementary section.

a) Type-section of Lower-UM7: Section-21

This section is exposed on a hill at about 380 m in altitude, westward from the main Kanalia-Mitropoli road (Fig. II. 1, locality-21 and Fig. II. 35). Section-21 is over 10 m thick.
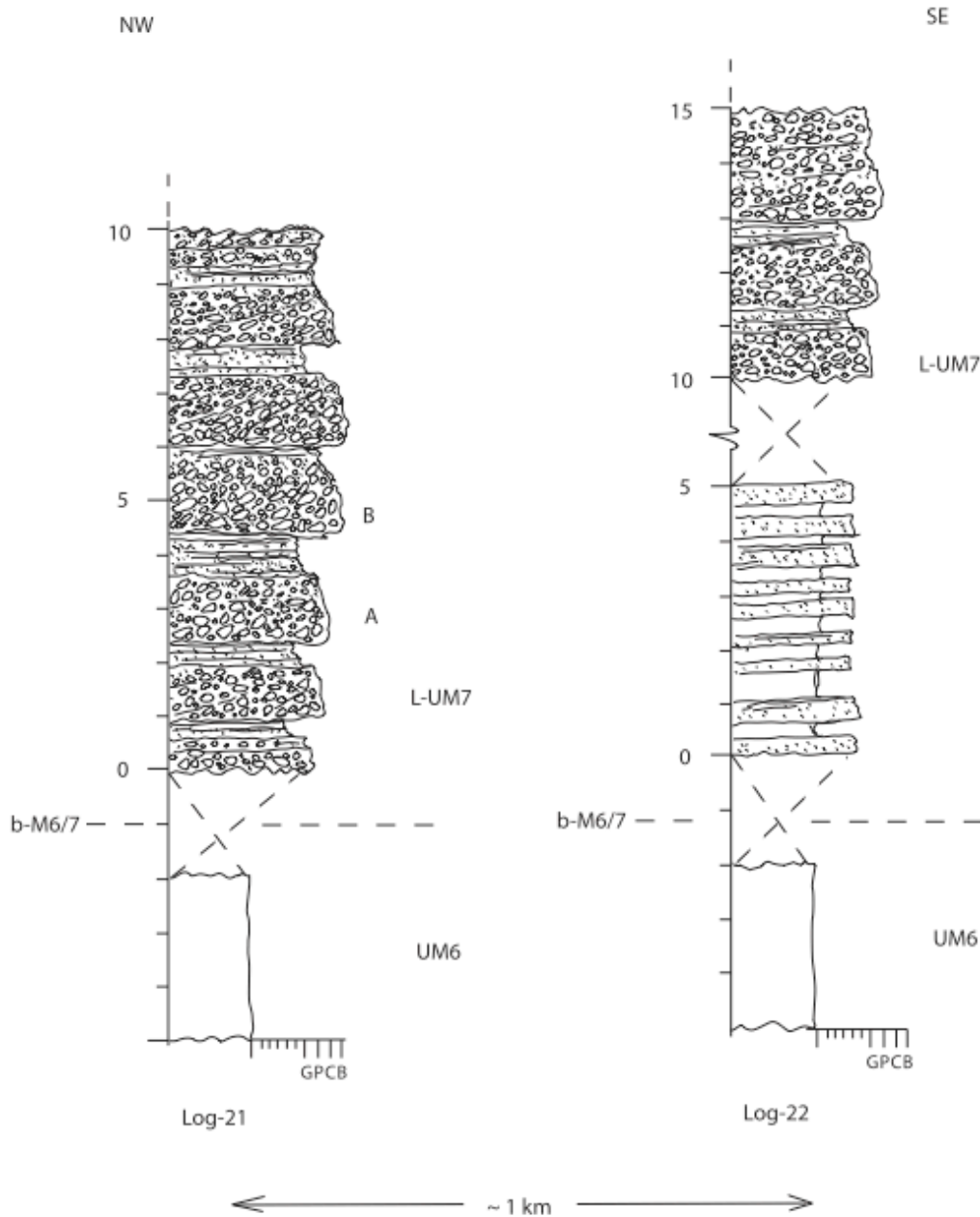
Fig. II. 35: Sedimentary log-21 and -22 showing L-UM7. L-UM7 corresponds to the first conglomerate and sandstone beds above the massive siltstone of UM6. A and B: see Fig. II. 36.

The succession is dominated by massive conglomerates interbedded with coarse-grained sandstones. The conglomerates are composed of 0.3 to 1 m thick, clast-supported, moderately- to poorly-sorted beds (Fig. II. 36A). They have sharp erosional bases and subtle large-scale cross bedding are locally observed.
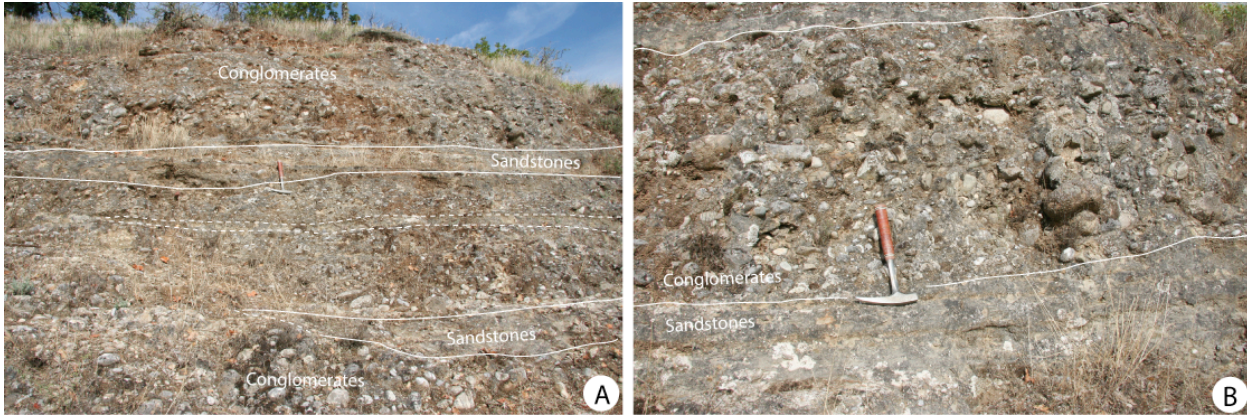
Fig. II. 36: Conglomerate facies of L-UM7 in section-21. A) Conglomerates show massive beds, 1-2 m thick, interbedded with 10-30 cm thick beds of coarse-grained sandstones. B) Close up view of the upper part of A, showing the clast-supported, poorly-sorted, non-grading, gravel- to cobble-conglomerates. It rests erosionnally above coarse-grained sandstones and is conformably capped atop by sandstones with the same facies as those below.

Clasts components include quartz, limestone, marble, gneiss and ophiolitic rocks. Clasts are sub-rounded to well-rounded and they are of gravel to pebble size (up to 10x20 cm). Clast imbrication (great axis vertical) indicates a shear towards the SW or S. Sandstones are a minor proportion of the succession (Fig. II. 35). They are mostly planar, thin- to medium-bedded, medium- to very coarse-grained (Fig. II. 36B). Occasionally, gravel- to pebble floating clasts occur within the sandstone beds.

b) Complements on L-UM7: Section-22

This section is exposed along Kanalia-Mitropoli road (Fig. II. 1, locality-22 and Fig. II. 35). Based on map extrapolation it rests above the sandy siltstones of UM6.

The measured section starts whit 5 m of thin- to medium-bedded, medium to coarse-grained sandstones interbedded with grey siltstones (Fig. II. 35, log-22). Above these sandstones, a massive conglomerate occurs of similar facies to that at section-21 (massive, reddish in weathered sections, gravel to pebble clast size, matrix- to clast-suported, moderately to poorly sorted). Coarse-grained sandstone beds are interbedded as well.

2. Middle part of UM7 unit (M-UM7): siltstones with plurimetric beds of sandstone (sections-23 and -24)

a) The lower part of M-UM7: Section-23

Section-23 is the type-section for M-UM7 (Fig. II. 37 and Fig. II. 38). It is located on the Kanalia-Mitropoli road about 500 m northward from section-22 (Fig. II. 1, site-23 and Fig. II. 37). The base of section-23 (Fig. II. 38, log-a) is exposed more eastward, down hill, at 370 m in altitude, about 300 m from the outcrop drawn as log-b (Fig. II. 39A).

Fig. II. 37: L- and M-UM7. Panorama view of localities-22 to -25 (see Fig. II. 1for location). Photo is taken from locality-13 in Fig. II. 1, looking to the north.

(1) Section-23, log-a

The basal part of M-UM7 (Fig. II. 38, log-a) is composed of alternating sandstone and siltstone beds with few conglomerates. The log-a exhibits at its base and top medium- to thick-bedded coarse-grained sandstone interbedded with siltstone.

In the middle part of the section, a 3 m thick package of sandstone and conglomerate beds is well exposed. The lower contact of this package is sharp and overlain by 1 m thick, very coarse-grained sandstone with large-scale cross bedding and floating mud clasts (Fig. II. 38 and Fig. II. 39B). Two successive, ca. 1 m-thick, massive, clast-supported, gravel conglomerate beds with well rounded floating cobbles at the base, are stacked above the cross-bedded sandstone. Planar beddings occur within the uppermost part of the conglomerates.

73
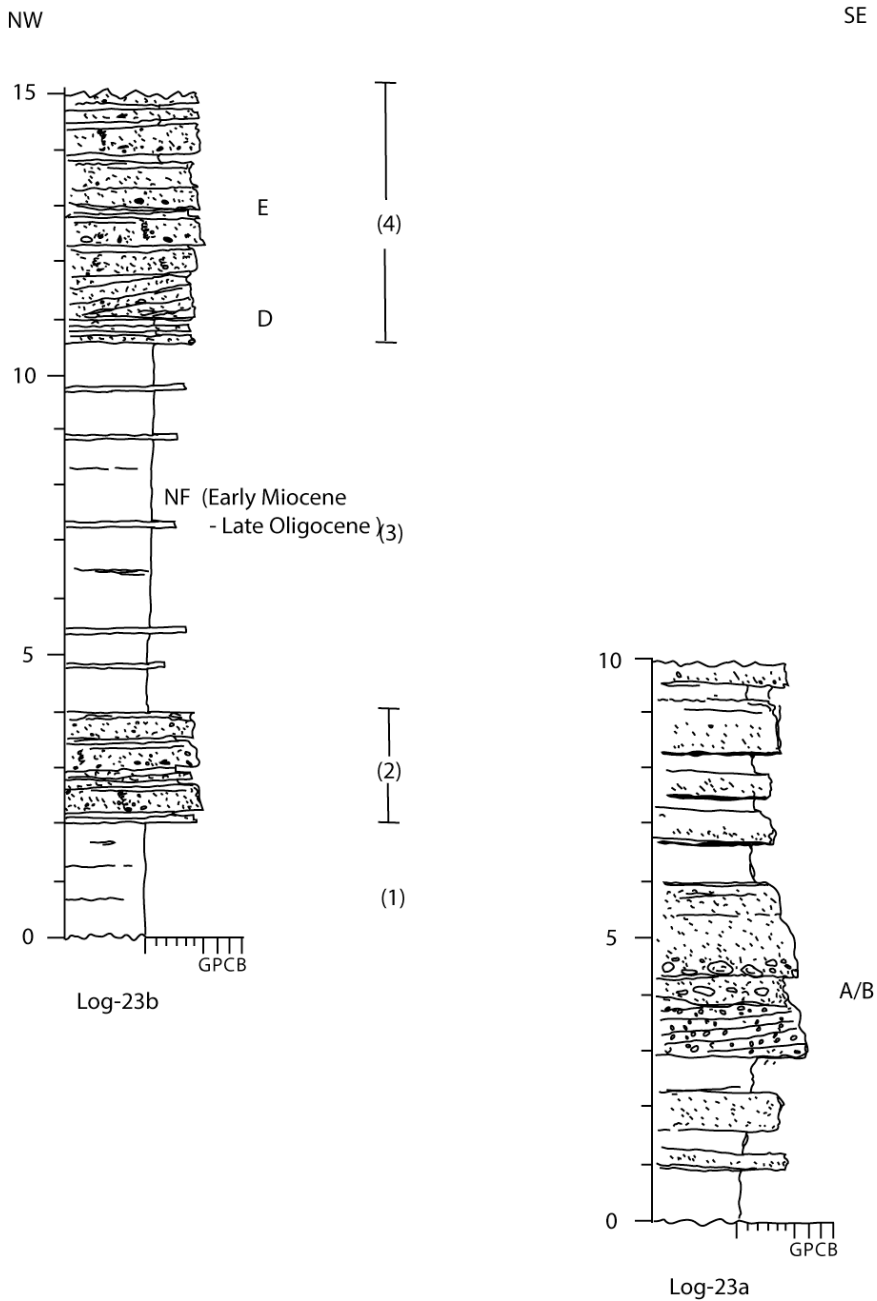
Fig. II. 38: M-UM7. Section-23. Log-a is located 300 m east of Log-b. 1 to 4 see text. Five samples for nannofossils have been collected along Log-b. One of them gave L.Oligocene-E.Miocene age. A to E: see Fig. II. 39.

(2) Section-23, log-b

Log-b outcrops on the road as an about 20 m thick succession of 4 sedimentary packages (Fig. II. 38; 1 to 4) of sandstones (2) and (4) (Fig. II. 39C) and massive siltstones (1) and (3).
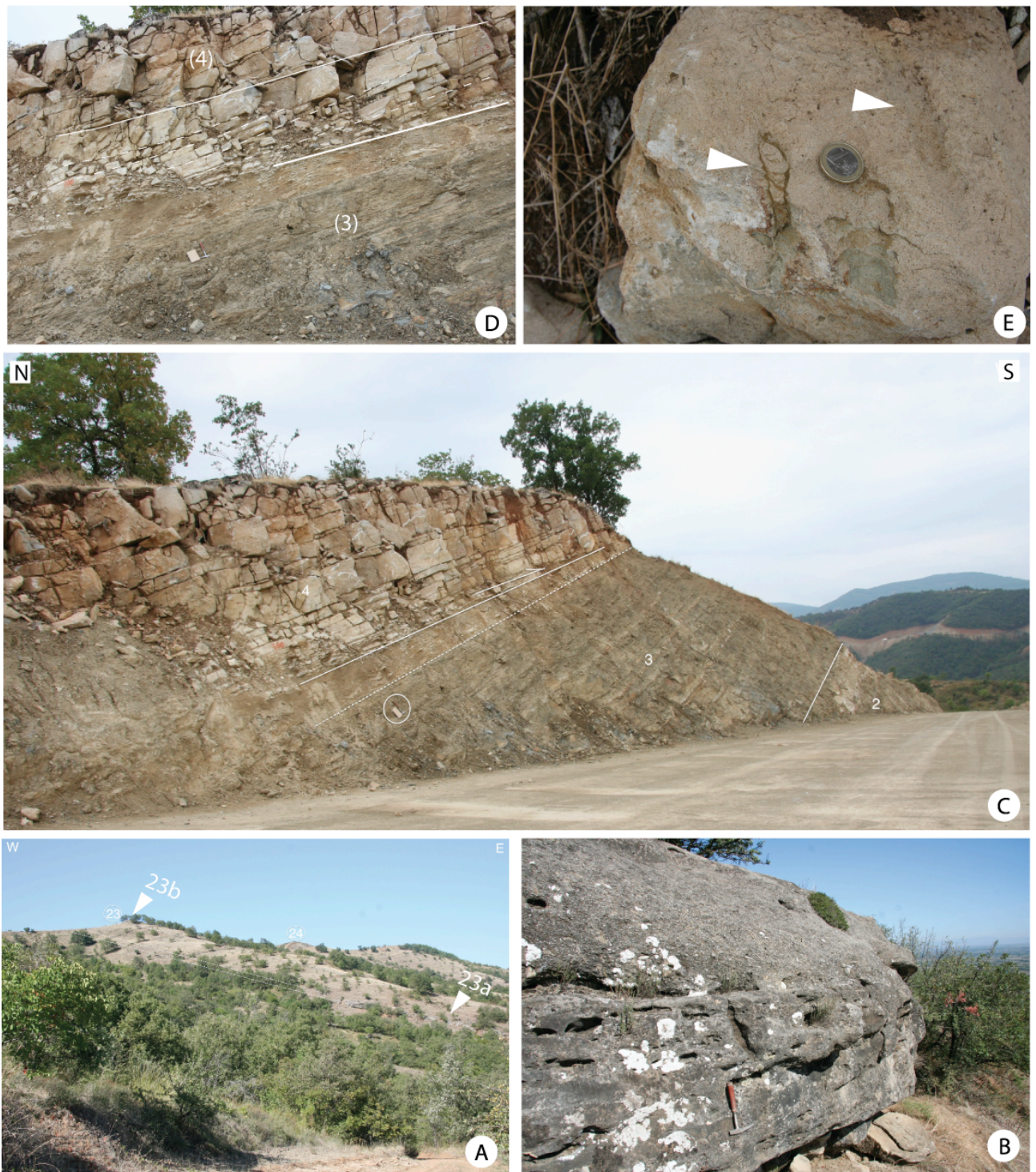
Fig. II. 39: Detailed of sedimentary facies from locality-23 (M-UM7). A) Panorama observation showing the lower part (log-a) of section-23 exposed at the eastern side of the Kanalia-Mitropoli road. B) Close up view of (A): large-scale cross bedding of 1 m thick, coarse-grained to gravelly sandstone overlain by massive, sharp erosional base, conglomerate with pebble- to cobble-clast floating at the bottom. C) Outcrop of section-23 (log-b). It shows a 6 m-thick greenish grey sandy siltstone (3) overlain by the upper sandstone (4). D) Tabular cross bedding at the bottom of the upper sandstone package (4). E) Bioturbations including vertical (Sk: *Skolithos*) and subhorizontal burrows occur within thin- to medium-bedded, very coarse-grained sandstones.

The siltsones (locally sandy siltstones), dark grey to greenish (Fig. II. 39C), are interbedded with minor sharp based, very thin-bedded sandstones. Two samples of fine-grained sediment have been collected. One of them delivered nannofossils of Late Oligocene to Early Miocene age (Fig. II. 38).

The sandstones are and medium- to very coarse-grained. They are sharp based, possibly erosionally, and locally with a sole of well-cemented, tabular crossbeds (Fig. II. 39D). Upward the packages they are thin- to medium-bedded, showing slithly normal grading. Mud clasts and vertical burrows are observed, increasing in abundance in the upper package, where *Skolithos* and *Ophiomorpha* are found (Fig. II. 39E).

b) The upper part of M-UM7: Section-24

Section-24 is exposed at the western side of the Kanalia-Mitropoli road about 150 m upward from section-23. It exhibits horst and graben structures (Fig. II. 40).
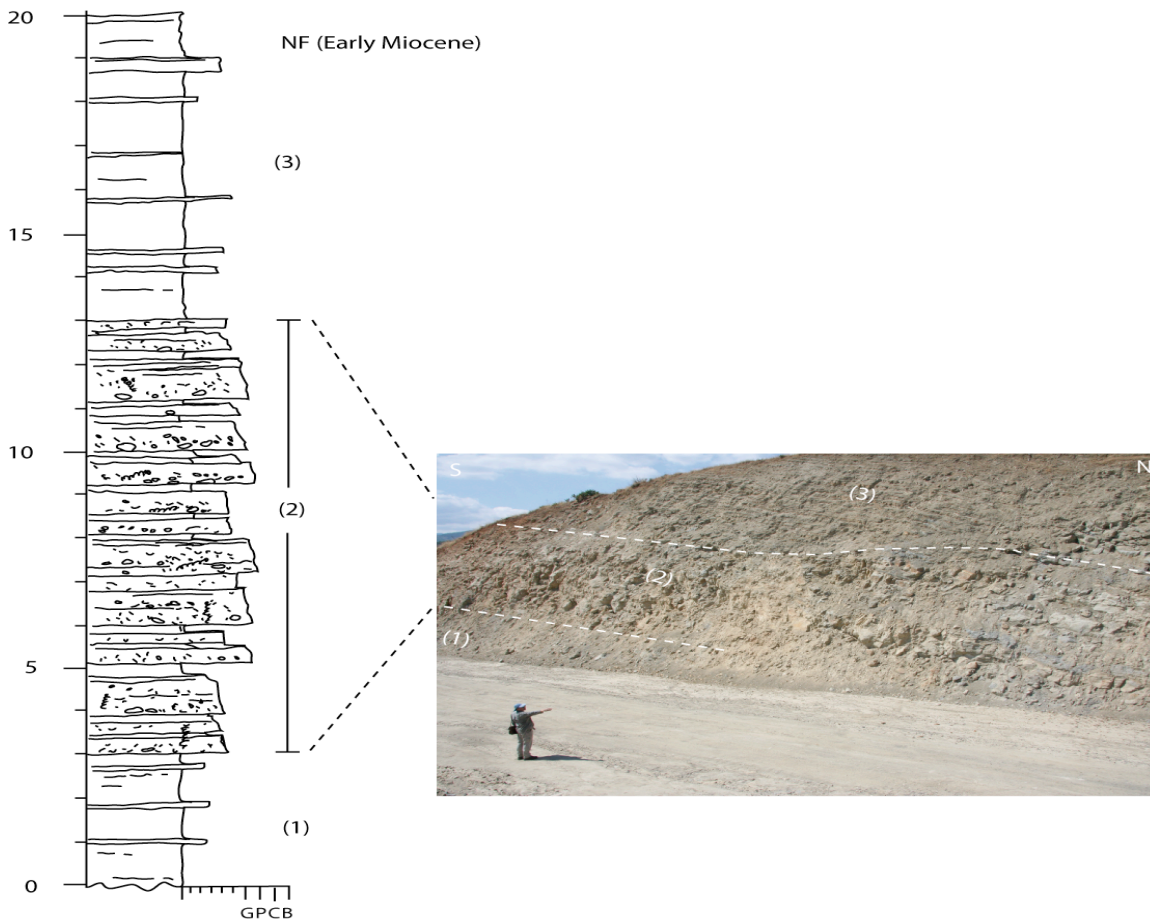
Fig. II. 40: M-UM7. (Left) Sedimentary log-24. (Right) View of the outcrop. 1 to 3: see text. NF: nannofossils.

As in section-23, it is composed of the alternation of similar silstone and sandstone bedset packages (Fig. II. 40, log-24). The siltstones, pale grey, are a bit sandier than their counterparts at section-23, and still interbedded with thin sandstone beds.

The sandstones in the sandstone bedset packages are medium- to very coarse-grained, forming 0.5-0.7 m thick, dominantly parallel beds. As in section-23, they have locally sharp erosional bases but a higher amount of floating gravel- to cobble-sized clasts. Bioturbations still include *Skolithos* and *Ophiomorpha.* By contrast to section-23, however, the sandstone package outcroping in section-24 is much thicker (about 10 m thick) and with a subtle upward thickening of the beds. The return of silstones above it is somewhat abrupt (Fig. II. 40).

3. Upper part of UM7 (U-UM7): Section-25, alternating turbiditic sandstones and siltstones with slumps

Section-25, about 20 m thick, is a combination from three distinct outcrops (Fig. II. 41).

Fig. II. 41: U-UM7. Panorama view from locality-14 (Fig. II. 1 for location), looking to NE. It shows the three sub-localities relative to section-25 (L-25, M-25 and U-25 as Lower-, Middle- and Upper-part of section-25).

They are exposed along the Kanalia-Mitropoli road at about 400 m in altitude (Fig. II. 1, locality-25) and show many normal faults. A combined sedimentary log of section-25 is presented in Fig. II. 42.

The lower outcrop (Fig. II. 42), 7 m thick, consists of parallel, tabular, medium to thick bedded gravelly coarse-grained sandstones alternating with thin-bedded siltstones (Fig. II. 43A). Sandstone beds have sharp and erosional bases and normal gradings. Occasional, maximum 1-5 cm extraformational clasts and mud clasts occur at the base. Sub-vertical

burrows of *Skolithos* type, 10-30 cm long, are not rare in these sandstones beds. The beds commonly grade upward to dm thick, grey, very thin- to thin-bedded siltstones.
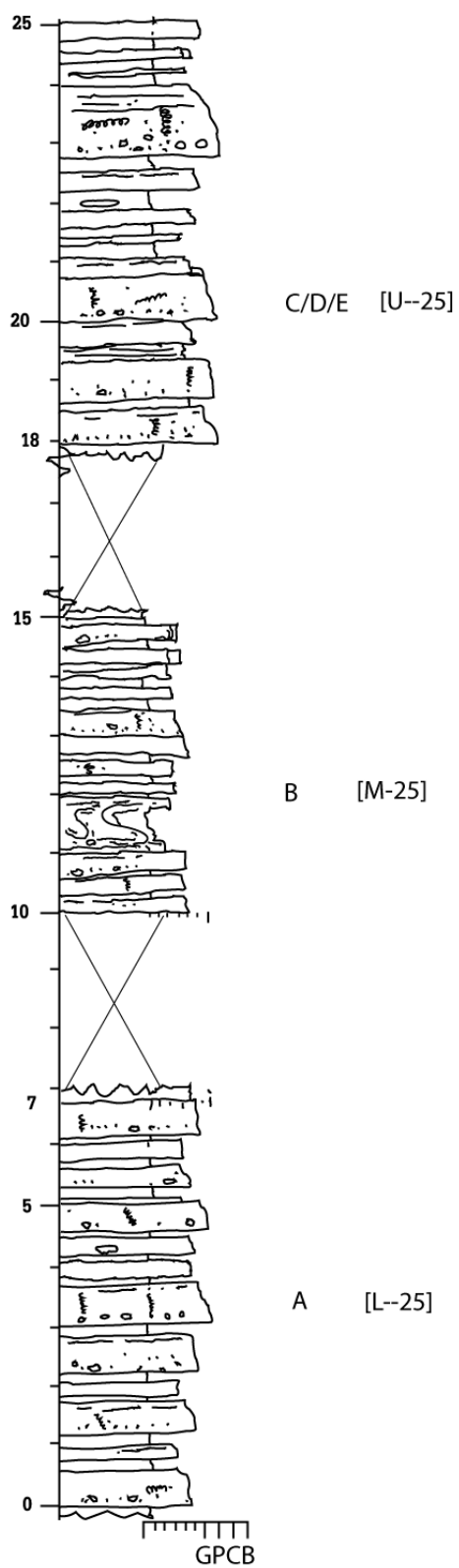
Fig. II. 42: U-UM7. Composite sedimentary log-25. A to F: see Fig. II. 43.

The middle outcrop (Fig. II. 42) consists in a 5 m thick sandstone succession similar to those in the lower one. Worthy, an interval 0.5-1 m thick, show a slumped organization sedimentary structure (Fig. II. 43B). This interval is thinning southward and the deformed layers indicate a southward or southwestward direction of shear.
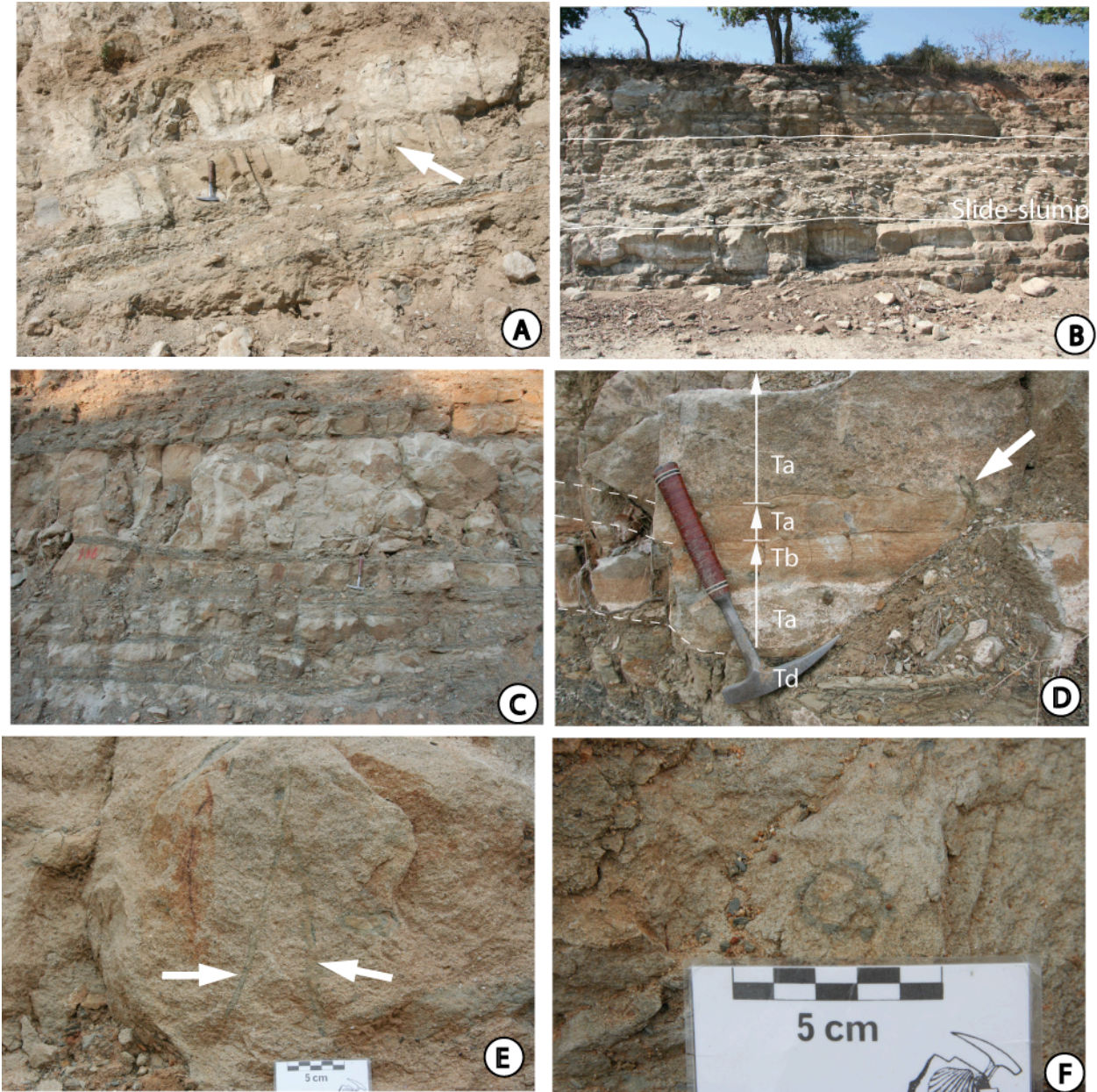
Fig. II. 43: U-UM7. A) Interbedded sandstone and siltstone from the lower part of log-25. B) Slumping bedding from the middle part of log-25. C) Medium- to thick-bedded sandstones interbedded with siltstones from the upper part of log-25. D) Planar bedding and flame structure. Ta-Td : Bouma sequences. Arrow indicated *Ophiomorpha*. E) Subvertical burrow *Skolithos* and F) *Ophiomorpha*.

The upper outcrop exhibits similar facies as well, but with coarser and thicker sandstones beds (Fig. II. 43C). The proportion of mudclasts and bioturbation degree is also increasing. Flame structures occur at the base of some beds (Fig. II. 43D).

Very coarse-grained to gravel and mudclasts are common at the bed base. As in the lower outcrops of section-25, the individual beds are fining upward, to planar bedded, medium sandstones topped by greenish grey siltstone (Fig. II. 43D: Ta, Tb and Te). In addition to *Skolithos* (Fig. II. 43E), *Ophiomorpha* (Fig. II. 43F) burrows are also present in these uppermost beds of section-25. There, bioturbation is intense with BI 1-2 (Droser & Bottjer, 1986), with regard to those two ichnospecies*.

4. UM7: Interpretation

Since the M-UM7 siltstones delivered planktic nannofossils in one place, and because this facies is homogenous throughout the unit, M-UM7 is interpreted as hemipelagic marine deposit emplaced in an averaged low energy setting, likely beneath the wave base. This does not imply a necessary deep setting because the basin was likely narrow at that time and the related fetch was small. The very thin sandstones interbedded in the silstone are interpreted as turbidites, because they are sharp-based and gradational to the silstone at the top.

The L-UM7 conglomerates are not easy to interpret. They are dominantly clast-supported, indicating tractive processes (water current drag). This is also indicated by the trough cross-stratification within some of those conglomerates and their erosional base. This general pattern is common in rivers but also in submarine channels. The sandstone beds that gradationally and conformably cap the conglomerates are interpreted as a waning flow stage of deposition, after the peak current stage. Because they are very extended laterally and somewhat isopachous, they more likely point to a marine setting.

The U-UM7 sandstones are interpreted as more proximal turbidites. The mudclasts are interpreted as rip-up clasts derived from erosion of the interbedded silts at the bottom of turbiditic flows. The tabular crossbeds at the base of the beds would represent the tractive part of the turbiditic deposit (traction carpet). As already stated for UM5, the occurrence of *Ophiomorpha* no longer can be taken as an evidence for a nearshore deposit, because some of these burrows exist in deep marine settings (Uchman, 2009).

VI. Kanalia block

Kanalia block is situated on the central part of the study area. It is bounded by Livadhia fault to the south and by Kanalia fault to the north (Fig. II. 44), localities of studied sections in Kanalia block). The exposed successions are well exposed in a dry river channel and along the roads joining Ligharies, Kanalia and north of Livadhia village. Sedimentary strata are generally NW-SE strike and dipping 20°- 40° to NE.
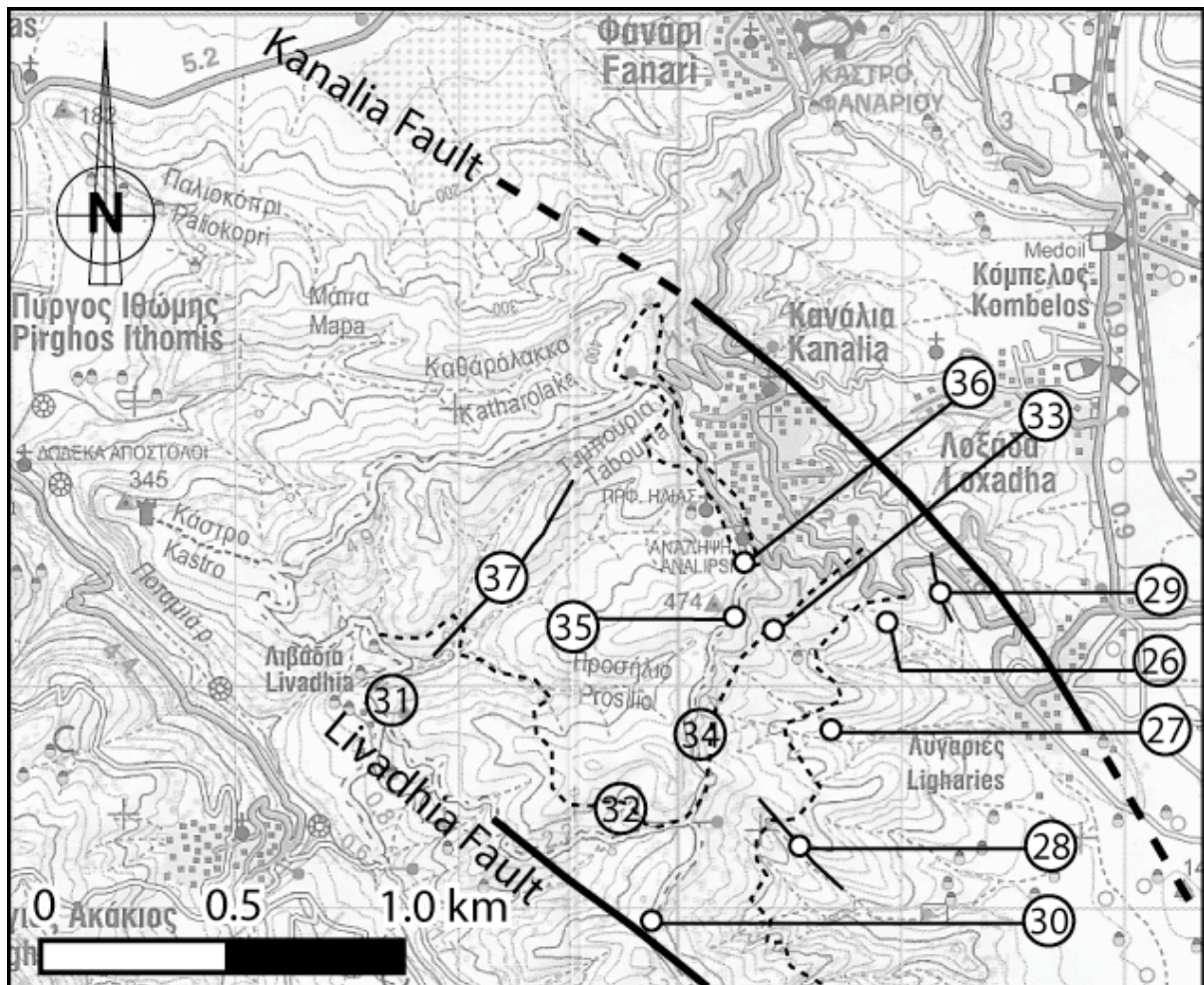
Fig. II. 44: Kanalia Block (UK). Map with the localities of sedimentary logs of Kanalia block (section-26 to −37).

Kanalia Block comprises three stratigraphic units (Fig. II. 45): two conglomerate-rich units termed UK1 and UK3, separated by a poorly exposed, high weathered, pale grey siltstone unit termed UK2.

Combining the outcrops with an areal mapping, a synthetic log of block-K is proposed (Fig. II. 46). The whole succession is approximately 200-250 m thick.
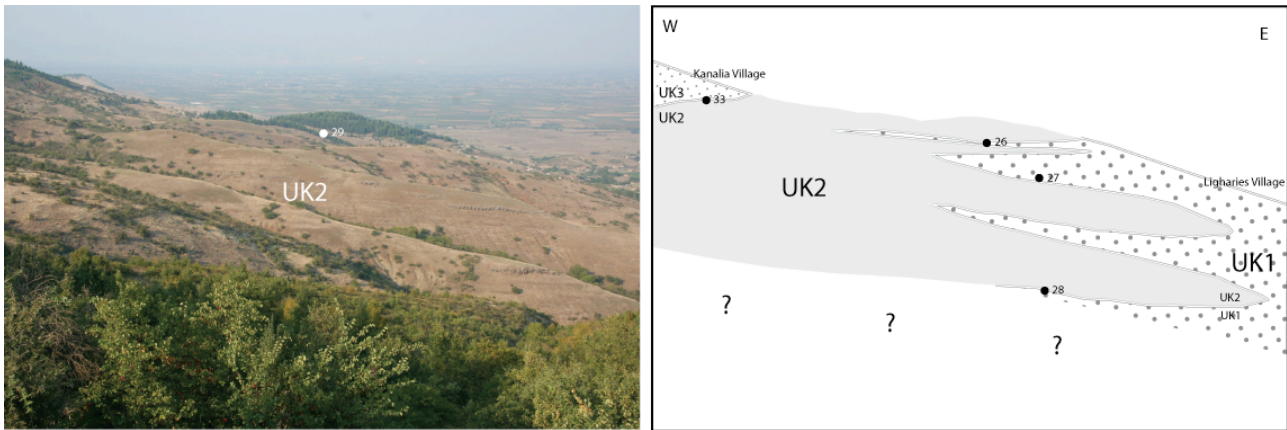
Fig. II. 45: Kanalia block, panoramic views (left) and line drawing (right) showing UK2 siltstones between UK1 and UK3 conglomerate-rich units. Looking to northward from locality-30.

From the bottom to the top, it comprises (Fig. II. 46): (i) Unit K1: Massive pebble to cobble conglomerates and medium- to thick bedded, planar- and cross beddded sandstones; (ii) Unit K2: Massive siltstones interbedded with thin- to medium planar bedded, sandstones; (iii) Unit K3: Medium- to thick bedded, tabular, gravel to pebble conglomerates interbedded with medium- to thick bedded, coarse grained sandstones.
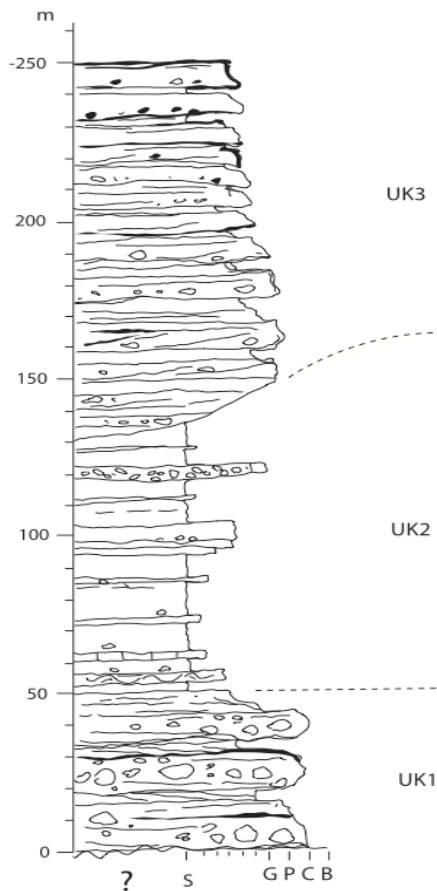
Fig. II. 46: Synthetic stratigraphic log of Kanalia Block (UK) with UK1, UK2 and UK3 units.

A. Unit K1 (UK1): Conglomerates interbedded with sandstones

UK1 is only exposed on the eastern part of Block-K. The exposure is commonly cropping out well on a dry river channel at the west of Ligharies village (at localities-30, -31, -32 and -37, Fig. II. 44).

The lower boundary of UK1 is not quite clear in the field, but might be detected on the panoramic view from site 31 looking northward. It rests erosionally on medium- to thick bedded, sandstones interbedded with siltstones. The upper boundary between UK1 and UK2 is probably gradational.

UK1 consists of massive gravel to cobble conglomerates interbedded with coarse-grained sandstones. The conglomerates are poorly sorted, massive, clast- to matrix supported with a pebble to cobble maximum clast size. Clasts are generally sub-rounded to rounded, consisting of gneiss, marble, ophiolite, radiolarite and limestone. Large floating clasts occur occasionally up to 30 cm in diameter. The conglomerates are commonly structureless, but locally thick sets display tiny large-scale trough cross beds at the base passing upwards to tabular beds up to 0.3-0.5 m thick.

The sandstones are commonly coarse to very coarse grained, moderately to poorly sorted, with trough- and planar cross-bedding. The cross-bed thickness ranges between 10 and 30 cm. Some sandstone beds are massive, structureless, with included conformable gravel to cobble conglomerates lenses. The proposed type section of UK1 is section-26.

1. Type section of UK1: Section-26

This section was observed on the northern bank of a NW-SE trending dry river channel. It is located about 500 m to the northwest of Ligharies village, at 200 m in altitude (Fig. II. 44, locality-26). It consists of a massive, pebble to cobble conglomerates interbedded with tabular, cross bedding sandstones (Fig. II. 47). The conglomerate beds, 20-50 cm thick, are stacked into about 1 m compact successions, each with an erosional, flat or irregular base. They are dominantly matrix-supported and poorly sorted, with subangulous to well rounded clasts 5-20 cm in diameter (max. 30 cm). The clast lithology comprises gneiss (40%), marble (30%), ophiolite rocks (20%) and radiolarite (10%)(Fig. II. 48A).

The conglomerates are dominantly tabular, either massive or, for the thickest packages, with oblique plane to trough cross bedding (Fig. II. 48D). Most of the conglomerate beds are non-graded to slightly normal graded (fining upward) but the thickest may have floating cobbles at their top (Fig. II. 47 and Fig. II. 48D, E).

The conglomerate beds may comprise inset lenses of cross-bedded sandstone (Fig. II. 48B and C). The interbedded sandstones are medium- to coarse grained, 10-30 cm-thick dominantly plane parallel beds. Some beds exhibit oblique plane to trough cross-laminations. Most of the deposit is reddish from the Fe-oxide coating of sand-grain size clasts, either in the conglomerate matrix or in the sandstones.
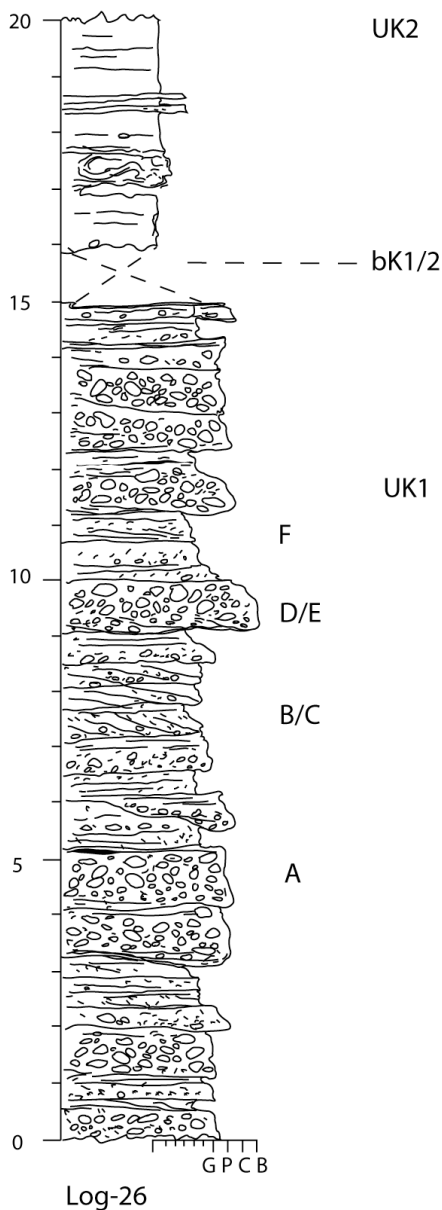
Fig. II. 47: UK1: Sedimentary log of section-26 (type-section). A to F see Fig. II. 48.

Fig. II. 48: UK1: facies deposits from section-26. A) Matrix supported, moderate to poorly sorted, gravel to cobble conglomerates. Clast component is composed of (g) gneiss, (m) marble, (o) ophiolite and (r) radiolarite. B) Three beds with tabular cross-bedding. C) Close up of a cross bedding showing fining upward from gravel conglomerate to medium-grained sandstone. D) A massive pebble to cobble conglomerate with large trough cross bedding. To the top, floating cobble clasts occur. E) An erosional base of massive pebble conglomerates cutting into the lower gravelly coarse-grained with planar cross bedding sandstone. F) Thick bed of massive coarse-grained sandstone with large cross bedding overlying massive pebble to cobble conglomerate.

2. Complementary data of UK1: Section-27

A moderately well exposed section occurs on the bank of a dry river channel at the eastern side of hill-474, about 600 m to the NE of the junction of Livadhia Kanalia-Morfovouni road and about 1 km west of Ligharies village (Fig. II. 44, site-27). UK1 is also exposed at the base of section-28 and section-29.

Section-27 is mostly composed of two facies, sandstones and conglomerates (Fig. II. 49; Fig. II. 50).
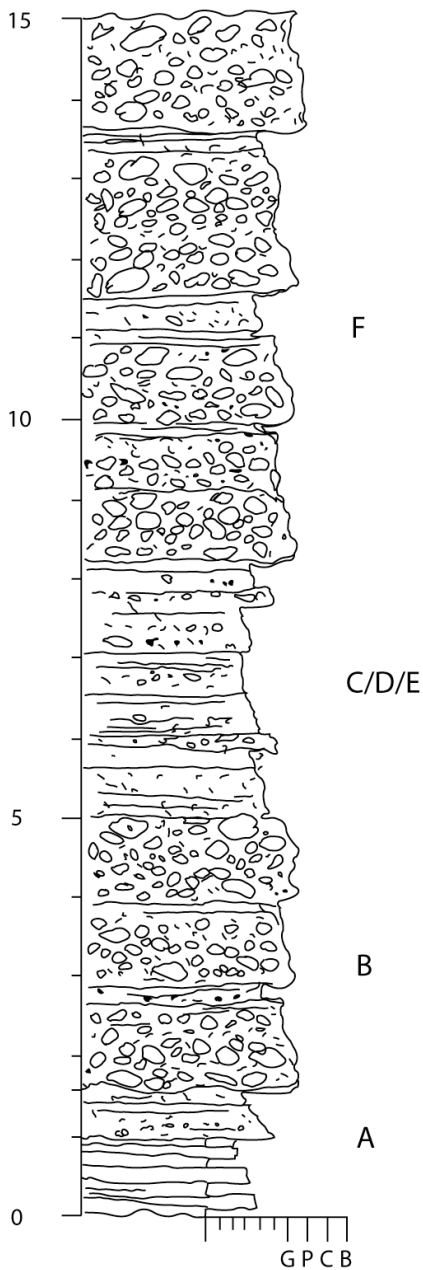
Fig. II. 49: UK1: sedimentary log of section-27. A to F: see Fig. II. 50.
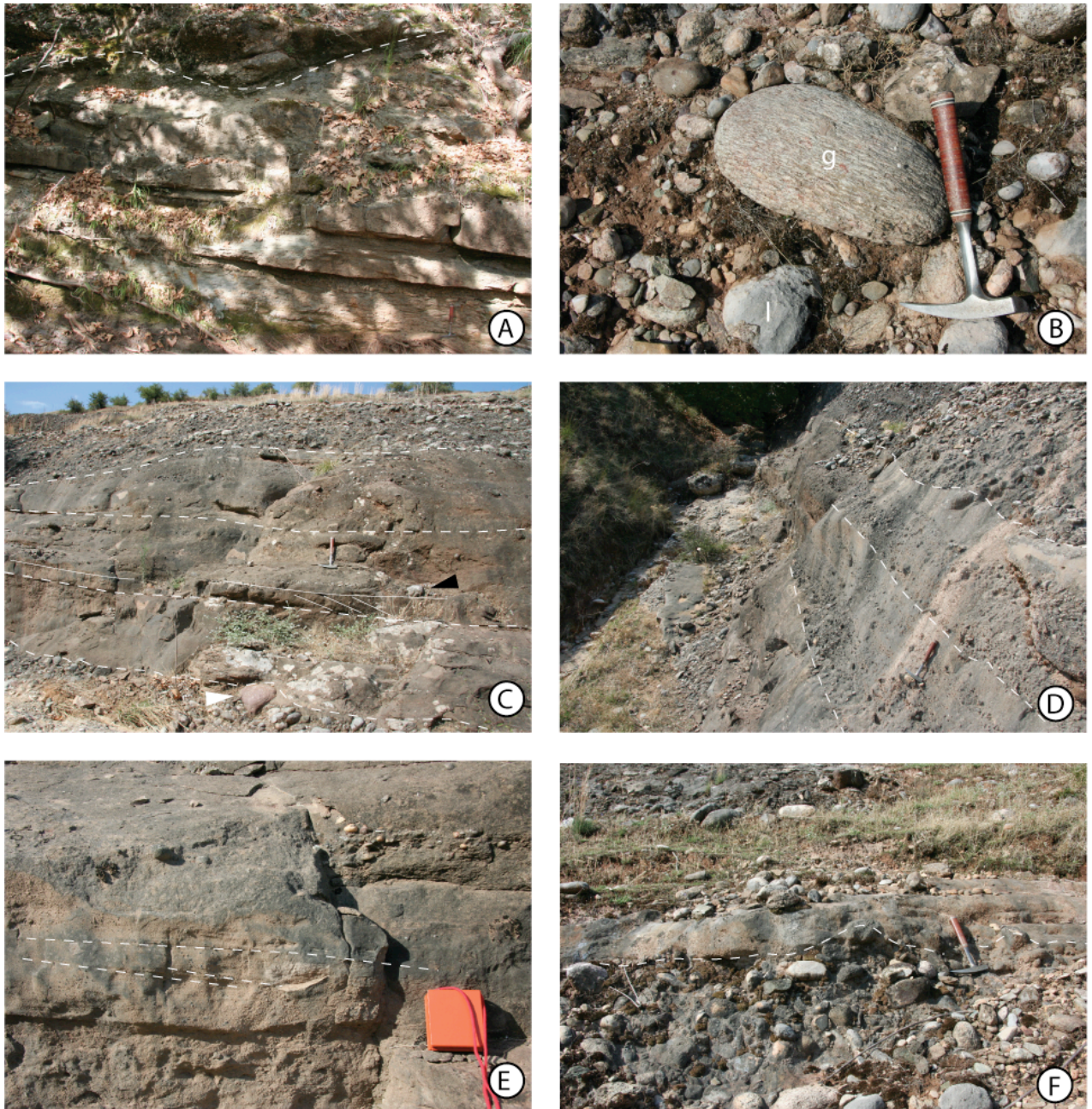
Fig. II. 50: Sedimentary facies of section-27 (UK1). A) Sharp base, thin to medium bedded fining-upward sandstone interbedded with pale grey, sandy siltstone and erosionally overlain by a gravel conglomerate. B) Poorly sorted, matrix-supported, pebble to cobble conglomerates (g: gneiss pebble). C) About 3 m thick of medium to thick bedded, medium- to coarse-grained sandstone with planar and cross bedding. D) Erosional based matrix supported, conglomerate lenses interbbed with sandstone beds. E) Close up on sandstone planar cross bedding. F) Thin to medium bedded sandstone with planar cross bedding overlying a pebble to cobble conglomerate bed.

The conglomerates are dominantly matrix-supported, with locally imbricated clasts pointing to a southwestward shear (long axis dip to NE). The clasts, sub-rounded to well-rounded, are of gravel to cobble size. Their lithology includes gneiss, white marble, limestone, ophiolite rocks and radiolarite. The conglomerate beds are from less than 30 cm to over 2 m thick, either massive and structureless (the case for the thickest beds) or composed by the

vertical stacking of 0.2-0.4 m thick plane parallel beds. In the latter case, they may exhibit scoured base and a slightly fining upward. Outsized cobbles are locally floating at the top of the thickest beds, in the upper part of section.

The sandstones are dominantly reddish due to Fe-oxide coating of gneiss. They are medium- to coarse grained and organized in tabular beds 10-40 cm thick with internal, plane parallel to trough cross-lamination. The sandstone beds are sharped-based, commonly fining-upward and they comprise rare vertical burrows (mostly crossing plane parallel laminae). At the bottom of section, they are interbedded with 0.1-0.2 m thick intervals of pale grey siltstone. In the mid part of section, they also are interbedded with decimeter-thick lenses of gravel conglomerates (Fig. II. 50D).

The overall organization of the section shows a larger scale interbedding of 3-4 m thick successions of conglomerate-dominated packages alternating with sandstone/siltstone dominated ones, and without clear gradational evolution.

3. UK1: Interpretation

The sand-sized quartz grains in UK1 are pervasively coated by limonite (Fe-oxide) in most outcrops. This is a hint for deposition in the subaerial realm. The sandstones are coarse- to very coarse grained, and poorly sorted. This suggests a relatively short distance of transportation and a high-energy setting of deposition. Almost all beds (sandstone and conglomerates) reflect deposition under tractive process (prominent bedding in the conglomerates and lamination in the sandstones, clast-supported fabric of the conglomerates). The large crossbeds were formed by meter-thick migrating bedforms in a high energy current, as evidenced by the floating pebbles in the sandstones. The complex interbedding of sandstone in the troughs of the conglomerates suggest that water-depth was shallow enough for the flow being sensitive to the bedform height variations. We therefore interpret the conglomerates and sandstone of UK1 as fluvial, likely braided plain deposits. The clast imbrications suggest that the river was sourced to the NE (Pelagonian) and flowing to the SW.

B. Unit K2 (UK2): Massive siltstones interbedded with thin-bedded sandstones

UK2 is exposed on a dry river west of Ligharies village, up to hill-474. It is also exposed along a small pathway going eastward from Livadhia near the Kanalia-Morfovouni road (Fig. II. 44, localities-30 to -33).

It comprises a minimum 80-100 m thick succession of massive, pale grey to pale brown siltstones interbedded with sheet-like, fine- to coarse-grained sandstones. The lower boundary of UK2 is generally sharp, above the massive pebble conglomerates and cross beddded sandstones of UK1 at localities-26, -27 and28 (Fig. II. 44). In the westernmost part of Kanalia-block, at locality-31, UK2 rests directly on the Koziakas Mesozoic basement. The upper boundary observed at site-33 is an erosional surface at the base of the incised channel linked to the conglomerate and sandstone deposits of UK3. The proposed type-section of UK2 is section-33.

1. Type section of UK2: log-33

This section (Fig. II. 51, log-33) is located northward from Ligharies going to Kanalia village, about 300 m from Kanalia (Fig. I. 7).

Siltstones of UK2 form the eastern escarpment of hill-474 (Fig. II. 44, locality-33). It is incised by several E-W directed dry river whereby UK2 is cropping out. Section-33 is from a wall of one of these dry river beds and combined with several outcrops around (Fig. II. 44, site-33 and Fig. II. 52A and B). Section-33 is dominated by massive siltstones of UK2, the lower boundary of which is not clearly exposed. The upper boundary of UK2 in this section is an erosional surface overlain by conglomerates and sandstones of UK3 (Fig. II. 52C and Fig. II. 53D and F).

The siltstone is massive, pale brown to pale grey, cemented by carbonates. Locally, well rounded gravel clasts (range from 0.5-2.0 cm) and leaf fragments occur within the siltstones (G, Fig. II. 51 and Fig. II. 53G). Sharp based, thin, sheet-like and nearly planar sandstone beds occur within the siltstone (Fig. II. 53E). Sliding/slumping evidence and also calcareous concretions are locally found. The siltstone is continously exposed over 15 m in thickness but can be extrapolated to >50 m thick.
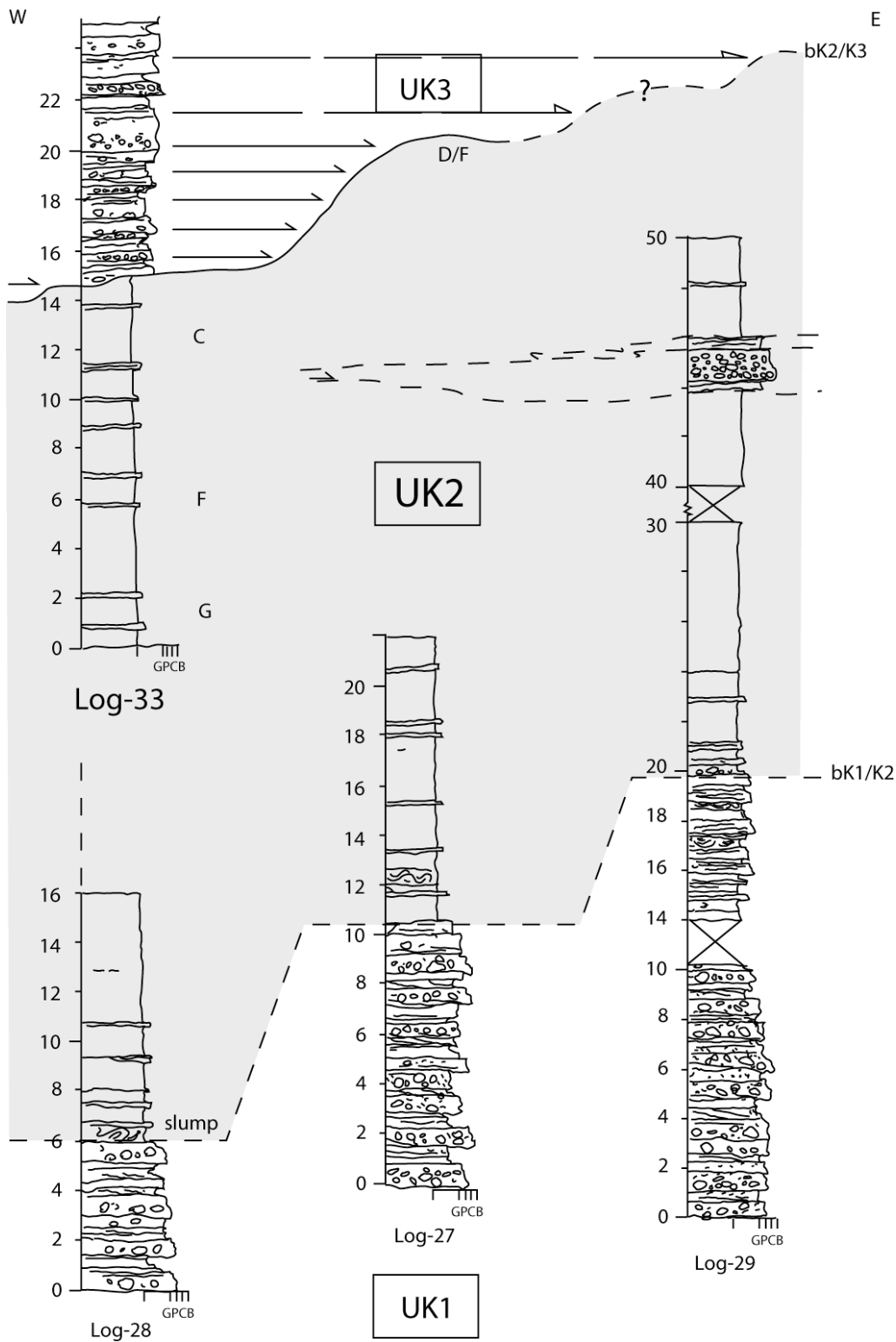
Fig. II. 51: UK2: Sedimentary log of UK2. Type section, Log-33 and complementary logs-27 to -29. C to G on log-33: see Fig. II. 52 and Fig. II. 53.

At the top of this section, the siltstone of UK2 is incised by a steep erosional surface at least 15-20 m in amplitude. This surface dips 20°-30° to NW and becomes subhorizontal to

the west. It is onlapped by conglomerates and sandstones of UK3. Sedimentary strata of both the lower UK2 and the upper UK3 are subparallel.
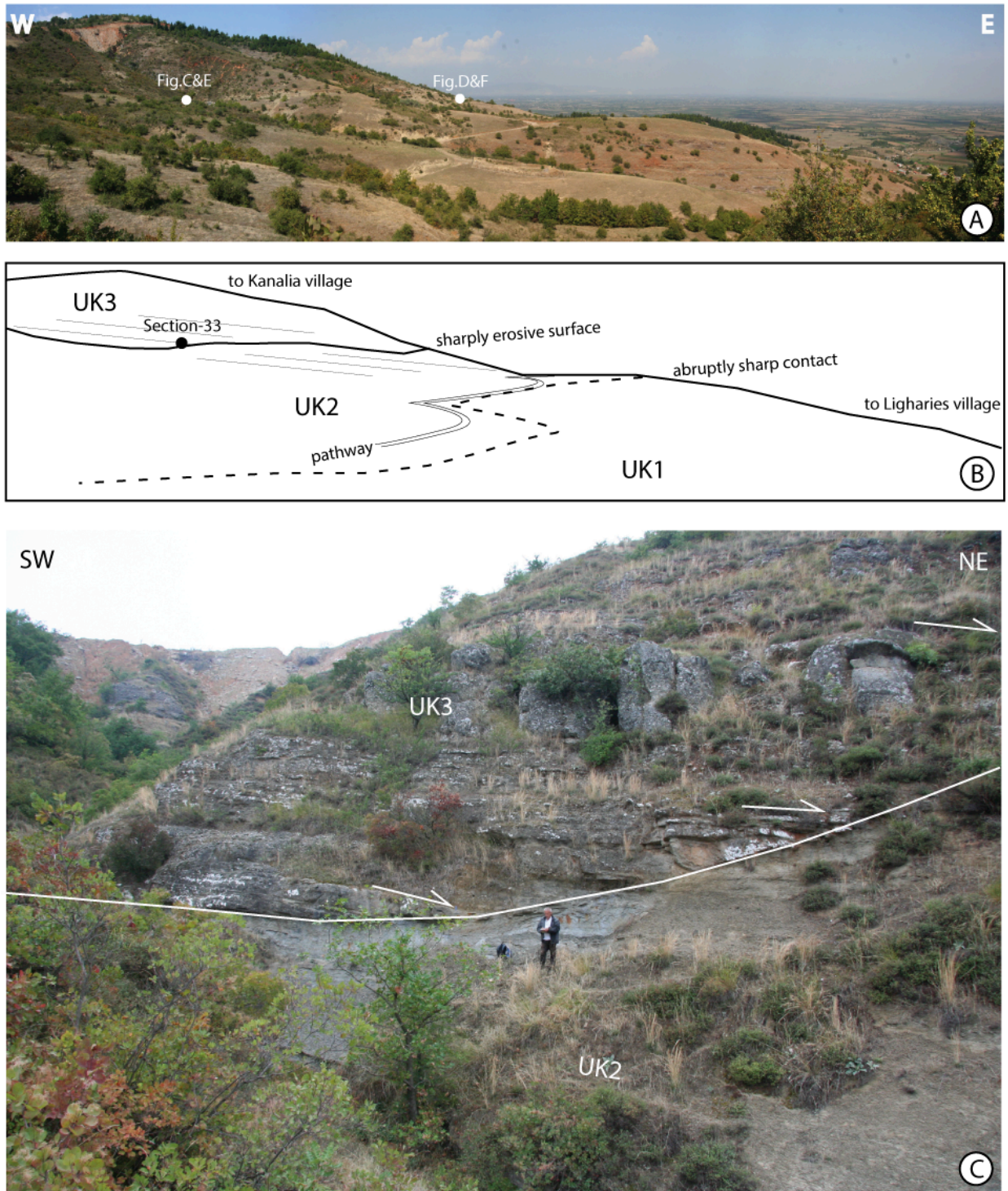
Fig. II. 52: UK2. A) and B) View to the north from section-30 showing UK2 between UK1 and UK3. C) Well-exposed erosional contact of conglomerates and sandstones of UK3 with underlying massive siltstones of UK2 at section-33. The contact is sharp with at least 15 m incision into the siltstone. It dips 20°-30° to NW and becomes subhorizontal to the west.

Fig. II. 53: UK2. D) Erosional contact between UK2 and UK3. For detail, see (F). E) Thin, sheet-like, sandstone beds insert in the grey siltstone of UK2 exposed in the dry river channel at section-33. F) Detail of (D). Medium to thick sandstone and conglomerate beds UK3 onlapping on the underlying UK2. Strike and dip direction of both the lower and upper strata across this unit boundary are the same. G) Leaf fossil in sandy siltstones of UK2.

2. Transition between UK1 and UK2

a) Description of Section-29: Upper UK1 to lower UK2.

Section-29 is located on a dry river, parallel to Ligharies-Kanalia road at about 100-200 m northwest of Ligharies village (Fig. II. 44, locality 29). Approximately, log-29 is 50 m in thickness.

This section shows a fining upward trend, with conglomerate packages and massive sandstones at the base belonging to UK1 (Fig. II. 54, log-29, 1). The lower part of section 29 comprises a poorly exposed and strongly weathered, pale brown to reddish in weathering, moderately cemented, massive, coarse-grained sandstone interbedded with gravel to pebble conglomerates (Fig. II. 55A). This coarse-grained deposit represents an equivalent to the upper part of conglomerates UK1 (Fig. II. 47 and Fig. II. 49). Although it is not well exposed,

the contact between UK1 and UK2 might be an abrupt grain-size shift to fine-grained sandstone and siltstone deposits.
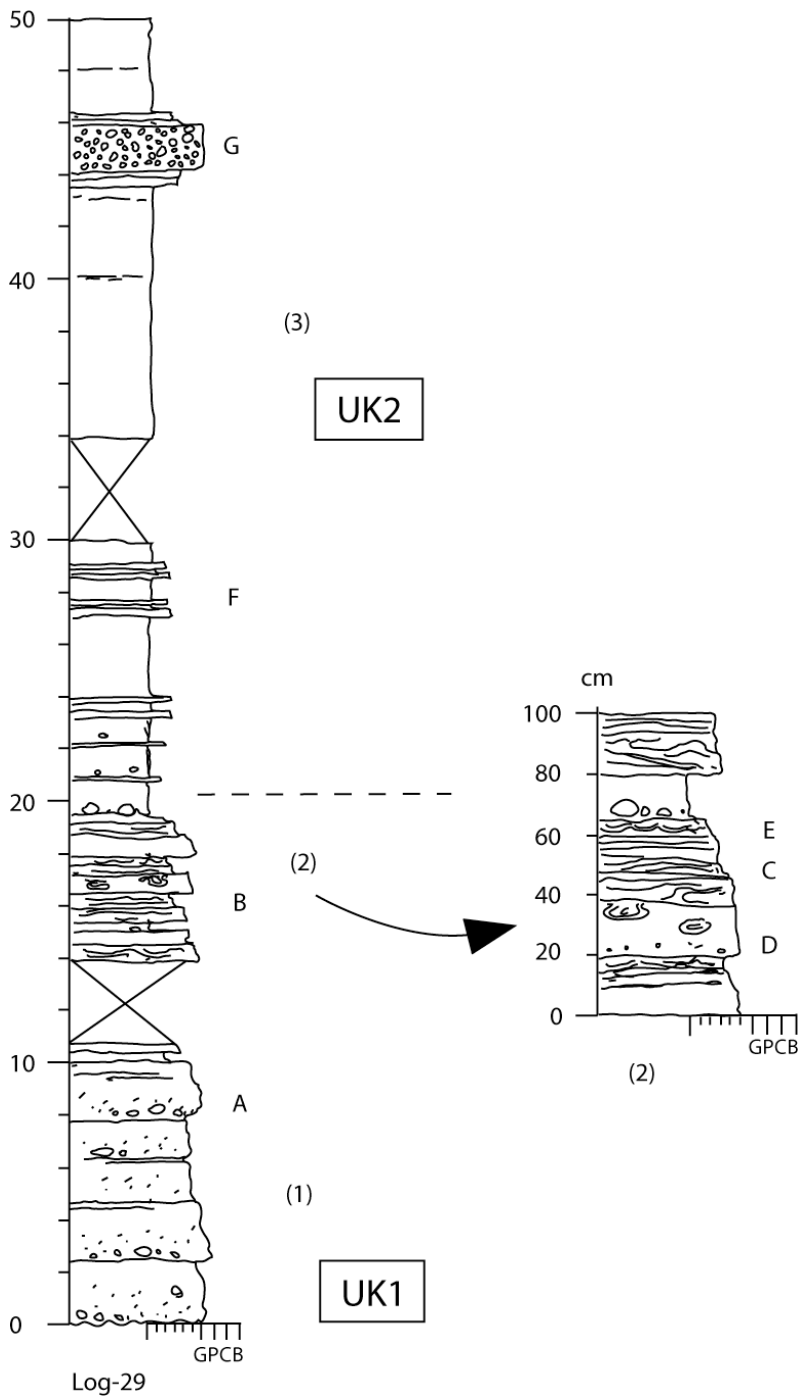
Fig. II. 54: Sedimentary log-29 with detail of a calcareous sandstone bed (log 29, 2): Transition between UK1 and UK2. 1 to 3: see text. A to G: see Fig. II. 55.

Above the contact a remarkable facies is outcropping, with well-preserved sedimentary structures (Fig. II. 54, log-29 (2)). It is a 3 m thick package of well-bedded, well-cemented, calcareous sandstone, organized in bedsets 20-60 cm thick (Fig. II. 55B).
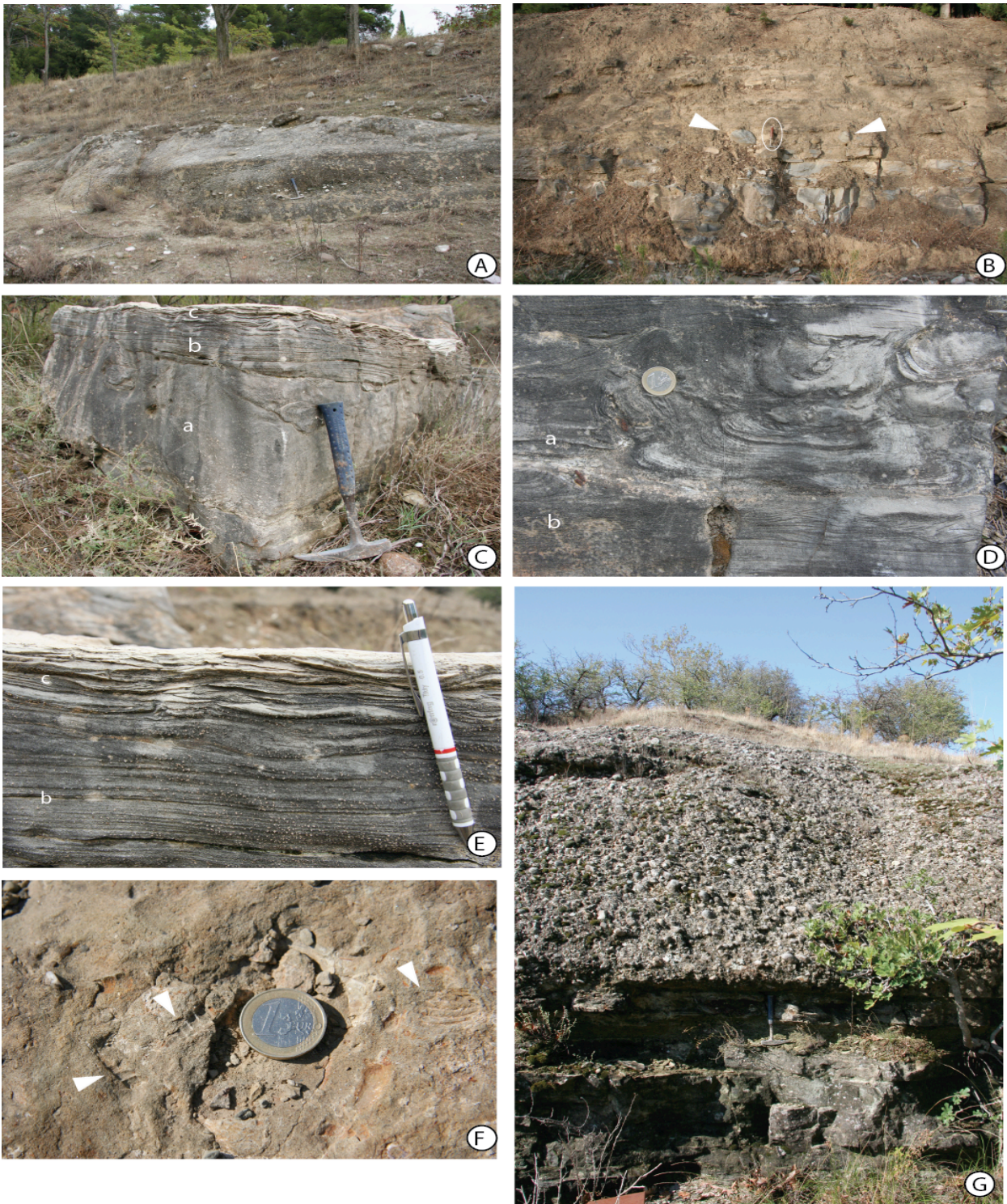
Fig. II. 55: Sedimentary facies from section-29 (transition between UK1 and UK2). Location of A to G: see Fig. II. 54. A) Poorly exposed, highly weathered, pale brown, gravelly to coarse grained, massive sandstone with pebble conglomerates at the lower part of section-29. B) Calcareous sandstone package (5 m thick) with gravel to cobble conglomerate floating at the top. Occasionally clasts are up to 25 cm in diameter (white arrow). In the circle, geologic hammer for scale. C) Fining upward calcareous sandstone bed with (a) massive and (?) pseudo nodule, (b)- hummocky-like, trough cross and planar cross stratification and (c) climbing ripple. D) Close up of (C): trough cross bedding (b) overlain by an erosional based, convoluted bedding with (?) pseudo nodule structure (a). E) Planar bedding (b) under climbing ripple or current ripple cross stratification (c). F) Fossil of gastropods and shell fragment. Coin for scale. G) About 2 m thick of massive grain supported, sub-rounded to well rounded, gravel to pebble conglomerate bed with, sharp base, coarse-grained sandstone at the bottom.

94

The bedsets have a sharply erosional base and a fining-upward trend. In the lower part the bedsets, the individual beds exhibit sliding/slumping structures, flames or bowls and pillows (Fig. II. 55C and D). They are grading upward to hummocky-like, trough-cross and planar cross bedding. Current ripple cross stratification (climbing ripples) is present at the top along with floating gravels and cobbles (Fig. II. 55E).

Above these beds, the UK2 facies in section 29 is similar to that in the type-section 33. Some shell fragments and entire gastropods are observed (Fig. II. 55F). The top is dominated by siltstones interbedded with thin- to medium bedded sandstones and an isolated thick, massive and clast-supported conglomerate bed (Fig. II. 54, log-29) and (Fig. II. 55G).

b) **Complementary data on the transition UK1 to UK2: section 26**

The upper part of section 26 is dominated by massive siltstones of UK2 (Fig. II. 47, a top of section; Fig. II. 56).
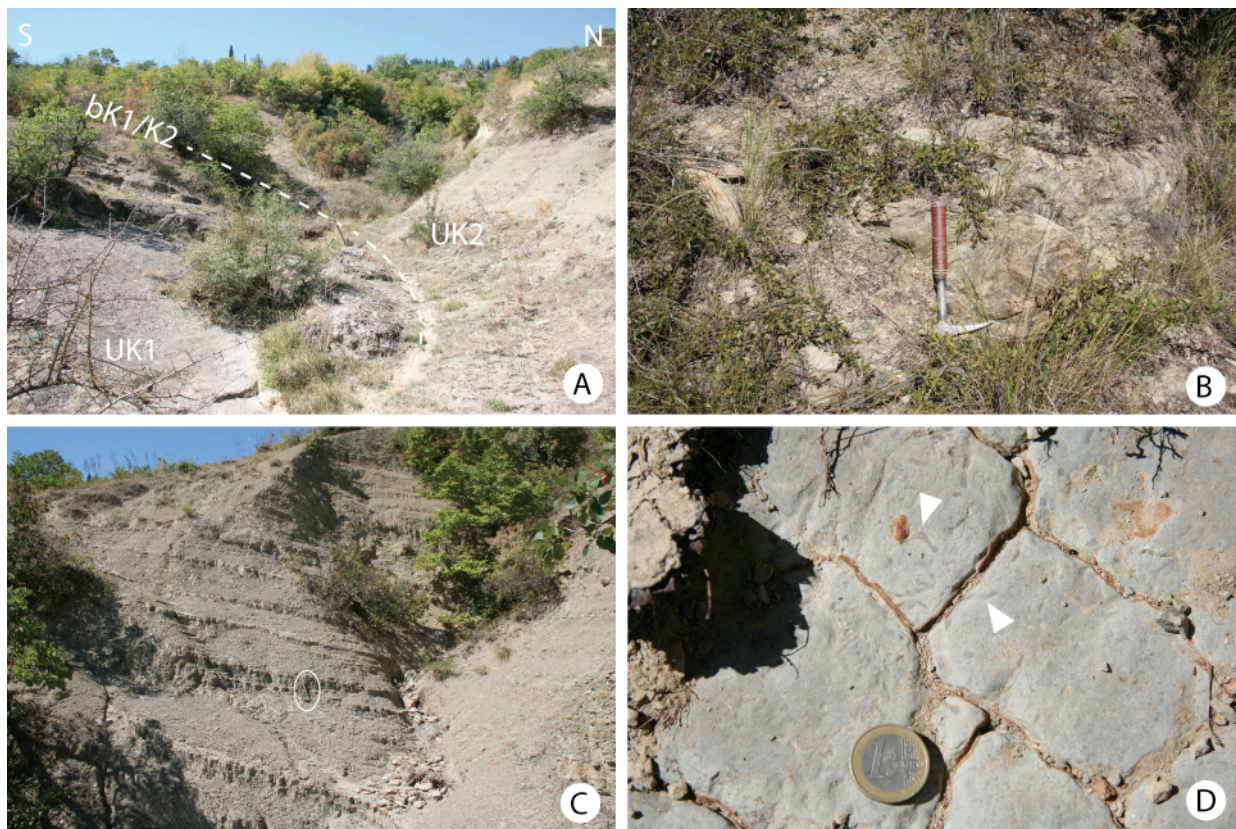
Fig. II. 56: UK2. Sedimentary detail of siltstones interbedded with sandstones of UK2 from the upper part of section-26. A) A sharp contact between the lower conglomerates of UK1 and the upper massive siltstones of UK2. B) About 1 m thick of slumping/sliding layer at the base of siltstones UK2. C) Massive pale grey siltstones interbedded with thin, sheet-like sandstones of UK2. Geological hammer for scale. D) Unidentified bioturbation (indicated by white arrow) at the top surface of calcareous sandstone encased by siltstone. Coin for scale.

The contact between UK1 and UK2 is sharp (Fig. II. 56A). Above the contact, the siltstone is pale brown with floating gravel clasts. About 50 cm thick of sliding/slumping bed is found 3 m above the contact (Fig. II. 56B). In the field, the massive siltstone can be followed upward on the sequence over more than 50 m thick. Continuing up the succession, pale brown siltstones become grey. Interbedded thin, sheet-like, medium to fine grained sandstone with calcareous cemented bodies encased by siltstone become more numerous (Fig. II. 56C). Unidentified bioturbations, about 0.2-2 cm long, are found on the surface of sandstone (Fig. II. 56D).

3. UK2: Interpretation

The silstone has a locally high amount of lime mud, marked by nodule layers. The siltstone is massive, and was not affected by hydrodynamic events, as evidenced by the delicately preserved leaf prints. The deposition rate was high enough for organic matter being buried. This is also suggested by the numerous floating granules in the siltstone. The interbedded thin sandstones are interpreted as distal turbidites. The thickest sandstone bedset at the base of the unit show a typical succession of high-density turbidite, with water escape features (convolutes) and climbing ripples. The 2m-thick conglomerate bed isolated in the siltstone could represent a slope channel-fill, which suggests that sediments coarser than the silts could be present further basinwards. Finally, it might be reasonable to interpret UK2 as a hemipelagic slope deposit.

C. Unit K3 (UK3): Pebble to cobble conglomerates and sandstones

In general, UK3 extends at the western part of Kanalia-block. It is very well exposed, especially along Kanalia-Morfovouni road (Fig. II. 1 at sites-34, -35 and -36). It is also cropping out at Kanalia village and in dry river beds west and northwest of hill-474, north of Livadhia village.

UK3 is a coarse-grained unit consisting of matrix- and clast-supported, pebble conglomerates interbedded with medium- to very coarse-grained sandstone which become dominant in the upper part of the unit. It has an erosive lower boundary, incising the underlying siltstones of UK2. To the western part of Kanalia-block, UK3 rests either

erosionally on UK2 or onlaps the Koziakas Mesozoic basement. The minimum thickness of UK3 is about 100 m. The unit is limited to the top by the Kanalia Fault.

Type-section of UK3 is section-35. Complementary sections include section-32 to -33, which correspond to lower boundary of UK3 and section-36 to -37, which correspond to the upper part.

1. Type-section of UK3: Section-35

Section-35 is exposed along Kanalia-Mitropoli road (at hill-474) and located about 400 m southward from Analipsi cemetery (Fig. II. 44, site-35; Fig. II. 57 and Fig. II. 59A). The outcrop on the western flank of the road is about 30 m wide and 15 m high (Fig. II. 58).
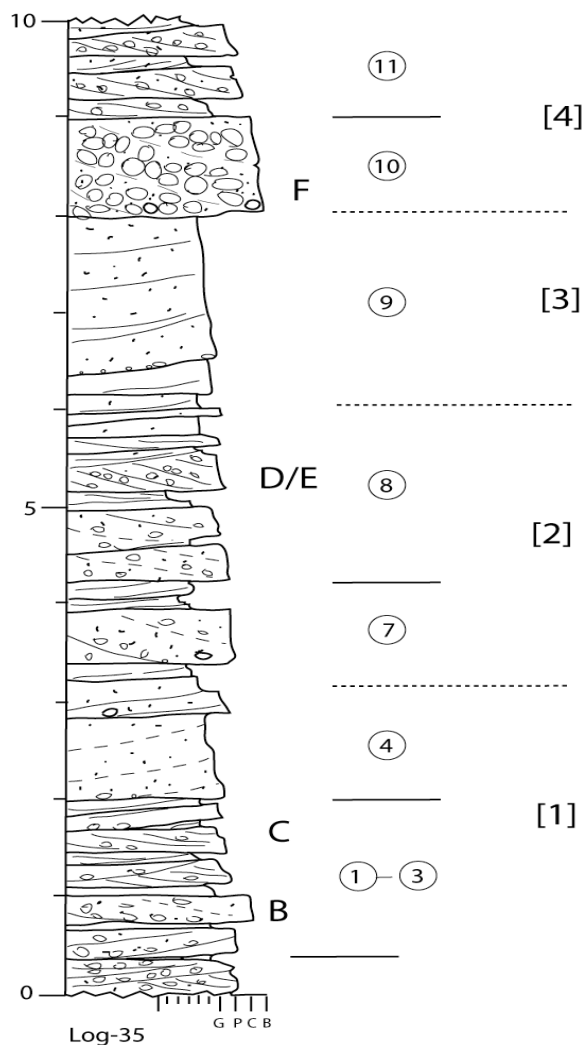
Fig. II. 57: UK3, Type section. Sedimentary log-35 with a view of the main outcrop. [1] to [4]: see Fig. II. 59A. A to F: see Fig. II. 59. 1-11 in circles: see Fig. II. 58.
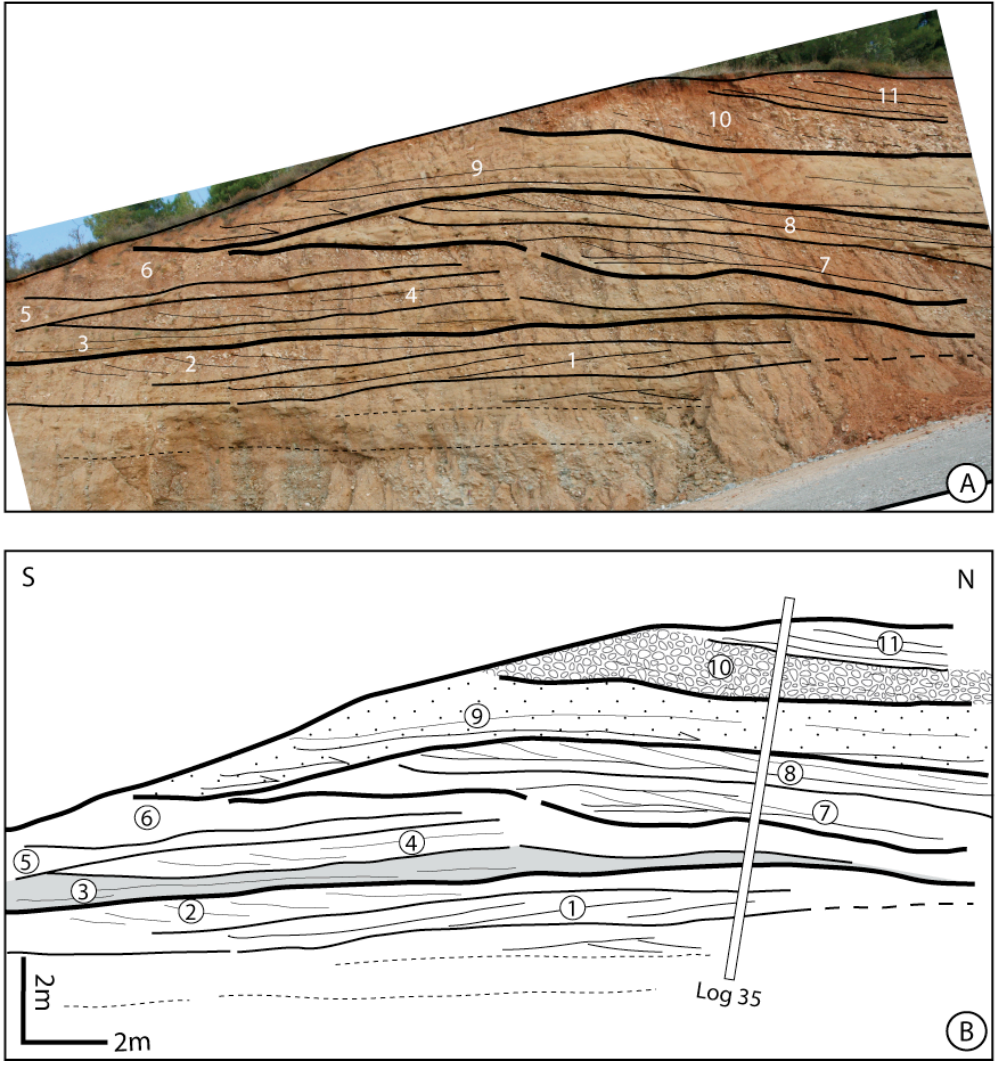
Fig. II. 58: UK3. View of section-35 with its interpretation. 11 beds have been distinguished, numbers only refer to this Figure. This section-35 is dominated by conglomerates (ie. 1 and 10) interbedded with sandstones (ie. 9). Large cross bedding exist (7 and 8).

The lower limit of UK3 is not observed on this section 35. However, this boundary is well exposed on the east of the hill-474 where it has been described before. It's a very clear erosional contact with huge channels (see Fig. II. 51, log-33; Fig. II. 52C Fig. II. 52A, C; Fig. II. 53D, F). The upper boundary of UK3 is not known because of the Kanalia Fault. This reddish succession exhibits a stack of interbedded conglomerates and sandstones.

The conglomerates are matrix- to clast-supported, moderately sorted and moderately- to well-cemented. Discrete large-scale trough cross bedding occur in the matrix-supported beds, while the clast-supported ones are more massive. Clast imbrications or large-scale crossbeds in these conglomerate beds indicate a transport to the SSW direction (Fig. II.63B). Clast components are dominated by gneiss and quartz (more than 50%), which are pebble

98

size and sub-rounded to well-rounded. Marble, ophiolite and red chert clasts are also well represented but less important. Maximum clast is up to 10x15 cm (Fig. II. 59C), at the exception of one massive, gneiss cobble bed at the top of section (Fig. II. 59F).
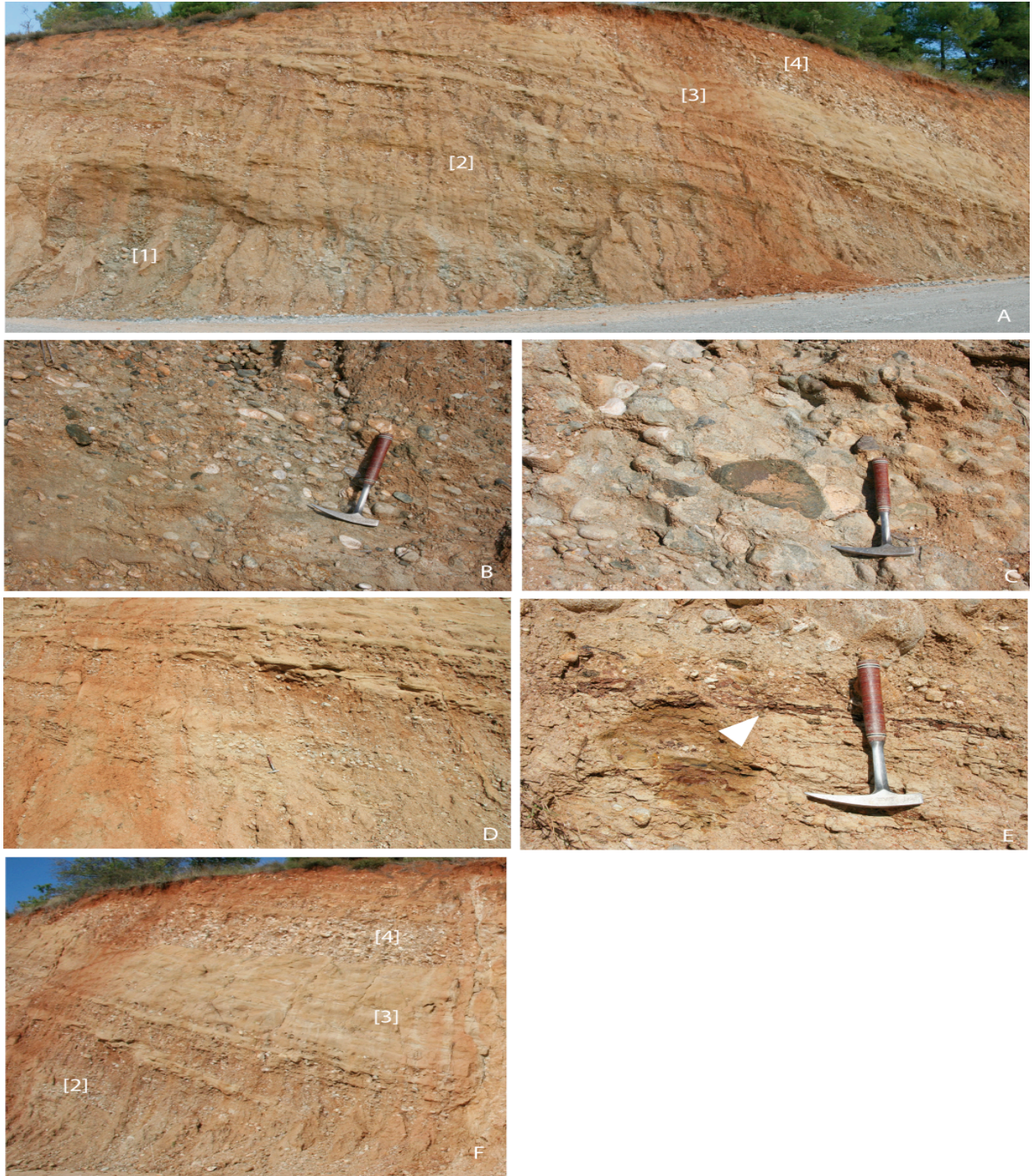
Fig. II. 59: UK3. Facies of log-35. A) Overview of section-35 outcrop [1 to 4, see Fig. II. 57]. B) Clast imbrications indicating NE to SW direction of paleoflow. C) Maximum clast size about 10x15 cm in matrix- to clast-supported conglomerate. D) Lenticular sandstones (bottom) and tabular, planar, large-scale cross bedding (top) interbedded in conglomerates. E) Sandy-siltstones layer containing weathered, red chert layer (white arrow). F) Massive sandstones with planar bedding [3] overlain by massive, cobble-conglomerates [4].

The sandstones are thin- to medium-bedded, coarse to very coarse-grained with a large amount of floating gravels and micas. Within the thicker beds, small pebble veneers are locally present. The sandstones are organized in tabular to lenticular bodies of >10 m in lateral extent, exhibiting planar- or large scale oblique cross bedding (Fig. II. 59D). Some beds show normal grading. Individual reddish sandy-siltstones may be interbedded, which contain abundant clasts of red chert (Fig. II. 59E).

These facies are more or less organized in about 5m-thick bedsets, bounded at the base by an erosion surface which incises over 1-2 m the underlying deposits. This surface is commonly floored by a discontinuous veneer of sandstone. Above, the idealized bedset comprises a fining-upward succession of (i) massive conglomerates, (ii) thinning-upward cross-bedded conglomerates interbedded with sandstones, (iii) cross-bedded sandstones with siltstones locally interbedded at the top.

2. Complementary sections

a) <u>The base of UK3: Section-32 and -33</u>

These sections show the lower boundary of UK3, in the southern and eastern parts of the area respectively*.* This lower boundary has also been drawn on Fig. II. 51, log-33.

The section-32, oriented in an E-W direction, is located along the pathway from Livadhia to Kanalia-Mitropoli road, (Fig. II. 44, site-32). Pale grey siltstones of UK2 form the base of this section but despite the road cut the contact is not well exposed.

The section-33 is the most interesting (Fig. II. 51 and Fig. II. 52, log 33). There, UK3 shows a very well exposed erosional lower boundary, incising UK2 over 10-20 m. The erosive surface is directed NE-SW and dip 20°-30° to the NW and is onlapped by UK3 deposits, which are there composed of conglomerates and sandstones similar to those in the type section.

b) <u>Complementary data on the upper part of UK3: Section-36</u>

The upper part of the exposed UK3 is represented in the section-36 along Kanalia-Mitropoli road, at about 420 m height altitude, close to Analipsi cemetery (Fig. II. 44, locality 36). Log-36 is established from more or less continuing outcrops along the road (Fig. II. 60). The section is

dominated by coarse-grained sandstones which show normal grading and upward-fining.
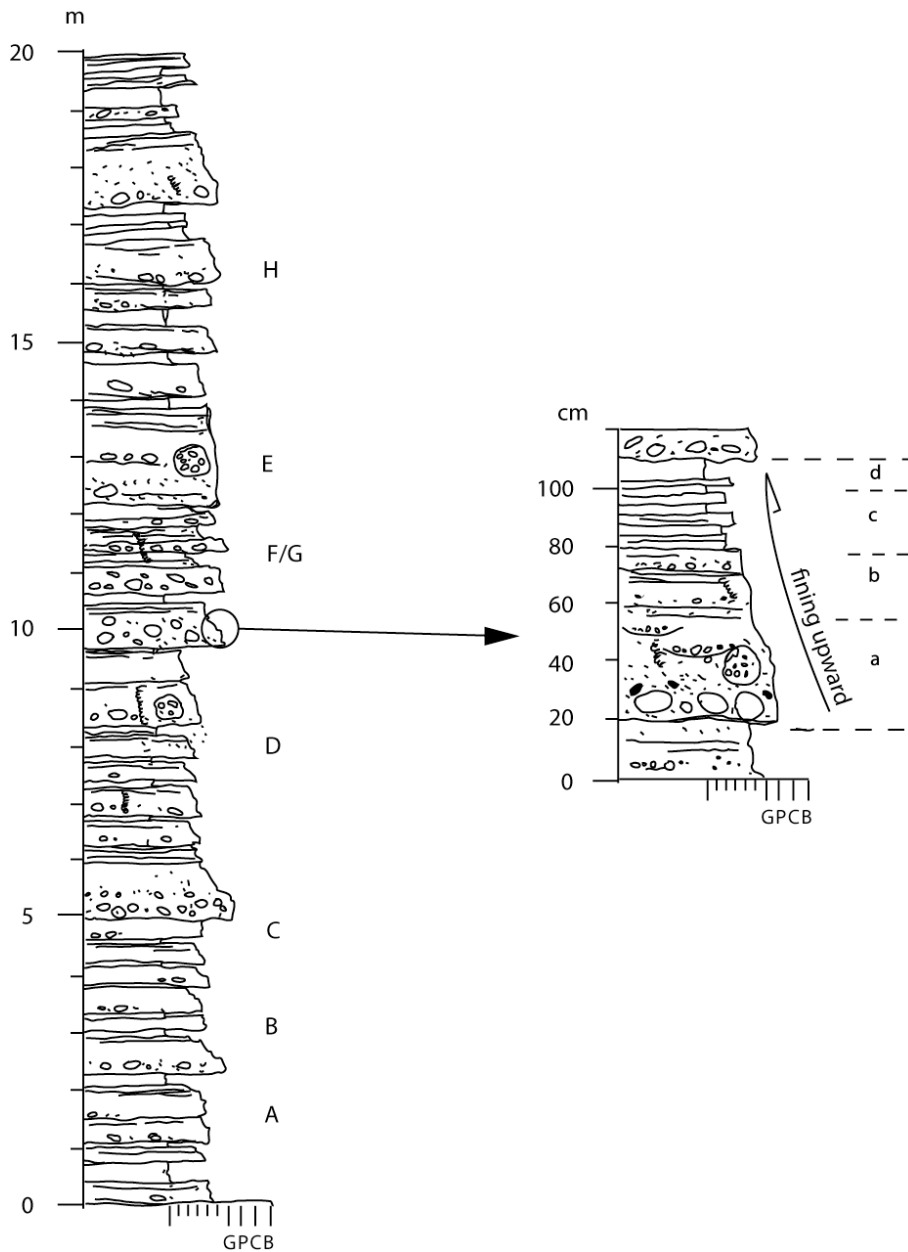
Fig. II. 60: Upper UK3. Sedimentary log-36 (left). A to H: see Fig. II. 61. Detail of massive coarse-grained sandstone bed showing normal grading (right).

      The sandstones are made up of thin- to very-thick, commonly fining-upward beds (Fig. II. 61C). They range from medium- to gravelly and very coarse-grained, and are moderately well sorted. The beds have sharp to irregularly erosional bases (Fig. II. 61D). Occasional (less than 25%) cobble conglomerates lenses, up to 0.7m thick, are embedded in the sandstones (Fig. II. 61A). They range from matrix-supported and well rounded (near the base of section) to poorly sorted, non-graded and clast-supported (at the top of section; Fig. II. 61D). Clast imbrication in these conglomerates indicates a shear direction toward the S or SW. Floating

pebbles or cobbles to even 1m large boulders (near the top section; Fig. II. 61E) are also found within the sandstone beds. Clast components are dominated by sub-rounded to well-rounded gneiss clasts. Sub-vertical *Skolithos* burrows are common (Fig. II. 61B, G). In place, scattered mud- and organic matter clasts are present (Fig. II. 61F, H).
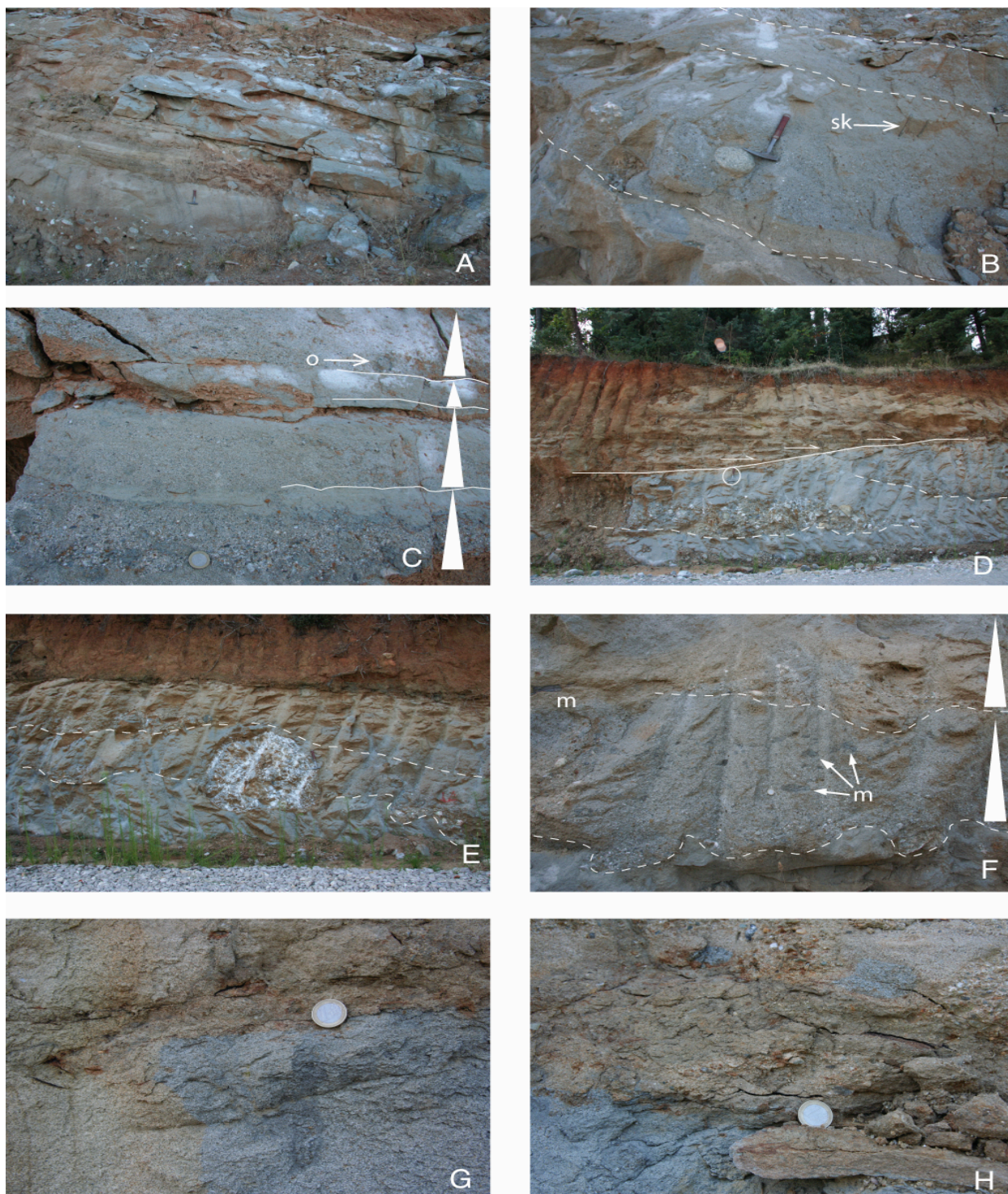
Fig. II. 61: Upper-UK3. Views of the outcrops of sedimentary section-36. For details: see text and Fig. II. 60. Sk: Skolithos (view B). m: mud clast (view F).

3. UK3: Interpretation

The lower unit part onlaps an incision surface cut down to 20 m into UK2. This surface strikes parallel to the paleocurrent pattern as indicated by the imbrications and the crossbeds of the onlapping deposit. Therefore we interpreted it as the wall of a valley or large channel that conveyed the sediments to the basin from its northeastern (Pelagonian) margin. The matrix-supported fabric of the cross-bedded conglomerates suggests that sediment load was very high. The idealized, 5m-thick fining-upward bedset-type in these conglomerates can be interpreted an individual channel-fill, with a conglomeratic sole (thalweg), and a stack of large crossbeds (bank) incorporating more silts at the top (decreasing energy along with channel infilling). The cut-and-fill architecture of the bedsets supports this interpretation. This is a common organization in coarse-grained braided fluvial plain deposits but can also take place in subaqueous channels. The fining-upward trend of the beds suggests that sediment supply was pulsed, maybe by floods.

The upper unit part has a much lesser amount of conglomerates and a more massive aspect of the sandstones beds. The presence of mud/organic clasts in the sandstones suggests that the deposit partly resulted from bed scour and that muddy deposits existed upstream. The massive aspect of the beds and the pebble-to-boulder floating clasts indicate that mass transport could have acted in this deposit. The long *Skolithos* traces argue in favor of a high deposition rate. Tractive processes may also occur and would explain the embedded lenses of clast-supported conglomerates. These could be thus small channels or gullies fed by larger conglomeratic bodies similar to those in the type-section. As a consequence, we inteprted the whole deposit as as debris flows and channel fills emplaced on a submarine slope fan.

VII. Fanari block

The Fanari block is the northernmost block of the studied area. The different sections are located on Fig. I. 7 and Fig. II. 62. Four stratigraphic units have been distnguished (UF1-4; Fig. II. 63). The younger one (UF4) is bounded by the Plio-quaternary Trikala plain.
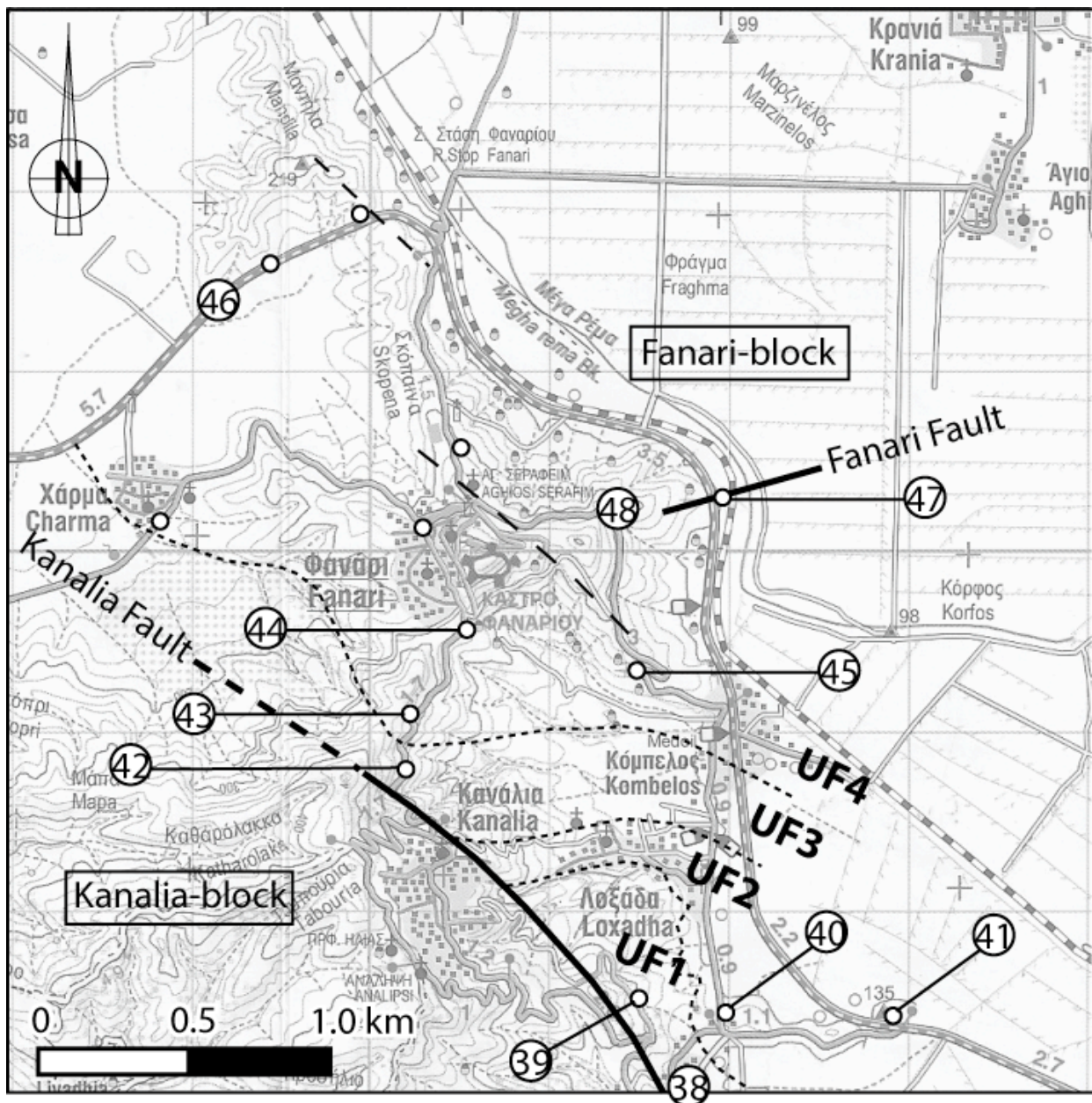
Fig. II. 62: Fanali block (UF). Location of the different sections (section-38 to -48).
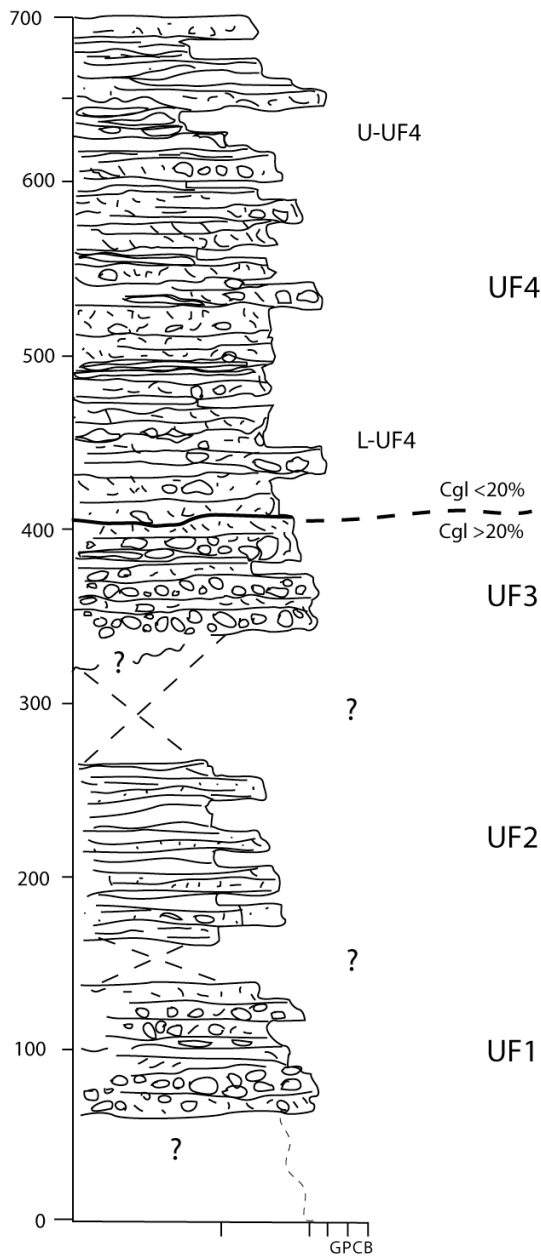
Fig. II. 63: Sedimentary log of Fanari Block.

A. Unit F1 (UF1): pebble to cobble conglomerates and sandstones

UF1 is rarely exposed on the Fanari-block. Outcrops exist on the southernmost Fanari-block, close to Kanalia fault, in the hill located north of Ligharies village (Fig. I. 7and Fig. II. 62, sites-38 and -39).

UF1 is limited by the Kanalia Fault to the south and its lower boundary is not found. The upper boundary is not clearly exposed in the field. However, in the landscape, we can see that UF1 is overlain by massive siltstones interbedded with sandstones attributed to UF2.

UF1 is dominated by reddish, moderately to poorly sorted, clast- to matrix-supported, gravel- to cobble-conglomerates and medium- to very-coarse grained sandstones. Thickness of UF1 is at least 50 m. The proposed section of UF1 is section-39.

1. Type-section of UF1: Section-39

This section, outcropping along the Ligharies-Kanalia road, is located on the small hill north of Ligharies village (Fig. II. 62, site-39). The unit is composed of more than 25 m of reddish, when weathered, sandstones and conglomerates (Fig. II. 64 and Fig. II. 65A).
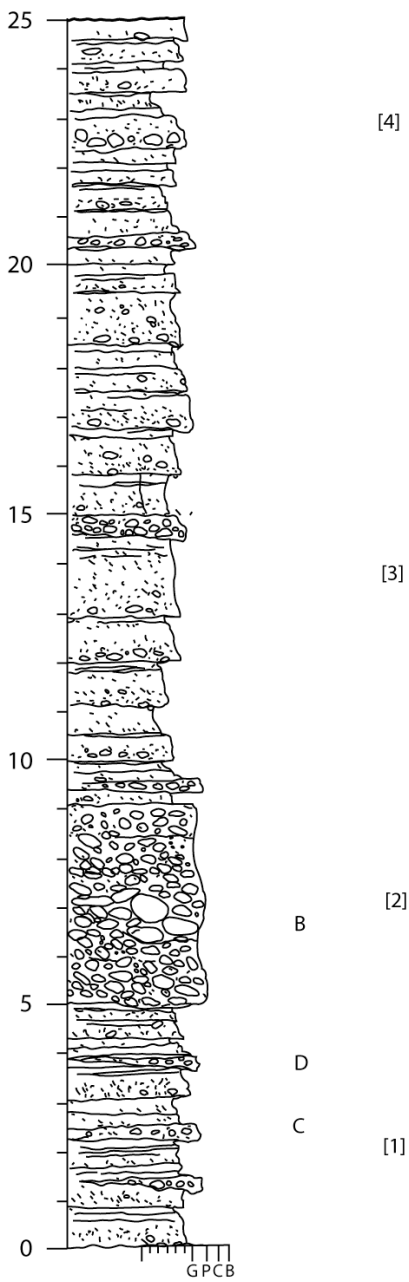
Fig. II. 64: Sedimentary log of section-39 (UF1 type-section). [1] to [4]: see text. B, C and D: see Fig. II. 65.

At the base of the studied section, about 4-5 m of reddish, gravelly to coarse-grained sandstones are present (Fig. II. 64, [1]). They are moderately bedded, well-cemented and range from medium- to thick-bedded. Some beds show planar lamination and normal grading (Fig. II. 65C). Erosional-based, clast-supported gravel- to pebble-conglomerate lenses or veneers occur. Thin siltstones beds may be present at the top of the sandstones.
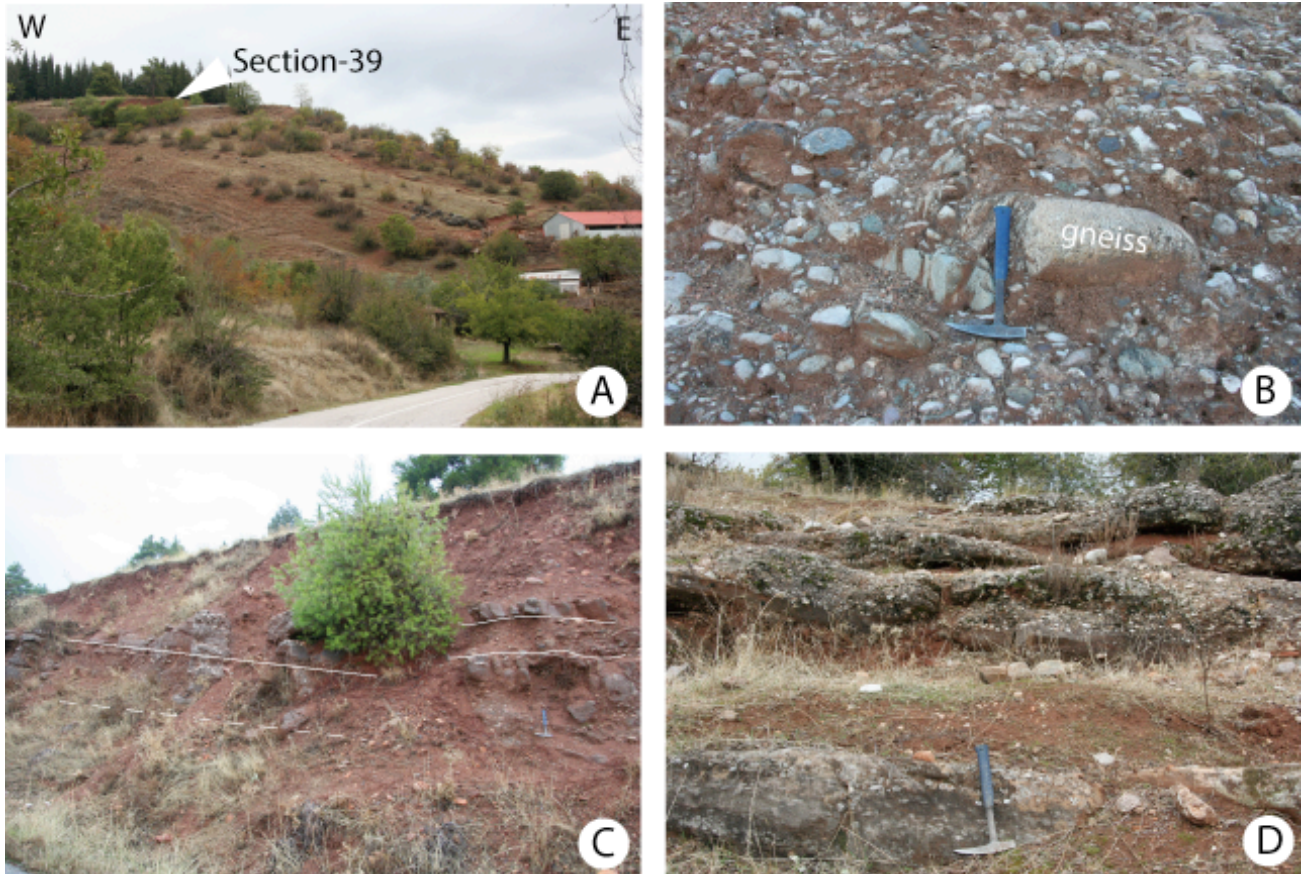
Fig. II. 65: Facies of UF1 unit. Views B, C and D: location on Fig. II.64. (A) Panorama view showing site 39 at the top of the hill, north of Ligharies village. The base of this section shows more than 25 m of thick reddish conglomerates. (This photo is taken from site 38 and is looking to the north, Fig. II. 62 for location). (B) A massive, clast-supported, poorly-sorted, pebble- to cobble-conglomerates. Gneiss clast is sub-rounded and up to 20x45 cm in diameter with a-axis oriented to SW. (C) Sandstones interbedded with matrix-supported, gravels- to pebble-conglomerates. (D) Medium- to thick-bedded, coarse-grained sandstones and gravel conglomerates. Sandstone beds at the lower part showing normal-grading and planar-bedding are overlain by sharp-base, matrix-supported, gravel to pebble conglomerates.

An impressive, 5 m-thick massive, pebble- to cobble-conglomerate is present in the middle part of the succession (Fig. II. 64, [2]). This conglomerate is clast-supported, poorly sorted and non-graded. Clasts are sub-rounded to well-rounded. They consist of gneiss 40%, quartz 30%, ophiolite rocks 15% and white marble 15%. Occasional gneiss clasts are up to 30 cm in diameter (Fig. II. 65B). Clast imbrications indicate a shear toward the SW. This conglomeratic bed is thinning down to 3 m laterally.

An upward-thickening of the sandstone beds is observed. Sedimentary structures are scarce in the thicker beds of the top, except some floating pebbles and cobbles. Also, interbedded siltsones are more developed than in the lower part (Fig. II. 64, [3] and [4]).

2. UF1: Interpretation

This unit is characterized by the embedding of conglomerate bodies which range from a few centimeters to up to 5 m thick, within a sandstone dominated succession. This architecture reflects a strong grain-size partitioning in the processes controlling deposition of the whole deposit. This is a very common architecture in coarse-grained braided river plains, where pebble/sand transitions are sharp at the bottom of channel bars. The lenses would then correspond to channel lags and the sandstone mostly the bar deposits. Other, subaqueous interpretations are still possible but less likely in our opinion due to the lens shape of the conglomerates and somewhat intimate cut-and-fill architecture of the two facies.

B. Unit F2 (UF2): Massive siltstones interbedded with thin- to thick-bedded sandstones Mitropoli Block

UF2 is exposed along the road at sites-40 and -41 (Fig. I. 7and Fig. II. 62 for location) and is also cropping out on a small hill at the southern side of Loxadha village.

The lower and the upper contact of UF2 are not found in the field. However, in the landscape, UF2 is seen resting on massive, pebble to cobble conglomerates of UF1 and overlying by tabular, gravel-to pebble-conglomerates of UF3. UF2 is commonly dominated by massive, pale grey siltstones interbedded with thin, sheet-like, sandstones. Sandstone beds are occasionally medium- to thick- while amalgamated, with occurrences of mud clasts and bioturbations. Thickness of UF2 is at least 80 m. A type-section of UF2 is section-41.

1. Type-section of UF2: Section-41

At hill-135, along the main Karditsa-Mouzaki road, section-41 is exposed at the junction to Kanalia village (Fig. II. 62, site-41). This road-cutting outcrop can be followed for up to 100 m along strike and up to 35 m height. The boundary between UF1 and UF2 is not exposed.

The succession (UF2) is dominated by grey siltstones interbedded with thin- to thick-bedded sandstones (Fig. II. 66, log-41). All along the succession, the finest-grained deposits are pale grey and massive siltstones.
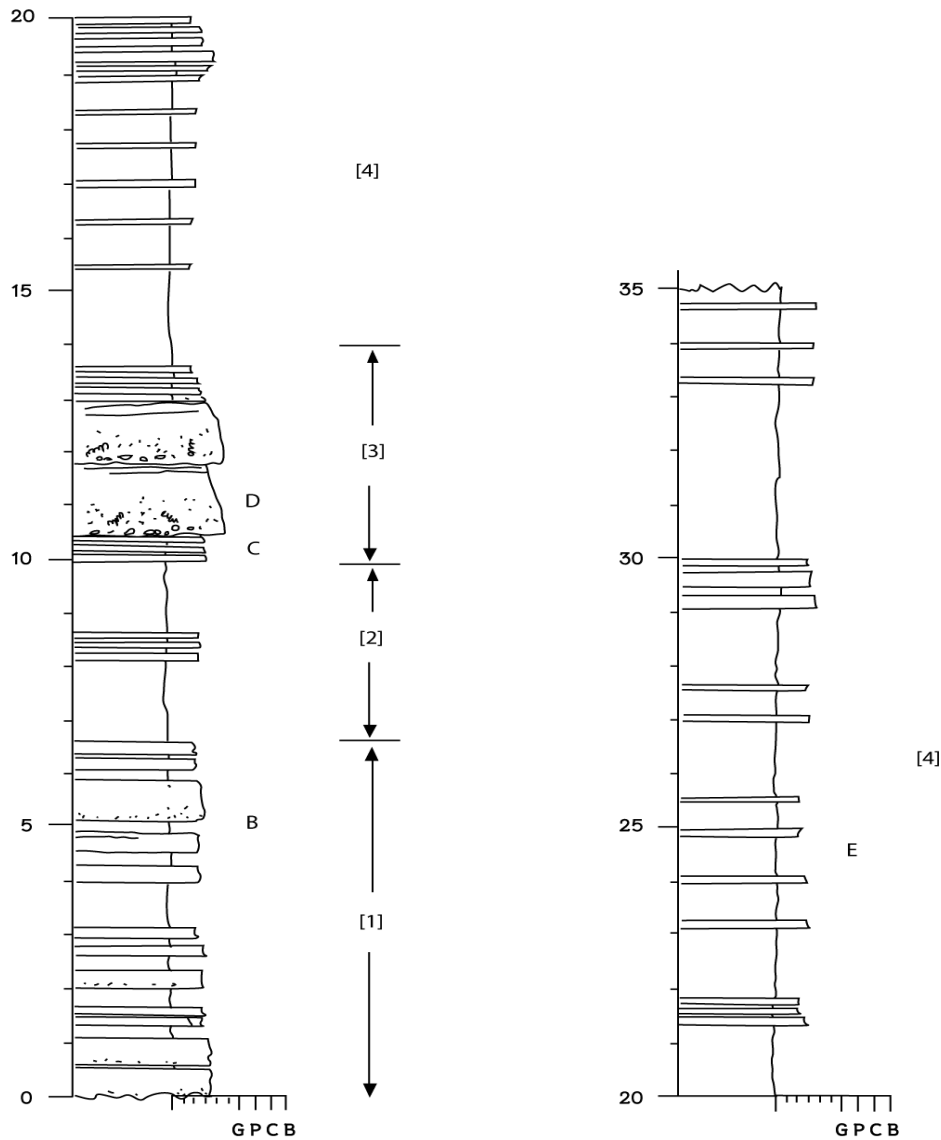
Fig. II. 66: UF2 type-section, Log-41. 1 to 4, B to E: see text and Fig. II. 67.

At the base, sandstones constitute 50% of the bulk deposit. They are sharp based and medium- to thick-bedded (Fig. II. 66, [1]). Upward in the sequence, massive siltstone dominates with only thin- to medium-thick interbedded sandstones, forming about 10% of the bulk deposit (i.e. Fig. II. 66, [2] and [4]). Locally, individual sandstones packages, up to 1 m thick, still occur (Fig. II. 67E). Throughout the succession, the sandstones are medium to very coarse grained, non-graded or slightly fining upward. Few mud clasts are observed within sandstone beds and some subvertical bioturbations are also found. The thick sandstone beds

109

show tabular to lens-shaped bodies. The lens-shaped bodies formed by bedsets exhibit an internal oblique accretion pattern to the west (apparent) (Fig. II. 67A).
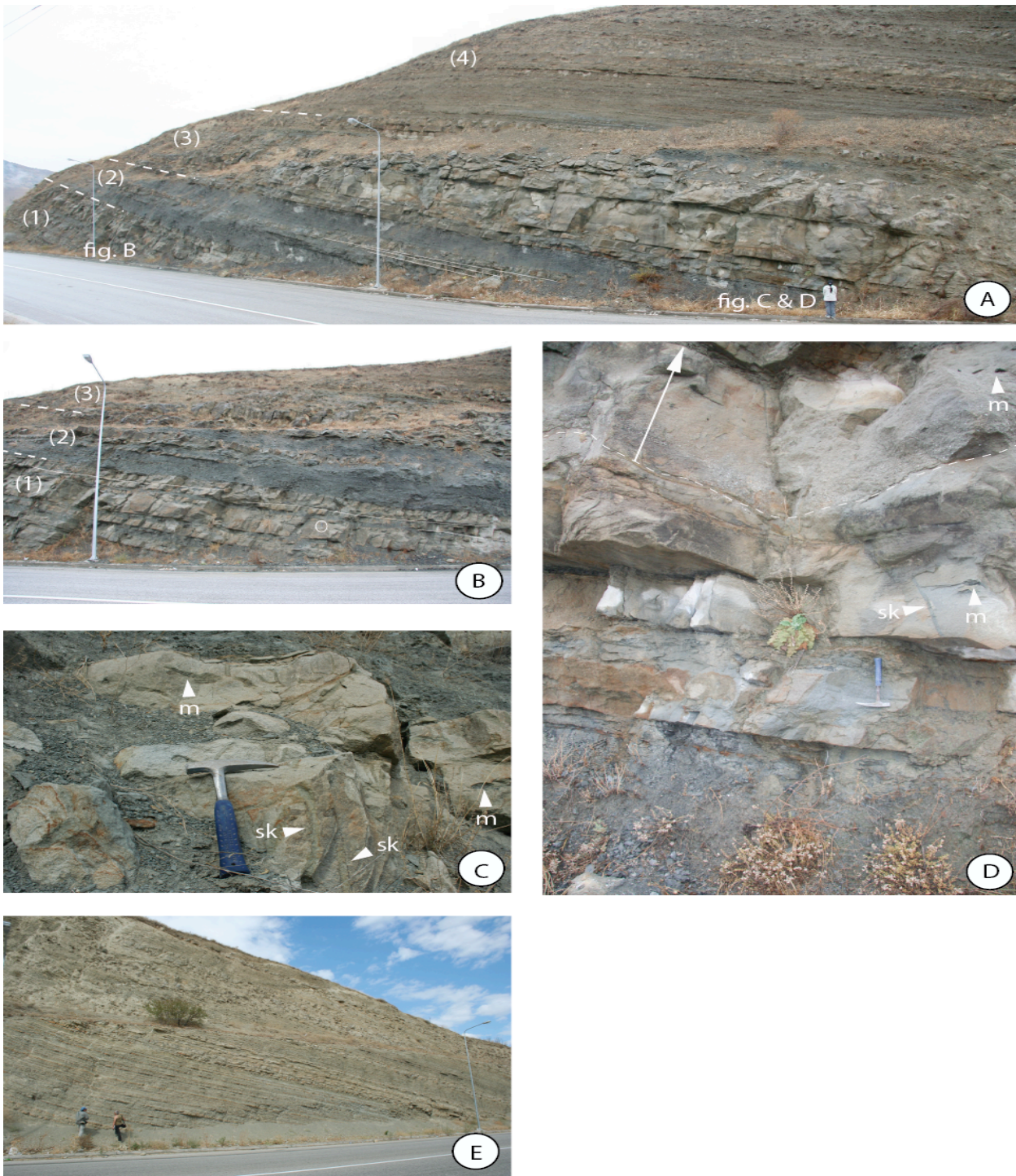
Fig. II. 67: Views of UF2 outcrops. (A) Panorama view of section-41 (hill-135). Numbers 1 to 4 on views A and B refer to Fig. II. 66. (B) The bottom of section consists of about 7 m of sharply based, medium- to thick-bedded sandstone packages. (C) Vertical burrows *Skolithos* and mudclasts are observed on thick, amalgamated beds (3 in Fig. II. 66). (D) Very thick sandstone bed with pebble lag at the base (3 in Fig. II. 66). It has a sharp erosional base and upward fining from gravel coarse-grained sandstone to siltstone. The sandstone shows vertical burrows of *Skolithos* (sk) and mud clasts (m). (E) Massive siltstones and thin bedded sandstones at the top of section-41 (4 in Fig. II. 66).

110

In this section, 10 m above the base of the outcrop, two very-thick and massive beds are floored by a pebble lag. These beds are composed of medium bedded sandstones which show a westward thickness decrease (Fig. II. 66A and D). Floating pebble clasts, mud clasts and bioturbations are observed. Bioturbations such as *Skolithos* are abundant (Fig. II. 67C).

2. Complementary section of UF2: Section-40

This section is located along Ligharies-Loxada road (Fig. I. 7 for location). Stratigraphically, it rests beneath section-41 and it overlies the UF1 conglomerates (section-39).

Section-40 shares similar facies with section-41. It is dominated by pale grey siltstones interbedded with rhythmic sandstones. Sandstones are commonly thin- to medium-bedded, sheet-like with sharp erosional base.

The structural dip of strata at this location is much steeper (40-60 degree to NE) than in other sections. This is due to the vicinity of the Kanalia Fault.

3. UF2: Interpretation

The siltstones were likely deposited as hemipelagites in a relatively deep marine setting, below wave-base (no ripples). We interpret the interbedded sheet sandstones as turbiditic deposits. The thickest beds have a pebble lag at the base, and floating gneiss clasts and mud pebbles. They are interpreted as high-density debrites. The numerous *Skolithos* traces in these beds are not the hint of a specific setting but reflect the ecological stress related to their abrupt deposition. Their lateral thinning suggests large-scale lobe geometry. Therefore, the depositional setting of UF2 could be the base of slope margin, close to the outlet of a river-connected canyon.

C. Unit F3 (UF3): Matrix-supported, pebble to cobble conglomerates and coarse-grained sandstones

UF3 is exposed along Kanalia-Fanari road (Fig. II. 62, locality-42). It is also cropping out on a dry river bed at Loxada village and along Loxada-Kanalia road.

In the landscape, UF3 can be seen above the grey siltstones of UF2. However, the limit between these two units is not well exposed in the field.

UF3 is characterized by massive, matrix supported, pebble to cobble conglomerates and thin to thick bedded, coarse grained sandstones passing gradationally to medium- to thick-bedded sandstones. Thickness is at least 50 m and the proposed type-section is section-42.

1. Type-section: Section-42

On the Kanalia-Fanari road, going from Kanalia to Fanari, at about 300 m from Kanalia exit junction, section-42 is well exposed at the western side of the road.

The bottom of this section is bounded to the south by Kanalia fault (Fig. I. 7, site-42). The section composed of conglomerates interbedded with sandstones/silstones (Fig. II. 68, [1]). Upward the section, the conglomeratic beds show a thick-up (Fig. II. 68, [2]) and then thin-up evolution (Fig. II. 68, [3]), which matches their abundance in the deposit.

Sandstones have a sharply to slightly irregular erosional base. They are medium to thick-bedded, very coarse grained, massive and structureless. Scattered granules to pebble clasts occur. Massive sandstone beds show a normal grading, and upward transition to planar bedding at the top (Fig. II. 69A).

The conglomerates are dominantly matrix-supported, moderately- to poorly-sorted (Fig. II. 69B, C). In the thickest beds, they may be clast-supported (Fig. II. 69D). Clasts range from granule to cobble size (up to 15 cm in diameter), sub-rounded to well-rounded and clasts consist of quartz, limestone, marble, gneiss, green volcanic rock and red chert (Fig. II. 69D). Clast imbrications indicate a S-SW direction of flow. Sedimentary structures such as large scale cross bedding are rarely found at the base of conglomerate beds (Fig. II. 69E). In other cases, their crude bedding is due to subtle variations of the amount of sandstone matrix in the stratification. Some conglomerate beds show a sharp erosional base (Fig. II. 69F) and slightly inverse grading occur.
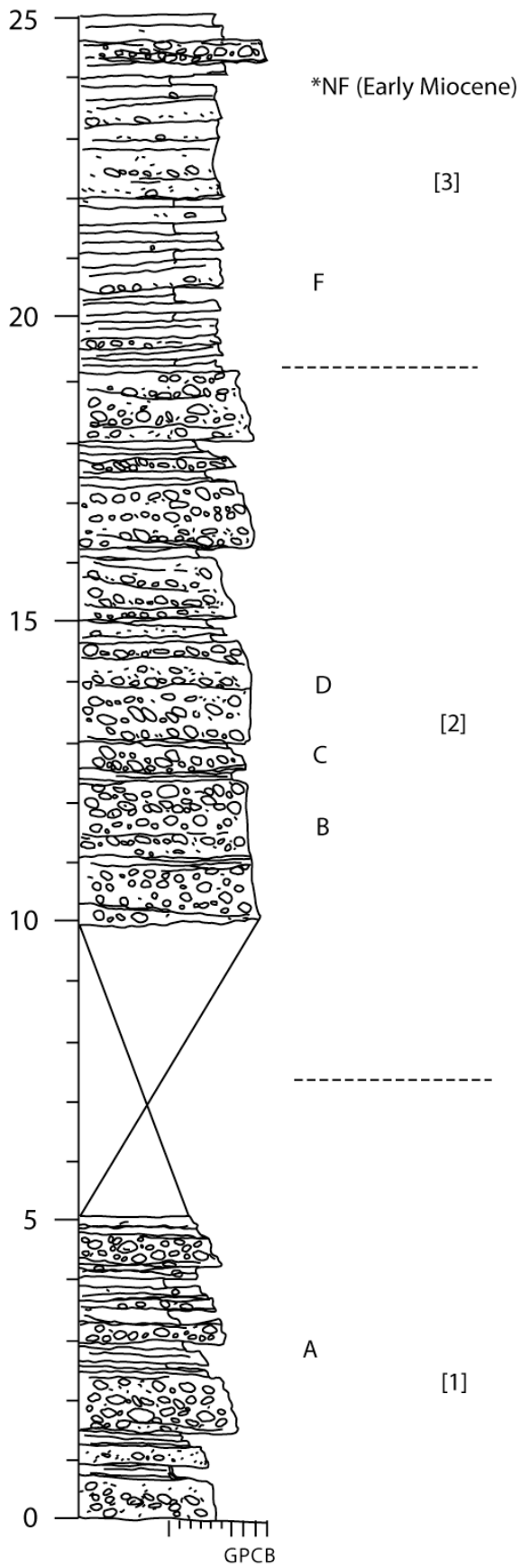
Fig. II. 68: UF3 type section. Sedimentary log of section-42. NF: nannofossils. 1 to 4 see text and A to F see Fig. II. 69.

Fig. II. 69: Views of sedimentary facies (UF3) from section-42. A to F: see text and Fig. II. 68.

2. UF3: Interpretation

The conglomerates are dominantly massive, matrix-supported and tightly mixed with varying amounts of sandstone in the course of stratification. This suggests they are emplaced as debris flows. The preserved reverse gradings suggest that flow was freezed and the clasts not settled out from the flow. This is common in high-density turbiditic currents. The sandstones, mostly massive, are not thought to represent distinct sedimentation events but the tail of the turbiditic flows. Their normal gradings record the normal waning stage of the

turbiditic flow. As a whole, this deposit is interpreted as a debrite- and turbidite-rich proximal slope fan.

D. Unit F4 (UF4) Interbedded sandstones and siltstones

UF4 is volumetrically the most important in Fanari block with a thickness of more than 400 m. It forms a prominent hill, where Fanari village is located, at the northern-most part of the studied region. The outcrops are surrounding Fanari village along the road, railway and dry rivers.

UF4 is a succession dominated by sandstones interbedded with siltstones. Overall of UF4 shows a fining upward trending. It conformably overlies UF3 and is capped at the top by the Plio-Quaternary Trikala plain. The lower boundary is a gradational contact, passing upward from coarse-grained sediments of UF3 to UF4. Conglomerates still occur in this unit but are minor in abundance (less than 20%) compared with UF3.

UF4 has been subdivided into a lower (L-UF4, sections-43 to -46) and upper (U-UF4, sections-47 and -48) part, respectively on the southern and northern sides of a main NW-SE fault located to the NE of Fanari village (Fig. II. 62). Section-47, which is an excellent rail-cutting outcrop with a good lateral continuity, is proposed as the type-section of upper UF4.

1. Lower part of UF4 (L-UF4): sections 43 to 46

The lower part of UF4 (L-UF4) is an about 200 m thick succession encompassing sections-43 to -46. It is exposed in scattered outcrops either at the base (section-43) or near the top of this succession (sections-44 to -46), along the Kanalia-Fanari road at the top of a hill between Kanalia and Fanari village (Fig. I. 7 and Fig. II. 62 for location of sections-43 to -46).

a) **The lower boundary of L-UF4: Section-43**

This section outcrops approximately at the middle of Kanalia-Fanari road (Fig. II. 62). It is assumed to show the lower limit of L-UF4 as defined where the proportion of conglomerate beds is less than 50%. The contact between UF3 and L-UF4 is a gradational one. From this boundary, the sequence of interbedded sandstones and siltstones is continuing upward until section-44.

b) Lateral and vertical variations in sections-44 to -46

Section 44 exposed on the Kanalia-Fanari road, at about 100 m before the entrance of Fanari village (Fig. II. 62, site-44) shows an example of the lower part of L-UF4 (Fig. II. 70). Section-45 is located in a road bend, about 1 km southeastward from Fanari village. It is up to 11 m thick and can be followed laterally to the west. Stratigraphically, strata dips show that section-45 is located above section-44 (maybe the base of log-45 could be a lateral equivalent to the upper part of log-44, Fig. II. 71A). Section-46 is exposed at the northwest of Fanari block, along Karditsa-Mouzaki road. Section-45 and -46 seem to be stratigraphically equivalent.
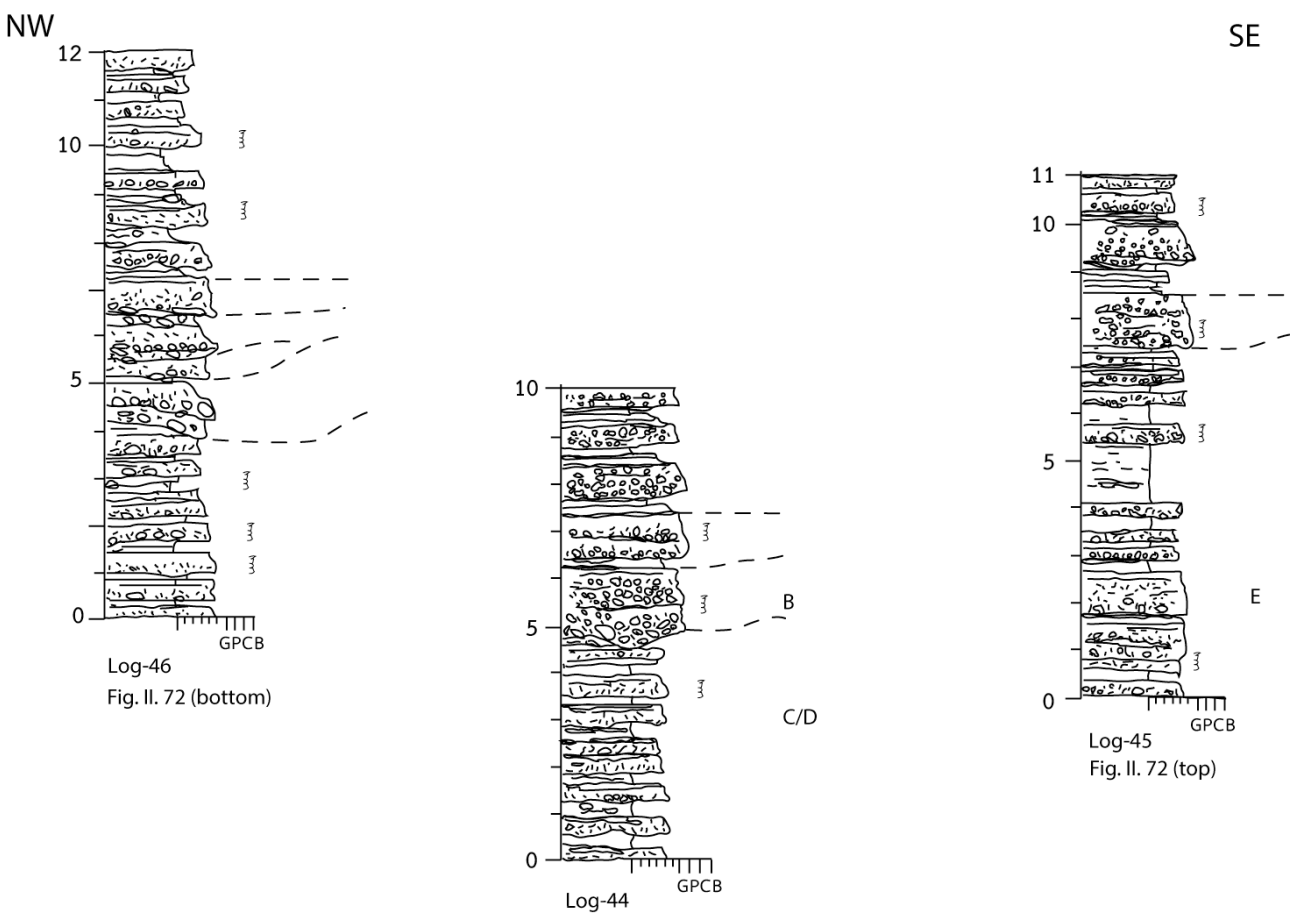
Fig. II. 70: Sedimentary logs of section 44, 45 and 46 (L-UF4). B to G: see Fig. II. 71. Mainly sandstones with mud clasts (gravel size).

These three sections combined (log-44 to -46) represent an about 20 m succession which is taken as the representative facies of the whole L-UF4 (Fig. II. 70). This flysch-like deposit is marked by erosional, fining-upward gravel beds (Fig. II. 71). The sandstones show locally metric to decametric channels forms (Fig. II. 72). They are coarser and more abundant near the lower part of the succession (log-44) and to the NW (log-46) than in the east (log-

116

45). Sandstones are thin- to thick bedded and also show sharp erosional base, with locally reverse gradings in their sole (Fig. II. 71C). Occasionally, thick amalgamated beds occur. Mud clasts up to 20x30 cm large is observed (Fig. II. 71B). Vertical burrows of *Skolithos* (Fig. II. 71D) and *Ophiomorpha* (Fig. II. 71E) are very common in the sandstones.

Fig. II. 71: Facies of L-UF4: sections-44, -45 and -46. (A) View of section-45 and location of section-44. (B) Scour base, erosional base of gravel conglomerates. (C) Inverse to normal grading coarse-grained sandstone. (D) Vertical bioturbation *Skolithos* from section 44. (E) *Ophiomorpha* and *Skolithos* from section-45.
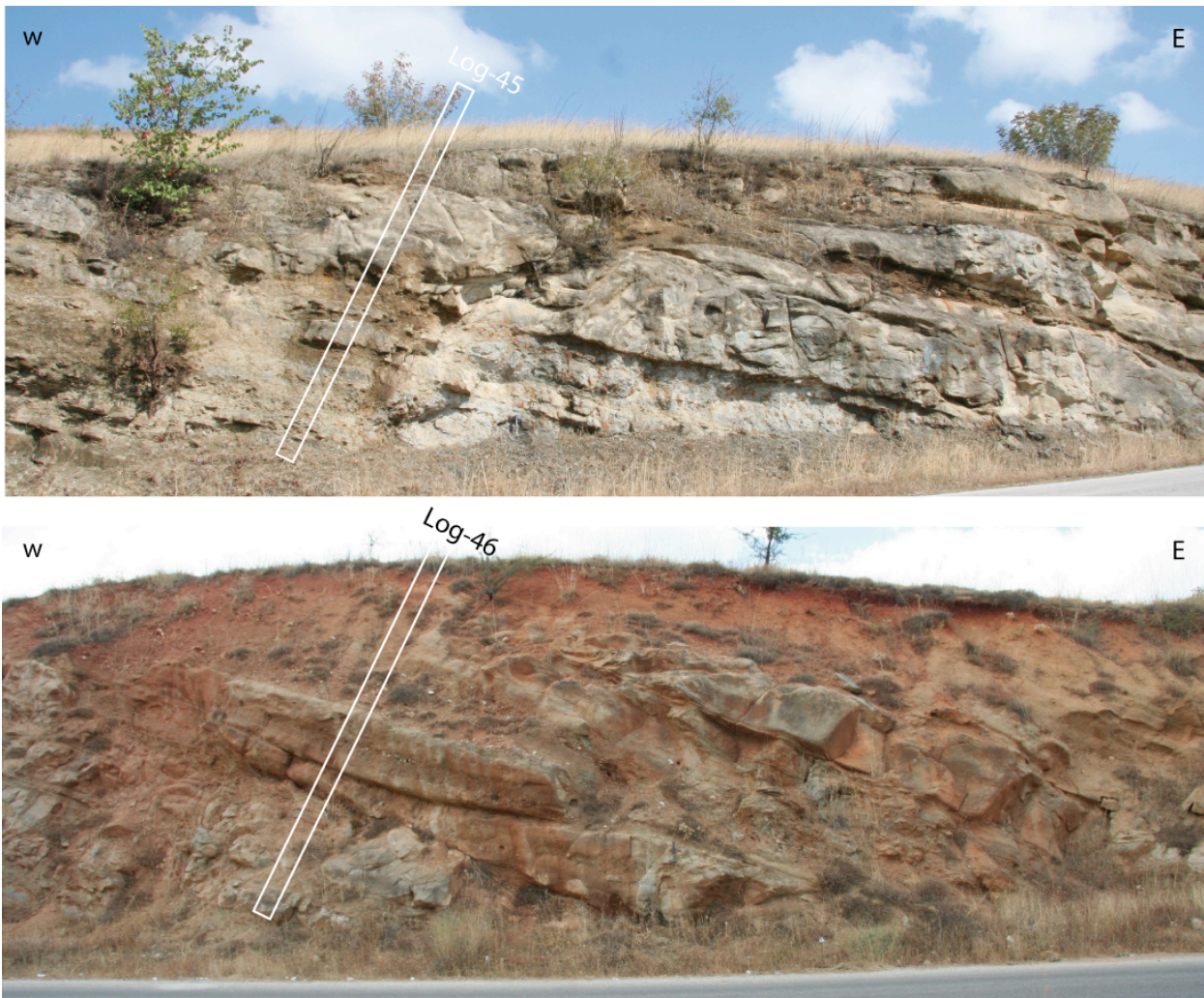
Fig. II. 72: L-UF4: Views of outcrops (sections-45 and -46). Top: Outcrop view of section-45 (eastern part). Bottom: Outcrop view of section-46 (western part), looking to north.

2. Upper part of UF4 (U-UF4)

a) Section-48 (U-UF4): nannofossils of Early-Miocene age in siltstones

This outcrop is located in a sharp curve of a main road, 750 m NE of Fanari Castle and 500 m west of the section-47, at about 200 m in altitude (Fig. II. 62, site-48). The strata dip 20-30° to NE. From these dippings we can conclude (in the absence of faulting evidence) that these strata are stratigraphically the lowermost part of U-UF4. The L-UF4/U-UF4 transition is not documented in the field. Section-48 is about 5-10 m thick, grayish and somewhat massive calcareous siltstone which delivered nannofossils of Early Miocene age. Taking into account

118

the dippings of UF4, this Early Miocene age could be the youngest age of all the deposits of the studied area (maybe as UM7).

b) Section-47: Type-section

Section-47 is a rail-cutting outcrop, situated 2.2 km southeast from Fanari rail station and about 2 km eastward from Fanari village (Fig. I. 7, site-47 and Fig. II. 62).

The succession is the continued deposit above the siltstone of section 48. It is up to more than 20 m thick and can be followed laterally continuous along strike up to more than 100 m. This excellent outcrop is proposed as a type-section of the upper part of UF4. Medium- to thick-bedded calcareous sandstones dominate and are interbedded with grey siltstones.

As an example, we describe some of the sedimentary structures observed in the sedimentary strata which have been subdivided into 6 subunits (Fig. II. 73 and Fig. II. 74).
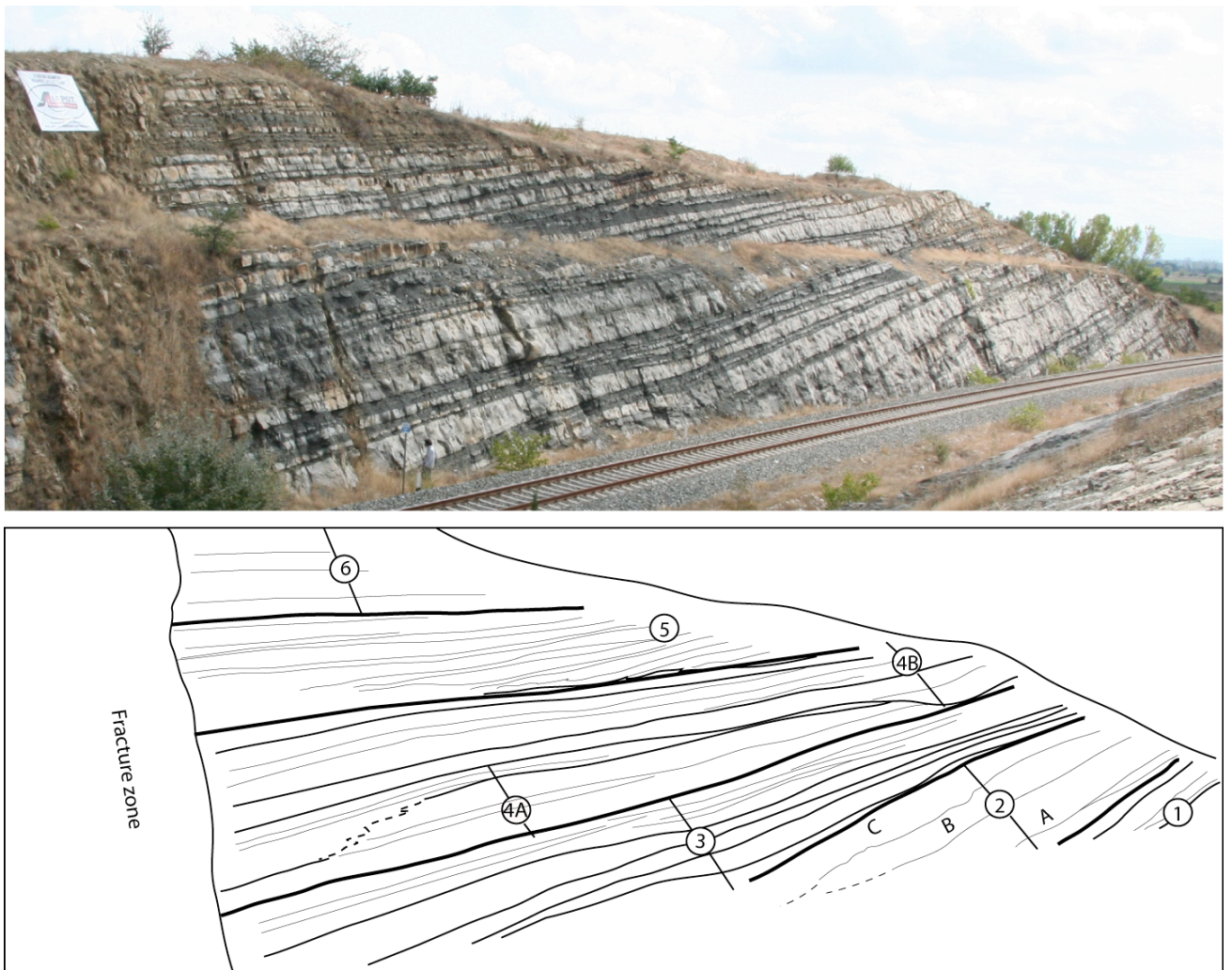
Fig. II. 73: U-UF4. Outcrop panorama view of section-47. See text and Fig. II. 74 for label description.

119
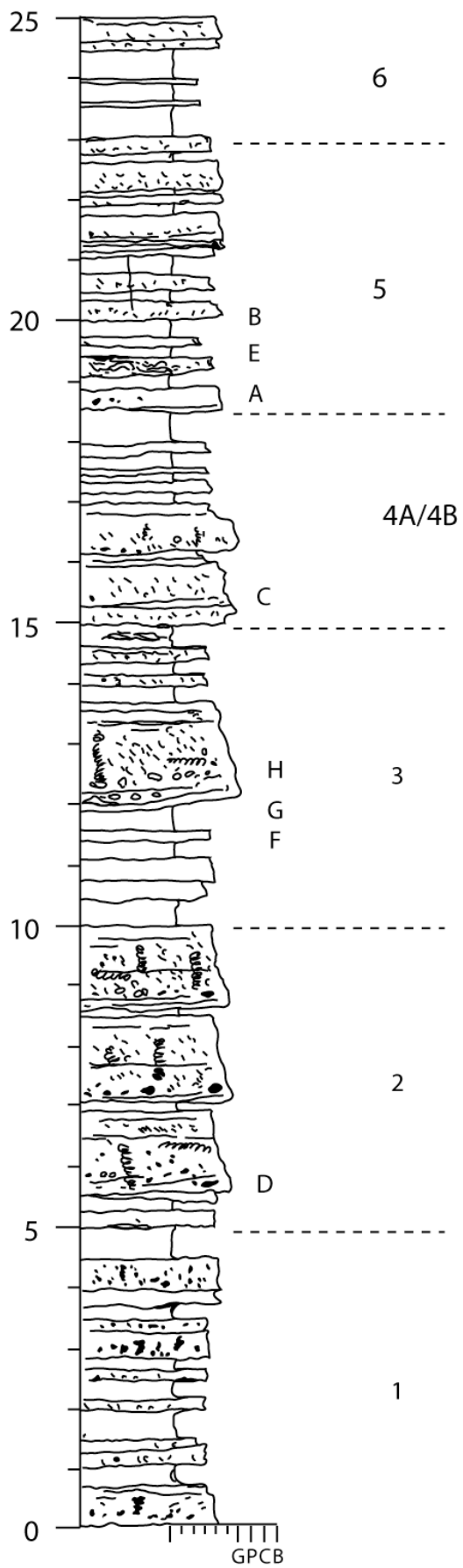
Fig. II. 74: U-UF4. Sedimentary log-47. For 1 to 6: see text and Fig. II. 73. A to H: see Fig. II. 75.

120
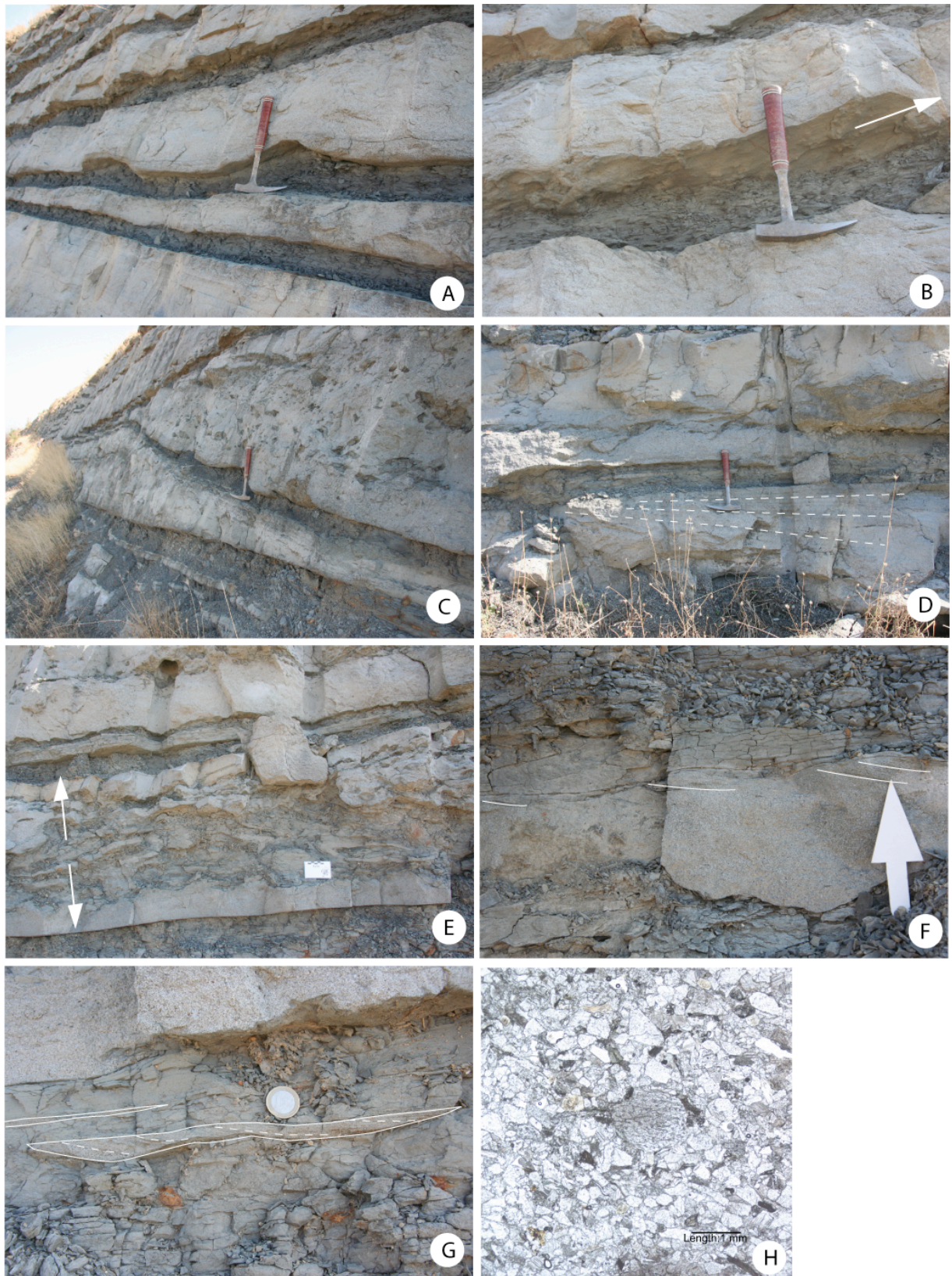
Fig. II. 75: U-UF4. (A) Load clast at the base of sandstone in subunit 5. (B) Flute mark at the bottom of sandstone bed in subunit 5. (C) Sharp-based sandstone with numerous mud clasts in subunit 4b. (D) Cross bedding in coarse-grained bed in subunit 2. (E) Slump (?) in sandstone and siltstone in subunit 5. (F) Current ripple at a top of sandstone bed in subunit 3. (G) Sandstone lens in siltstone bed in subunit 3. (H) Coarse grained sandstone of subunit 3 (thin section, 6x6 mm).

The sandstones in this outcrop, 0.1-2m thick, range from medium- to very coarse-grained, with grains of quartz, muscovite, feldspar and calcite (Fig. II. 75H) and mud clasts (namely in subunit 4b) or organic matter lenses (subunit 5). The thickest ones comprise also floating gravels (subunit 2). They are either massive, planar- or cross-bedded (Fig. II. 75D, F, G), with common normal gradings (Fig. II. 75F). Groove- and flute casts are locally present at their base, indicating a SW paleocurrent (Fig. II. 75B). Sub-vertical *Skolithos* burrows as well as sub-horizontal bioturbations have been observed in subunits 2 and 3. The sandstones are either stacked on eachother or interbedded with m-thick siltstone layers. In the latter case, many load structures deform their contacts (Fig. II. 75A), and somes beds may be totally disorganized by slumps (Fig. II. 75E).

The large scale organization of strata in this outcrop show that the sandstones form lens-shaped bodies, about 3-5 m thick and 60-80 m in (apparent) lateral extent. These bodies are either convex-up, bounded by a flat, overall agradational surface (subunit 2, 4a and 5), or flat-topped and with an erosional channel form at the base (subunit 4b). The channel-like subunits infill the troughs between the convex-up ones. Their lower part exhibit massive sandstone with numerous mud clasts (Fig. II. 75C). Alternatively, the space between the convex-up bodies is infilled by siltstone dominated beds which laterally thin and pinch out against the sandstone-dominated bodies. Accretion of the convex-up bodies might be partly lateral, as suggested by the dominance of beds dipping to the NW. The overall sandstone:mudstone ratio decreases upward the section.

3. UF4: Interpretation

L-UF4 is a thick succession of flysch-like sandstones interbedded with thin conglomerates. Both the marine nannofossils found at the top of those deposits in the lower part of U-UF4 and the gradational transition of UF4 above UF3 deposits (interpreted as slope fan debris flows and proximal turbidites) point to a turbidite interpretation of this subunit, and therefore we suggest that L-UF4 is part of a submarine slope fan. The numerous mud clasts in the sandstone beds were likely supplied by erosion of the slope fan margins. As already mentioned for other units, the occurrence of *Ophiomorpha*, which is generally associated with nearshore environments, may be due to a peculiar species of the Nereites association, such a *Ophiomorpha rudis* (Uchman, 2009).

U-UF4 is interpreted as a channel and lobe system emplaced at the lower end of a more mature turbiditic system. The convex-up sandstone-dominated bodies correspond to lobe elements and the siltstone-dominated trough fills the interlobe depositional phases. Mud clast-rich channel fills are preserved inset in the lobe deposits (subunit 4b). The paleocurrents were to the SW, which is consistent with the observed lateral accretion of the lobes to the NW. A rapid deposition rate, together with the development of permeability barriers caused by the silstone layers, was responsible for basal load features and hydroplastic deformation and slumping.

VIII. Synthesis and conclusions

In the light of all outcrops investigated, seven facies can be used to build out a facies model (Fig. II. 76) that reflects the geometric relationships of facies as observed in the three blocks. These are (with in brackets the units where they ar observed):

Carbonates:

- Facies A: heterozoan carbonate shelf dominated by large benthic foraminifers (UM1);

Conglomerates:

- Facies B: fluvial conglomerate and sandstone (UK1, UF1);

- Facies C1: submarine channel conglomerate and sandstone (UM2, L-UM5, L-UM7, L-UK3);

- Facies C2: conglomeratic debris flows, locally interbedded with proximal turbidites (UM3, L-UM4, UF3);

Sandstones:

- Facies D1: Proximal turbiditic sandstones interbedded with thin conglomeratic channels (U-UM5, U-UM7, U-UK3, L-UF4);

- Facies D2: Turbiditic sandstone channels and lobes (U-UF4);

- Facies E: Hemipelagic silstone, with interbedded distal turbidites (U-UM4, UM6, M-UM7, UK2, UF2).
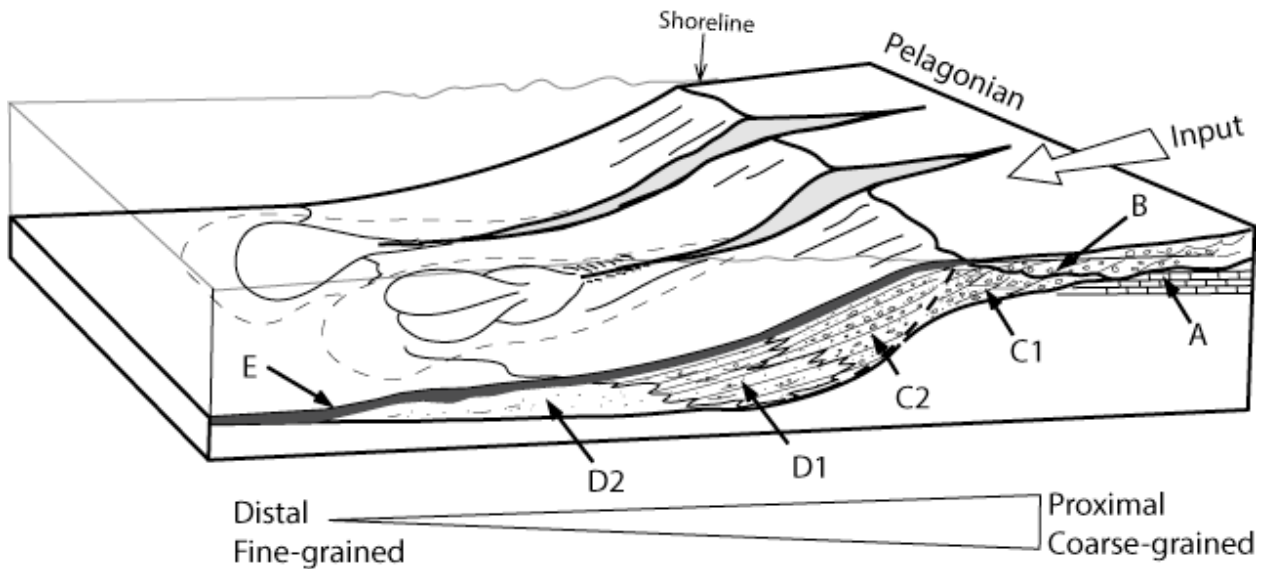
Fig. II. 76: Idealized facies model of the depositional system of the study area. Note the "almost ramp-like" topography of the basin margin, at the exception of incised canyons that convey the sediments to the slope fan.

In this facies model, the fluvial to marine conglomerates are mostly channelized while prograding on the shelf or entrenched in the canyons. Dowstream, they are comprised of a slope fan, where they grade basinward to sandy debris flows and turbidites. The hemipelagic facies is found above each type of marine facies.

In the following paragraphs, we analyze the facies tracts in each block and propose a sequence stratigraphic interpretation of the vertical succession of the stratigraphic units based on this facies model. In chapter IV, with additionnal tectonic data and 2D cross-sections, a more general assessment of stratigraphic units in the frame of the basin evolution will be attempted.

A. Mitropoli Block

The Mitropoli-Block comprises the most complete record of the MHB in the study area, with 7 units. UM1 to UM4 show local onlaps on the basement. The total thickness of the deposits is in excess of 600 m. Foraminifera in the limestones and nanofossils in the siltstones show that the series begin in Late Oligocene and continue in Lower Miocene. Most of the

siliciclastic facies were emplaced above UM1 in response of paleoflows running from the NE (Pelagonian source rocks) in a subsiding marine basin.

The major unconformities are associated to major base-level falls and they are onlapped by facies tract as follow, from base to top:

- A-B   (UM1-UM2)
- C2   (UM3)
- C2-E   (UM4)
- C1-D1-E   (UM5-UM6)
- C1-E-D1   (UM7)

In sequence stratigraphic terms, these facies tracts thus record either transgressive (UM4, UM5-6) or transgressive-regressive (UM1-2, UM7) successions of deposits bounded at the base by unconformities (although, there is no evidence that these unconformities are subaerial erosion surfaces). Therefore, they can be considered as depositional sequences (SM, as Mitropoli sequence; Fig. II. 77):

- UM1 (-UM2):   SM1
- UM3:   SM2
- UM4:   SM3
- (UM2-) UM5-UM6:   SM4
- UM7:   SM5

In general terms, most of the facies models are covered through a sequence. The conglomerate facies above the sequence boundaries are interpreted as the lowstand systems tracts (except in SM2 where no facies tract can be observed). The above, locally subtle shift toward a more sandy deposit is interpreted as the transgressive surface (L/U-UM5 boundary, upper part of L-UM4 and L-UM7). The maximum flooding surface is located at the maximum shaliness (U-UM4, M-UM7) or carbonate content of facies E (UM6). The highstand systems tract has a slightly higher percentage of sandstone in facies E (UM6), or is marked by the return of slope-fan sandy turbidites (U-UM4, U-UM7).

However, units UM1 to UM3 do not comprise the Facies E and only the conglomeratic ones, so they are therefore less easy to interpret in sequence stratigraphic terms:

- UM1 could record the transgressive tract and UM2 the higstand tract of the first depositional sequence of the basin. However, UM2 was sourced from the Pelagonian, and not from the Koziakas as UM1. Also, at the map scale, UM2 is surrounded by UM5, which is preserved at the same elevation against the basement. Therefore, UM2 could be a lateral, more proximal equivalent of UM5. In this (preferred) hypothesis, UM2 would be part of the SM4 sequence.

- Because UM3 is a syntectonic deposit entrenched within/capping active faults, it is also difficult to see regional base level variations across it, and facies changes might be related to local slope destabilizations. However, it is the only unit which records this active faulting event in its deposits, that makes it timely significant. As a consequence, UM3 is proposed as separate depositional sequence SM2.
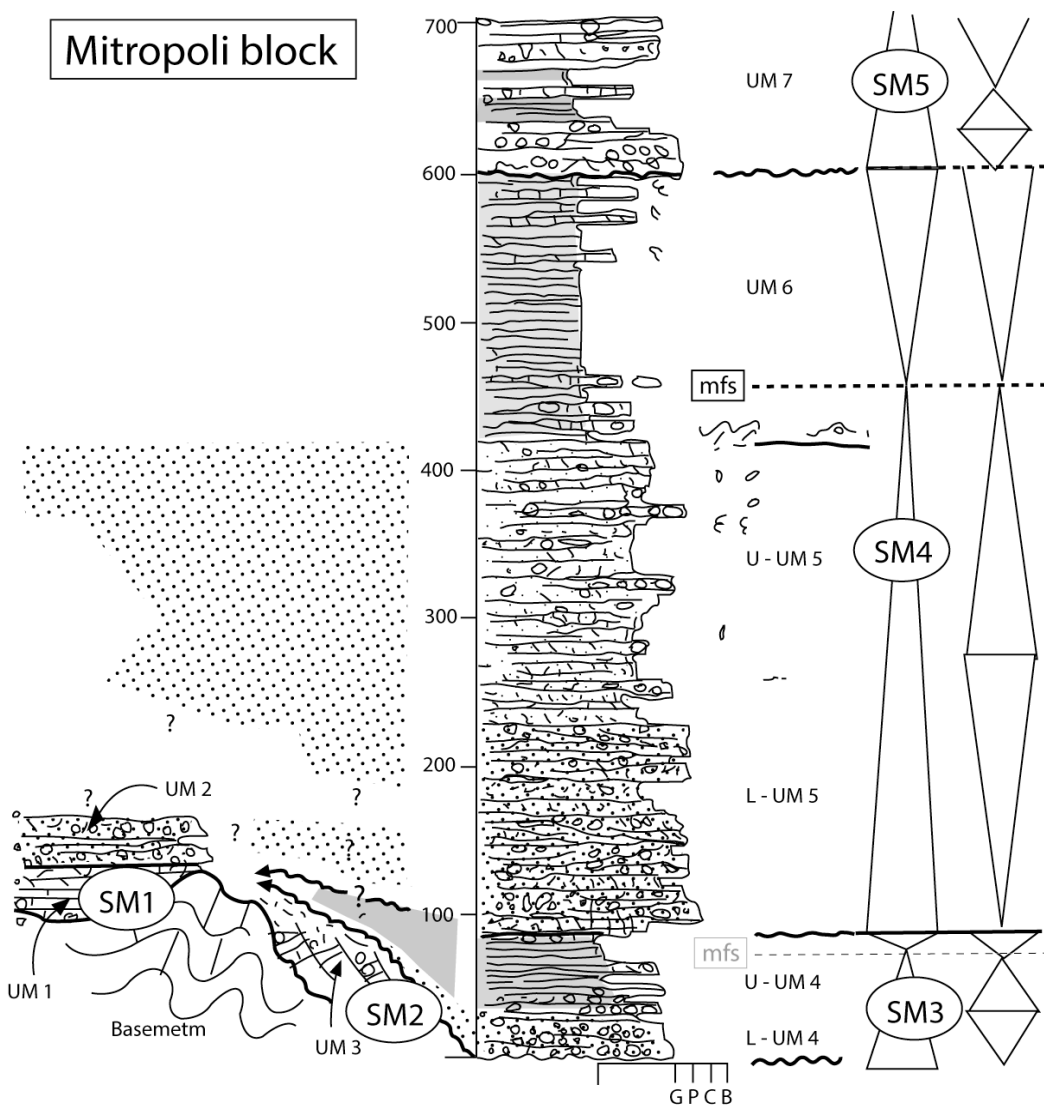
Fig. II. 77: Synthetic sketch of Block-UM with preliminary sequence stratigraphic interpretations.

The Mitropoli block sequence set records an overall transgressive evolution, marked by the deepening-up of the basal conglomerate fluvial (UM2) to turbiditic facies (L-UM7). In the same time, the thickness of hemipelagites increases.

B. Kanalia Block

The stratigraphic succession in Kanalia Block, about 250 m thick, is thinner than that of Mitropoli Block, but it could not be correlated to it due to the presence of Livadhia Fault. UK2 and UK3 onlap the Koziakas basement at lower elevations than similar facies units in Mitropoli Block. Sediments are only terrigenous, mostly conglomerates and siltstones and there are sandstones than in Mitropoli Block. Nanofossils observed in the siltstones give a Early Miocene age in the middle part of the block (UK 2) and locally Late Oligocene-Early Miocene.

The UK1 and UK2 deposits, although drastically different, might constitue a conformable succession of strata within a B-E facies tract. This facies tract is truncated at the top by a major erosional unconformity, with associated incised-valleys or at least large channels. This unconformity is interpreted in the same way as its counterparts in Mitropoli Block: a sequence boundary. The UK1-UK2 succession thus forms one depositional sequence (SK1) and the UK3 above succession is part of another one (SK2), composed of a C1-D1 facies tract (Fig. II. 78). Both sequences record an overall transgressive evolution, but their lower part probably comprises the LSTs. Then, the transgressive surfaces are marked by a seaward shift of facies (slumped sandstones in the upper part of UK1 and the top of C1 in UK3). The MFS, missing in SK2, might be associated to the carbonate nodules in SK1 (base of UK2). As in UM6, this could be the effect of abrupt flooding of the valley interfluves and landward shift of terrigenous supply.

The SK1 TST illsutrates a conspicuous pattern of the facies model as we see it: it passes rapidly from the fluvial realm to the most distal facies of the basin with only a thin slumped sandstone in between. This sandstone is likely a transgressive shallow-water deposit corresponding to the retreating river mouth sands. Their small thickness and the absence of slope fan deposits show that little accommodation was developed at that time and place in Kanalia block.

The overall sequence set recorded in Kanalia Block is transgressive, because the conglomerates in both sequences record a seaward shift of facies from fluvial (UK1) to submarine (UK3).
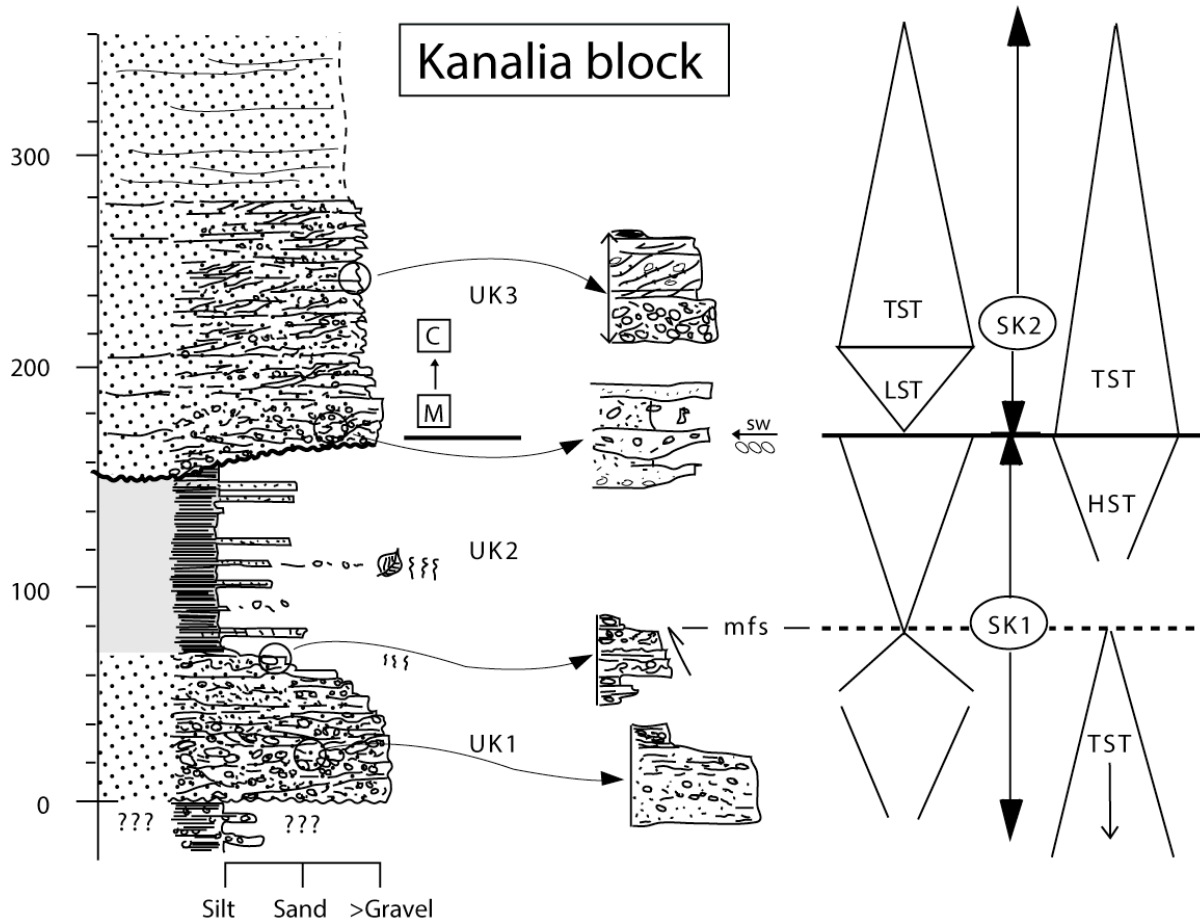
Fig. II. 78: Synthetic sketch of Block-UK with preliminary sequence stratigraphic interpretations.

C. Fanari Block

The stratigraphic succession in Fanari Block is about 370 m thick, but none of the 4 units could be correlated directly with units of the other blocks, due to the presence of the Kanalia Fault. The silty facies at the base of U-UF4 provided a Lower Miocene age.

One major unconformity is determined in Fanari Block, at the base of UF3. As in other blocks, it is interpreted as a major sequence boundary. Therefore, we consider that UF1-UF2 is part of a sequence (SF1) and UF3-UF4 part of another one (SF2; Fig. II. 79). The facies tracts below and above this unconformity are: B-E (SF1) and C2-D1-E-D2 (SF2). Both facies tracts record an overall transgressive evolution.

The transition between facies B and E is abrupt in SF1, but this may be due to a lack of observation. The C2-D1-E facies tract in SF2 is also basically interpreted as transgression. The change from the hemipelagite E to the topmost D2 channel and lobe deposit may only reflect the general interbedding of facies E with the most distal sands of the basin, and in that case the 10 m thick hemipelagite would only be a landmark in the course of transgression – the peak of which would then be the topmost D2 channel and lobe sandstone. Alternatively, these D2 sandstones would to the turnaroud to sea-level fall and the start of another sequence (SF3) with LST deposits.
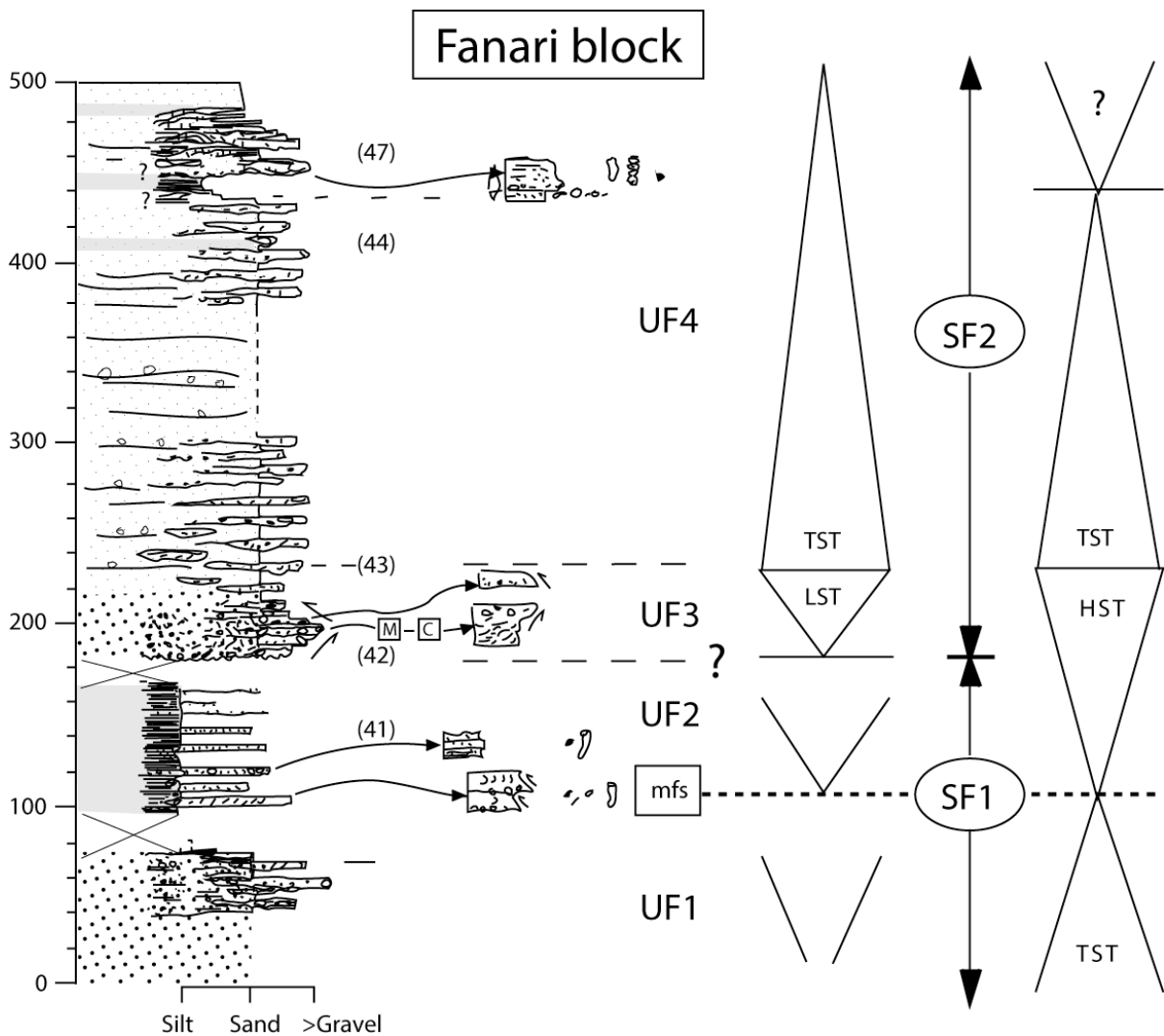
Fig. II. 79: Synthetic sketch of Block-UF with preliminary sequence stratigraphic interpretations.

IX. General tectonic framework of the studied area

Sedimentary strata overall the study area are commonly NW-SE striking (N100°E to N140°E) and dipping 20 to 50° toward the NE. The major faults within the area are striking NW-SE. The two main faults (Livadhia Fault and Kanalia Fault, see Fig. III. 1) define the three main tectonic blocks described in the stratigraphic section (Chapter I, Fig. I. 9A and B; Chapter II).

Other faults of less importance in terms of offsets could be measured and described. They show a wide range of orientation and some of them are clearly synsedimentary. In this tectonic section, we will present and discuss the brittle deformation of that area and insist notably on the synsedimentary faulting that highlights the tectonic development of this part of the Mesohellenic Basin. The variety of structures and synsedimentary deformations show that the area experienced several episodes of faulting.

Previous published work on tectonic pattern consists mainly on geological mapping (Savoyat, 1969b; Jaeger, 1979; Lekkas, 1988). More recent work on this part of Greece focused on recent tectonic activity. These studies, based on recent geomorphology, focal mechanisms, and geodetic data showed that the present activity is exclusively extensional with a dominant North-South direction of extension (Caputo, 1995; Hatzfeld *et al.*, 1999; Papadimitriou & Karakostas, 2003; Kamberis *et al.*, 2012).

After a brief presentation of the tectonic framework of this area of western Thessaly (section **IX**), we describe the structural pattern and precise the chronology of deformation on the basis of field data in the studied area (Fig. III. 1). Our analysis focused on:

X) Synsedimentary extensional deformation
XI) Kinematics analysis of the major NW-SE faults
XII) Transverse faults
XIII) Metric-scale brittle deformation

130
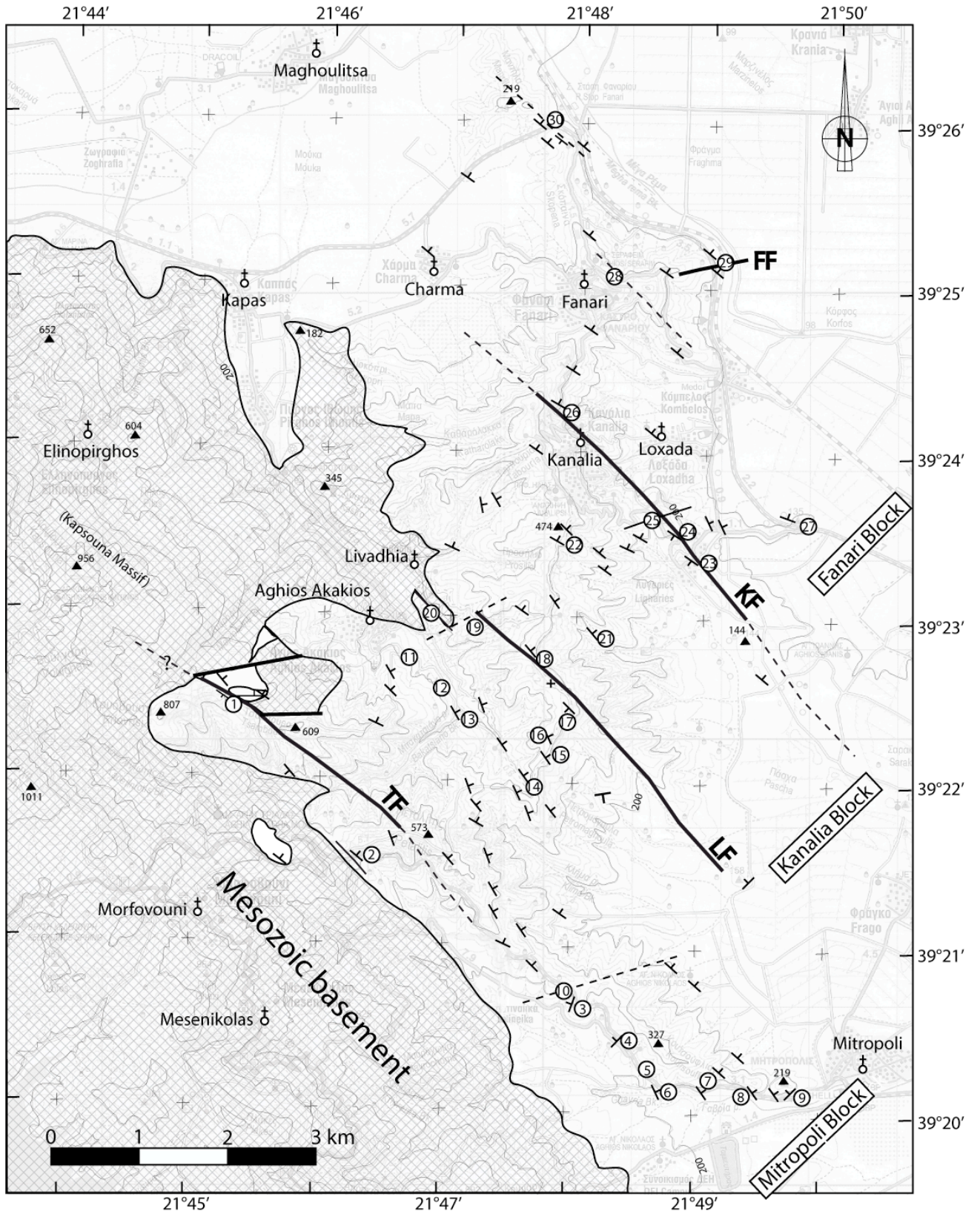
Fig. III. 1: Structural map of the studied area with report of the main faults, bedding planes and localities of tectonic data described in this chapter (circled numbers).

131

A. Previous work

Savoyat (1969b) established the 1/50000 scale geological map and cross-section of the studied area (Fig. III. 2).
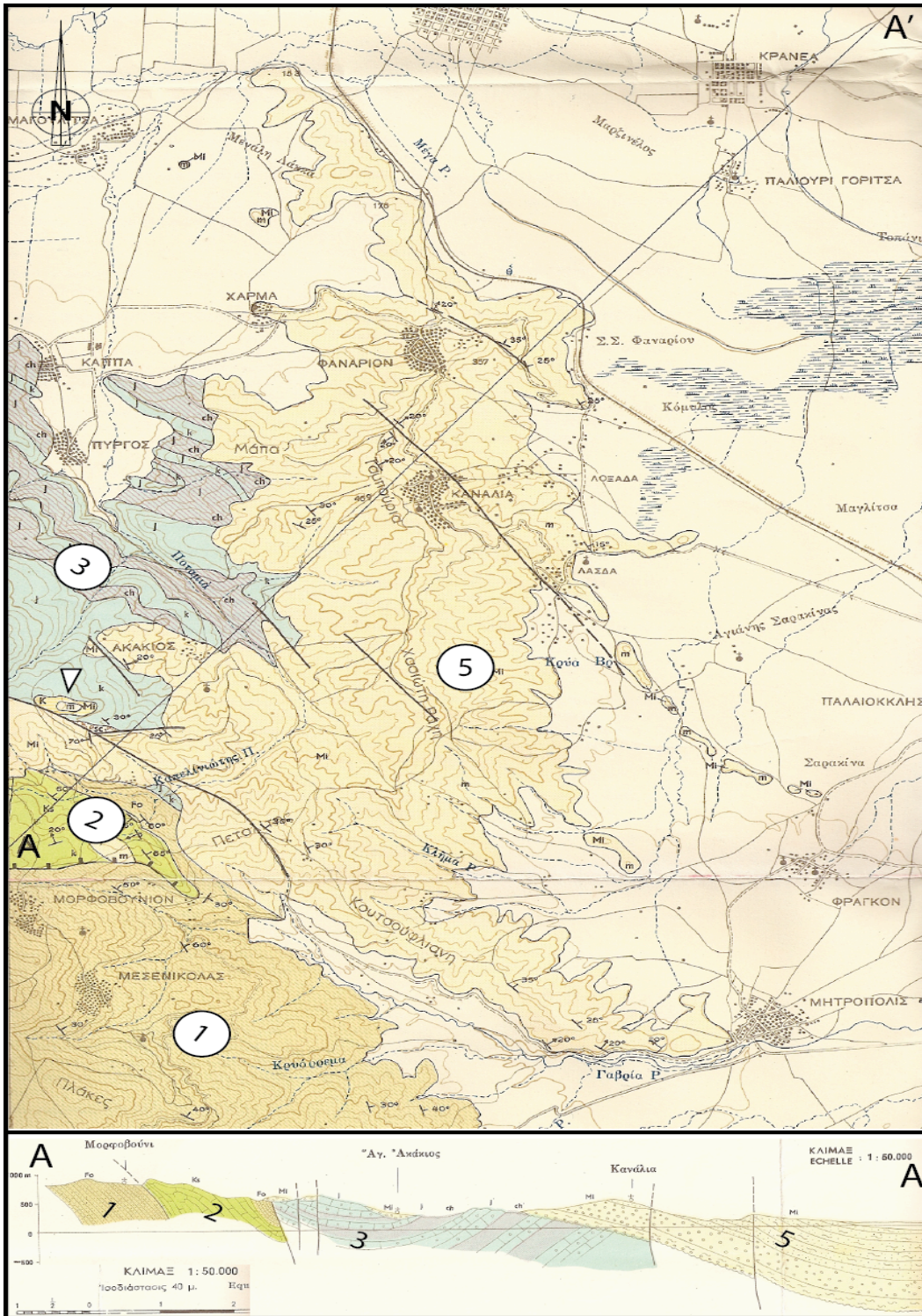
Fig. III. 2: Geological map (1/50000 scale) and cross-section from Savoyat (1969b). 1: Early Tertiary Pindos flysch units; 2: Cretaceous limestones; 3: Koziakas units; 5: Neogene deposits.

He distinguished the neogene deposits (5, Fig. III. 2) uncomformable on the deformed Mesozoic basement constituted of Pindos paleogene flysch (1), Cretaceous limestones (2) and Koziakas Mesozoic series (3). All these units (1, 2, and 3, Fig. III. 2) were deformed during early Tertiary and earlier tectonic episodes during Hellenides convergence (Brunn, 1956; Aubouin, 1958; Ferrière, 1982; Jacobshagen, 1986).

Further work by Jaeger (1979) proposed another geological map of that area, but it mainly differs from the previous one (Savoyat, 1969b) on the interpretation of structures in the pre-Neogene basement.

On both of these works, the neogene series are all considered as undifferentiated post-orogenic molassic deposits. Mapping by Lekkas (1988) consider three different sedimentary units within the Neogene deposits on the basis of various dominant lithologies (see Fig. I. 5).

B. Recent tectonic activity in Central Greece

Several studies have reported and synthesized the seismic activity of central Greece (*e.g.* Caputo, 1995; Papazachos and Kiratzi, 1996; Hatzfeld *et al.*, 1999; Papadimitriou and Karakostas, 2003). The location of epicenters reveals a distribution mainly along the E-W directed faults that have therefore to be considered as active (Fig. III. 3).

Focal mechanisms indicate clearly normal faulting with a dominant N-S direction of extensional deformation (Fig. III. 4).

The study of recent faulting in and at the borders of Thessaly plains includes also geomorphological analysis, fault scarps recognitions, trenching of main faults and geophysical prospecting. This work led to establish precise maps of the Pliocene to Quaternary faults (Fig. III. 5, Caputo, 1995).

The detailed analysis of individual faults showed that the normal faulting occurred along NW-SE faults during the Pliocene to the early Pleistocene and that it changed to approximately E-W directed faults since the late Pleistocene (Caputo and Pavlides, 1993; Mercier *et al.*, 1998; Caputo *et al.*, 2006).
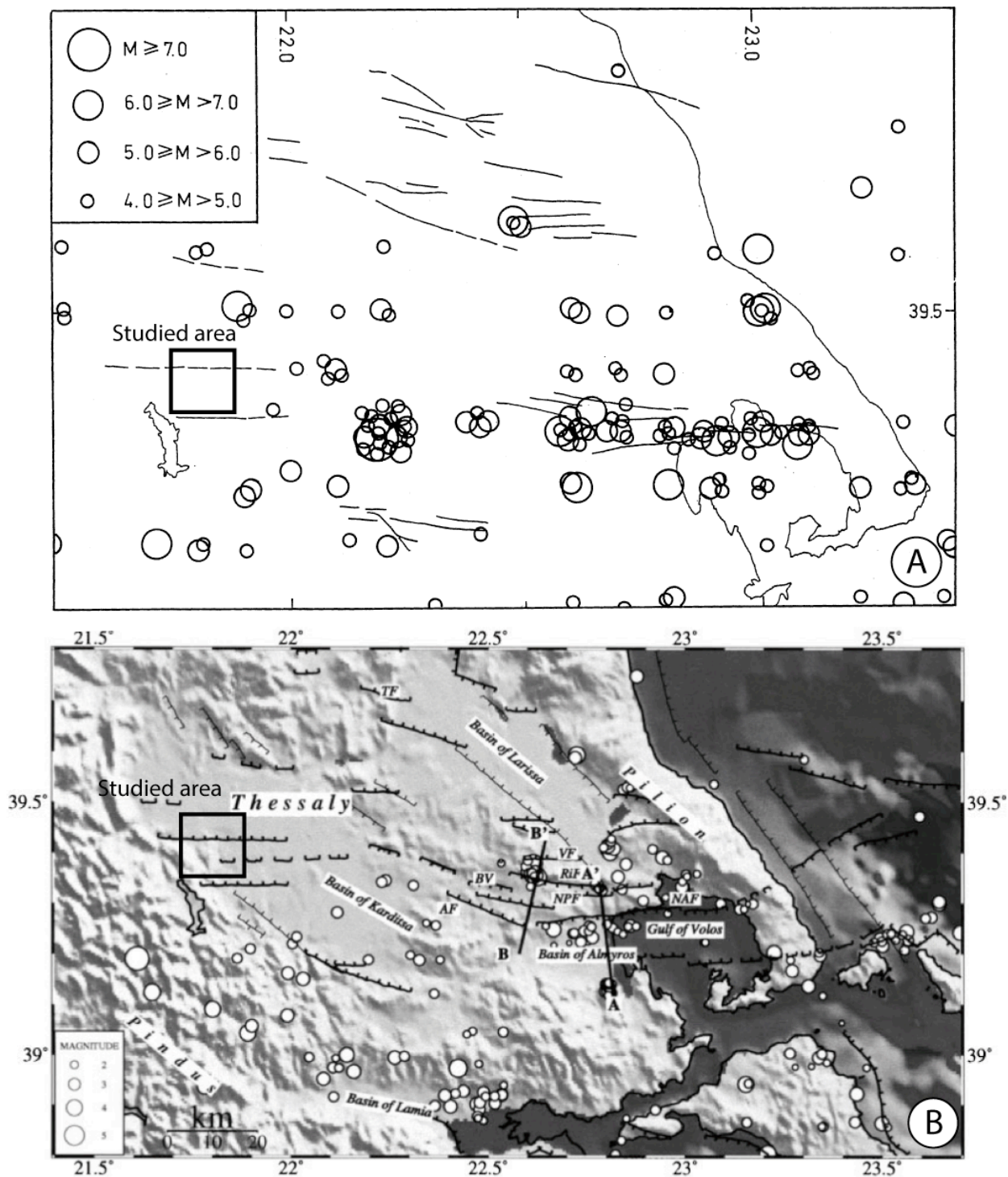
Fig. III. 3: A - Distribution of epicenters for main earthquakes in Thessaly Region for the period 1901-1985, from Caputo (1995) and, B - location of recent earthquakes from Hatzfeld *et al*. (1999).
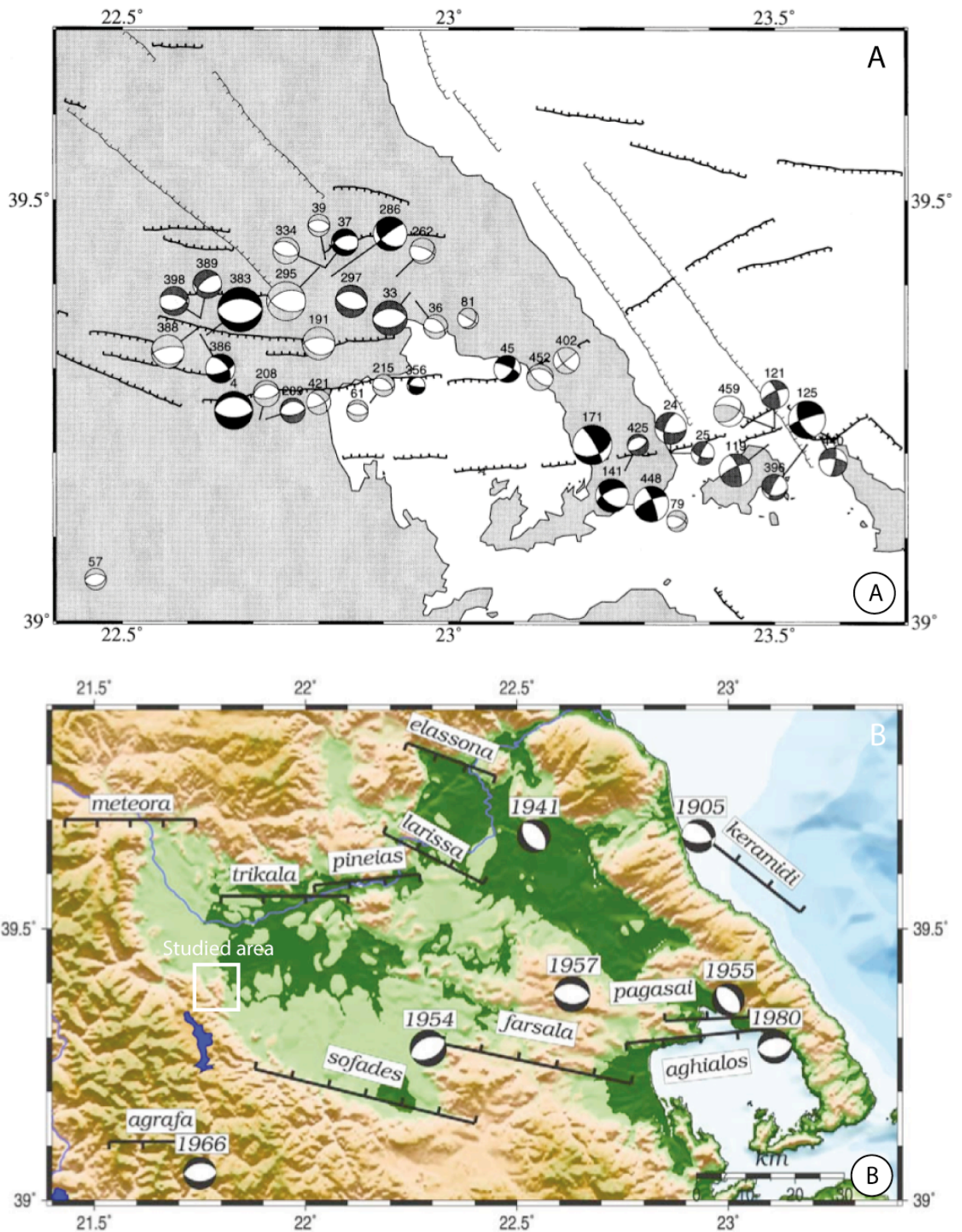
Fig. III. 4: A - Map of the focal mechanisms computed for Thessaly and the Gulf of Volos. Note the largely dominant N–S-trending pure extension in Thessaly, the western half of the map (Hatzfeld *et al.*, 1999). B – Map of focal mechanisms from large earthquakes (M$_w$ > 6) in Thessaly Region (Papadimitriou and Karakostas, 2003).
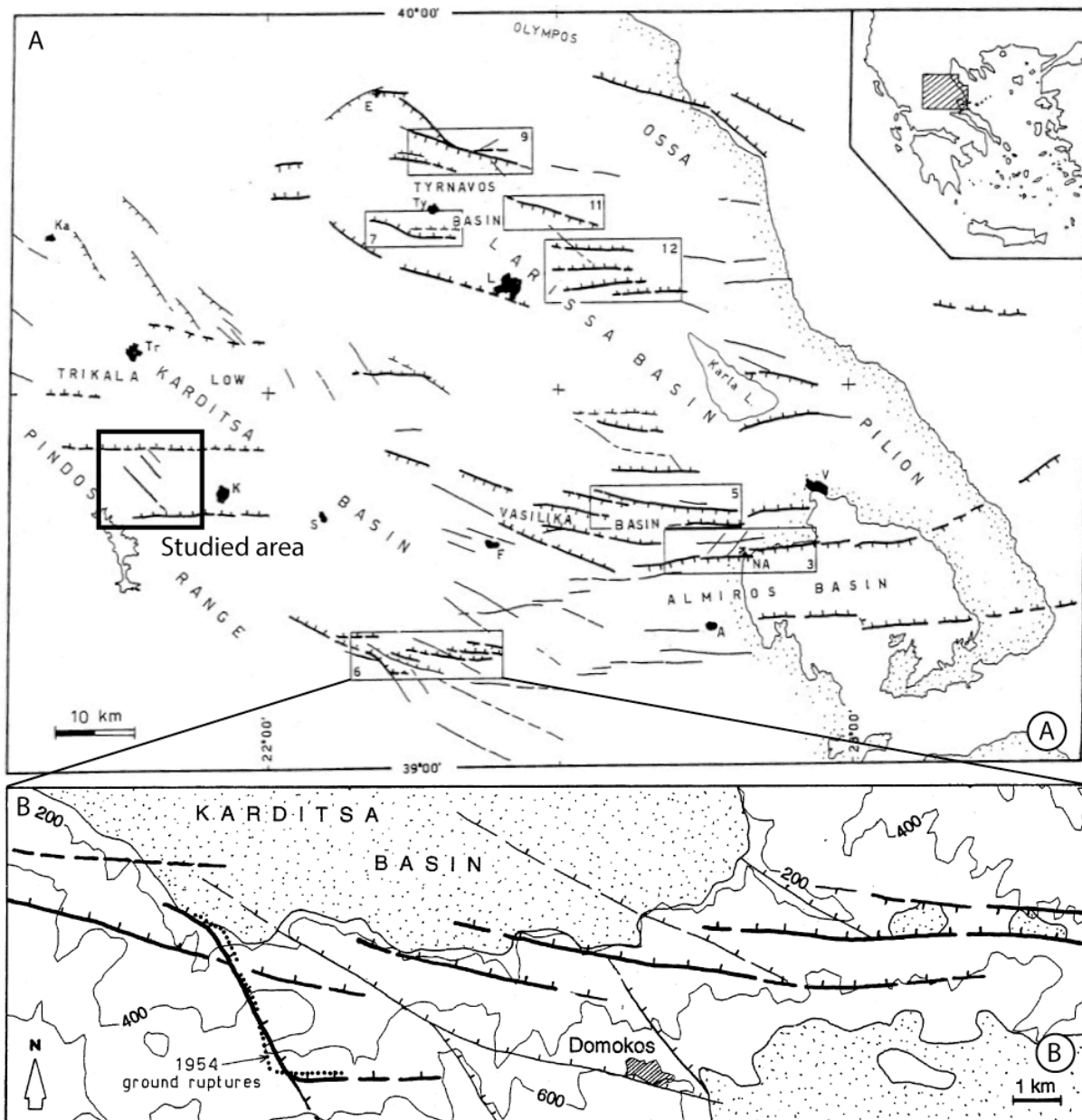
Fig. III. 5: Distribution of active faults in Thessaly Region of Central Greece (A), with a detail of Domokos area in southern Thessaly (B, frame n°6 on A), from Caputo (1995).

Studies from GPS measurements (Kreemer *et al.*, 2004; Hollenstein *et al.* 2008) also give similar results with a c. 10 mm/yr southward shift of central Thessaly relative to Eurasian plate (Hollenstein *et al.*, 2008). Other recent studies, based on geomorphology, hydrographic pattern and brittle deformation analysis in western Thessaly showed extensional faults changing from a NW-SE direction in the Pliocene to an E-W direction in the Quaternary (Fig. III. 6, Kamberis *et al.*, 2012). Their conclusions on fault pattern and timing is

in good accordance with results from earlier authors in southern and eastern Thessaly (Caputo and Pavlides, 1993; Mercier *et al.*, 1998; Caputo *et al.*, 2006).

Fig. III. 6: Evolution trough time of the direction of normal faulting in western Thessaly according to Kamberis *et al.* (2012). Note the persistence of extensional deformation from the Serravallian-Tortonian to present-day and the change in extensional direction from NE-SW in the late Pliocene to N-S in the Quaternary.

The extensional deformation that dominates in the Aegean domain since the Miocene (and even earlier farther North) is generally interpreted as the result of the African Slab retreat beneath the Aegean/Anatolian plate (*e.g.* Jolivet & Brun, 2010). This extensional deformation associated to slab retreat is considered to have started in Northern Greece (Rhodope zone) as early as Eocene times and migrated gradually southward through time.

X. Syn-sedimentary extension at the onset of basin development

Along Mitropoli-Morfovouni road, at the southern part of Mitropoli-block (Fig. III. 1, localities-2 to 4), we observed a succession of syn-sedimentary normal faults within the basal conglomeratic units (UM3 mainly). Occasionally, such normal faults also appear up to the basal beds of the overlying unit (L-UM4), These faults are good markers of the important unstabilities, of tectonic and/or of gravitational origin, that control the initial development of the Mesohellenic Basin in that particular area.

These synsedimentary faults are nicely exposed along the Mitropoli-Morfovouni road cutting (Fig. III. 1), at about 6 km west of Mitropoli village and about 2 km east of Morfovouni village (locality-2, Fig. III. 1). The outcrop show deformed conglomeratic series that are directly overlying the Mesozoic basement that is exposed about 50 m to the west. The outcrop is continuous through more than 300 m. The exposed serie is described in the Stratigraphy section (Chapter II; type-section of UM3 and UM4). The outcrop displays several types of structures, dominated by normal faulting, and we focused here on the detailed description of synsedimentary structures.

At this locality 2 (Fig. III. 1 and Fig. III. 7), we observe a series of east-dipping normal faults within the conglomerates-dominated unit (UM3). The overlying siltstones and turbidites (UM4) are overlapping the normal faults and associated tilted blocks.

Most fault planes are directed NW-SE (N120°E to N150°E) and dipping 30° to 70° toward the NE. A few conjugate faults are dipping 70° to 80° toward the SW.

Measurements of fault planes are plotted on stereonet diagrams (Fig. III. 8C). This set of faults reveals a NE-SW direction of extension. Slickensides are absent from fault surfaces, probably because of their synsedimentary nature, they were not deep enough to be

mineralized by calcite. However, motions of sedimentary strata are clear, indicating normal motions.

On this outcrop (Fig. III. 7 and Fig. III. 8) a 1 to 2 meter-thick layer of pale-grey to orange siltstones of UM3 conglomeratic unit is a good marker bed (layer d). Offsets along the faults range from 1 to 3 meters. The offsets slightly decrease toward the northeast. For instance F2 has an offset of about 3 m and F7 has an offset of about 1 m (Fig. III. 8A and B).
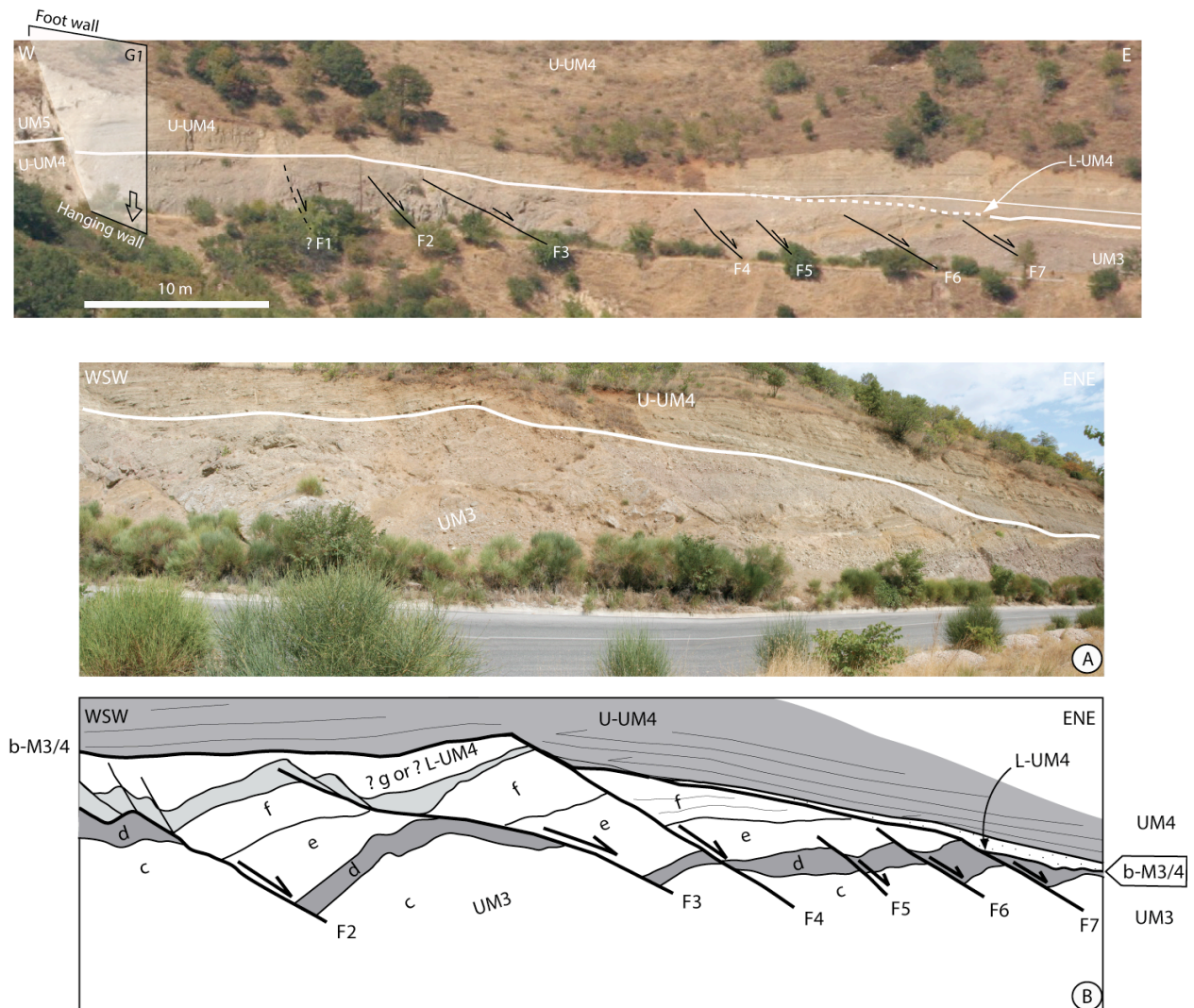
Fig. III. 7: Top) Panoramic view of section at locality 2 (Fig. III. 1), looking toward the NE from Mitropoli-Morfovouni Road. We can observe the UM3-UM4 stratigraphic units and a serie of east-dipping normal faults that affect only UM3 (except from the large fault on the western side that affect the whole UM3-UM5 units). Bottom) A: Closer view of normal faults within UM3 and covered by UM4. B: sketch drawing of the various strata from A.
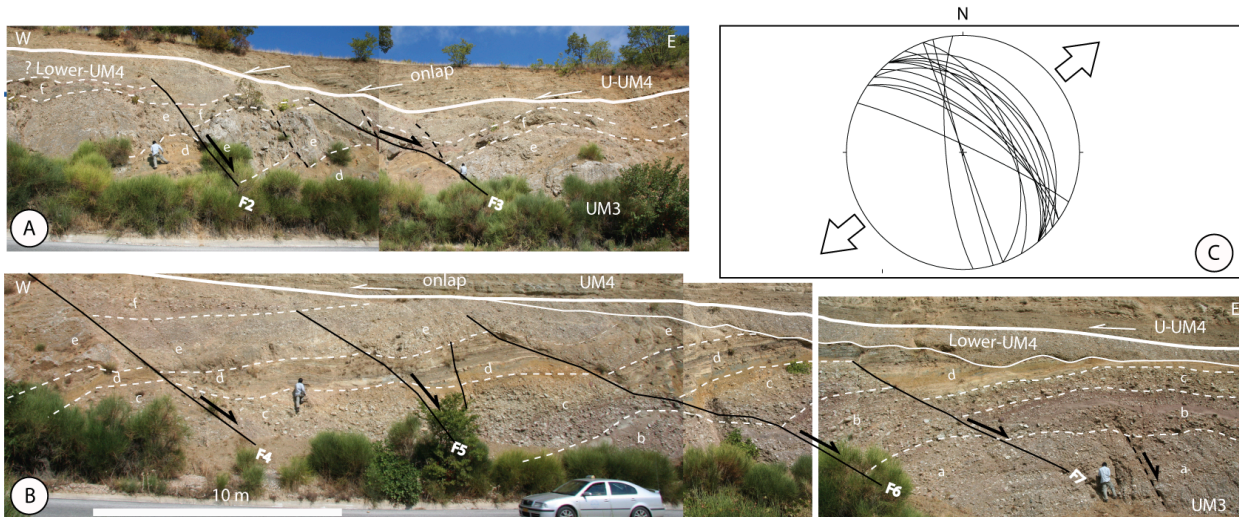
Fig. III. 8: A-B, Detailed interpretation of some of the synsedimentary faults (F2 to F7, see also Fig. III. 8B) affecting UM3 at locality 2, along the Mitropoli-Morfovouni Road (Fig. III. 1 for location). C, Measured fault planes reported on a stereonet diagram (equal area, lower hemisphere).

Some wedge-shaped sedimentary bodies can be observed on the footwall of the main faults. For example, on the footwall of fault F4 (Fig. III. 8, and details on Fig. III. 9) the layer-f, constituted of conglomerates, is thickening significantly toward the fault. The geometry of individual beds within this layer-f is unclear because of its very coarse-grained lithology, but the fan-shaped geometry can be distinguished from outcrop (Fig. III. 9).
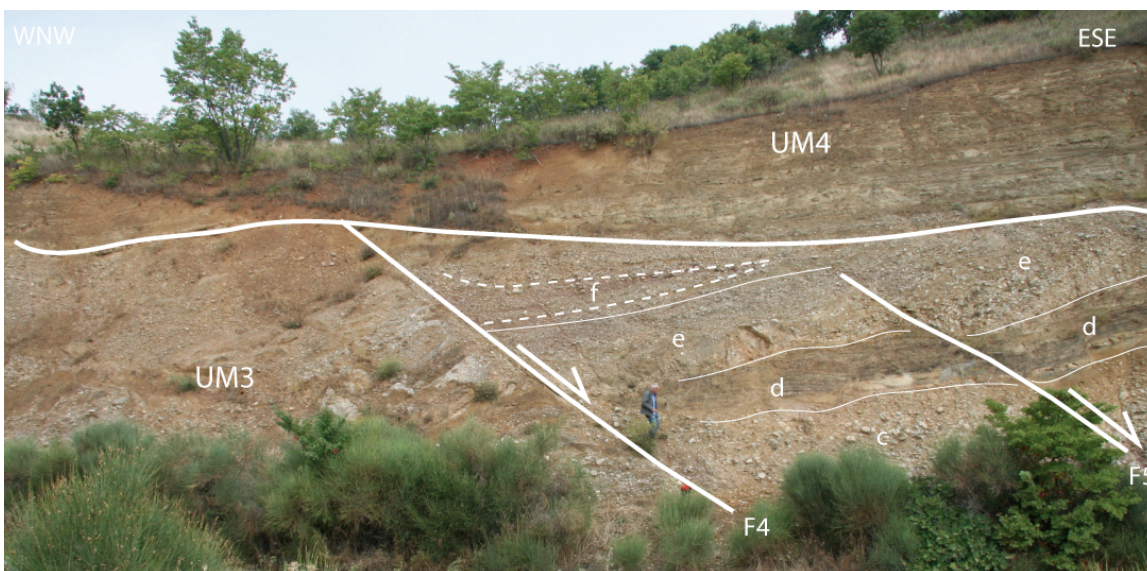
Fig. III. 9: Close-up view of fault F4 showing a sedimentary wedge (in dashed lines, within unit f) with thickening toward the fault.

Because of rotation along the observed listric faults, bedding planes in UM3 can be largely tilted. Within this unit UM3, affected by synsedimentary faulting, general bedding

direction is NW-SE (N130°E to N150°E). These bedding plane are dipping up to 40-50° on the footwalls, close to the fault, and flatten progressively away from the fault plane, getting subhorizontal on the hangingwall of the next fault (e.g. F2 and F3 on Fig III.8). Some drag folds can also be observed on the footwall of some of these synsedimentary faults (e.g. F4 and F5 on Fig. III. 8).

In summary, we observe from this locality that these synsedimentary listric faults are striking NW-SE and mainly dipping toward the NE. They are clearly normal faults that represent a NE-SW direction of extension during deposition of UM3 and mostly prior to the deposition of UM4 that is uncomformably overlying these structures. A few normal faults, with moderate displacements, were observed also in the overlying beds of UM4. They are covered with onlap geometry by the conglomeratic beds of UM5 (Fig. III. 10). This spectacular tectonic pattern, in the early stages of the neogene sedimentation in this area, testifies for the occurrence of a significant NE-SW extensional episode at the onset of the basin development.
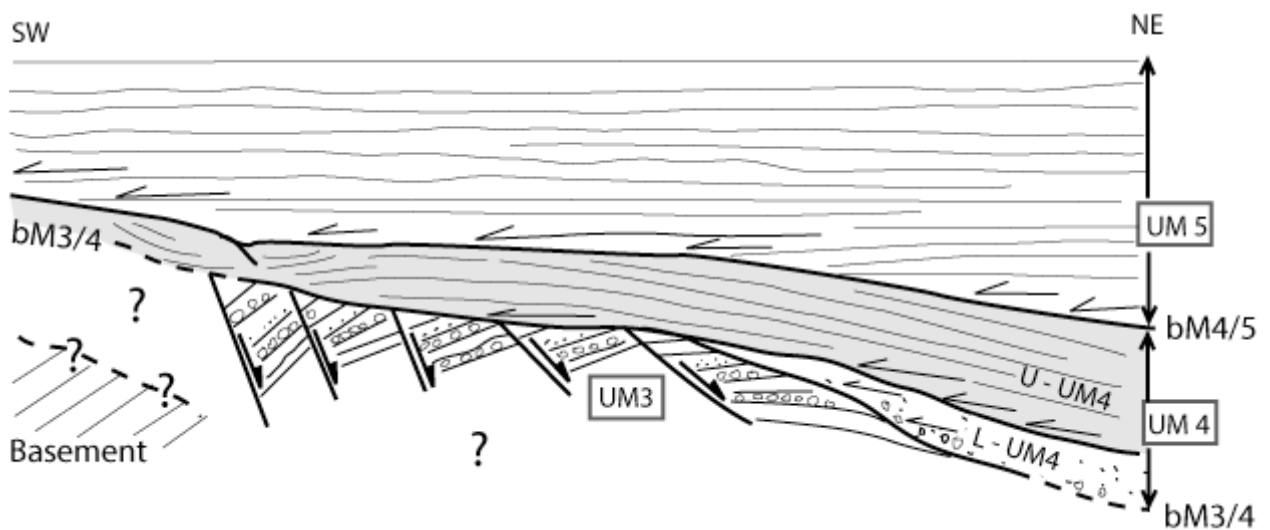
Fig. III. 10: Interpreted schematic cross-section at locality 2, presenting the geometric relationships between sedimentary units on top of the synsedimentary faults of UM3.

XI. Description and analysis of the Main NW-SE Faults

The studied area is transected by large faults directed NW-SE. Their kinematics analysis show that they are quite complex and reveals that they correspond certainly to polyphased tectonic activity on these individual faults. We describe and define in this section

the 3 main faults of that area, from the SW to the NE: Tsambouro, Livadhia, and Kanalia that are named from this study.

A. Tsambouro Fault (TF)

This fault, appearing on the southwest part of the Mitropoli block, has been mapped by previous authors (Savoyat, 1969b; Jaeger, 1979; Lekkas, 1988) with similar NW-SE orientation but not exactly at the same location. We named this fault (Tsambouro Fault, TF) from the name of a hill (summit at elevation 609 m, Fig. III. 1), close to the type-section of the fault.

One of the best outcrop of this fault is along a small track North of Morfovouni (locality 1, Fig. III. 1). This Fracture zone shows an approximatively N120°E direction. Because of intense surface weathering, no evidence of striations could be observed directly in this fault zone. Some fracture planes could be measured in the fault zone. They range from N100°E to N120°E and are steeply dipping toward the North (dips ranging from 75 to 85°N).

At this locality, we observed conglomeratic beds of UM5 that are getting subvertical close to the fault, on its southwestern side. On the northeastern side of the fault, we observe the following succession from base to top: Mesozoic limestones of Koziakas basement; Oligocene limestones of UM1; conglomeratic strata of UM2. UM1 and UM2 strata on this NE side of the fault show gentle dipping toward the NE (Fig. III. 11A). The bedding planes were reported on stereonet diagrams in order to construct the fold axis that is obviously related to the faulting. This relation between fractures and severe folding in the vicinity of the main faults is consistent regarding the geometric relationship of stereonet (Fig. III. 11B). Indeed, the constructed axis of the fold is subhorizontal and in the fracture planes.

From the offset of sedimentary series, we assume that the NE-side of Tsambouro Fault is a moving upward compartment, relative to the SW-side moving downward. Deformation of strata on both side of the fault zone, and particularly the UM5 conglomerates and sandstones going vertical close to the fault (Fig. III. 11), also demonstrates a drag fold in accordance with that relative motion. The total offset is in the range of 50-150 m, according to the total offset of the sedimentary units.

The overall geometry of the Tsambouro Fault is not very well constrained but if we admit that the small scale brittle deformation in the fault zone is reflecting the attitude of the main fault (c. N110°E 80°N), we therefore have to consider that the Tsambouro Fault is a reverse fault.
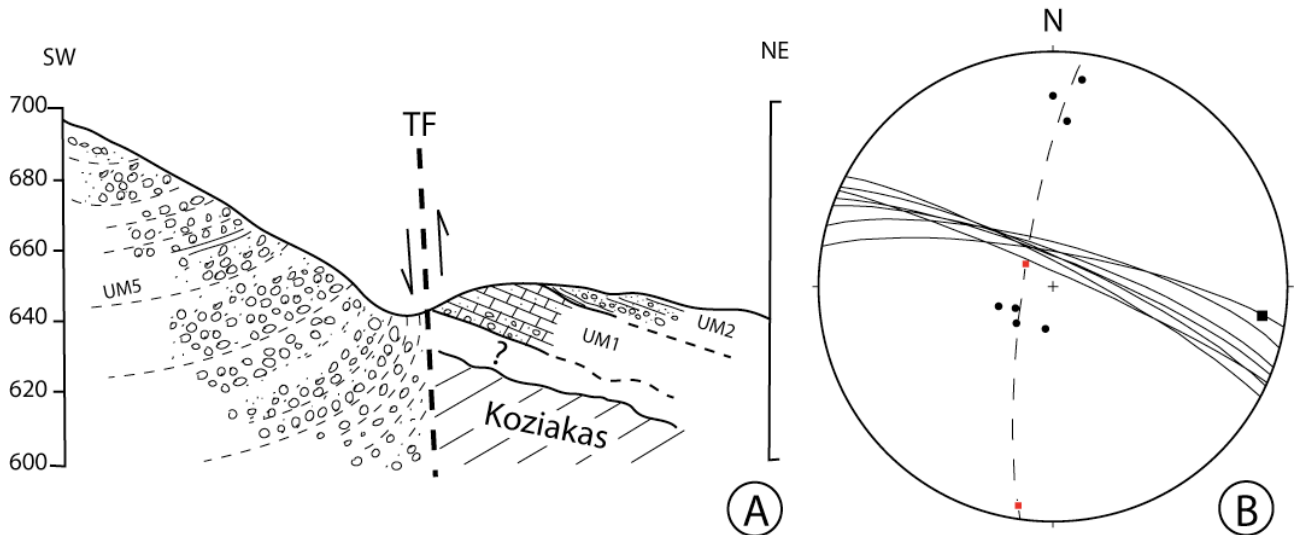
Fig. III. 11: A: Schematic cross section of Tsambouro Fault (TF); and B: stereonet diagram reporting secondary fracture planes (solid lines), poles of bedding planes (circles), and the drag fold axis constructed from poles of bedding planes (square). See text for comments.

B. Livadhia Fault (LF)

Livadhia Fault crosses the middle part of the studied area and it separates the Mitropoli block and the Kanalia block. The fault is also directed NW-SE (strike from N140°E to N150°E) and it is steeply dipping, nearly vertical. The Fault was directly observed from outcrop at three localities (18, 19, and 20) (Fig. III. 1 and Fig. III. 12).

Along the new Kanalia-Morfovouni road (Fig. III. 12, locality 18), the fresh road-cut shows a good outcrop of the fault. It forms a 5-6 m thick crushed zone and separates UM7 from UK1-UK2 sedimentary units.

On the SW from Livadhia Fault, UM7 consists of medium- to thick-bedded bioturbated sandstones alternating with siltstone beds. These strata are dipping gently toward the NE. On the NE compartment, the series are fine- to very coarse-grained. They consist of channelized pebble conglomerates alternating with siltstones and sandstones. This sedimentary unit has been attributed to the top of UK1 (see map Fig. III. 12 and Chapter 2). These strata are striking NW-SE (N110°E to N140°E) and they are dipping 20-30° toward the NE.

143
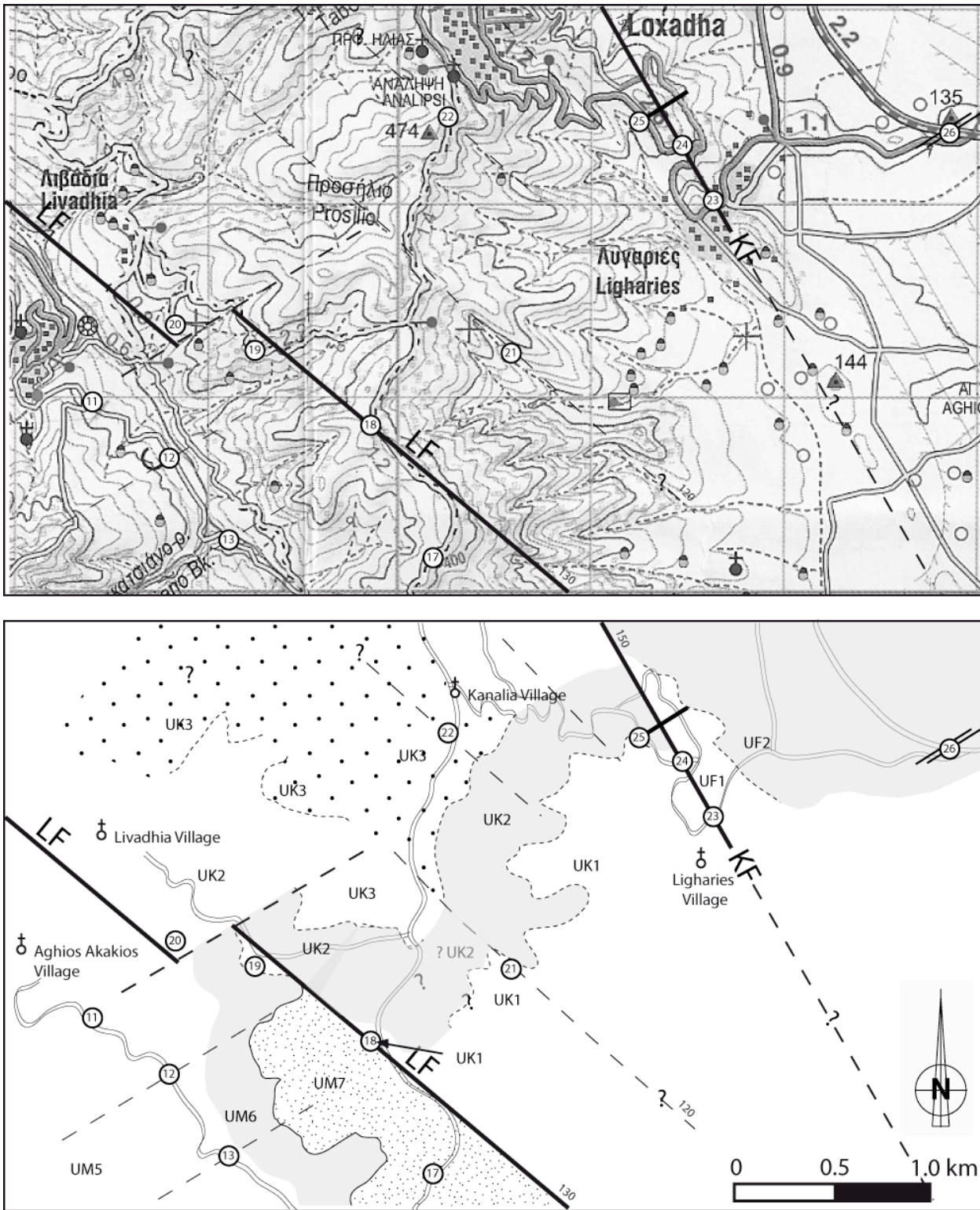
Fig. III. 12: Topographic (A) and geological maps (B) of the central part of the studied area showing the Livadhia Fault (LF), southern extension of Kanalia Fault (KF) and localities refered in the text (circled numbers).

Within the deformed zone (Fig. III. 13), sedimentary strata are chaotic and most of the remaining beds are steeply dipping (50° to 70°) toward the SW. The main fault is directed

N140°E to N150°E and some dip-slip striations could be measured within the crushed zone (Fig. III. 14A).
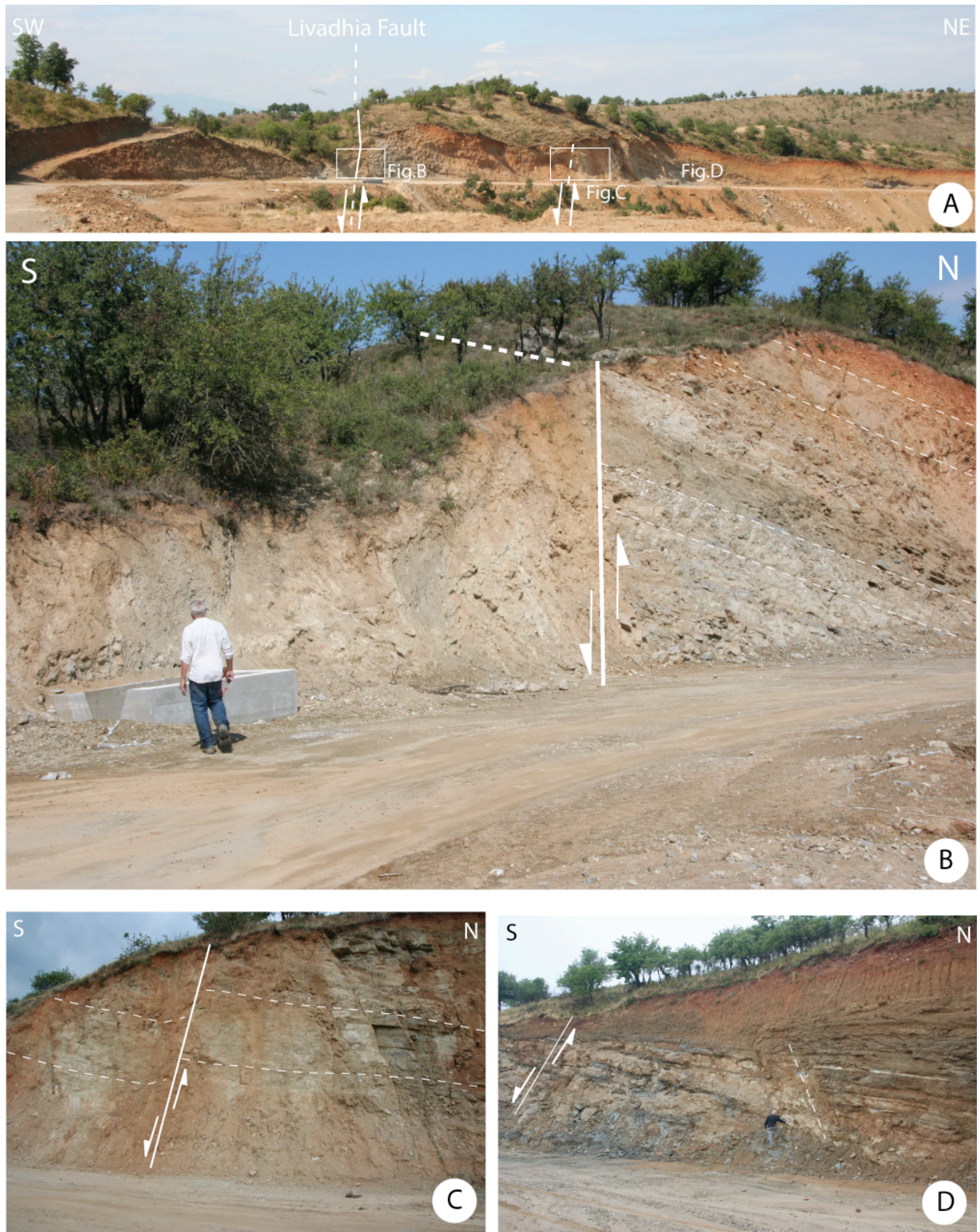
Fig. III. 13: Views of Livadhia Fault zone at locality 18 . - (A) General view from locality-18 ; (B) Closer view of Livadhia crushed zone in the main fault ; (C) and (D) Normal faults in the vicinity of Livadhia main crushed zone.

Kinematics analysis of this crushed zone is not clear because of chaotic deformation but all indicators (striations, steep beds) suggest mainly vertical motion along the fault. From stratigraphic relationships on both sides of the fault, we propose a mainly normal displacement. Moreover, the brittle deformation in the vicinity of the main fault is clearly characterized by normal faulting. These normal faults have similar orientations and also show dip-slip slickensides. The bedding offsets, ranging from 0.5 m to 2 m, confirm the normal faulting in this zone (Fig. III. 13C and D, and Fig. III. 14B).
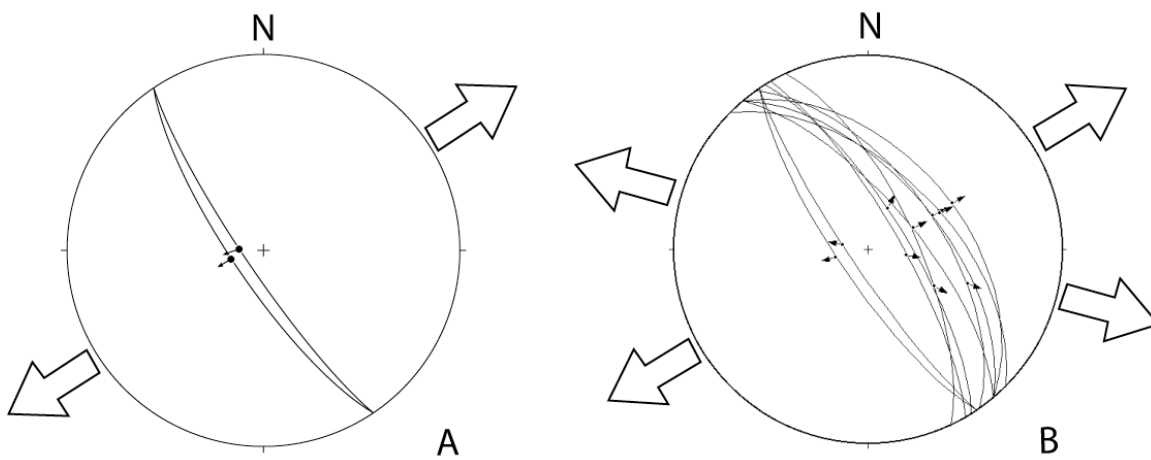
Fig. III. 14: Stereonet diagrams from measured planes and striation within the main Livadhia crushed zone (A) and from normal faults measured close to Livadhia main fault zone (B).

The Livadhia Fault could also be observed from other localities (*e.g.* locality 19, Fig. III. 12). The fault location can be deduced from large offsets within the sedimentary units in the structural continuity of the previous outcrop, but the exposure is not sufficient to undertake any kinematics analysis of the fault surface.

Further to the NE, at about 1km South of Livadhia village (locality-20, Fig. III. 12), a large fault is deduced from the significant offset between Koziakas basement (Mesozoic limestones) and neogene series. This fault is not strictly in the continuity of Livadhia Fault but it can be the same fault if we admit that it is offset by a transverse fault (Fig. III. 12 and Fig. III. 15). This transverse fault shows an apparent sinistral displacement but had also probably some dip-slip motion, similarly to other transverse faults in this area (see section XII).

146

Fig. III. 15: Panoramic view looking NE from Aghios Akakios with the position of Livadhia Fault (LF) separating UM and UK sedimentary units. We propose an apparent sinistral offset of that major fault on the NW side of that view.

In conclusion, we can propose that the Livadhia Fault is a major normal fault, steeply-dipping southwestward, with a minimum offset of approximately 50-100 m. No evidence of strike-slip motion could be observed from this fault. The fault could be observed in several places (Fig. III. 16), and we consider that the large fault, dipping SW, and separating Koziakas basement to neogene siltstones corresponds also to the same Livadhia fault. This Livadhia Fault has therefore to show an apparent sinistral offset along a transverse fault (Fig. III. 15). The fault can be polyphased, as expected from the complex chaotic zone of the fault plane, but only vertical displacements could be deduced from our analysis.
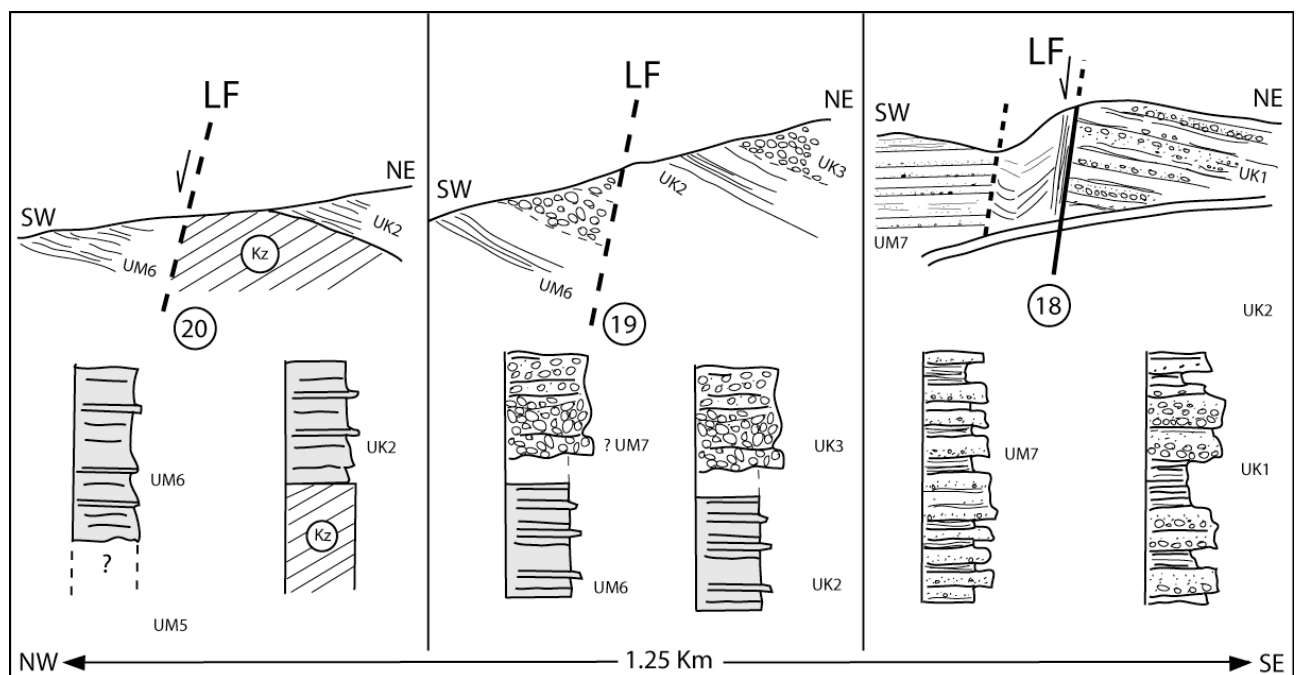
Fig. III. 16: Schematic Cross-section of Livadhia Fault zone at localities 18, 19 and 20 (NE-SW direction).

147

C. Kanalia Fault (KF)

This fault is named here from the village of Kanalia, located in the central part of the studied area. This fault has been reported on the 1/50000 geological maps (Savoyat, 1969b; Lekkas, 1988) but was not studied in details.

We could observe and describe outcrops of the Kanalia Fault at three localities (23, 24, and 26 on Fig. III. 1). The best place to observe that fault is along the road between Kanalia and Fanari, just outside Kanalia Village (locality-26, Fig. III. 1).

1. Kanalia Fault "type section"

The Kanalia Fault (Fig. III. 17) is well exposed on the western side of Kanalia-Fanari road, at about 300 m North of the exit of Kanalia village (locality-26, Fig. III. 1).

The main fault separates massive medium- to coarse-grained sandstones with few scattered pebbles, in the SW, and alternating conglomerates and sandstones, in the NE (Fig. III. 17A and C). The bedding on both side of the fault is moderately dipping about 15° toward the NNE. The main fault plane is striking NW-SE (N110°E to N120°E) and is dipping 60-75° to the NE.

Striations on the main fault plane could not be observed but some of them could be measured on secondary faults obviously related to the main fault plane. These striations, as well as the fault planes measured in this fault zone are reported on a stereonet diagram (Fig. III. 17B). The striations on these secondary faults showed mainly some dip-slip displacements. Folding of strata on both sides of the fault zone reveals some reverse motion (Fig. III. 17A and C). Moreover, a secondary fault within this fault zone clearly shows a reverse motion from the offset of conglomeratic beds and from the offset of individual broken pebbles.

The stratigraphic succession also supports this interpretation with overall reverse motion as the hangingwall (NE side of the fault) present the reappearance of conglomeratic layers evolving upward to massive sandstones with sparse pebbles (Fig. III. 17). This later facies corresponds very well to the one observed on the footwall of the fault below the sandstones (SW side).

Fig. III. 17: (A) view of the Kanalia Fault, dipping NE, at locality-26, and interpretative sketch of that fault zone (B). Stereonet diagram (C) with fault orientations and measured slickensides on fault planes within Kanalia Fault zone.

2. Additional data on Kanalia Fault (localities 23 and 24)

We could follow the Kanalia fault zone southeastward and we found some relatively significant outcrops that permitted to obtain some additional structural information. These outcrops could be observed between the villages of Kanalia and Ligharies (locality-24, Fig. III. 18) and at the eastern entrance of Ligharies village (locality-23, Fig. III. 18).

149
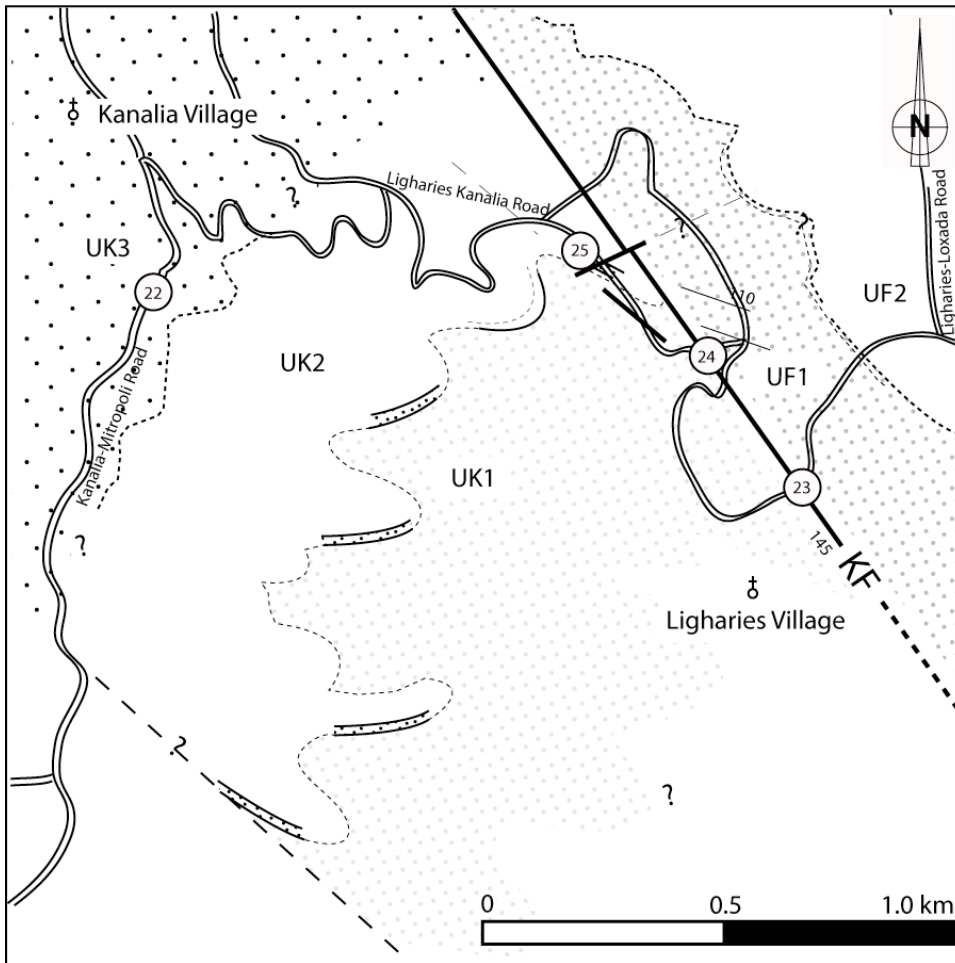
Fig. III. 18: Detailed map of the Kanalia area with the location of outcrops along the Kanalia Fault (KF).

At this locality-23, just outside Ligharies, the fault zone itself is relatively crushed and weathered (Fig. III. 19 and Fig. III. 20). Consequently, it could not provide many reliable displacement features. However, we could find some cleavage development in the fault zone that indicates reverse motion (Fig. III. 19C). In addition, some preserved striations are dip-slip and indicate therefore vertical displacements. We also could distinguish a few horizontal striations indicating some strike-slip displacements.

About 350m farther toward the NE, at locality-24 (Fig. III. 18 and Fig. III. 21), The Kanalia Fault zone also showed some strike-slip striations, with probably a sinistral displacement as deduced from slickensides (Fig. III. 20). These observations showed that the Kanalia Fault had not only reverse displacement but also experienced some strike-slip displacement at some stage of its development.

Fig. III. 19: (A) Outcrop view from the Kanalia Fault at locality-23 (location on Fig. III. 18). (B) closer view of the fault line ; (C) Tectonic cleavage in the fault zone that confirms the reverse component along this fault.
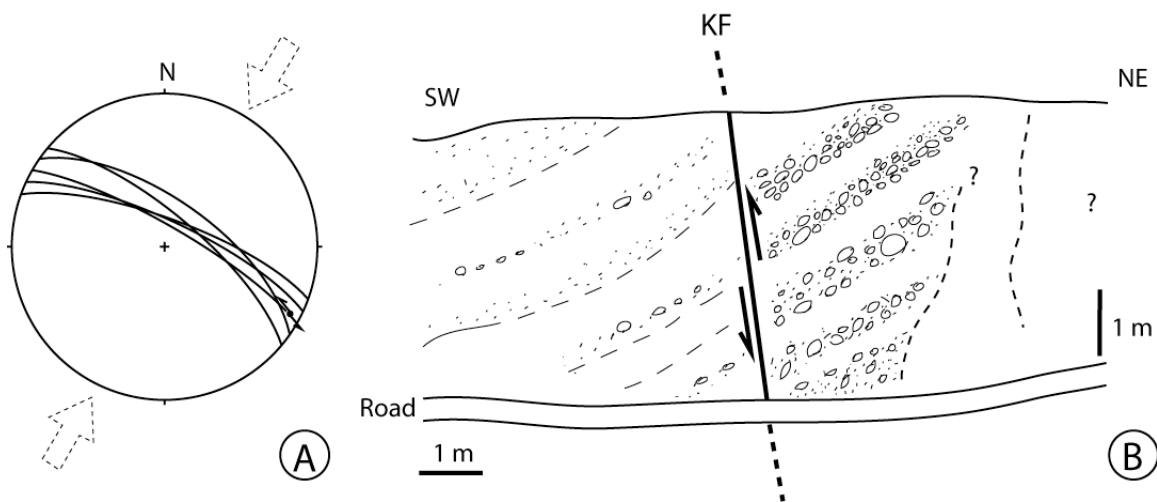
Fig. III. 20: (A) Stereonet diagrams (equal area, lower hemisphere) presenting the brittle deformation measured from the outcrops of Kanalia Fault Zone at localities 23 and 24 (location on Fig. III. 18 and Fig. III. 1). (B) Interpretative sketch of Kanalia fault zone at locality-23.

However, at all the localities, the significant steepening of bedding in the vicinity of the fault zone correspond to metric-scale to decametric-scale drag folds that confirms the reverse faulting along this structure. On locality-23 (Fig. III. 19), on the SW side of the fault, bedding is progressively increasing from 28°SW to 65°SW close to the fault zone. It shows clearly that these strata form a large syncline below the fault with the northeastern limb that is highly steepened near the fault. Conglomeratic beds from the NE compartment are also steeply dipping southwestward (45 to 55° SW). They then flatten as we move away from the fault, until dipping gently to the NE. They thus represent an anticline developing on this NE side of the fault (Fig. III. 20B). On locality-24 (Fig. III. 21), the folding is not so obvious but the SW side of the fault also present significant steepening of bedding, comparable with the one described above at locality 23.
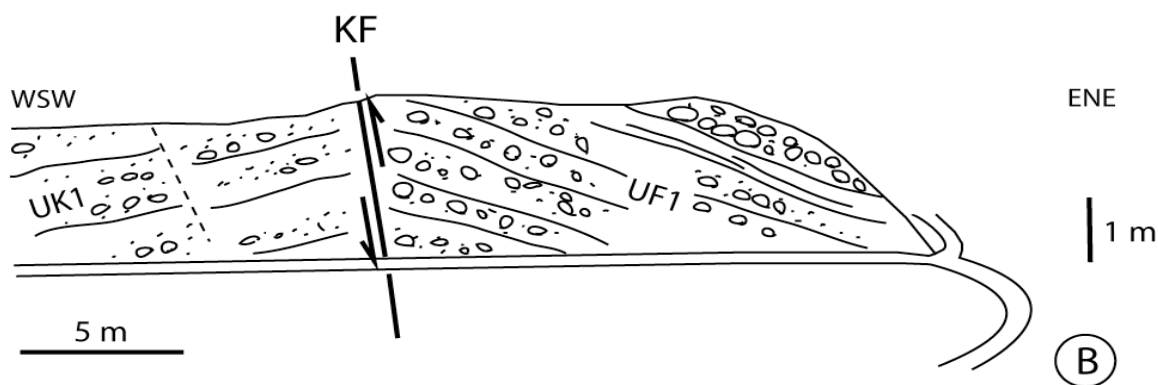
Fig. III. 21: (A) Outcrop view from the Kanalia Fault at locality-24 (location on Fig. III. 18 and Fig. III. 1). (B) Interpretative sketch of Kanalia fault zone at locality-24.

3. Conclusion

Our mapping and analysis of the Kanalia Fault showed that it corresponds to a significant fault within this area with an important lateral continuity. The main fault is directed N100°E to N130°E and is dipping 60-80° toward the NE. Our observations on that fault zone demonstrated some reverse displacement that is confirmed by the overall stratigraphic offset along the fault zone. Strike-slip movement, probably sinistral, has also been observed. The total reverse offset remains unclear because of the absence of a reliable marker bed on both sides of the fault. However, because of the general offset of the stratigraphic succession, we propose a minimum total offset in the range of 30-50 m along this fault.

D. Conclusion on NW-SE major faults

The studied area is presents three major NW-SE faults. They are all associated with a complex crushed zone 2 to 5 meters-thick.

We analyzed the fault surfaces and the deformation of strata on both sides of each fault and these results are illustrated on Fig. III. 22.

This analysis showed that at least two of these large faults had a significant reverse component. Their orientation and their steep attitude suggest strongly that they correspond to former normal faults inverted during a compressional episode.

Only the Livadhia Fault is apparently only normal and do not show any inversion.
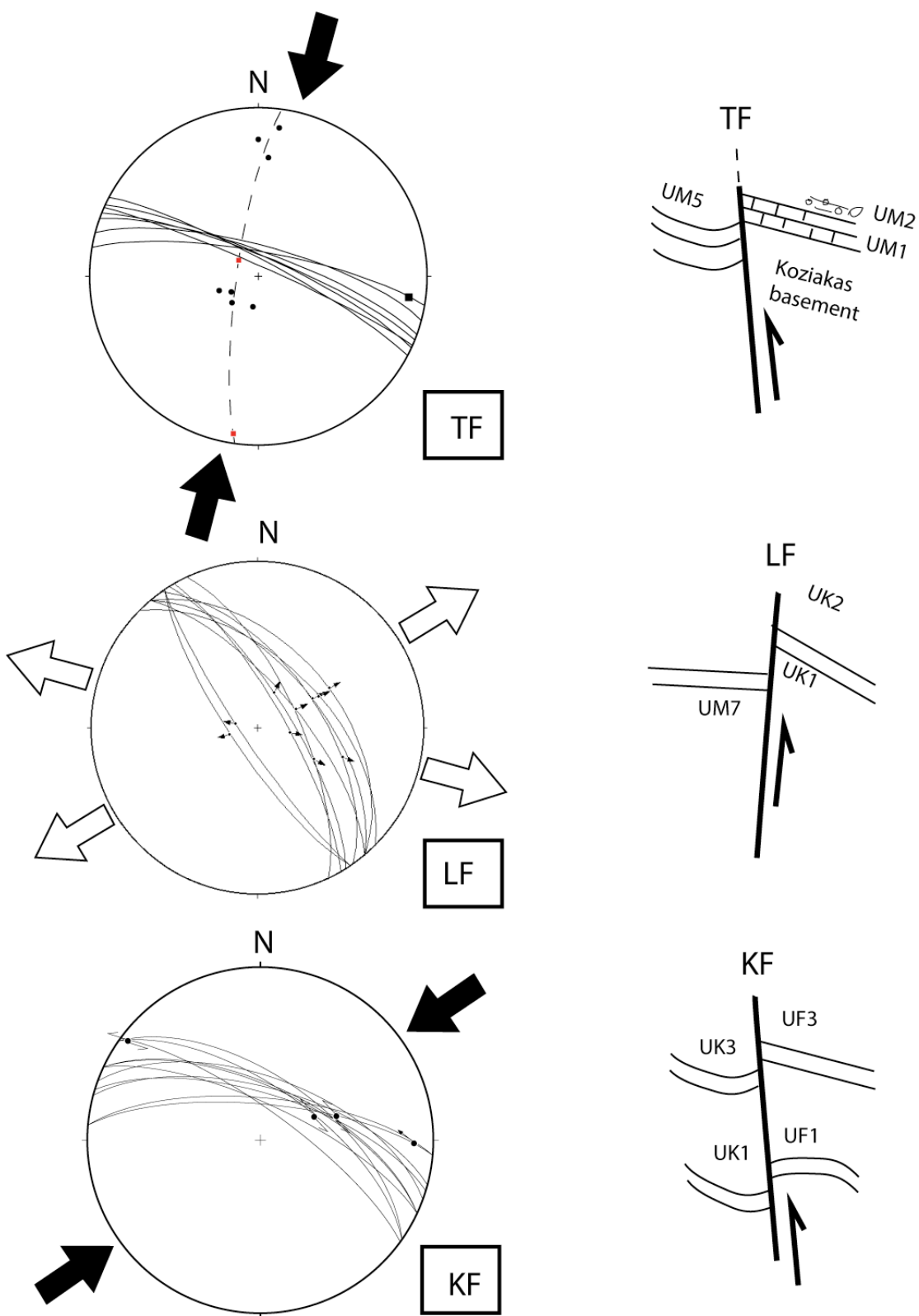
Fig. III. 22: Summary of observed structural data on the major NE-SW faults in the studied area: Tsambouro Fault (TF), Livadhia Fault (LF), Kanalia Fault (KF).

XII. Transverse faults

From our mapping of that area, it appeared obviously that some sedimentary units and some of the main regional NW-SE faults are locally offset by some transverse faults. Some of these faults were observed directly from outcrops and we describe here some of these faults that are well constrained and that can provide information on the tectonic development of the studied area.

Some of the transverse faults were not observed directly but only deduced from our mapping. For example, we can notice that the Livadhia Fault present a significant offset close to Livadhia village (see Fig. III. 1). This is interpreted as the result of a transverse fault striking N060°E to N080°E (Fig. III. 23). The apparent motion is sinistral but the total offset of Livadhia Fault can also be associated to vertical offset (normal or reverse) along the transverse fault.
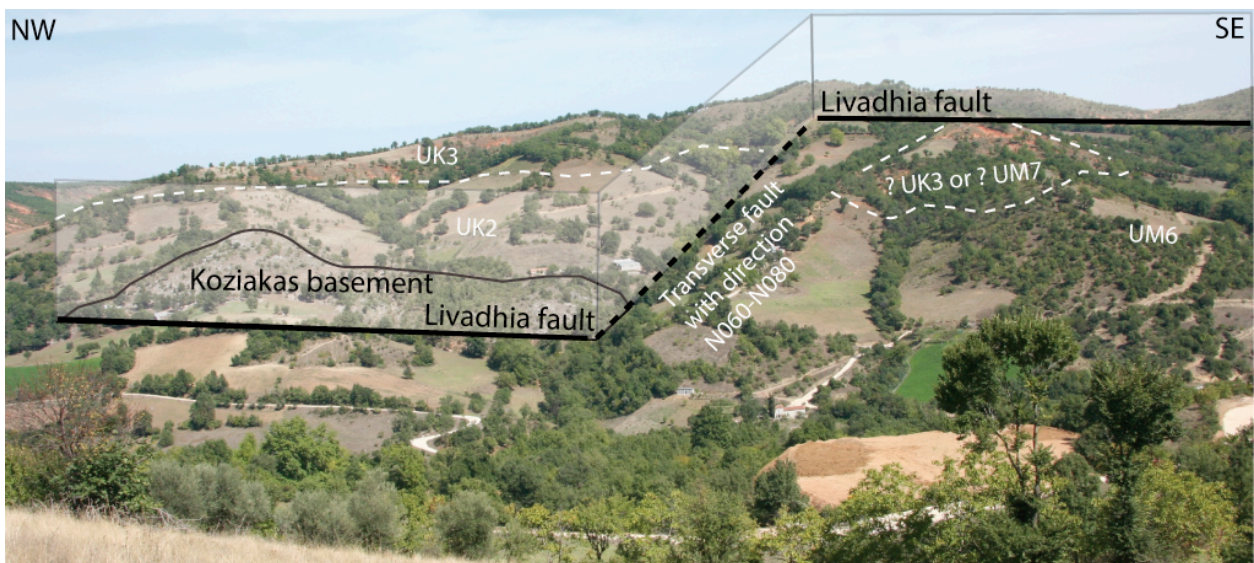
Fig. III. 23: Panoramic view toward the NE showing the apparent left-lateral offset of Livadhia Fault.

The direct observation of fault planes in fracture zones of similar orientation can help to propose a coherent interpretation of the motion along these faults, and therefore participate to the overall tectonic model of the studied area.

A. Fanari fault (FF)

The Fanari Fault is nicely exposed in a railway cutting, about 1 km east of Fanari village (locality-29, Fig. III. 1). We named this fault by the name of the nearby village. At this locality, the Fanari fault forms a fracture zone that is about 4 to 5 m wide (Fig. III. 24).
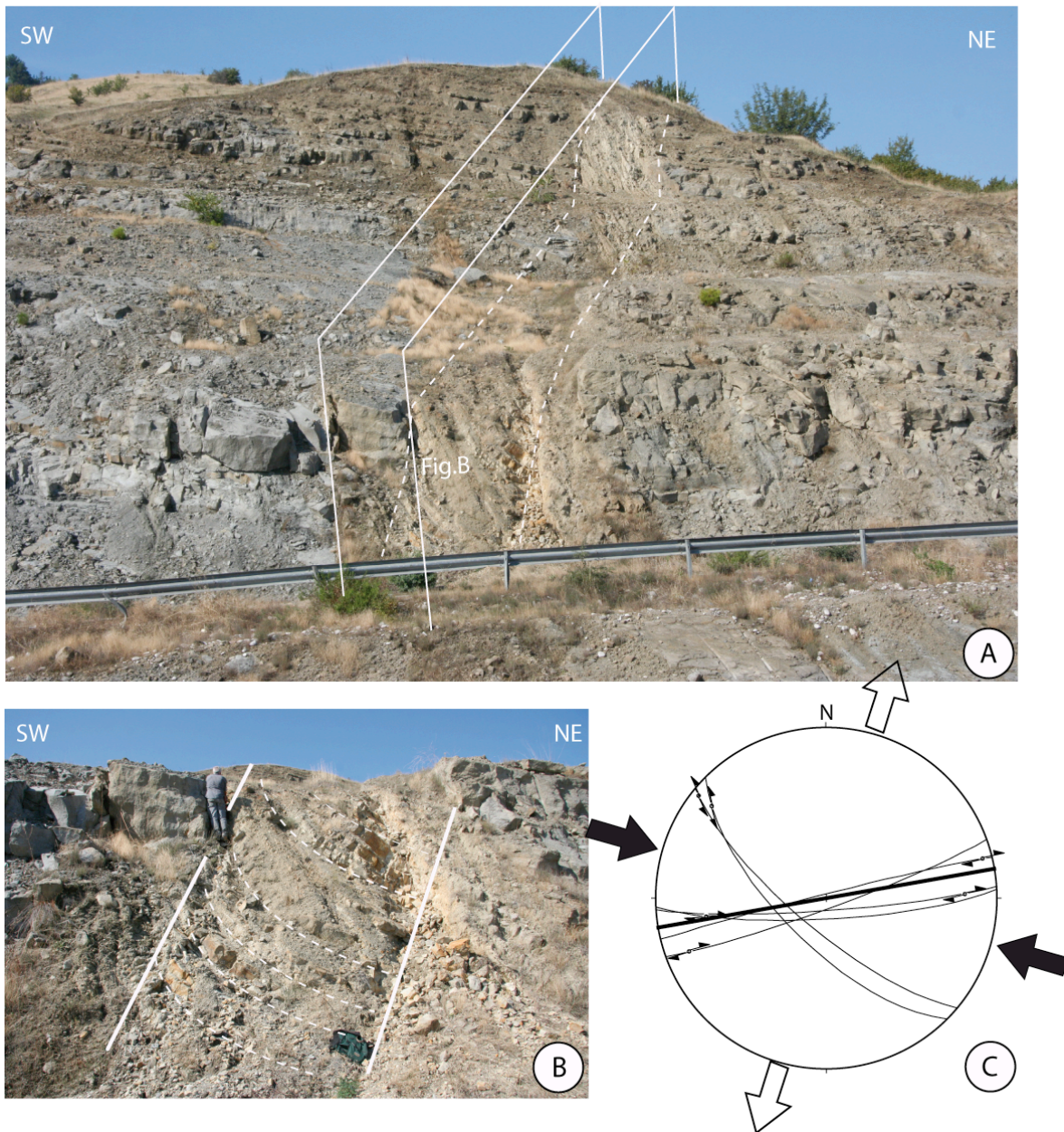
Fig. III. 24: A and B) views of Fanari Fault at locality-29, looking toward the NW (location on Fig. III. 1). C) Stereonet diagram (equal area, lower hemisphere) showing the Fanari Fault (thick line), conjugate strike-slip faults, and normal faults.

The fault zone strikes N070°E to N080°E and shows subvertical dipping. Sedimentary strata on both sides of the fault are interbedded sandstones and siltstones of UF4. These turbiditic beds are dipping homogeneously at about 25° toward the NE (N135°E to N140°E,

156

24 to 27° NE). Within the 4-5 m wide fracture zone, bedding is much more steep and shows changes in strike, getting directed N080°E similarly as the fault orientation. Fault planes within the fault zone present low angle slickensides indicating for dextral displacement. Other small-scale fault planes in this area, striking N130°E to N140°E, show sinistral strike-slip displacements (Fig. III. 24C). Some normal faults, with dip-slip striations, could also be measured in this fault zone but no clear relative chronology between strike-slip and normal faults could be observed.

B. Transverse faults from Ligharies – Loxada area

A few transverse faults could be observed in that NE part of the studied area. One of them can be seen on the side of the road between Ligharies and Kanalia (locality-25, Fig. III. 1 and Fig. III. 18).
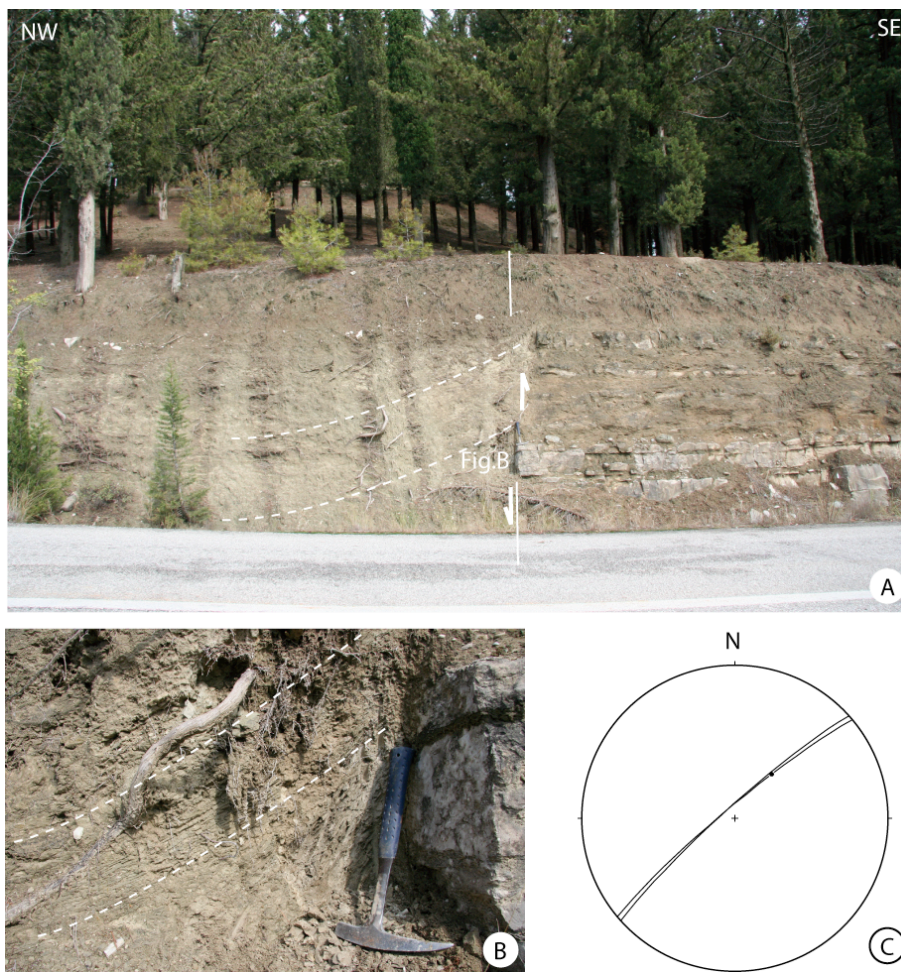
Fig. III. 25: (A) Transverse fault in pelitic series of UK2 at Locality-25 (Location on Fig. III. 1 and Fig. III. 18) with detail (B) and stereonet diagram with fault planes and striation (C).

At this place, fine-grained sediments of UK2 are cross-cut by a fault directed N050°E and dipping 75 to 80° toward the NW (Fig. III. 25). Some fine striation indicates some oblique slip motion (pitch 60°NE) and the drag fold on the hangingwall confirms some normal component (Fig. III. 25A and B).

C. Conclusion

From all the observations we could obtain on these transverse faults, we can see that they show a relatively large diversity in attitude and kinematics. However, some general trends can be deduced from our analysis: they are generally dipping very steeply (80 to 90°) and they strike mostly from NE-SW to ENE-WSW (N045°E to N080°E). We can also notice that most of them have a normal component.

XIII. Metric-scale brittle deformation

We analyzed the brittle deformation from many sites within the studied area. These sites were selected from the good quality of fault data with reliable striations indicating the sense of movement along faults.

A. Post-depositional normal faulting

In southern and central part of the study area, mainly within Mitropoli-block, we observed many normal faults that are locally well organized in conjugate faults, but in some places more chaotic in distribution. They have generally offsets that range from a few centimeters to a few tens of meters. They are very well exposed at least at four localities (Fig. III. 1, locality-2, -15, -16 and -17).

The road-cut exposure along Mitropoli-Morfovouni road (Fig. III. 1, locality-2) shows not only synsedimentary normal faults (Chapter III, section-2) but also some normal faults cross-cutting the whole series of UM3 to UM5 (Fig. III. 26). The normal offsets along these faults are up to 25-30 m. The direction of extension is not clear from these faults that are not well organized spatially, as shown by the stereonet diagram (Fig. III. 26F).

158
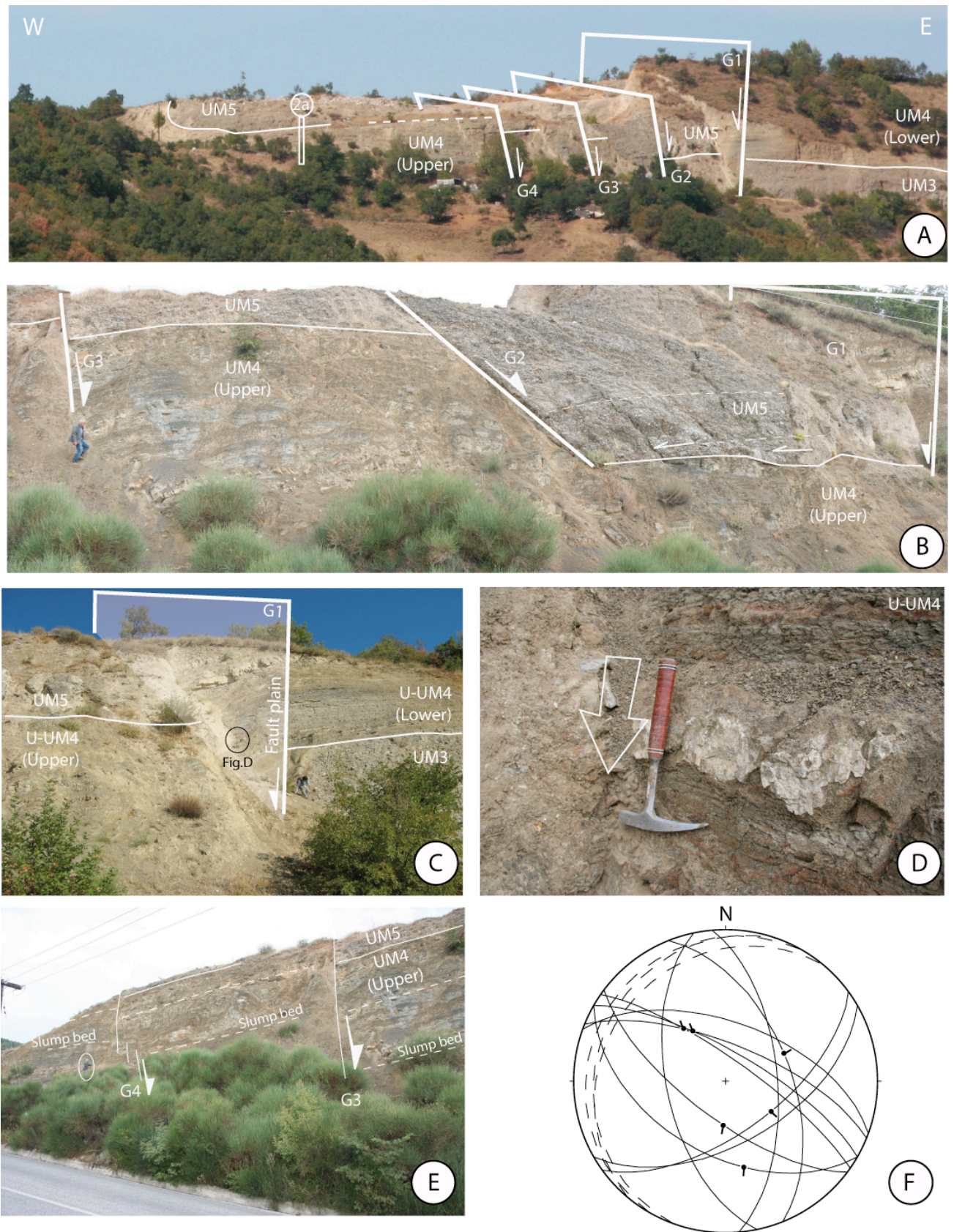
Fig. III. 26: (A) Panoramic view from the western side of locality-2. It shows the large normal faults across the UM3-UM5 units (Faults G1 to G4). (B), (C), (D) and (E) are closer views of some of these faults. (F) Stereonet diagrams (equal area, lower hemisphere) showing the post-UM5 normal faults at locality 2. Bedding planes are in dashed lines. These faults are not well organized and do not reflect a very coherent extensional direction.

159

Further NE, at localities-15, -16 and -17 (Fig. III. 1, and Fig. III. 27), some sets of normal faults are exposed on the side of the Kanalia-Morfovouni road-cut.

Fault planes and associated slickensides are reported on stereonet (Fig. III. 27B) and indicate NE-SW direction of extensional deformation.
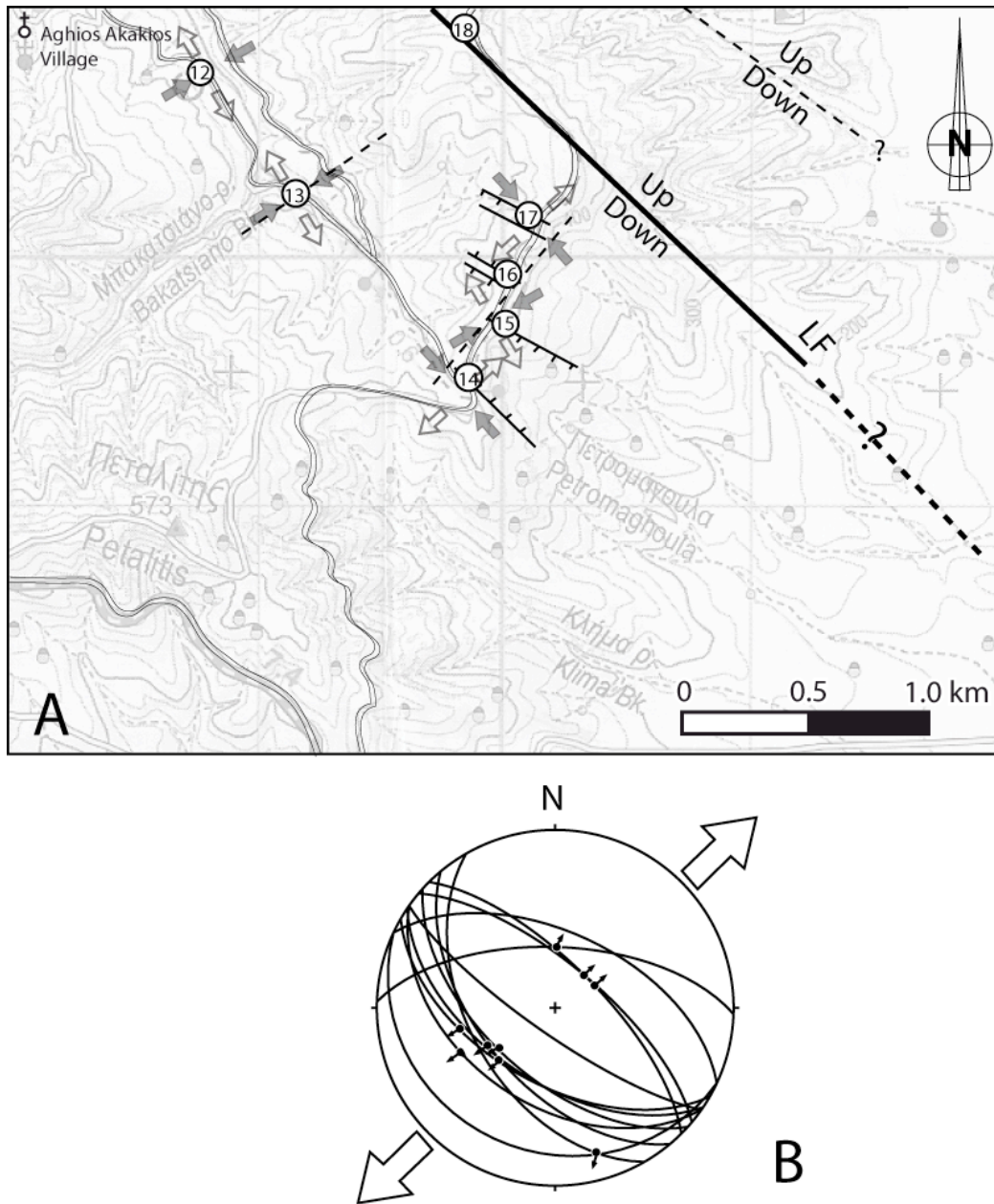
Fig. III. 27: (A) Enlargement of the central part of the studied area and location of the main normal faults. (B) Stereonet diagram (equal area, lower hemisphere) showing the normal faults at localities 16 and 17. These sets of faults are showing clearly some NE-SW extensional deformation in that area, at least after deposition of UM7.

At locality-17, some sets of normal faults can also be observed and also correspond to a NE-SW direction of extensional deformation (Fig. III. 28). These faults are also appearing in the interbedded sandstones and siltstones of upper UM7.
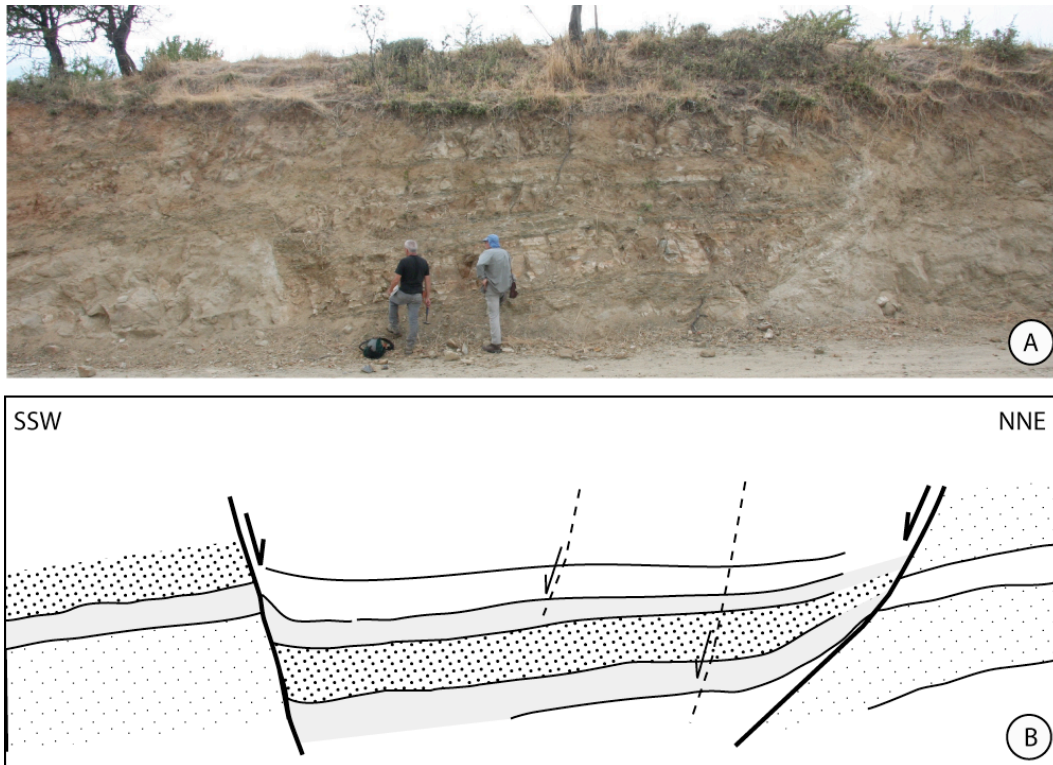
Fig. III. 28: Normal fault sets at locality-17 (Fig. III. 1 for location).

From our observations, the post-deposition tectonic history of the area includes some significant extensional deformation. The normal faults are not always coherently organized, evoking some quite complex changes in deformation axis. However, some sets of faults are nicely organized with a clear NW-SE direction of extension.

B. Conjugate strike-slip faults

We measured some conjugate strike-slip faults on many sites across the studied area (Fig. III. 29). Among the best constrained locations, we expose here the data from three of them.

Firstly, along the Mitropoli to Morfovouni road (location-2 and -3, Fig. III. 1), in the area also characterized by synsedimentary normal faults, many subvertical faults display horizontal striations. The distribution of slickensides on the fault planes clearly reveals a set on ENE-WSW dextral faults and a set of WNW-ESE sinistral faults (Fig. III. 29, B). These sets of faults are representative of E-W compressional deformation and N-S extensional deformation.
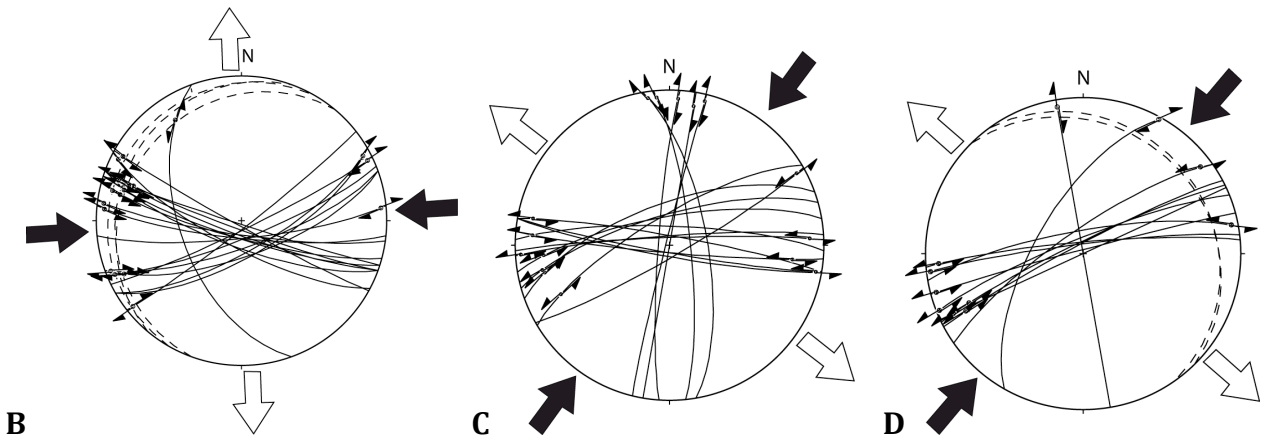
Fig. III. 29: (A) Subhorizontal sinistral slickensides on a fault plane at locality 2, along Mitropoli to Morfovouni road; B, C, and D: Stereonet diagrams (equal area, lower hemisphere) reporting the conjugate strike-slip faults measured in UM3-UM5 along the Mitropoli-Morfovouni Road at localities 2 and 3 (B), in the siltstones beds (UM7) at locality 15 (C), and next to Aghios Akakios at localities 11 and 12 (D). The localities are reported on Fig. III. 1.

Secondly, in the siltstones beds of UM7, at the locality-15 (Fig. III. 1), the distribution of strike-slip faults and associated slickensides (Fig. III. 29C) reveals a slightly different orientation. The conjugate strike-slip faults from this site correspond of NE-SW compressional deformation and NW-SE extension.

Thirdly, in the area close to Aghios Akakios (localities-11 and -12, Fig. III. 1), the sets of conjugate strike-slip faults also indicate NE-SW compression and NW-SE extension (Fig. III. 29D).

All these faults are compatible with the direction of compressional deformation deduced from the analysis of some of the major NW-SE faults in that area (*cf.* Tsambouro Fault and Kanalia Fault, see above in section XI).

XIV. Conclusion on tectonic analysis

From our tectonic analysis, we demonstrated a complex deformation history of this southern area of the Mesohellenic Basin.

One of the main results is the evidence for synsedimentary extensional deformation at the onset of development of the basin in that particular area. The first coarse-grained detrital deposits (UM3) are coeval with the extension on NW-SE trending normal faults. This episode is apparently very short in time as the normal faults are covered by UM4-UM5 series. Very few of these faults possibly moved slightly after deposition of UM4 and before UM5, but most of the motion occurred before UM4.

Some sets of normal faults also affect the whole early Miocene sedimentary series and is responsible notably for the development of decametric-scale grabens and of at least one of the major faults of the area (Livadhia Fault). We consider that the other main faults (Tsambouro and Kanalia faults), with similar shape and orientation, were also formed during that extensional episode, before being later inverted. This extension can be locally relatively chaotic in orientation, but some sites and the main faults express a dominant NE-SW direction of extension.

After this period of extension and deposition, the area is affected by compressional deformation. This episode was evidenced mainly from the deformation of some of the larger faults of the area from which we could clearly identify reverse displacements. Sets of conjugate strike-slip faults, throughout the whole area, are compatible with that compressional direction (NE-SW to E-W) and are therefore possibly linked to that episode. We propose that this compressional event had a significant impact on the uplift of Koziakas Mountain on the western side of the Mesohellenic Basin.

The last episode is extensional. It corresponds to the present-day deformation deduced from focal mechanisms and GPS studies. This episode of extension is considered to have

started in the area as early as the late Miocene (early Tortonian) with a N-S direction of extension (Kamberis *et al.*, 2012). The directions of extensional deformation range from NW-SE to NE-SW, changing regularly during Pliocene and Quaternary times (Kamberis *et al.*, 2012). The present direction of extension is N-S, demonstrated by focal mechanisms, GPS studies, and morphological analysis (*e.g.* Caputo and Pavlides, 1993; Hatzfeld *et al.*, 1999; Papadimitriou and Karakostas, 2003; Kreemer *et al*, 2004; Caputo *et al.*, 2006; Hollenstein *et al.* 2008). This N-S extension (early Tortonian ?, or present-day) could be responsible for some normal motion along some of the transverse faults that are post-dating all the other faults and structures within the studied area.

In summary, we can tell from our tectonic analysis that the area experienced at least 4 successive episodes:

1. NE-SW Extension: onset of the depocenter in this part of southern MHB (earliest Miocene, syn-UM3)

2. Probably pre-tilt extension, mainly NE-SW directed, creating grabens and large regional faults

3. NE-SW to E-W compressional deformation, with inversion of some of the major faults

4. Extensional deformation, variable in direction, but dominated by N-S direction of extension (Plio-Quaternary extension, still active).

CHAPTER IV - Conclusions

XV. Summary of the results on stratigraphy

The MHB in this area had never been studied in detail before (see Chapter I). Hence, we provided diverse results about sedimentology, stratigraphy and tectonics.

A. Stratigraphic units definition and analysis

The presence of major faults led us to consider separately the stratigraphic successions within three main blocks, Mitropoli (UM), Kanalia (UK) and Fanari (UF) blocks. Within each block, stratigraphic units have been defined (UM1-7, UK1-3 and UF1-4).

The most complete and diverse stratigraphic succession is that in Mitropoli block:

(i) it rests on the Mesozoic Koziakas (limestones) or Koziakas/Maliac (lavas, shales and radiolarites) basement;

(ii) the lowermost deposits are diverse : Oligocene limestones to the West (UM1), conglomerates to the SE (UM3);

(iii) synsedimentary faults are observed near the base (UM3);

(iv) the succession above is marked, at the scale of hundred meters, by alternating shaly (siltstone) and coarse-grained (conglomerate to sandstone) deposits.

The other blocks (UK and UF) also exhibit such alternating shaly- and coarse-grained units. This asks the question of correlating the stratigraphic units across the block boundaries (see below).

B. Lithologic diversity

There is only one limestone outcrop, about 25 m thick (UM1). All other deposits are siliciclastic, at the exception of few carbonate beds associated to some siltstones (UM6 and UK2). These deposits are conglomerates (7 units or subunits), sandstones (3 units) and siltstones (4 units or unit parts).

Where marked, the clast imbrications in conglomerates indicate a southwestward shear and therefore a paleocurrent in that direction (see additional data after references).

A progressive change in lithology of the Pelagonian sediment source is observed between UM3 and UM5. The basal conglomerates (UM3) comprise many clasts derived from the Pelagonian Mesozoic cover (limestones, radiolarites, ophiolites), which crop out to the east of Mitropoli. A major change takes place at the start of UM5, with an increase of pebbles derived from the Pelagonian basement (gneiss and marbles), which are exposed much farther to the NE of the study area. This is the hint of an important tectonic event (see below).

C. Paleontologic results

Large benthic foraminifers especially Lepidocycline of Late-Oligocene age have been observed in the UM1 limestone.

The sandstones delivered some shell fragments and a few entire shells of marine gastropods, but they are overall very rare. Trace fossils are also observed, mostly burrows of *Ophiomorpha* and *Skolitos* type. Tiny network of *Rhizocorallium* might also be present at the top of some turbidites.

Some silstones have a calcareous nannofossil content, some of which could deliver a mostly Early Miocene age (Chapter II and additional data after References). Other, located to the SW of the study area, delivered a larger time-span (Late Oligocene-Early Miocene).

D. Sequence stratigraphy

Several depositional sequences have been identified in each block, based on facies tracts and separated by major unconformities (details in conclusions of Chapter II).

In Mitropoli block, UM1 and UM3 form separate sequences SM1 and SM2.

- SM1 is the older sequence in the study area and SM2 shows the initial stage of basin subsidence and terrigenous sedimentation.

- SM3 is onlapping to the western basin border and likely incorporates L-UM4 and U-UM4.

- SM4 is the thickest sequence in the basin, and comprises UM5 and UM6.

- SM5 comprises UM7 and is the youngest sequence in the basin.

Kanalia and Fanari blocks exhibit two sequences each (SK1-2, and SF1-2), except if we consider U-UF4 as a separate sequence (SF3), which is debatable (see Chap. II).

The main sequences are interpreted as composed by LST, TST and HST, except SM1 and SM2 (TST only), SK2 (LST and TST, due to an abrupt termination of the sequence against Kanalia fault), SF2 (LST and TST), and SF3 (LST). It is worth noting that this interpretation is not directly dictated by data, as the facies tract in each complete sequence are generally a fining- and deepening-upward succession of facies. But a

(i) base-level fall is necessary to emplace the lower sequence part and

(ii) the highstand phase is noticeable in some returning sandstone abundance at the top of siltstone successions.

In the three blocks, the sequence might form overall transgressive sequence sets.

XVI. Stratigraphic correlations

The studied area is characterized by a 20-40° dip of strata toward the NE. The tectonic deformations (see Ch. III) are not large enough to make the three blocks belonging to remote parts of the basin and therefore the sequences in each block may be correlated with its counterparts in the other blocks. Several arguments can be used to assess the correlations:

(i) tectonics, and namely the motion direction and throw on the fault planes ;

(ii) the map and log comparisons based upon lithology ;

(iii) sedimentology and sequence stratigraphy.

Mitropoli block is considered as the most complete record of the area, although it is located at the basin edge, because it is composed of 5 depositional sequences and it is the only one for which the bottom is observed. The sequences in Kanalia and Fanari are either part-equivalents of the Mitropoli ones or above them. The paleontologic data do not allow to address the correlations.

By extrapolating the dip of strata, the Mitropoli, Kanalia and Fanari deposits would be stacked on top of eachother. This is unlikely because UM1 and UK3 rest on the same basement at almost the same elevation (Fig. I. 9). Therefore, we consider in the rest of this section that Kanalia and Fanari sequences are part of the whole Mitropoli sequence set.

We haven't ranked these sequences and in our analysis we suggest that they all are of same order, despite the important thickness variations from one to the other. We also put apart SM1 and SM2 because they have specificities that are absent in Kanalia and Fanari sequences (carbonates shelf for SM1 and synsedimentary faults for SM2). The absence of carbonates in SM1 by itself is not a sufficient reason for excluding the possibility of correlating SM1 with other sequences in Kanalia or Fanari blocks but as we will see it is more likely that the sequences in those blocks correlated with sequences higher in the Mitropoli sequence set.

The overall trend in sequence sets in the three blocks is transgressive and this neither could be used as a pattern template to guide the correlation. Instead, we proposed two alternatives: either (i) the thicker LSTs or (ii) the thicker HSTs are to be correlated (Fig. IV. 1 and Fig. IV. 2).

168

In the first option (Fig. IV. 1), the idea is that the L-UM5 and L-UK3 thick conglomeratic facies are very similar (subaqueous conglomeratic channel fills) and that, because they are very thick, they point to a stage of basin evolution where lowstand accommodation is high.
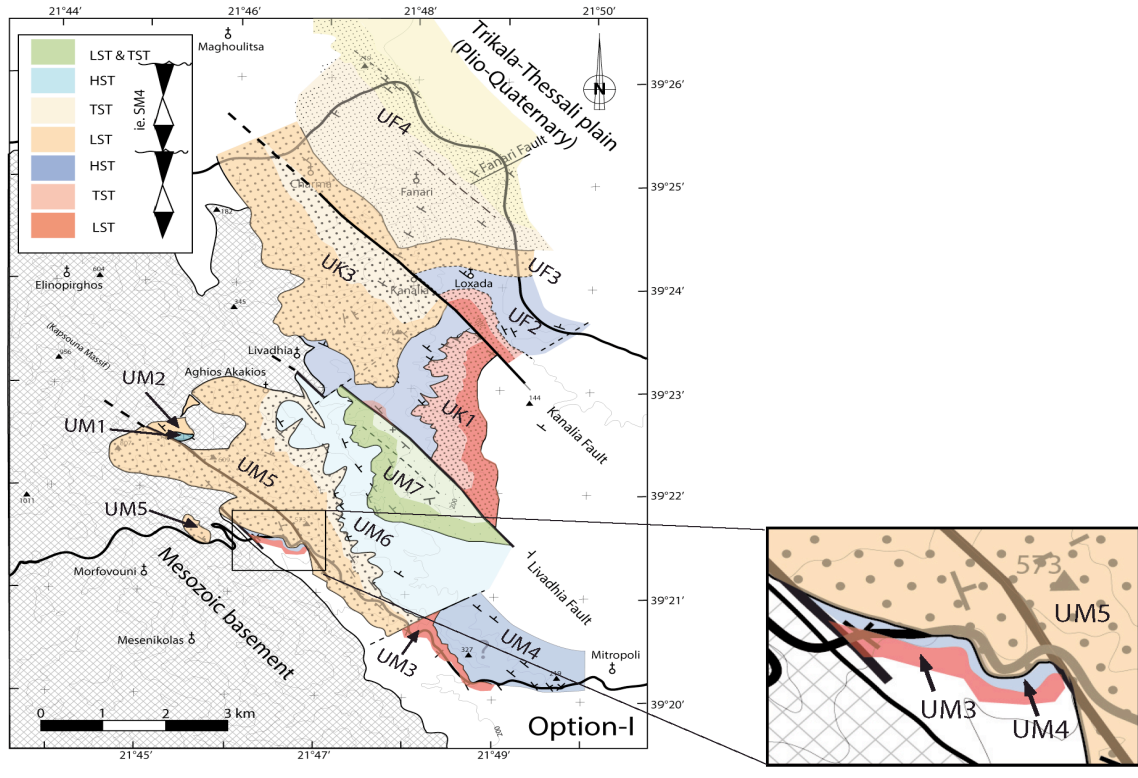
Fig. IV. 1: Correlation of sequences across the blocks of the study area. Option 1: thick conglomerates correlated. Above: in map (colors correspond to systems tracts). Below: cross-sections (colors indicate depositional settings as in the caption).

In this option, this conglomeratic belt most likely correlated to the east with UF3 in the Kanalia block, because it is also a conglomerate and because it points to the largest accommodation space at maximum lowstand throughout the Kanalia sequence set (if one exludes the possibility that the U-UF4 belongs to a SF3 sequence).

The implications of this option are that (i) the basin axis is clearly identified above the Fanari block, while the Kanalia and Mitropoli block record more proximal deposition, at the basin edge; (ii) the HST of the preceding sequence drastically (and somewhat abruptly) thins toward the basin edge between the Kanalia block (thick UK2) and the Mitropoli block (thin U-UM4). This possibility cannot be ruled out and some features on the field could support it, as for instance the westward onlap of U-UM4 above L-UM4, associated with a small angular unconformity between both subunits which indicates a basinward tilt at this time. Also, the probable southeastward thickness increase of U-UM4 around Mitropoli is consistent with such an option.

To summarize, in this option we correlate SM3 with SK1 and SF1, and SM4 with SK2 and SF2 (we postulate that no sequence is missing above the correlation line). This option implies a >700 m throw on the Livadhia fault to the southeast (in the basin), while it would be almost zero in the northwest at the contact with the basement (Fig. I. 9). This is unlikely, while not impossible.

In the second (preferred) option (Fig. IV. 2), the idea is that the thick HSTs must be correlated because they must represent much more time than the conglomeratic series. This is based upon the idea that the diffusion and deposition rate of silts in the basin, owing to Stoke's law, is several orders longer than that of the conglomerates. In this respect, we correlate UM6 with UK2 and UF2.

UM6 and UK2 have in common a carbonate-rich content, with limestone nodules at the base of the siltstone succession. UF2 is not well documented throughout but share the same E facies and thickness (around 80 m) with the two others. In this option, the basin axis is also identified above the Fanari block, as the following LST preserved there is more distal (C2) than that in the other blocks (C1). Worthy, the above TST is much thicker in the basin (L-UF4) than at its edges (M-UM7). This could reflect the height of the slope margin (and accommodation space of the slope fan) or be the hint of a larger subsidence in the basin at that time (or both).
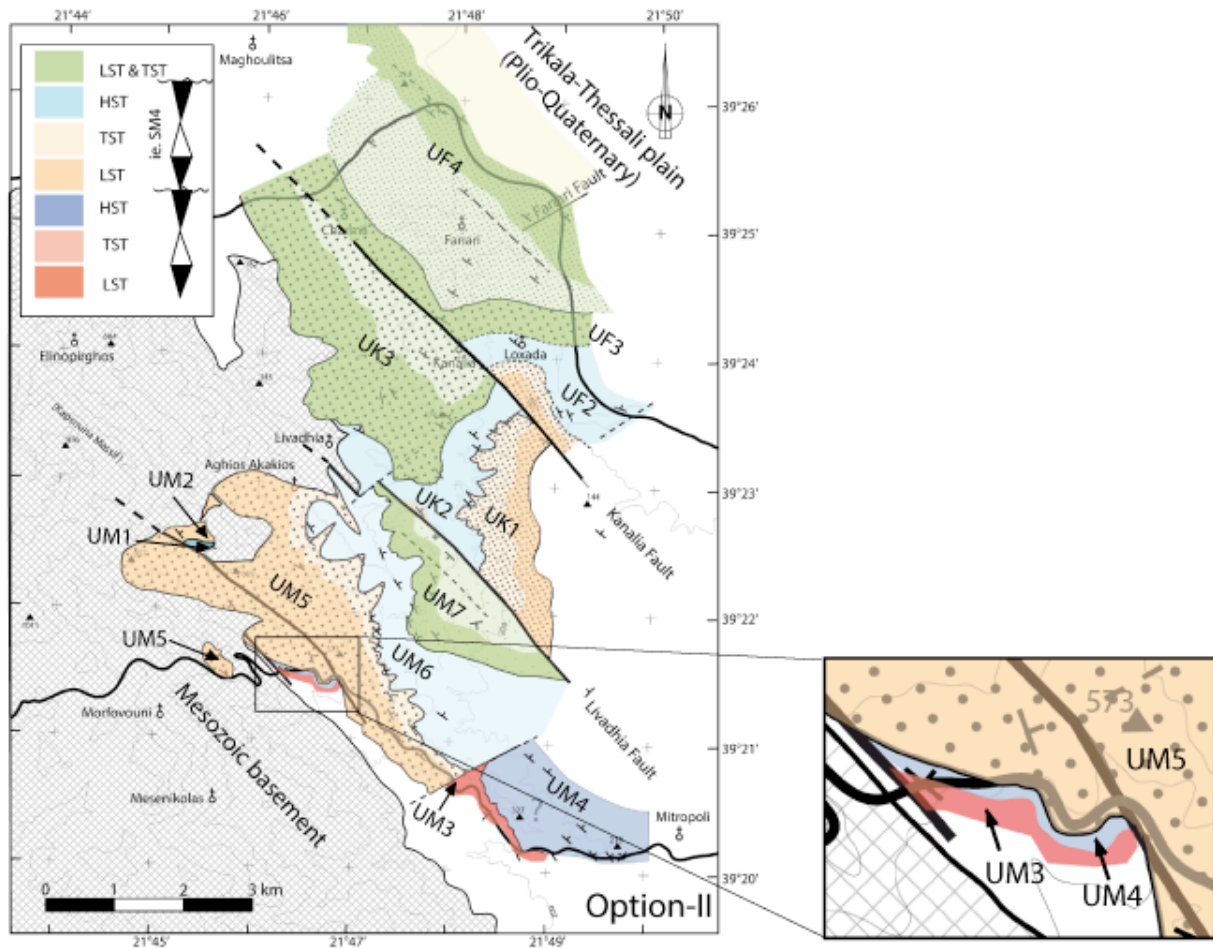
170
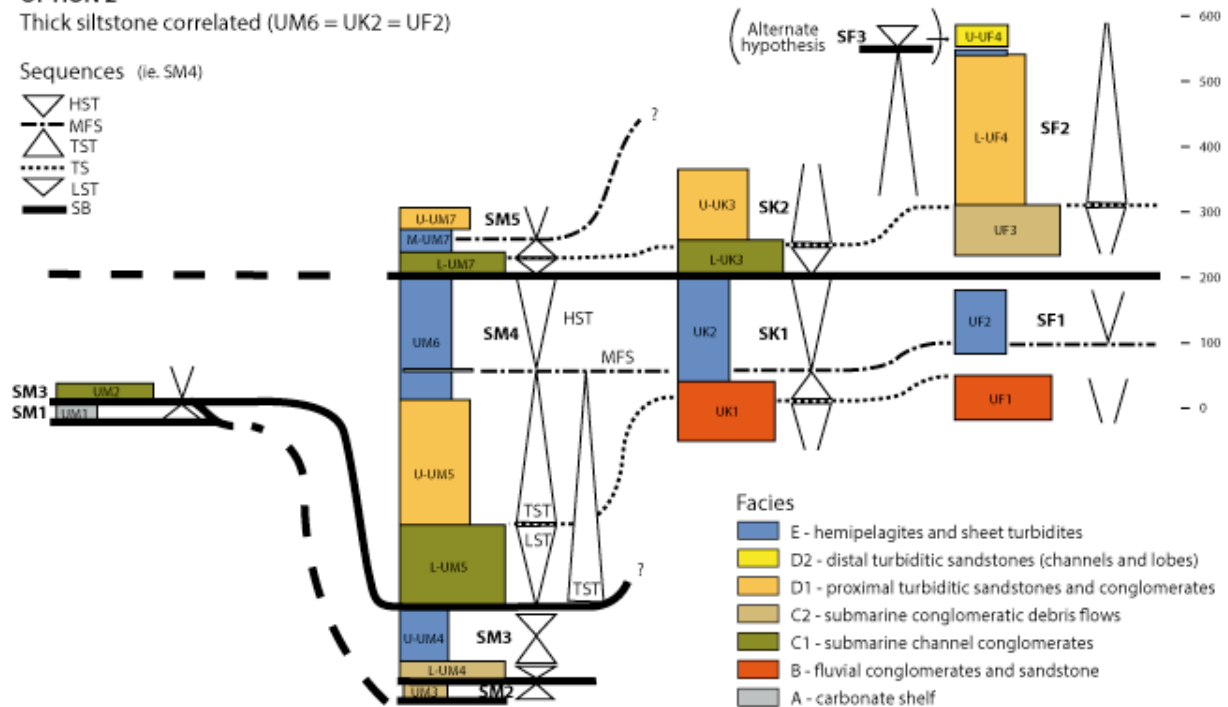
Fig. IV. 2: Correlation of sequences across the blocks of the study area. Option 2 (preferred): thick silstones correlated. Above: in map (colors correspond to systems tracts). Below: cross-sections (colors indicate depositional settings as in the caption).

171

We think indeed that the height of the slope margin increases along the basin fill, because the most distal and evoluted sandy turbiditic channel and lobe system appears in its final evolution stage (U-UF4). To summarize, in this option we correlated SM4 with SK1 and SF1, and SM5 with SK2 and SF2. This option is likely. It implies that the major faults would have played so as to uplift their NE side, which is not unconsistent with our tectonic results.

In these two options, we identified the basin axis above the Fanari block, and a basin edge to the west (Mitropoli block ?). It is important to note that, however, this western basin edge was not the source or the proximal part of the depositional system in 3D. Indeed, above UM1, most of the sediment is derived from erosion of the Pelagonian basement to the NE and the paleocurrents are oriented to the SW. This helps to solve an apparent contradiction which is that the lowstand deposit in UK1 and UF1 is fluvial (closer to the basin axis), while correlated to submarine conglomerates in L-UM4 or L-UM5 (closer to basin edge). This illustrates that the basin was deepening southwestward, and implies that the Koziakas basin border was further to the SW at that time, and/or that the basin was bent to a more NS striking direction to the south of the study area.

XVII. Results on tectonics

The MHB is a piggyback basin, and therefore its infilling may have been influenced by deformation. There are no large folds and structural surfaces are homogenous in dip (20-40°) and strike (NE), except close to the major faults.

The faults are numerous, mostly striking NW-SE. Some transverse faults are perpendiculary to the main strike direction (Fig. I. 9 and Chapter III). Some are undoubdtly syndepositional, as those in UM3, where syn- and post-tectonic strata are observed. These are listric faults, trending NW-SE with the eastern compartment collapsed. They mark the initiation of subsidence in the study area. Other normal faults cross-cut the whole stratigraphic succession. Some bound graben-like structures as observed in UM7.

The major faults (Tsambouro Fault TF, Livadhia, LF, and Kanalia, KF, faults) are nearly vertical and might be polyphased. The Kanalia fault has a late compressional play but the throw direction and length could not be determined. The same result was obtained for the

Livadhia fault, where subhorizontal streaks have also been observed. The compressional stress axes on these faults are most commonly NE-SW.

It is worth noting that some of the faults cross-cuting the most recent units could have been generated short after the basin fill and may even be partly syndepositional, as slumps are preserved in these deposits (UM7), but these slumps are rare and other syn-tectonic features are not observed.

So, a younger age is more probable. Some of these normal faults could be of Plio-quaternary age as the study area is near the Trikala plain but some others seem to be tilted by a compressional event probably of Miocene age (middle ? upper ?) therefore they are older than this event.

This compressional event is well printed in the main faulted zones (see chapter III). It could be synchronous with the uplifts of the borders of the basin (Koziakas series in the SW, pelagonian series in the NE). It likely is the cause of the inversion on pre-compressional normal fault (as the Kanalia fault for instance).

The northeastward dip of strata seems to be linked to the uplift of the Koziakas at the western border of the MHB that took place after the Early Miocene.

It might be that the major faults already exist at that time because the great axis of the reconstructed stress fields against the faults also shows a northeastward tilt. Thus, the subvertical faults were less steep and dipping toward the NE by the time they formed.

XVIII. Geologic evolution of the studied area

A. Sequence control, eustatic vs tectonic

As previously stated, the basin developed and was filled at the same time as tectonics structures, mostly faults (i.e. UM3 unit), were formed. This caused accommodation to increase, mostly in localized areas. The sequence boundaries, in several places, are slight angular unconformities associated to truncation surfaces. They therefore are interpreted as the consequence of fault activity (tectonic control).

We think that the eustatic cycles had only a subdued influence on the basin stratigraphy, as for instance causing a hypothetic regression at the base of SF3 (Fig. IV. 2). The hundreds of meters of inflilled accommodation in SM4 or SF2 could not be the result of eustatic transgressions and a 20-50 m eustatic cycle would be difficult to unravel in the observed stratigraphic signal. There is also a frequency limitation to such an analysis. As regarding to glacioeustatic cycles, there should be many of them recorded and we must conclude that the stratigraphic signal is therefore not sensitive to such a control (no parasequence-like successions are systematically observed on the field). As regarding to longer-term (3rd order) eustatic variations, they are of about the same number in the considered period as the sequences recorded (Haq et al., 1987; Abreu et al., 1998), so that their influence cannot be evidenced in the absence of a more detailed sequence stratigraphic assessment (which is beyond the resolution of our data).

Moreover, the paleontological data are not accurate enough to compare the sequence with eustatic charts. The overall transgressive sequence set recorded in the study area reflects a continuously active subsidence over the time of deposition (Late-Oligocene/Early Miocene). Moreover, it suggests that the sediment supply was not enough to keep pace with the increase in accommodation in the basin axis. Thus, the basin deepened along its axis. One consequence of this was the increase in height of the basin slope margin. This is evidenced by the progressive development of sandy turbiditic systems within the LSTs upward the sequence set.

Combining all the available data, we propose a three-stage basin evolution of this part of the MHB:

B. First submarine troughs

The Late Oligocene carbonate shelf (UM1) overlying the basement is the paleolandscape on which the basin initiated. The shelf was likely discontinuous, because it is not found elsewhere above the basement and beneath the siliciclastic deposits of the basin. Almost in the same time (Late Oligocene), this landscape was dissected by synsedimentary normal faults with eastward collapse and, in the same time, conglomerates were supplied in the related hemi graben-like depressions from the local Pelagonian reliefs to the east (UM3). This occured in a fluvial to shallow marine environment. The western (Koziakas) border was

174

not uplifted at that time and therefore it could not act as a source for these first deposits. (By the way, it was uplifted after the main basin fill so that almost no sediments from the Koziakas are reworked in the MHB in the study area, Fig. IV. 3).
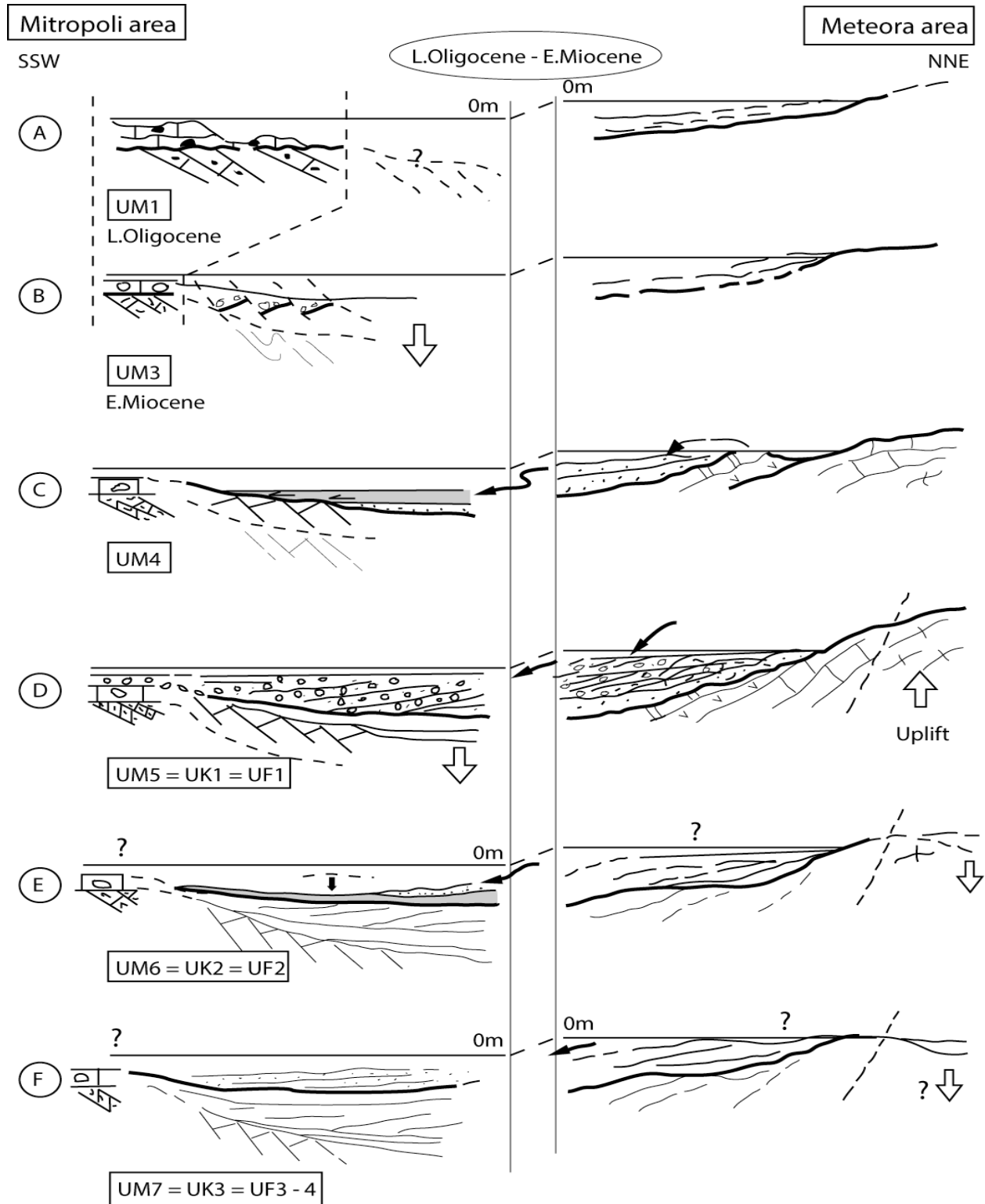
Fig. IV. 3: Chronologic evolution of the study area (Mitropoli block) with an equivalent corresponding to Option-II.

C. Installment of the NE-SW routing of sediments

Post-fault deposits unconformably onlap this submarine paleotopography in the southern part of the study area (UM4). These deposits thicken to the SE, in the direction of the basin axis and start to record relatively deep marine setting during relative sea-level highstands. The basal, lowstand submarine conglomerates also start to record paleocurrents from the NE, but no time-equivalents of these deposits are exposed in the NE part of the study area. If there were, they should likely be fluvial ones.

The next sequence is the first one that correlates throughout the study area. In our preferred correlation option, it starts with conglomerates which are fluvial to the NE (UK1 and UF1), passing downstream to submarine conglomerates (L-UM5). In the distal part of the depositional system, the deposit following the conglomerate is a thick proximal turbiditic facies tract (U-UM5) which is backstepped by highstand siltstones. The siltstones reach the more proximal parts of the system to the NE where they rapidly overlain the fluvial conglomerates.

The thickness of this sequence suggests that it could not be supplied by a small catchment area. Indeed, there is an increase of sediments derived from the Pelagonian basement which located far upstream to the NE (Fig. I. 1). This also suggests that the Pelagonian hinterland experienced a strong denudation at that time, as compared to the previous stages when only its Mesozoic cover was also eroded and provided the sediments recorded in the basin.

This stage ends with the deposition of a thick highstand silstone (UM6) which was used as trackline in our preferred correlation option.

D. Generalized deepening and turbiditic sedimentation

The last stage is marked by the development of sandy turbidites which are locally slumped (UM7). This is the hint of a well-developed submarine slope and a longer submarine routing system. The most distal sandy facies, a channel and lobe turbiditic deposit (U-UF4), appears at the top of the TST of the last sequence.

The final infilling history of the basin is not recorded in the study area.

E. Post-sedimentary events

After the youngest deposits observed in the study area, this area was affected by tectonic events:

i)   post-deposits normal faults (probably the main ones);

ii)   a compressional event giving birth to a clear inversion movement on the main faults probably in the middle-late Miocene times (Mercier et al., 1979; Vamvaka et al., 2006);

iii)   the Plio-quaternary extensional event well known in this area, with the development of the Trikala plain.

XIX. The studied area versus MHB

The study area is the southernmost part of the MHB where sediments of this basin are exposed. However, as explained in our introduction (Ch. I), it was probably somewhat isolated from the main MHB by a narrow pass in the south of the Meteora area.

Our results show that the study area develops later than the main MHB to the north. The MHB had its initial stages in the Upper Eocene (isolated bassins) and its main stage in the Lower Oligocene on its western border (Albano-Thessalian bassin). The later stages of subsidence of the main MHB, in the Lower Miocene, correspond to more eastward depocenters, and this is when deposition started in the studied area. In this respect, the studied area could be considered as the southern continuation of the Meteora area only (Pentalofon Fm and Tsotyli Fm).

It is worth noting that the Meteora deposits (Ori R. & Roveri M., 1987; Ferrièr J., et al., 2012) corespond to a renewed deposition of conglomerates above fine-grained sediments. These conglomerates are the result of the uplift of the Pelagonian indentor, which is located to the NE of our study area, upstream of the Pelagonian-sourced, preserved depositional systems. There are many similarities between the conglomerates in the Meteora (Gilbert deltas: our facies C1, see conclusions of Ch. II) and L-UM5 or L-UF4. The UM3 syn-sedimentary faults and arrival of Pelagonian pebbles in the study area could thus be the southern

expression of a major tectonic phase in the Pelagonain area begining at the Oligocene/Miocene boundary.

The study area shows spectacular synsedimentary normal faults linked to the Early Miocene events. These tectonic events were previously suspected in the Meteora area but the relative structure could not be clearly identified in this Meteora area.

Our studies also show that the present day SW border of the MHB was only feed with NE Pelagonian sources. A question arises: is it the true SW Early Miocene border of the MHB (if the synsedimentary E.Miocene normal faults) or was this basin border farther westward (resting on Pindos series ?) at this time ?.

REFERENCES

Abreu V.S. & Haddad G.A. (1998) - Glacioeustatic fluctuations: the mechanism linking stable isotope events and sequence stratigraphy from the early Oligocene to middle Miocene. In de Graciansky P.C., Hardenbol J., Jacquin T. & Vail P. (Eds.), Mesozoic and Cenozoic sequence Stratigraphy of European Basins, SEPM Special Publication n°60, p.245-259.

Allen P.A., Homewood P. & Williams G.D. (1986) - Foreland basins: an introduction. In: Foreland Basins (Ed. by P.A. Allen and P. Homewood), Spec. Publ. Int. Ass. Sediment., vol.8, p. 3-12.

Aubouin J. (1959) - Contribution à l'étude géologique de la Grèce septentrionale: les confins de l'Epire et de la Thessalie. Ann. Géol. Pays hellén., vol.10, p.14-84.

Barbieri R. (1992) - Foraminifers of the Eptachori Formation (early Oligocene) of the Mesohellenic Basin, northern Greece. J. Micropalaeontology, vol.11, p.73-84.

Bizon G., Lalechos N. & Savoyat E. (1968) - Présence de l'Eocène transgressif en Thessalie. Incidences sur la paléogéographie régionale. Bull. Soc. Géol. Fr., vol.10, p.36-38.

Bornovas J. and Rondogianni-Tsiambaou T. (1983) - Geological Map of Greece, 1:500,000. IGME, Athens.

Bouma A. (1962) Sedimentology of some Flysch deposits : A graphic approach to facies interpretation. PhD, Utrecht University, 168 p.

Bourcart J. (1925) - Observations nouvelles sur la Tectonique de l'Albanie moyenne. Bull. Soc. Géol. Fr., vol.25, p.391-428.

Brunn J.H. (1956) - Etude géologique du Pinde septentrional de la Macédoine occidentale. Ann. Géol. Pays helléniques, vol.7, p.13-58.

Brunn J.H. (1969) - Geological Map of Greece, Pentalofon Sheet, scale 1:50.000, IGME, Athens.

Caputo R. (1995). Inference of a seismic gap from geological data: Thessaly (Central Greece) as a case study. Ann Geofisica. vol.38, p.1–19.

Caputo R., and Pavlides S. (1993) Late Cainozoic geodynamic evolution of Thessaly and surroundings (central northern Greece). Tectonophysics, vol.223, p.339–362.

Caputo R., Helly B., Pavlides S., and Papadopoulos G. (2006). Archaeo- and palaeoseismological investigations in Northern Thessaly (Greece): Insights for the seismic potential of the region. Nat Hazards, vol.39, p.195–212. DOI 10.1007/s11069-006-0023-9

Collinson J.D (1996) Alluvial sediments. In: Reading H.G. Ed., Sedimentary Environments : Processes, Facies and Stratigraphy, third edition, Blackwell Science, pp. 37-82.

Desprairies A. (1979) - Etude sédimentologique des formations à caractère flysch et molasse, Macédoine, Epire (Grèce). Mém. Soc. Géol. Fr., 136, 180p.

Doutsos T., Pe Piper G., Roronkay K., Koukouvelas I. (1993) – Kinematics of the central Hellenides, Tectonics, 12, p.936-953.

Doutsos T., Koukouvelas I., Zelilidis A. & Kontopoulos N. (1994) - Intracontinental wedging and postorogenic collapse in Mesohellenic Trough. Geol. Rundsch., vol.83, p.257-275.

Dunham, R. J. (1962). Classification of carbonate rocks according to depositional texture. In Ham, W. E. (ed.), Classification of carbonate rocks: American Association of Petroleum Geologists Memoir, p. 108-121.

Ferrière J. (1982). Paléogéographies et tectoniques superposées dans les Hellénides Internes: les massifs de l'Othrys et du Pélion (Grèce continentale). Mem. Soc. Geol. Nord., vol.7, 970p.

Ferrière J., Reynaud J.Y., Migiros G., Proust J.N., Bonneau M., Pavlopoulos A. & Houzé A. (1998) - Initiation d'un bassin transporté : l'exemple du "sillon mésohellénique" au Tertiaire (Grèce). C. R. Acad. Sci. Paris, 326, p.567-574.

Ferrière J., Reynaud J.Y., Pavlopoulos A., Bonneau M., Migiros G., Chanier F., Proust JN. and Gardin S. (2004). Geological evolution and Geodynamic controls of the Intramontane Piggyback MesoHellenic Basin, Greece. Bull. Soc. Geol. France. t. 175, n°4, p. 361-381.

Ferrière J., Chanier F., Reynaud J.Y., Pavlopoulos, A., Ditbanjong P., Migiros G., Coutand I. & Bailleul J. (2011). Tectonic control of the Meteora conglomerates (Meso-Hellenic Basin, Greece). Bull. Soc. Geol. France, vol.182, p. 437-450.

Ferrière J., Chanier F., Ditbanjong P. (2012) The Hellenic ophiolites: eastward or westward obduction of the Maliac Ocean, a discussion. Int. Journ. Earth Science, vol. 101, Issue 6, p.1559-1580. DOI: 10.1007/s00531-012-0797-9.

Folk R.L. (1959) - Pratical petrographic classification of limestones. Bull. Amer. Assoc. Petrol. Geol., 43/1, p.16-38.

Godfriaux I. (1968) - Etude géologique de la région de l'Olympe (Grèce). Ann. Géol. Pays hellén., 19, p.12-81.

Haq B.U., Hardenbol J. & Vail P.R. (1987) - Chronology of fluctuating sealevels since the Triassic (250 Myrs ago to present). Science, vol. 235, p.1156-1167.

Hatzfeld, D., Ziazia, M., Kementzetzidou, D., Hatzidimitriou, P., Panagiotopoulos,D., Makropoulos, K., Papadimitriou, P., Deschamps, A. (1999) Microseismicity and focal mechanisms at the western termination of the north Anatolian fault and their implications for continental tectonics. Geophys. J. Int., vol.137 (3), p.891–908.

Jacobshagen V. (1986). Geologie von Griechenland, Gebrüder borntraeger, Berlin-Stuttgart , 363p.

Jaeger P. (1979) - Geologie du massif du Koziakas et de la chaine du Pinde face à Mouzaki (Grèce continentale). Thèse «3ème cycle, Univ. Paris, 146 p.

Jolivet L. and Brun J.-P. (2010). Cenozoic geodynamic evolution of the Aegean. Int. Journ. Earth Sciences, vol.99, p.109-138. DOI: 10.1007/s00531-008-0366-4.

Hollenstein, Ch., Müller, M.D., Geiger, A., Kahle, H.-G. (2008) - Crustal motion and deformation in Greece from a decade of GPS measurements, 1993–2003. Tectonophysics, vol.449, p.17–40.

Kamberis, E., Bathrellos G.D. , Kokinou E. , Skilodimou H. D. (2012) - Correlation between the structural pattern and the development of the hydrographic network in a portion of the Western Thessaly Basin (Greece). Cent. Eur. J. Geosci., vol.4(3), p.416-424. DOI: 10.2478/s13533-011-0074-7

Karfakis J. Skourtsis-Coroneou V., Ioakim C.H., and Mavridou F., (1993) Geological Map of Greece, « Mouzaki Sheet », scale 1:50,000, IGME, Athens.

Kontopoulos N., Fokianou T., Zelilidis A., Alexiadis C. & Rigakis N. (1999) Hydrocarbon potential of the middle Eocene middle Miocene Mesohellenic piggyback basin (central Greece): A case study. Marine and Petroleum Geology, vol.16, p.811-824.

Koumantakis J., Matarangas D., TsaïlaMonopolis S. & Georgiadou E. (1980) Geological Map Panayia Sheet, 1:50,000, IGME, Athens.

Kreemer C., Chamot-Rooke N., Le Pichon, X. (2004). Constraints on the evolution and vertical coherency of deformation in the Northern Aegean from a comparison of geodetic, geologic and seismologic data. Earth Planet. Sci. Lett., vol.225 (3–4), p.329–346.

Lekkas E. (1988). Geological structure and geodynamic evolution at the Koziakas mountain range (western Thessaly). National and Kapodistrian University of Athens, Dept. Of Geology. Geol. Monogr.1, 281p.

Lowe D.R. (1982) Sediment gravity flows ; II, Depositional models with special reference to the deposits of high-density turbidity currents. Journal of Sedimentary Research, 52:279-297.

Mavridis A., Kelepertzis A.K., TsaïlaMonopolis S. & SkourtsiKoroneou V. (1993) Geological Map Knidi Sheet, 1:50,000. IGME, Athens.

Mavridis D., Matarangas D., TsaïlaMonopolis S. & Mostler H. (1979) Geological Map Ayiofillon Sheet, 1:50,000. IGME, Athens.

Mercier, J.L., Delibassis N., Gauthier A., Jarrige J.J., Lemeille F., Philip H., Sebrier M. et Sorel D. (1979). La néotectonique de l'Arc Egéen. Rev. Geol. Dyn. Geogr. Phy., XXI, p. 67-92.

Mercier J.L., Sorel D. & Vergely P. (1989) Extensional tectonic regimes in the Aegean basins during the Cenozoic. Basin Research, vol.2, p.49-71

Mulder T. and Alexander J. (2001) The physical character of subaqueous sedimentary density flows and their deposits. Sedimentology, vol.48, p.269-299.

Mutti E. (1979) Turbidites et cônes sous-marins profonds. In: Homewood P. Ed., Sédimentation détritique. Institut de Géologie, Université de Fribourg, pp. 353-419.

Normark W.R. (1970) Growth pattern of deep-sea fans. AAPG Bulletin, vol.54, p.2170-2195.

Ori G.G. & Roveri M. (1987) Geometries of Gilberttype deltas and large channels in the Meteora Conglomerate, MesoHellenic basin (OligoMiocene), Central Greece. Sedimentology, vol.34, p.845-859.

Papadimitriou, E. & Karakostas, V. (2003) - Episodic occurrence of strong (Mwv6.2) earthquakes in Thessalia area (central Greece). Earth Plan. Sci. Let., vol.215, p.395-409.

Papanikolaou D., Lekkas E., Mariolakos H. & Mirkou R. (1988) Evolution of the Mesohellenic Basin. Bull. Soc. Géol.Gr., vol.20, p.17-36.

Papazachos C.B. and Kiratzi A.A. (1996) - A detailed study of the active crustal deformation in the Aegean and surrounding area. Tectonophysics, vol.253, p.129-153.

Posamentier H. and Vail P.R. (1988) Eustatic controls on clastic deposition II-sequence and systems tract models. In: Wilgus C.K. et al. Eds., Sea-level Changes – An Integrated Approach. SEPM Special Publication 42, pp. 126-154.

Savoyat E., Lalechos N. & Bizon G. (1969a) Geological Map Trikala Sheet, 1:50,000. IGME, Athens.

Savoyat E., Lalechos N. & Bizon G. (1969b) Geological Map Karditsa Sheet, 1:50,000. IGME, Athens.

Savoyat E., Lalechos N., Philippakis N. & Bizon G. (1972a) Geological Map Kalambaka Sheet, 1:50,000. IGME, Athens.

Savoyat E., Monopolis D. & Bizon G. (1971a) Geological Map Nestorion Sheet, 1:50,000. IGME, Athens.

Savoyat E., Monopolis D. & Bizon G. (1972b) Geological Map Grevena Sheet, 1:50,000. IGME, Athens

Savoyat E., Verdier A., Monopolis D. & Bizon G. (1971b) Geological Map Argos Oresticon Sheet, 1:50,000. IGME, Athens.

Soliman H.A. & Zygojiannis N. (1980) Geological and Paleontological studies in the Mesohellenic Basin, Northern Greece. I Oligocene smaller Foraminifera. II Eocene smaller Foraminifera Geol. Geophys. Research, XXII, 1: 166, 27 plates; IGME Athens

Posamentier H. and Vail P.R. (1988) Eustatic controls on clastic deposition II-sequence and systems tract models. In: Wilgus C.K. et al. Eds., Sea-level Changes – An Integrated Approach. SEPM Special Publication 42, pp. 126-154.

Stow D.A.V. and Shanmugam G. (1980) Sequence of structures in fine-grained turbidites : Comparison of recent deep-se and ancient flysch sediments. Sedimentary Geology, vol.25, p.23-42.

Stow, D.A.V., Reading H.G. and Collinson J.D. (1996) Deep seas. In : Reading H.G. Ed., Sedimentary Environments : Processes, Facies and Stratigraphy, third edition, Blackwell Science, pp. 395-452.

Shanmugam G. (2000) 50 years of the turbidite paradigm (1950s-1990s) : deep-water processes and facies models-a critical perspective. Marine and Petroleum Geology, vol.17. P.285-342.

Vamvaka, A., Kilias, A., Mountrakis, D., and Papaoikonomou, J. (2006). Geometry and structural evolution of the Mesohellenic Trough (Greece), a new approach. In Robertson, A.H.F., and Mountrakis, D., eds., Tectonic Development of the Eastern Mediterranean Region: Geological Society London Special Publication 260, p.521–538.

Vidakis M., Papazeti E. & TsaïlaMonopolis S. (1998) Geological Map Nestorion Sheet, 1:50,000. IGME, Athens.

Wilson J. (1993) The Anatomy of the Krania Basin, NW Greece. Bull. Geol. Soc. Greece, vol.28, p.361-368.

Zelilidis A. & Kontopoulos N. (1996) Significance of fan deltas without toesets within rift and piggyback basins: examples from the Corinth graben and the Mesohellenic trough, Central Greece. Sedimentology, vol.43, p.253-262.

Zelilidis A., Kontopoulos N., Avramidis P. & Bouzos D. (1997) Late Eocene to early Miocene depositional environments of the Mesohellenic basin, NorthCentral Greece: implications for hydrocarbon potential. Geologica Balcanica, vol.27, p.45-55.

Zelilidis A., Piper D. & Kontopoulos N. (2002) Sedimentation and basin evolution of the Oligocenemiocene Mesohellenic Basin, Greece. AAPG Bulletin, vol.86, p.161-182.

Zygojiannis N. & Müller C. (1982) Nannoplankton Biostratigraphie der tertiären Mesohellenischen Molasse (NordwestGriechenland). Z. dt. geol. Ges., vol.133, p.445-455.

ANNEXE-I

Nannofossil analysis

Fanari-block

UF4
UF3

900
800
700
600

2008 2009 2010

8) 09FNR_01 Mio inf
14) 08FNR_05 Oligo sup - Mio inf
7) 08KNL_01 Mio inf

KF + ? − ?
UF2

6) 08NR OR_08 Mio inf ***

Kanalia-block

UK3
UK2
UK1

600 500 400 300 200 100 0 ?

13) 08KNL_11 Oligo sup - Mio inf
7) 09KNL_01 Mio inf
5) 09KNL_13 Mio inf
6) 09KNL_74 Mio inf
5) 09KNL_71 Mio inf ***

LF + ? − ?

2008 2009 2010

Mitropoli-block

UM7
UM6
UM5
UM4
UM3
UM2
UM1

900 800 700 600 500 400 300 200 100 0

1) 09LVD_21 Oligo sup
4) 09KNL_57
4) 09KNL_12 Oligo sup - Mio inf
Mio inf
3) 09KNL_55 Oligo sup - Mio inf
1) 09LVD_21 Oligo sup
12) 08LVD_03 Oligo (probably)
2) 09AGH_14 Oligo sup
1) 09KNL_08 Oligo sup

08MFV_02   08MFV_10
08MFV_04   08MFV_09
08MFV_01   08MFV_08
08MFV_03
08MFV_07

Mio inf 09FNR_01

08FNR_03
Mio inf 08FNR_05
08FNR_04

08FNR_32   08KBL_01   08FNR_01
08FNR_30
08FNR_22   08LXD_02   08LST_02
08FNR_20   08LXD_01   08LST_01
08LST_03
08KNL_03
08KNL_02   08CDF_03
Mio inf 08KNL_01

08NR_07
08NR_06
08NR_04
08NR_03
08NR_02
08NR_01

Mio inf *** 08NR OR_08

KF

09KNL_73   08KNL_11 Mio inf
09KNL_71   08KNL_10
Mio inf ***   09KNL_02
09KNL_01 Mio inf

09KNL_13 Mio inf

09KNL_74 Mio inf

LF

09KNL_57 Oligo sup-Mio inf
09KNL_12 Mio inf
? 09LVD_21   09KNL_55 Oligo sup-Mio inf
Oligo sup   09KNL_11
09KNL_10

08LVD_03 Oligo probably
08LVD_02
08LVD_01
09AGH_14 Oligo sup
09AGH_13
09AGH_10   09KNL_09
09KNL_08 Oligo sup
09KNL_53

Mitropoli 2008

5) 08MFV_27 Mio inf
4) 08MFV_24 Mio inf
? UM4
? UM3
Basement

08MFV_28
08MFV_27 Mio inf
08MFV_26
08MFV_24 Mio inf
08MFV_23
08MFV_22
08MFV_21
08MFV_20
09MFV-08

ANNEXE-II

Paleocurrent measurements

Arrows indicate paleoflows as determined by mostly conglomerate clast imbrications.

Table of illustrations

CHAPTER I

CHAPTER II

190

of (A), showing clearly sharply erosive and truncated surface of b-M4/5. C) Upward from section-2a, at an ancient quarry, b-M4/5 is sharp and slightly incised into underlying UM4 with the overlying conglomerates of UM5 downlapping westward. D) Clast-supported, poorly sorted, gravel to pebble conglomerate. Clast components include ophiolite (o), radiolarite (r), marble (m), quartz, limestone and gneiss (g). E) Massive, thick bedded, matrix to clast-supported, normal grading, pebble to boulder conglomerates capped by very coarse-grained sandstones...52

198

CHAPTER III

CHAPTER IV

Table of contents

RESUME

Le bassin méso-hellénique est un bassin oligo-miocène intra-chaîne situé dans le nord de la Grèce continentale, à la limite entre les zones externes et les zones internes de la chaîne des Hellénides. Ce mémoire présente une analyse détaillée des séries sédimentaires affleurant sur la bordure occidentale du bassin dans sa partie la plus méridionale. Trois blocs, séparés par des failles majeures, sont étudiés successivement, du point de vue des faciès, de leur stratigraphie et des structures tectoniques. Une carte géologique détaillée est produite, fondée sur les formations lithologiques élevées au rang d'unités stratigraphiques. La structure est un monoclinal faillé à vergence vers le bassin. Les failles sont essentiellement des failles normales, mais des mouvements compressifs existent. Des failles listriques synsédimentaires précoces sont enregistrées à la base du comblement. Les failles majeures interblocs sont inversées tardivement. Les faciès indiquent pour l'essentiel des épandages sous-marins d'origine gravitaire. Les sources sédimentaires sont d'abord locales (couverture mésozoïque) puis, pour l'essentiel du comblement, lointaines (socle pélagonien des zones internes). Les directions de paléocourants indiquent un approvisionnement depuis le NE, dans le secteur des Météores. La succession stratigraphique est marquée par des ruptures de faciès abruptes et érosives ainsi que des discordances enregistrant essentiellement un signal tectonique. Les analyses micropaléontologiques permettent de préciser l'âge des séries sur l'intervalle Oligocène supérieur-Miocène inférieur. Cet âge est plus jeune que le démarrage du bassin méso-hellénique plus au nord, mais sub-contemporain de la mise en place des conglomérats des Météores, dont le contrôle tectonique a également été mis en évidence.

ABSTRACT

The Mesohellenic Basin is an Oligo-Miocene intermontane basin preserved in Northern continental Greece, at the boundary between the external and internal zones of the Hellenides. This memoir presents a detailed analysis of the deposits outcroping in the southernmost part of the basin, on its western border. Three fault-bounded blocks are presented successively, including facies, stratigraphic and tectonic data. A detailed geological map is provided, featuring lithological formations of chronological significance. The main structure is a faulted monocline dipping toward the basin. Faults are mostly normal faults, although compressional features are observed. Synsedimentary listric faults are recorded in the lower part of the basin fill. The major block-bounding faults were lately inverted. The facies indicate mainly submarine gravity flows and associated turbidites. The sediments were supplied first locally (erosion of the mesozoic cover) and then, for most of basin fill, from denudation of the pelagonian basement (internal zones). Paleocurrent directions, related to this main part of the infill, indicate a source to the Northeast, in the area of the Meteora. The stratigraphic succession is marked by facies gaps and erosional unconformities which point to a dominant tectonic control. The micropaleontologic analyses provide an overall Upper Oligocene-Lower Miocene age of the series. This age is younger than that of the early stages of the basin more to the north, but rather contemporaneous with the Meteora conglomerates, the tectonic origin of which was previously demonstrated.